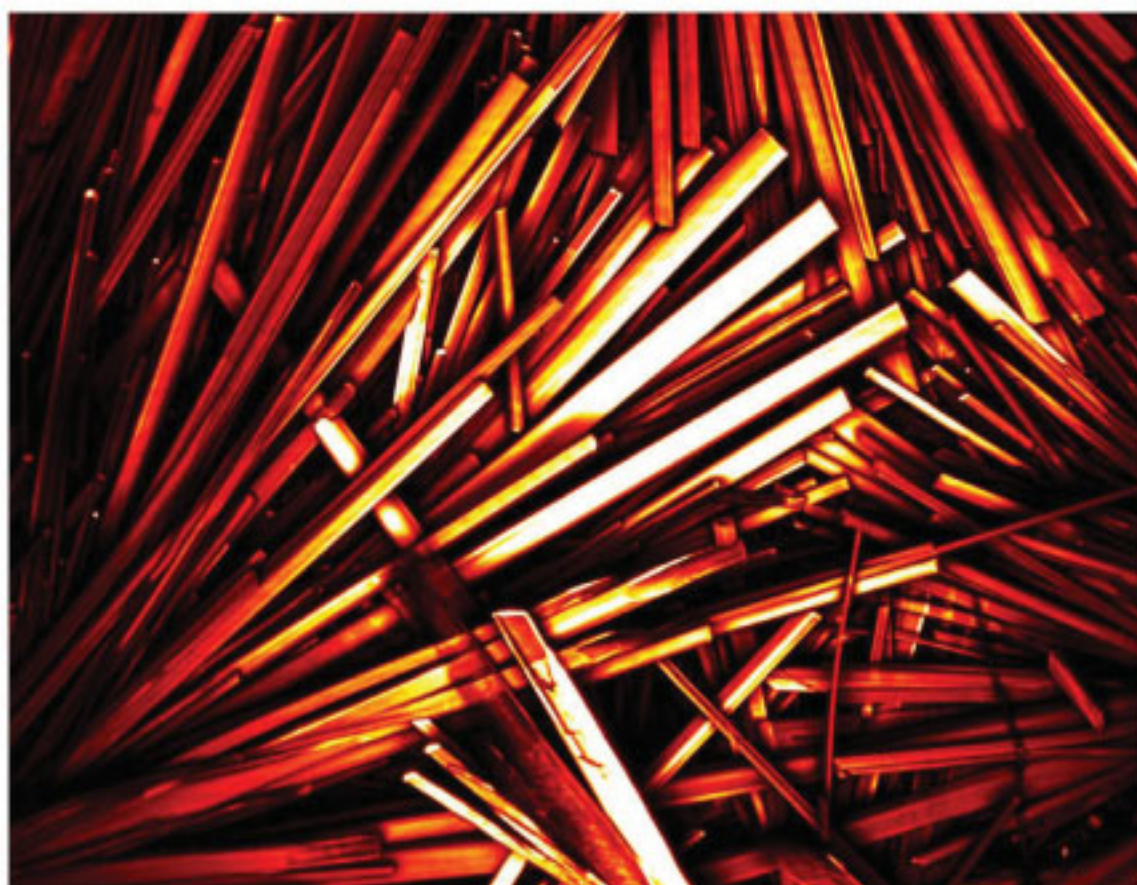


Maike Windbergs

**Towards a better understanding
of lipid-based matrices**
**Innovations in the production and analysis of
physically stable solid lipid extrudates with tailor-
made dissolution profiles**



Cuvillier Verlag Göttingen
Internationaler wissenschaftlicher Fachverlag



**Towards a better understanding of lipid-based
matrices – Innovations in the production and
analysis of physically stable solid lipid extrudates
with tailor-made dissolution profiles**

Inaugural-Dissertation

zur Erlangung des Doktorgrades
der Mathematisch-Naturwissenschaftlichen Fakultät
der Heinrich-Heine-Universität Düsseldorf

vorgelegt von

Maike Windbergs

aus Düsseldorf

Düsseldorf, April 2009

aus dem Institut für pharmazeutische Technologie und Biopharmazie
der Heinrich-Heine Universität Düsseldorf

Gedruckt mit der Genehmigung der
Mathematisch-Naturwissenschaftlichen Fakultät der
Heinrich-Heine-Universität Düsseldorf

Referent: Prof. Dr. Peter Kleinebudde

Koreferenten: Prof. Dr. Jörg Breitzkreutz

Prof. Dr. Thomas Rades

Tag der mündlichen Prüfung: 30.04.2009

Bibliografische Information der Deutschen Nationalbibliothek

Die Deutsche Nationalbibliothek verzeichnet diese Publikation in der Deutschen Nationalbibliografie; detaillierte bibliografische Daten sind im Internet über <http://dnb.ddb.de> abrufbar.

1. Aufl. - Göttingen : Cuvillier, 2009

Zugl.: Düsseldorf, Univ., Diss., 2009

© CUVILLIER VERLAG, Göttingen 2009

Nonnenstieg 8, 37075 Göttingen

Telefon: 0551-54724-0

Telefax: 0551-54724-21

www.cuvillier.de

Alle Rechte vorbehalten. Ohne ausdrückliche Genehmigung des Verlages ist es nicht gestattet, das Buch oder Teile daraus auf fotomechanischem Weg (Fotokopie, Mikrokopie) zu vervielfältigen.

1. Auflage, 2009

Gedruckt auf säurefreiem Papier

978-3-86955-072-5

Table of contents

Table of contents	I
Figures.....	VII
Abbreviations and symbols	XI
List of original publications	XIII
1. Introduction and theoretical background.....	1
1.1. Lipids as excipients for the formulation of oral pharmaceutical dosage forms.....	1
1.2. Solid-state behaviour of lipids and problems during manufacturing.....	4
1.3. Dissolution testing of oral lipid-based dosage forms and its correlation to solid-state analysis	6
2. Aims of the study	9
3. Experimental	11
3.1. Introduction	11
3.2. Materials	11
3.2.1. Lipids.....	11
3.2.2. Polyethylene glycols	11
3.2.3. Model drugs.....	11
3.3. Methods	12
3.3.1. Manufacturing	12
3.3.1.1. Mixing	12

3.3.1.2. Extrusion.....	12
3.3.1.3. Tableting.....	12
3.3.1.4. Resolidification of lipid melts in thin layers	13
3.3.2. Analytics.....	13
3.3.2.1. Differential scanning calorimetry (DSC)	13
3.3.2.2. X-ray powder diffraction (XRPD)	13
3.3.2.3. Attenuated total reflectance infrared (ATR- IR) spectroscopy	14
3.3.2.4. Near infrared (NIR) spectroscopy	14
3.3.2.5. Raman spectroscopy	15
3.3.2.6. Raman mapping.....	15
3.3.2.7. Coherent anti-Stokes Raman microscopy (CARS).....	15
3.3.2.8. Dissolution testing.....	16
3.3.2.9. Intrinsic dissolution testing in combination with <i>in situ</i> Raman spectroscopy.....	16
3.3.2.10. Intrinsic dissolution testing in combination with CARS microscopy.....	17
3.3.2.11. Scanning electron microscopy (SEM).....	17
3.3.2.12. Hot-stage microscopy.....	17
3.3.2.13. Contact angle measurements	18
3.3.2.14. Storage.....	18
3.3.2.15. Karl Fischer titrimetry	18
3.3.2.16. Moisture sorption analysis.....	18
3.3.2.17. Laser diffraction	19

4. Results and discussion.....	21
4.1. Solid lipid extrudates – solid-state characterization of lipids after processing and storage in correlation to dissolution characteristics	21
4.1.1. Introduction	21
4.1.2. Understanding the solid-state behaviour of triglyceride solid lipid extrudates and its influence on dissolution	21
4.1.3. Influence of the composition of glycerides on the solid-state behaviour and the dissolution profiles of solid lipid extrudates	25
4.2. Investigating and understanding the principles of lipid solid-state behaviour during processing and storage.....	29
4.2.1. Introduction	29
4.2.2. Investigating the principles of recrystallization from glyceride melts	30
4.3. Combining lipid and hydrophilic polymer in one matrix.....	34
4.3.1. Introduction	34
4.3.2. Tailor-made dissolution profiles by extruded matrices based on lipid polyethylene glycol mixtures.....	35
4.3.3. Influence of structural variations on drug release from lipid/polyethylene glycol matrices	38
4.4. Development and establishing of novel dissolution methods with focus on <i>in situ</i> monitoring of drug release and solid-state behaviour.....	42
4.4.1. Introduction	42
4.4.2. Investigating the relationship between drug distribution in solid lipid extrudates and dissolution behaviour using Raman spectroscopy and mapping	43

4.4.3.	Chemical imaging of oral solid dosage forms and changes upon dissolution using coherent anti-Stokes Raman scattering microscopy <i>and</i>	48
	Coherent anti-Stokes Raman scattering microscopy to monitor drug dissolution in different oral pharmaceutical tablets	48
5.	Summary and conclusions	53
6.	Zusammenfassung der Arbeit	55
7.	References	57
8.	Acknowledgements	67
9.	Original publications	69
9.1.	Article 1: Understanding the solid-state behaviour of triglyceride solid lipid extrudates and its influence on dissolution	69
9.2.	Article 2: Influence of the composition of glycerides on the solid-state behaviour and the dissolution profiles of solid lipid extrudates	78
9.3.	Article 3: Investigating the principles of recrystallization from glyceride melts	87
9.4.	Article 4: Tailor-made dissolution profiles by extruded matrices based on lipid polyethylene glycol mixtures	109
9.5.	Article 5: Influence of structural variations on drug release from lipid/polyethylene glycol matrices	116
9.6.	Article 6: Investigating the relationship between drug distribution in solid lipid matrices and dissolution behaviour using Raman spectroscopy and mapping	125

9.7. Article 7: Chemical Imaging of Oral Solid Dosage Forms and Changes upon Dissolution Using Coherent Anti-Stokes Raman Scattering Microscopy	146
9.8. Article 8: Coherent anti-Stokes Raman scattering microscopy to monitor drug dissolution in different oral pharmaceutical tablets.....	154

Figures

Figure 1: DSC thermograms of tristearin and theophylline powders and extrudates.....	22
Figure 2: Variable temperature XRPD patterns of resolidified tristearin melts.	23
Figure 3: Dissolution curves of triglyceride extrudates. (a) comparison of different triglycerides and (b) comparison of tristearin extrudates produced at different temperatures (n = 3, mean, cv < 3%, not shown).....	24
Figure 4: SEM images of extrudate surfaces containing 50% theophylline anhydrate produced at different temperatures (a) glyceryl monostearate 65 °C (b) tristearin/ glyceryl monostearate (5+5 w/w) 65 °C (c) tristearin 65 °C (d) tristearin/ glyceryl monostearate (9+1 w/w) 65 °C (e) tristearin 55 °C and (f) tristearin/ glyceryl monostearate (9+1 w/w) 55 °C.....	27
Figure 5: Dissolution curves of different lipids and their mixtures at different extrusion temperatures directly after manufacturing (TG = triglyceride tristearin, PG = partial glyceride glyceryl monostearate) (n = 3, mean, SD < 2%, not shown).	28
Figure 6: XRPD patterns of resolidified triglyceride melts during storage. Trilaurin (a) at room temperature, (b) at 40 °C, tripalmitin (c) at room temperature, (d) at 40 °C, tristearin (e) at room temperature and (f) at 40 °C.....	31
Figure 7: DSC thermograms of resolidified melts during storage. (a) 90% tristearin/10% glyceryl monostearate and (b) tristearin at room temperature.	33
Figure 8: Dissolution curves of extrudates (TG = triglyceride tripalmitin, PEG = polyethylene glycol, n = 3, mean, SD < 4%, not shown).....	36

- Figure 9: SEM images of extrudates before and after dissolution (a) tripalmitin before dissolution, (b) tripalmitin after dissolution, (c) tripalmitin/polyethylene glycol (9+1 w/w) before dissolution, (d) tripalmitin/polyethylene glycol (9+1 w/w) after dissolution, (e) tripalmitin/polyethylene glycol (5+5 w/w) before dissolution and (f) tripalmitin/polyethylene glycol (5+5 w/w) after dissolution. 37
- Figure 10: Dissolution curves of extrudates containing different matrix compositions based on tripalmitin and polyethylene glycol (PEG) (9+1 w/w) (mean, n = 3, SD < 3%, not shown). 40
- Figure 11: Dissolution profiles of extrudates based on different triglycerides and PEG 10000 (9+1 w/w) (mean, n = 3, SD < 4%, not shown). 41
- Figure 12: Cross section of an extrudate. Raman maps of (a) theophylline anhydrate, (b) tripalmitin, (c) both components and (e) optical image of the area mapped. 44
- Figure 13: Surface of an extrudate. Raman maps of (a) theophylline anhydrate, (b) tripalmitin, (c) both components and (e) optical image of the area mapped. 44
- Figure 14: Raman spectra from *in situ* analysis during intrinsic dissolution testing of tablets compressed from physical mixture (a) and extrudate (b) containing tripalmitin and theophylline anhydrate. 46
- Figure 15: Solid dosage forms consisting of lipid (red) and drug (green) after different immersion times in dissolution medium. (a-c) tablet of tripalmitin/theophylline monohydrate, (d-f) tablet of tripalmitin/theophylline anhydrate and (g-i) tablet of extrudates of tripalmitin/theophylline anhydrate. 49
- Figure 16: In-line visualization of theophylline monohydrate crystal growth on the surface of a tablet in water consisting originally of tripalmitin/theophylline anhydrate. 51

Figure 17: In-line visualization of drug release from a tablet of tripalmitin (red) and theophylline monohydrate (green) during dissolution testing.....	51
--	----

Abbreviations and symbols

API	active pharmaceutical ingredient
ATR-IR	attenuated total reflectance infrared spectroscopy
a.u.	arbitrary units
CI	confidence interval
CFR	Code of Federal Regulations
cv	coefficient of variation
DSC	differential scanning calorimetry
FDA	Food and Drug Administration
GRAS	generally recognized as safe
HPLC	high pressure liquid chromatography
n	number of experiments
PEG	polyethylene glycol
PG	partial glyceride
R ²	coefficient of determination
RH	relative humidity
SD	standard deviation
SEM	scanning electron microscopy
TG	triglyceride
USP	United States Pharmacopeia
w/w	weight/weight

w/v	weight/volume
XRPD	X-ray powder diffraction
Θ	angle X-ray diffraction

List of original publications

- I. Windbergs M, Strachan CJ and Kleinebudde P. Understanding the solid-state behaviour of triglyceride solid lipid extrudates and its influence on dissolution. *European Journal of Pharmaceutics and Biopharmaceutics* 71 (2009) 80-87.
- II. Windbergs M, Strachan CJ and Kleinebudde P. Influence of the composition of glycerides on the solid-state behaviour and the dissolution profiles of solid lipid extrudates. *International Journal of Pharmaceutics* doi: 10.1016/j.ipharm.2009.03.002.
- III. Windbergs M, Strachan CJ and Kleinebudde P. Investigating the principles of recrystallization from glyceride melts. *AAPS Pharm Sci Tech* (submitted).
- IV. Windbergs M, Strachan CJ and Kleinebudde P. Tailor-made dissolution profiles by extruded matrices based on lipid polyethylene glycol mixtures. *Journal of Controlled Release* 137 (2009) 211-216.
- V. Windbergs M, Strachan CJ and Kleinebudde P. Influence of structural variations on drug release from lipid/polyethylene glycol matrices. *European Journal of Pharmaceutical Sciences* 37 (2009) 555-562.
- VI. Windbergs M, Haaser, M, McGoverin C, Gordon K, Kleinebudde P and Strachan CJ. Investigating the relationship between drug distribution in solid lipid matrices and dissolution behaviour using Raman spectroscopy and mapping. *Journal of Pharmaceutical Sciences* (accepted).
- VII. Windbergs M, Jurna M, Offerhaus HL, Herek JL, Kleinebudde P and Strachan CJ. Chemical imaging of oral solid dosage forms and changes upon dissolution using coherent anti-Stokes Raman scattering. *Analytical Chemistry* 81 (2009) 2085-2091.
- VIII. Jurna M, Windbergs M, Strachan CJ, Hartsuiker L, Otto C, Kleinebudde P, Herek JL and Offerhaus HL. Coherent anti-Stokes Raman scattering microscopy to monitor drug dissolution in different oral pharmaceutical tablets. *Journal of Innovative Optical Health Sciences* 2 (2009) 37-43.

1. Introduction and theoretical background

1.1. Lipids as excipients for the formulation of oral pharmaceutical dosage forms

The introduction of high throughput methods in drug discovery has led to potential active pharmaceutical ingredients (APIs) exhibiting increasingly high binding affinities for the designated target receptor in the human body. Unfortunately, the high specificity of these substances is often accompanied by a complex chemical structure and strong hydrophobicity (Kerns, 2001). The bioavailability of the API in the human body and the resulting therapeutic effect strongly depends on parameters like solubility of the API in the gastrointestinal tract and permeability across the gastrointestinal wall (Amidon et al, 1995). The formulation of hydrophobic drugs to overcome these barriers is challenging. As APIs are most commonly administered orally, there is a strong need to develop new methods to formulate such substances.

Lipids have recently generated substantial interest as a basis for oral dosage forms (Pouton and Porter, 2008; Jannin et al, 2008). Being naturally based, lipids are physiologically non-toxic and biodegradable. They are also often used in the food industry and therefore in most cases classified as GRAS (generally recognized as safe). The Food and Drug Administration (FDA) in the United States has published the list of GRAS substances in the Code of Federal Regulations (CFR) (Chen, 2008).

In general, lipids show a high variability in their physico-chemical properties and therefore there are various possibilities for different types of pharmaceutical formulations. Several lipid-based systems for the delivery of drugs have already been introduced onto the market, with their physical and chemical characteristics including drug release depending on both the choice of lipid and processing technique. Nearly all of the established processing techniques have the advantage of being solvent-free. Therefore no subsequent drying step is necessary, which is cost and time efficient and avoids additional stress for the product. One can distinguish between processes which involve mechanical compression and thermal formation of the dosage form, with the latter being more frequently used. Combinations of mechanical and thermal processing may also be used.

One of the first lipid-based formulation approaches involved capsules being filled with liquid or semi-solid lipid formulations in which the active pharmaceutical ingredient (API) was either suspended or dissolved (Cole, 1989; Bowtle, 2007). Another formulation approach involved the production of small drops of molten lipid with incorporated API that were then resolidified (Pallagi et al, 2004).

The most common formulation approach involves melting the lipid with the solid API and then resolidifying it to form a coherent matrix in which the API is embedded. The resolidified melt can be granulated (Ozdemir and Agabeyoglu, 1990) resulting in irregular spheres which can be filled into capsules or tableted. Solid particles can also be produced in one step with a variety of different methods including melt extrusion (Prapaitrakul et al, 1991; Liu et al, 2001; Breitenbach, 2002) and melt granulation (Evrard et al, 1999; Zhang and Schwartz, 2003). In addition, processes like spray cooling (Cavallari et al, 2005; Erni et al, 1980) or spray drying (Chaunhan et al, 2005) have been investigated. The resulting particles can either be processed into tablets or filled into capsules. Other established systems include solid lipid nanoparticles (Bunjjes et al, 1996; Mehnert et al, 2001) and nanostructured lipid carriers (Ricci et al, 2005), which can be produced by different techniques. Furthermore, liquid lipids can be used in a fluid bed process to coat particles (Barthelemy et al, 1999).

One advantage of lipid-based formulations is their high potential for the development of controlled release systems. In particular, they can be used for prolonged drug release (Hamdani et al, 2002). In addition, they are able to enhance the solubility and permeability of drugs with poor oral bioavailability (Prabhu et al, 2005; Humberstone et al, 1997), a fact that is increasingly important since a large proportion of the newly developed APIs have low solubility and permeability, according to the commonly used Bioclassification System (Amidon et al, 1995; Löbenberg and Amidon, 2000). Furthermore, taste masking is also feasible with the help of lipids (Qi et al, 2008) and APIs which are sensitive against humidity can be protected in a lipid-based dosage form. Lipids are also used in small quantities as lubricants in tableting processes and as mould releasing agents.

Another approach for the formulation of lipid-based dosage forms is to manufacture at temperatures below the melting point of the lipid, either at room temperature or with moderate heating. Tableting is one such approach which has previously been performed (Li et al, 2006). Extrusion is another approach, and is defined as forcing a

plastic mass through a hole of defined size by applying pressure (Kleinebudde, 1997). Successful studies have already been conducted with a rotary ring die press (Breitkreutz et al, 2003) and a ram extruder (Pinto and Silverio, 2001).

This idea has been further developed with screw extrusion, which has the advantages of being a continuous process with controllable pressure and temperature application. In addition, the mass inside the extruder barrel is subjected to agitation in three dimensions providing intensive mixing. The temperature of the extruder barrel can be adjusted below the melting point of the individual lipid to allow suitable extrusion conditions. For this process, the powdered lipid(s) and API are mixed in a laboratory mixer and the resulting powder blend is transferred to the dosing device which gravimetrically feeds the powder into the barrel in order to provide a consistent feed. As the lipid mass does not melt, the process has been called solid lipid extrusion. Reproducible extrudates with a smooth surface and favourable properties for further processing can be obtained. They can either be spheronized to pellets or cut into cylinders of suitable size for the applicable dosage form. In addition, milling is possible.

Solid lipid extrusion has been used for the production of sustained release matrix pellets (Reitz and Kleinebudde, 2007). Furthermore, solid lipid extrudates have been used as the basis for dosage forms exhibiting taste masking properties. The extrudates have been either spheronized into pellets (Reitz and Kleinebudde, 2007; Krause et al, 2009) or milled down into granules (Michalk et al, 2008).

Unfortunately, lipid-based dosage forms including solid lipid extrudates do exhibit some challenges. Both the choice of the lipids and the manufacturing technology strongly influence the subsequent properties of the dosage form, including surface structure, solid-state behaviour and reproducibility. They can also exhibit stability problems, largely due to their complex solid-state behaviour (Hamdani et al, 2003). These issues will be covered in the next section.

1.2. Solid-state behaviour of lipids and problems during manufacturing

Lipids encompass a very diverse group of substances exhibiting a wide range of structural differences. They include both naturally occurring and semisynthetic substances. The most important group for the manufacturing of lipid pharmaceutical dosage forms are glycerides. The central molecule in these substances is glycerol which is esterified with fatty acids. Depending on the degree of esterification, glycerides can be classified as mono-, di- and triglycerides. Physicochemical properties of a specific glyceride primarily depend on the degree of esterification and the structure of the esterified fatty acids. By increasing the degree of esterification (with a lower fraction of free hydroxyl groups) the glyceride exhibits as higher melting point, and is more lipophilic and brittle. In addition, the properties of the fatty acids have to be taken into consideration. Chain length, branching and the existence and position of double bonds affect the physicochemical properties of glycerides.

The diversity of possible structural combinations in lipids provides a building kit for the construction of pharmaceutical excipients with desired properties. Modifications can be made by methods such as transesterification, fractionation or hydration. Furthermore, hydrophilisation of the substance can be achieved by the esterification with hydrophilic molecules. A very prominent example is the esterification with PEG (Gelucire[®]), but other substances such as lactic and citric acids have also been used. In most cases, the lipids which are used for the production of dosage forms are heterogeneous mixtures of different glycerides.

Glycerides are able to exhibit polymorphism, a phenomenon which has been the subject of many scientific investigations (Larsson, 1996; Timms, 1984). Monoacid triglycerides are mainly used as research substances. They usually exhibit three different polymorphic modifications with a monotropic relationship: the thermodynamic least stable α -form, the metastable β' -form and the stable β -form (Sato, 2001; Sato et al, 1999). Each of these forms is defined by a specific packing mode of the fatty acid chains, with the stable β -form exhibiting the densest packing mode and thus having the highest melting temperature. Transformations from a less stable to a more stable form can occur, during which an increasing degree of order is achieved. The rate of transformation depends both on the chemical structure of the

lipid and external influences like temperature and pressure (Thoma and Serno, 1983). The more complex the glyceride the more complex is its solid-state behaviour. Heterogeneous glycerides form additional polymorphic structures to those exhibited by monoacid triglycerides.

An analytical technique that is widely used for the investigation of glyceride solid-state behaviour is differential scanning calorimetry (DSC). This technique can be used to gain insight into the existence of polymorphic forms and their transformations (Brittain et al, 1991). The shortcomings of this technique are that the sample is changed during measurement as a polymorphic form whose melting point has been exceeded during measurement is able to recrystallize in another polymorphic form. Complementary non-destructive techniques include X-ray powder diffraction (XRPD) and vibrational spectroscopy methods such as infrared and near infrared spectroscopy as well as Raman spectroscopy (Bugay, 2001). Despite the variety of techniques the analytical investigation of the often complex solid-state behaviour of glycerides can be challenging.

Due to their versatile solid-state behaviour as mentioned above glycerides exhibit difficulties in the processing of lipid-based dosage forms. The processing is often accompanied by transformations associated with melting and recrystallization (Hamdani et al, 2003). The lipid polymorphic behaviour is quite difficult to predict, and a dosage form produced with a metastable lipid modification and the desired properties may subsequently change with the polymorphic transformation to a more stable form (Whittam et al, 1975; Sutananta et al, 1994). The result is usually a deterioration of the product quality with respect to desired properties including drug release profiles.

Furthermore, the processed dosage forms often show transformations during storage, which may also affect the dissolution behaviour (Choy et al, 2005). This effect is often called 'aging' in the literature, and is mostly due to the appearance of a metastable lipid modification during processing which eventually transforms to a more stable modification during storage (Whittam et al, 1975). These effects might also result in alterations of the drug release (San Vicente et al, 2000). Therefore, the solid-state behaviour of lipids during processing and its relationship to drug release and storage must be understood to obtain reproducible dosage forms.

At present, there is a lack of understanding of the physicochemical behaviour of lipid-based dosage forms during processing and storage. Due to the lack of understanding and hence control of the processing conditions that result in the formation of metastable forms of lipids, the number of lipid-based formulations on the market is still limited.

1.3. Dissolution testing of oral lipid-based dosage forms and its correlation to solid-state analysis

Dissolution testing is universally used in the development, production and quality assurance of oral solid dosage forms. The Pharmacopoeias describe suitable and established standard dissolution methods with their requirements. The results gained from such investigations are used to predict the bioavailability and hence they are surrogate parameters of therapeutic efficacy. For quality issues, dissolution data can be used as a control tool as in most cases the dissolution behaviour of a dosage form is sensitive to variations during manufacturing which affect the dissolution performance.

The dissolution behavior of drugs from solid oral dosage forms is a critical quality attribute since, in almost all cases, therapeutic efficacy of the medicine depends on this very behaviour. In general, drug dissolution from oral dosage forms is investigated by analyzing the concentration of the released drug in a defined volume of stirred or flowing dissolution medium. The concentration of released drug in the medium is measured at defined time intervals using techniques such as UV spectroscopy or HPLC (Costa and Lobo, 2001). A combination of chemical and physical properties of both the solid dosage form and the dissolution medium determine the drug dissolution behaviour. Important properties of the solid dosage form include the apparent solubility of the drug and the other components, particle size and drug distribution. These characteristics and hence the dissolution rate change during drug dissolution (Brittain and Grant, 1999).

In addition, in the special case of matrices which remain intact during dissolution, such as solid lipid extrudates, there is evidence that the dissolution behaviour is largely a function of drug distribution at the surface and within the core of the matrix, and at present this distribution is not well understood.

As solid-state properties of the components affect dissolution behavior to a large and sometimes even unpredictable extent there is a strong need for monitoring and especially visualizing solid-state properties in real time during dissolution testing. Established dissolution testing as described above provides no direct information on the changing dosage form phenomena, and hence the dissolution behaviour of drugs cannot be completely understood with such analysis alone. Therefore, there is a need to monitor the changing chemical and physical properties of dosage forms during dissolution.

Initial attempts to characterize such changes involved the bulk characterization of samples *ex situ* using methods such as X-ray diffraction (Phadnis and Suryanarayanan, 1997). Recently, Raman spectroscopy has been used to detect solid-state transformations during dissolution *in situ* (Aaltonen et al, 2006; Savolainen et al, 2009). However, since drug release from dosage forms is largely dependant on spatial phenomena, it is obviously pertinent to obtain spatially resolved information. Spatially resolved analysis of oral dosage forms has experienced a surge of interest within the last decade (Gowen et al, 2008), in part due to much advanced analytical technology. Scanning electron microscopy has been used to characterize dosage form morphology changes after dissolution testing (Aaltonen et al, 2006), and X-ray powder diffraction has been used to depth-profile dissolution related phase transformations (Debnath et al, 2004).

Methods exhibiting chemical selectivity that are suitable for imaging dosage forms include near-infrared (NIR), mid-infrared (IR), terahertz and Raman imaging (Sasic, 2007; Zeitler et al, 2007) as well as imaging based on secondary ion mass spectrometry (Belu et al, 2000; Mahoney et al, 2004). While these methods are all appropriate for imaging physical and/or chemical changes of dosage forms after dissolution testing *ex situ*, they all exhibit serious shortcomings with respect to *in situ* imaging. Demands for *in situ* analysis include an absence of analysis-related dosage form destruction, a sampling setup that does not interfere with the dissolution medium flow, an ability to obtain data in the presence of dissolution media and sufficient temporal resolution. Secondary ion mass spectrometry cannot be used to sample materials in a dissolution medium. With respect to NIR (Reich, 2005), IR (Coutts-Lendon et al, 2003; Van der Weerd and Kazarin, 2004) and terahertz imaging, the radiation used with these techniques is strongly absorbed by water which severely

limits their use in aqueous environments. For IR imaging, this problem has been circumvented by the use of an attenuated total reflectance (ATR) set-up, whereby an ATR crystal is interfaced with both a tablet and dissolution medium in a flow through cell dissolution testing setup (Van der Weerd et al, 2004; Van der Weerd and Kazarin, 2005). However, the requirement for intimate contact between the dosage form and ATR crystal severely limits sampling set-up flexibility making analysis of different kinds of solid dosage forms problematic and the high pressure applied to the samples during analysis can be destructive. Furthermore, commonly observed particle sizes in oral solid dosage forms may be below the spatial resolution of this technique (Pajander et al, 2008). Raman imaging has potential for *in situ* analysis of solid dosage forms dissolution due to its lack of water sensitivity and relatively high spatial resolution (up to about 1 μm), but potential disadvantages include a typically longer data acquisition time (minutes or hours for 512 by 512 pixels) and possible interference from fluorescence (Uzunbajakava et al, 2003; Ling et al, 2002).

In conclusion, solid lipid extrudates are a promising new oral lipid-based dosage form where it is likely that the crystal structure of the lipid could be controlled during manufacturing and storage. Unfortunately, as in case of other lipid-based dosage forms, there is a lack of understanding the underlying principles of the lipid solid-state behaviour during extrusion and storage. In addition, the correlation of solid-state structure and dissolution characteristics has not been completely understood partly due to the fact that suitable analytical methods for investigating these issues have not yet been developed.

2. Aims of the study

The aim of this work was to understand structural characteristics of solid lipid extrudates during the extrusion process, storage and dissolution, and to relate these characteristics to drug dissolution behaviour. A correlation between the matrix structure, from the bulk to molecular levels, and dissolution behaviour should be established to provide a basis for the formulation of extrudates with predictable and tailor-made incorporated drug release profiles.

More specifically the aims were:

- To gain deeper understanding of the solid-state behaviour of lipids during the extrusion process below their melting points and during storage.
- To establish extrusion conditions leading to stable solid lipid extrudates.
- To correlate the solid-state behaviour of the lipids and drug distribution in the extrudates with the dissolution characteristics.
- To vary the composition of the extrudates in order to broaden the range of dissolution profiles.
- To develop and establish novel dissolution analysis methods with a focus on *in situ* monitoring of drug release and solid-state behaviour of excipients and drug.

3. Experimental

3.1. Introduction

A more detailed description of the materials and methods is given in the original publications. In the methods part each method description contains the references for those publications in which the described method is used.

3.2. Materials

3.2.1. Lipids

Different lipids were chosen as matrix forming excipients. The pure powdered monoacid triglycerides trilaurin (Dynasan 112[®]), tripalmitin (Dynasan 116[®]) and tristearin (Dynasan 118[®]) containing fatty acids with different chain lengths were used as received. The average of the batches which were used contained 98% pure triglycerides. In addition, the powdered partial glycerides glyceryl monostearate (Imwitor 491[®]) and glyceryl stearate (Imwitor 900 P[®]) possessing different degrees of esterification were used. The lipid batches which were used provided an average of 96% purity. All lipid powders were supplied by Sasol (Witten, Germany).

3.2.2. Polyethylene glycols

Powdered polyethylene glycols with different mean molecular weights were used as release modifying agents. Polyethylene glycols with a mean molecular weight of 10000 (Polyglykol 10000[®]) and 20000 (Polyglykol 20000[®]) were supplied by Clariant (Waalwijk, The Netherlands). Polyethylene glycols with mean molecular weights of 100000 (Polyox WSR N10[®]), 1000000 (Polyox WSR N12K[®]) and 7000000 (Polyox WSR 303[®]) were provided by Dow Chemical (New Milford, Connecticut, US).

3.2.3. Model drugs

Powdered theophylline anhydrate and theophylline monohydrate were used as model drugs. Theophylline anhydrate was produced by BASF (Ludwigshafen, Germany). Theophylline monohydrate was recrystallized from theophylline anhydrate which had

been dissolved in purified water. The crystal form of each substance was verified with X-ray powder diffraction and compared to the theoretical pattern available from the Cambridge Structural Database (Cambridge Crystallographic Data Centre, Cambridge, United Kingdom) using the associated Mercury software (v. 1.5).

3.3. Methods

3.3.1. Manufacturing

3.3.1.1. Mixing

For extrusion experiments powdered excipients were weighed in a 1:1 ratio with the model drug and blended in a laboratory mixer (LM20 Bohle, Ennigerloh, Germany) for 15 min at 25 rpm.

For tableting excipients and model drug were weighed in a 1:1 ratio and blended in a Turbula mixer (Willi A. Bachofen AG, Basel, Switzerland) at 62 rpm for 15 min.

Performed in articles 1, 2, 4, 5, 6, 7 and 8.

3.3.1.2. Extrusion

Pure excipients or blended powder mixtures containing excipients and model drug in a 1:1 ratio (w/w) were fed from a gravimetric dosing device (KT20K-Tron Soder, Lenzhard, Switzerland) into the barrel of a co-rotating twin-screw extruder (Mikro 27GL-28D, Leistritz, Nürnberg, Germany). Extrusion was performed with a constant screw speed of 30 rpm and a feeding rate of 40 gmin⁻¹. The extruder die plate exhibited 23 holes (diameter 1 mm, length 2.5 mm). The processing temperature was individually chosen depending on the melting temperature of the excipients.

Performed in articles 1,2,4,5,6,7 and 8.

3.3.1.3. Tableting

Blended powder mixtures were compressed on a tableting machine (Korsch EK 0, Erweka Apparatebau, Berlin, Germany) using flat-faced punches (diameter 9 mm). In addition, extrudates were compressed to tablets (150 mg). The crushing strength was

determined (Schleuniger 2E, Dr. Schleuniger Pharmatron AG, Solothurn, Switzerland) resulting in values around 40 N.

Performed in articles 6, 7 and 8.

3.3.1.4. Resolidification of lipid melts in thin layers

The powdered lipids were either purely or in physical mixtures completely melted 20 °C above their melting points. Each melt was held for at least 3 min before they were poured out into purpose-built Teflon moulds. The melts resolidified in thin lipid layers of 2 mm in ambient conditions.

At certain time points small quantities of the lipid layer surface were removed with a medical scalpel and investigated. Analysis was performed on the freshly resolidified sample and after 24 and 48 hours. Afterwards, measurements were conducted in a 2 days interval up to 16 days. The following measurements were accomplished after 24, 36, 48 and 60 days.

Performed in article 3.

3.3.2. Analytics

3.3.2.1. Differential scanning calorimetry (DSC)

Differential scanning calorimetry was performed using a DSC 821e or a DSC 823e calorimeter (Mettler-Toledo, Gießen, Germany). Approximately 5 mg of sample was weighed into hermetically sealed aluminium pans (40 µl). The samples were heated from 20 to 300 °C with a heating rate of 10 °Cmin⁻¹. All experiments were conducted twice.

Performed in articles 1, 2, 3 4 and 5.

3.3.2.2. X-ray powder diffraction (XRPD)

Diffraction patterns were recorded using a theta-theta X-ray powder diffractometer (D8 Advance, Bruker AXS GmbH, Karlsruhe, Germany). Measurements were performed in symmetrical reflection mode with CuK α radiation ($\lambda=1.54 \text{ \AA}$) using Göbel mirror bent multilayer optics. The angular range measured was 5-40° (2θ), with a step size of

0.05° (2θ). The measuring time was 1 s per step. The samples were put in the sample holder and gently compressed to smooth the surface. All experiments were conducted in triplicate.

Variable temperature measurements were also performed with the same diffractometer with resolidified melts of excipient powders. The powdered samples were heated up to 10 °C above their individual melting temperature and held at that temperature for at least 3 min before pouring the melt into the sample holder on ice to rapidly resolidify them. Measurements were directly performed in the temperature range of 25 °C up to the individual melting temperatures of the excipients.

Performed in articles 1,2,3,4 and 5.

3.3.2.3. Attenuated total reflectance infrared (ATR-IR) spectroscopy

Samples were measured using an FTIR spectrometer (Bruker FTIR Vertex 70, Bruker, Ettlingen, Germany) with an ATR accessory fitted with a single reflection diamond/ZnSe crystal plate (MIRacle ATR, PIKE Technologies, Madison, WI, USA). The samples were placed in the ATR device without any preparation and measured using 64 scans for each spectrum. Spectra were collected between 4000 and 650 cm^{-1} with a resolution of 4 cm^{-1} . All experiments were conducted in triplicate.

Performed in articles 1 and 2.

3.3.2.4. Near infrared (NIR) spectroscopy

For NIR measurements a NIR spectrometer (NIR-256L-2.2T2, Control Development Inc., South Bend, IN, USA) with a thermoelectrically cooled 256 element InGaAs array detector, tungsten light source and a fiber optic reflectance probe (six illuminating optical fibers around one signal collecting fiber) was used. A reference spectrum was recorded with a Teflon background. The spectra were collected from 1100 nm to 2200 nm with 30 ms integration time and 500 scans per spectrum. All experiments were conducted in triplicate.

Performed in article 1.

3.3.2.5. Raman spectroscopy

Raman spectra were recorded with a 1600 pix CCD camera (Newton DU-970N, Andor Technology, Belfast, Northern Ireland). The samples were irradiated by a Kr ion Laser (coherent, Innova 90K, Santa Clara, CA) at 647.1 nm of 30 mW and focused by 40x 0.65NA microscope objective lens.

Performed in articles 6, 7 and 8.

3.3.2.6. Raman mapping

The Raman mapping data were collected using a Senterra dispersive Raman microscope (Bruker Optics, Ettlingen, Germany). An excitation wavelength of 785 nm, with 100 mW power and a 1200 groove per millimetre grating were used. The resulting resolution was 3-5 cm^{-1} across the spectrum. For the maps, each spectrum was the co-addition of three 5 s exposures, and collected from 50-1530 cm^{-1} with a step size of 2 μm . An Olympus 100x objective (N.A. 0.9) with a 50 μm confocal pinhole was used to collect the Raman signal. The resolution was estimated to be 5 μm (axial) and 2 μm (lateral) using the full width half maximum of the intensity profile of the 520 cm^{-1} band of silicon. Peaks unique to each component were integrated with the integration function in OPUS 6.5, and, for each component, normalized as a percentage of the maximum signal observed for that component in the analyzed area.

Performed in article 6.

3.3.2.7. Coherent anti-Stokes Raman microscopy (CARS)

The CARS setup consisted of a coherent Paladin Nd:YAG laser and an APE Levante Emerald optical parametric oscillator (OPO). In this setup, the fundamental (1064 nm, 80 MHz, >15 ps) of the laser was used as Stokes, whereas the signal from the OPO (tunable between 700-1000 nm and spectral width of 0.2 nm) was used as the pump and probe. The beams were scanned over the sample by galvano mirrors (Olympus FluoView 300, IX71) and focused by a 20x 0.5NA objective lens into the sample. Both beams had a power of several tens of mW at the sample. Due to the highly scattering samples the forward generated CARS signal was collected in the backward direction. The collected signal was filtered and detected by a photo multiplier tube. All images were 512x512 pixels over the full field of view and were obtained in a 2 s

interval. Images at different wavelengths required tuning of the OPO but no realignment of the optics. Different images were collected consecutively. For the dissolution testing the tripalmitin matrix was imaged before and after dissolution to verify the absence of change in the matrix material. During the dissolution only the theophylline was imaged in real time.

Performed in articles 7 and 8.

3.3.2.8. Dissolution testing

Dissolution studies were performed according to the USP 29 Methods 1 (basket) and 2 (paddle) with a dissolution apparatus (Sotax AT7 smart, Sotax, Lörrach, Germany). Extrudates were cut to lengths of approximately 1 cm, and a sample size of 140 mg was used in each vessel. Experiments were conducted in purified water containing 0.001% polysorbate 20 at 37 ± 0.5 °C with a stirring speed of 50 rpm. The absorption of the medium was measured at 2.5 or 5 min intervals using a UV-Vis spectrometer with an absorption wavelength of 242 nm (Lambda 40, Perkin–Elmer, Rodgau-Juegesheim, Germany) in a continuous flow-through cuvette. The experiments were conducted in triplicate taking the mean for the dissolution curve. The standard deviation was below 4% in all cases.

Performed in articles 1, 2, 4 and 5.

3.3.2.9. Intrinsic dissolution testing in combination with *in situ* Raman spectroscopy

Experiments were conducted using a channel flow intrinsic dissolution test apparatus with a quartz window for the Raman probe. The drug concentration of the dissolution medium was measured with a UV-VIS spectrometer (Ultraspec III, Pharmacia Biotech, Uppsala, Sweden) in a flow-through cuvette. For these studies a Raman spectrometer (Control Development Inc., South Bend, IN, USA) equipped with a fiber optic probe (Raman Probe RPS785/12-5, InPhotonics, Norwood, MA, USA) was used. The spectra were recorded in a 30 s interval between 200 and 2200 cm^{-1} with an integration time of 1 s and by averaging 3 scans per spectrum.

Performed in article 6.

3.3.2.10. Intrinsic dissolution testing in combination with CARS microscopy

The dissolution flow-through cell consisted of a Teflon chamber in which two metal bars were used to fix the dosage form in the centre of a flowing dissolution medium. A hose pump circulated the medium through the chamber via suitable conduits at a constant rate of 5 mL/min. On one side, the cell was equipped with a thin microscope cover glass that was transparent to the incident and scattered radiation. The dissolution medium was purified water and the measurements were conducted at room temperature. Such a set-up allowed the solid-state properties of a solid oral dosage form to be visualized *in situ* with an appropriate medium flow for dissolution testing of oral solid dosage forms.

Performed in articles 7 and 8.

3.3.2.11. Scanning electron microscopy (SEM)

The samples were mounted on aluminium stubs using double-sided carbon tape and sputter-coated with platinum for 20 s or with gold for 150 s (Agar Manual Sputter Coater B7340, Agar Scientific, Stansted, UK). SEM micrographs were recorded using either a DSM 962 scanning electron microscope (Carl Zeiss, Oberkochen, Germany), or a Leo 1430VP scanning electron microscope (Leo Elektron Microscopy, Cambridge, UK) with a working voltage of 20 kV.

Performed in articles 1,2,4,5 and 6.

3.3.2.12. Hot-stage microscopy

Thermomicroscopic investigations were performed with a hot-stage FP 900 (Mettler-Toledo, Giessen, Germany) in combination with an optical microscope (Leica, Wetzlar, Germany). The powdered lipids were heated above their melting points and the melt was held for at least three minutes before monitoring the resolidification at room temperature.

Performed in article 3.

3.3.2.13. Contact angle measurements

Contact angle measurements were performed with an optical contact angle meter (Drop shape analysis system DSA 100, Krüss, Hamburg, Germany). A 0.8 μL drop of distilled water was placed on the extrudate surface and the contact angle was directly determined by using the associated software (Drop shape analysis DSA1, v1.90, Hamburg, Germany). For each sample eight measurements were performed and the mean was calculated.

Performed in articles 2, 4 and 5.

3.3.2.14. Storage

Samples were exposed to different climatic conditions to investigate their stability. A climate chamber (KBF 240, Binder, Tuttlingen, Germany) provided a constant climate with 40 °C and 75 %RH. The samples were placed in open Petri dishes. In addition, storage experiments were performed in a drying cabinet at 40 °C (Ehret, Emmendingen, Germany). Furthermore samples were stored in room conditions.

Performed in articles 1, 2, 3, 4 and 5.

3.3.2.15. Karl Fischer titrimetry

The water content of the extrudates was verified using a Karl Fischer titrator (DL 18, Mettler-Toledo, Gießen, Germany). The medium consisted of Hydranal[®]-methanol dry and Hydranal[®]-formamide dry combined in equal parts. Hydranal[®]-composite 5 was used as one-component reagent. Calibration was performed with Hydranal[®] water standard. The mean of three measurements was calculated.

Performed in article 4.

3.3.2.16. Moisture sorption analysis

A dynamic vapor sorption analyzer SPS 11 (Projekt Messtechnik, Ulm, Germany) was used to expose the samples to a specific climate in controlled temperature and humidity. Approximately 1500 mg of the sample was weighed into aluminium cups and the sample weight was monitored during the measurements. Measurements were

performed in duplicate at room temperature in the humidity range between 0% and 80% with steps of 10% each. Based on these data sorption isotherms were constructed.

Performed in articles 4 and 5.

3.3.2.17. Laser diffraction

The particle size of the powders was determined with a laser diffractometer (Helos, KF-Magic, Clausthal-Zellerfeld, Germany) using the dry dispersion method. The median and the 90% quantile were determined three times. The mean was calculated for each material.

Performed in articles 5 and 6.

4. Results and discussion

4.1. Solid lipid extrudates – solid-state characterization of lipids after processing and storage in correlation to dissolution characteristics

4.1.1. Introduction

Even though solid lipid extrusion has already been performed in different working groups (Breitkreutz et al, 2003; Pinto and Silverio, 2001; Reitz et al, 2007), complete understanding of the lipid solid-state behaviour during extrusion has not been achieved. In this section, a comprehensive overview of the underlying principles of solid-state behaviour of different lipids during processing and storage is given that could be correlated to the dissolution behaviour. In addition, the influence of the matrix composition of solid lipid extrudates on solid-state behaviour and drug release could be elucidated.

Corresponding articles: 1 and 2.

4.1.2. Understanding the solid-state behaviour of triglyceride solid lipid extrudates and its influence on dissolution

Three pure monoacid triglycerides differing in their fatty acid chain lengths (trilaurin, tripalmitin and tristearin) were extruded below their melting points. The aim of extrusion in general was to obtain reproducible cylindrical extrudates with a smooth surface and high mechanical stability. Therefore, the equipment variables were kept constant whereas the process variables, screw speed and feed rate, were adjusted to obtain a continuous product flow. As the lipids melt at different temperatures depending on the chain length, the extrusion temperature was individually chosen for each lipid. The best extrusion results were obtained a few degrees (6-11 °C) below the melting point of the stable polymorphic form of the individual lipid. The physical characterization of powders and extrudates with a combination of DSC, XRPD and vibrational spectroscopy techniques gave further insight into the solid-state behaviour of the lipids during processing and storage. Depending on the extrusion temperature, the extrudate contained different polymorphic forms of the lipid after extrusion (figure

1). All lipid powders were in the stable β -form before manufacturing. Tristearin extrudates exhibited α - and β -form of the lipid after extrusion at 55 °C having their melting endotherms with the onsets at 50.2 °C (α -form) and 70.7 °C (β -form) respectively whereas extrusion at 65 °C resulted in pure tristearin β -form (figure 1) (Hagemann, 1988).

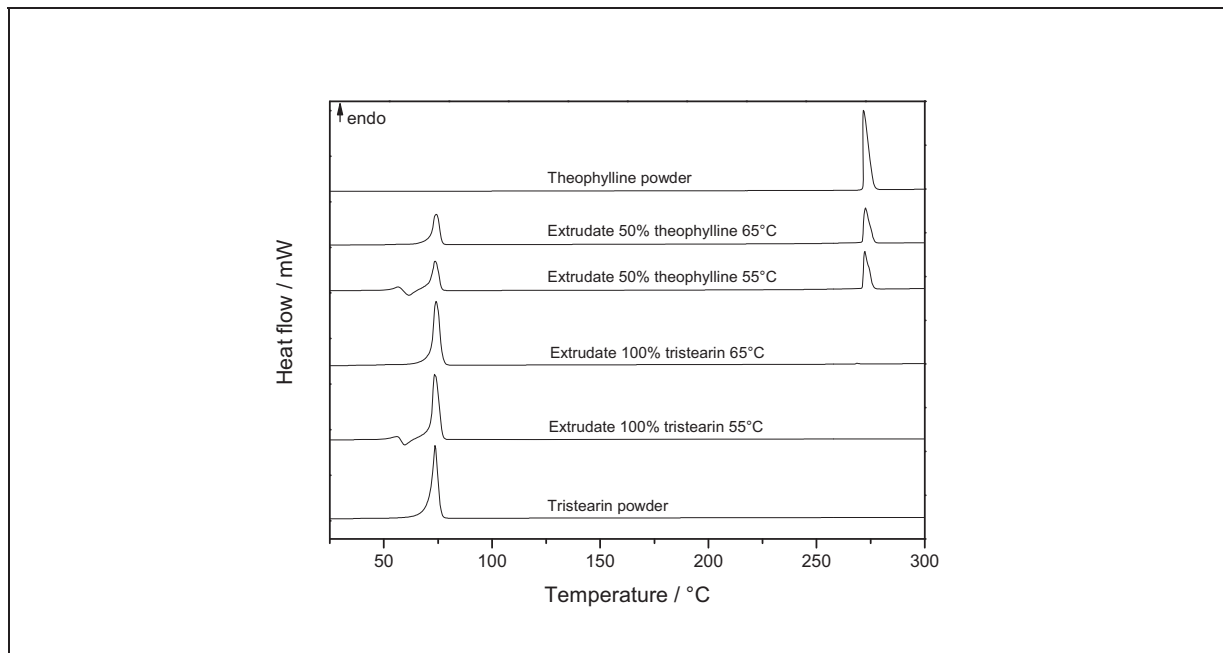


Figure 1: DSC thermograms of tristearin and theophylline powders and extrudates.

The combination of extrusion temperature and friction was found to be a key factor for the polymorphic behaviour of the lipid after extrusion. Friction causes temperature to rise which leads to melting at the edges of the lipid mass inside the extruder barrel. After leaving the die plate the molten parts of the lipid directly resolidify. The temperature at which the extrudate leaves the extruder determines the crystallization behaviour from the molten component of the extruded lipid (MacNaughtan et al, 2006).

This hypothesis was backed up with XRPD measurements during which the sample was heated up in the range of 25-75 °C in 5 °C steps. There was no incidence of solid-state changes until melting and as the polymorphs exhibit a monotropic relationship the α -form must be created via the melt (Sato, 2001; Sato et al, 1999). Variable temperature XRPD was also performed on the resolidified melts of the lipid powders as figure 2 depicts for tristearin. Depending on the temperature the α -form peak (21.4°)

or the β -form peaks (19.4° , 23.1° and 24.05°) were detected (Kellens et al, 1991; Van Langevelde et al, 2001). The results were in good agreement with the results obtained for the extrudates and could be corroborated with ATR-IR measurements (Kobayashi, 1988; Yano et Sato, 1999). The influence of pressure applied to the lipid mass inside the extruder barrel could be excluded as it was too low to have an effect on polymorphic transformations. The pressure during extrusion never exceeded 0.7 MPa and the previously reported pressure values which affect lipid polymorphic transitions are above this range (Wagner and Schneider, 1996). In conclusion, to obtain extrudates which only contain the stable β -form of the lipid the extrusion temperature has to be adjusted above the melting point of any unstable polymorphic form.

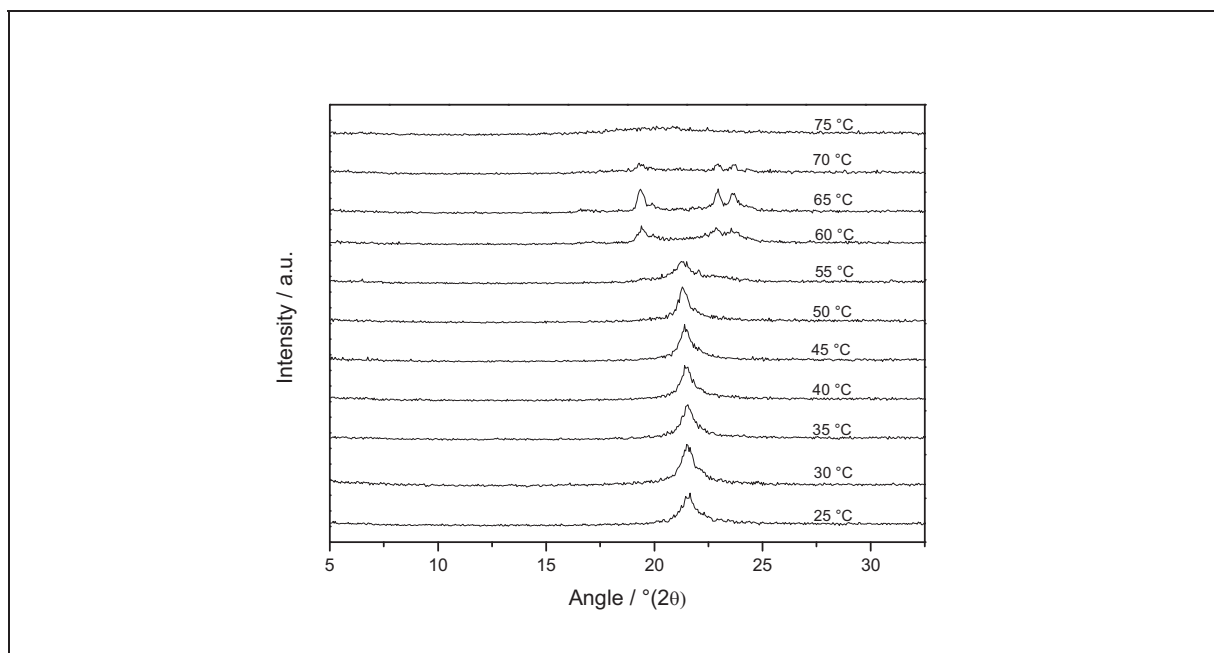


Figure 2: Variable temperature XRPD patterns of resolidified tristearin melts.

Release of the incorporated model drug theophylline anhydrate was found to be chain-length dependant (figure 3a) as lipids with a shorter chain length like trilaurin (12 C-atoms) led to faster release profiles than tripalmitin (16 C-atoms) or tristearin (18 C-atoms). Polymorphic transitions after manufacturing had a strong influence on the dissolution behaviour due to crystallization of the stable β -form from the unstable α -form on the surface of the extrudate. In case of tristearin the extrudate produced at 55 °C exhibiting partly α -form which transforms to β -form over time was found to exhibit a slower dissolution rate than the pure β -form tristearin extrudate produced at 65 °C (figure 3b). On the first glance these results are unintuitive as the release is purely

diffusion controlled and the α -form is the less dense packing mode which should therefore lead to an equal or higher dissolution rate. But SEM images of the surface revealed sharp fractal structures covering the surface ('blooming effect'), increasing the contact angle and hence being expected to decrease the wetting and the dissolution rate (Khan and Craig, 2004; Fang et al, 2007).

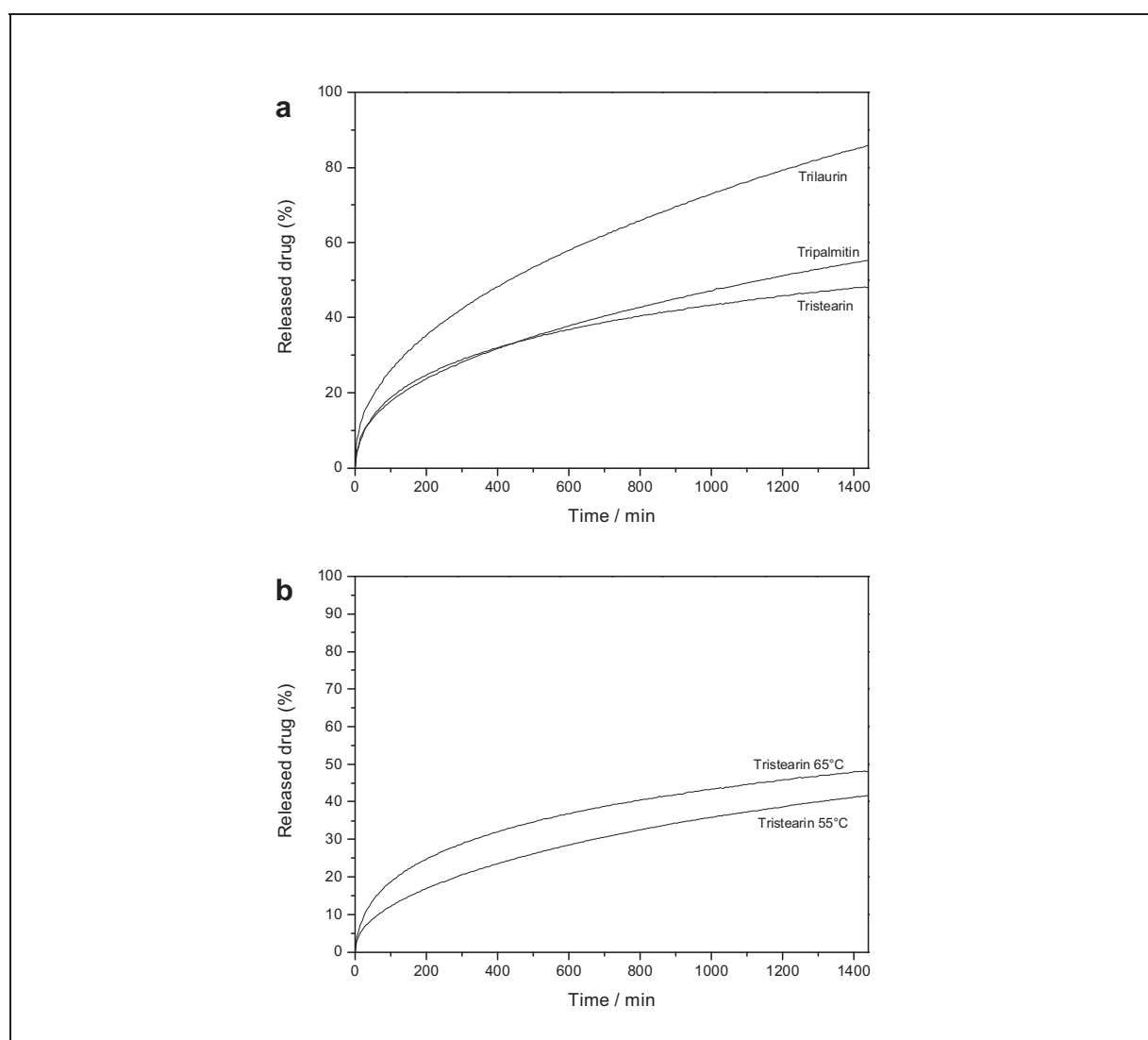


Figure 3: Dissolution curves of triglyceride extrudates. (a) comparison of different triglycerides and (b) comparison of tristearin extrudates produced at different temperatures ($n = 3$, mean, $cv < 3\%$, not shown).

Triglyceride solid lipid extrudates remained stable during open storage in accelerated conditions ($40\text{ }^{\circ}\text{C}$; 75 \%RH) for 10 months. There was no evidence of solid-state changes of lipid and drug and no interactions could be detected. Despite there being

some evidence that theophylline monohydrate is the thermodynamically stable form in these conditions the drug remained as the anhydrate (Ticehurst et al, 2002). This is probably due to the hydrophobic barrier provided by the lipid matrix and a slow transformation rate.

In conclusion, these results led to a deeper understanding of the solid-state behaviour of lipids during extrusion and storage and help to avoid process conditions which lead to undesirable dosage form properties. The solid-state behaviour of triglycerides is influenced by different factors during processing and has to be well understood and monitored to obtain reproducible dosage forms of high quality. Understanding the polymorphic behaviour of triglycerides in solid lipid extrudates and its effect on dissolution will help in the development of solid lipid extrudates with desired dissolution behaviour.

4.1.3. Influence of the composition of glycerides on the solid-state behaviour and the dissolution profiles of solid lipid extrudates

Based on the results of the study performed on the extrusion of triglycerides, the composition of the lipid matrix was modified under controlled conditions to broaden the range of dissolution profiles from these dosage forms. A partial glyceride was extruded alone and in different ratios with a triglyceride to evaluate the effect of the lipid matrix composition and possible interactions between either the lipids or lipid and model drug. Solid-state analysis was conducted on the powders and on the extrudates and correlated to the results of dissolution testing. In addition, the storage stability under accelerated conditions was tested.

The partial glyceride, glyceryl monostearate, was successfully extruded alone and with 50% theophylline anhydrate as a model drug. The extrudates contained pure β -form of the lipid (Hagemann, 1988). DSC measurements revealed a limited interaction between lipid and drug during the measurement as the drug is able to partially dissolve into the lipid when the melting temperature of the lipid is exceeded (Chen et al, 1997). Non-destructive analysis of the extrudates using XRPD (Yajima et al, 2002) and ATR-IR spectroscopy (Nolasco et al, 2006; Kobayashi, 1988) revealed that no polymorphic transitions occurred in the lipid or drug.

Mixtures of the monoglyceride, glyceryl monostearate, and the triglyceride tristearin in two ratios (9+1 tristearin/glyceryl monostearate and 5+5 tristearin/glyceryl monostearate (w/w)) could successfully be extruded containing 50% drug. Solid-state analysis of the extrudates revealed interactions between the two lipids as the unstable tristearin α -form could be detected even though the temperature was sufficiently high enough to prevent this formation compared to a pure tristearin extrudate. Modified DSC measurements led to deeper insight into these solid-state phenomena. The extrudates were measured once and stored at room temperature for 24 hours in ambient conditions. These resolidified melts were measured a second time by DSC. Comparison of the thermograms of these samples led to the conclusion that the partial glyceride is able to hinder the formation of the β -form in the triglyceride. The structure of the partial glyceride exhibits some compatibility with the triglyceride structure and therefore stabilizes the less packed α -form of the triglyceride during recrystallization after melting (Garti et al, 1988; Garti, 1988). This effect is known in the literature and used in the chocolate industry to stabilize the favoured polymorph of cocoa butter (Schlichter-Aronhime and Garti, 1988). As a small quantity of the lipid mass in the extruder barrel melts due to the combination of temperature and friction the same phenomena can be observed for the extrudates. The degree of α -form formation can be correlated to the amount of partial glyceride in the matrix.

During storage, recrystallization of the tristearin α -form to the more stable β -form was detected. In this context, surface analysis using SEM and contact angle measurements was performed as the surface is very important with regard to dissolution behaviour. The release of the drug is purely diffusion controlled and the matrix stays intact, therefore transformations at the surface can have a pronounced effect on the release profile. Figure 4 depicts the SEM images of the extrudate surfaces with their corresponding contact angles. The glyceryl monostearate extrudate exhibits a smooth surface (figure 4 a) and the lowest contact angle due to its surfactant properties. The 5+5 (w/w) mixture of tristearin and glyceryl monostearate (figure 4b) also provides a relatively smooth surface. The increased contact angle of 116° is due to the presence of tristearin. Differences between the pure triglyceride (figure 4c) and the 9+1 (w/w) mixture of tristearin and glyceryl monostearate both produced at 65°C were revealed using solid-state analysis. The mixed extrudate should be expected to exhibit a significantly lower contact angle than the pure triglyceride sample. Instead, the mixed extrudate surface was partly covered with needle-like structures increasing the contact

angle. This effect was accentuated at a processing temperature of 55 °C. Figure 4e depicts the surface of the tristearin extrudates whereas figure 4f depicts the surface of the tristearin / glyceryl monostearate (9+1 w/w) mixed extrudate. The surface of both extrudates was completely covered with sharp needles and the contact angle was 125° in both cases. As the contact angle defines wettability it is evident that the needles at the extrudate surface strongly affect the dissolution behaviour (Fang et al, 2007; Khan and Craig, 2004).

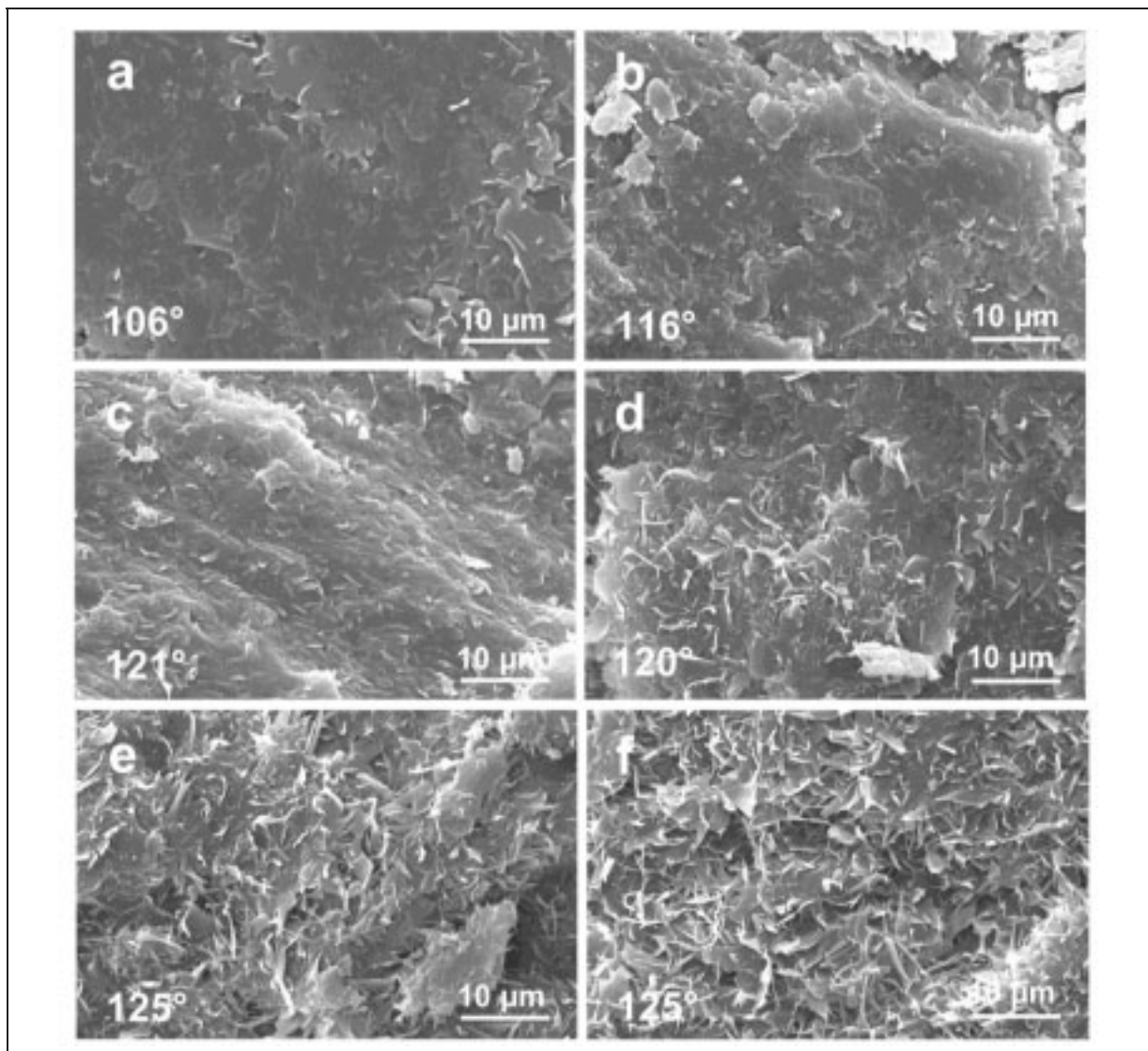


Figure 4: SEM images of extrudate surfaces containing 50% theophylline anhydride produced at different temperatures (a) glyceryl monostearate 65 °C (b) tristearin/ glyceryl monostearate (5+5 w/w) 65 °C (c) tristearin 65 °C (d) tristearin/ glyceryl monostearate (9+1 w/w) 65 °C (e) tristearin 55 °C and (f) tristearin/ glyceryl monostearate (9+1 w/w) 55 °C.

As already stated the dissolution from solid lipid matrices is purely diffusion controlled. Figure 5 depicts the dissolution characteristics of the processed batches.

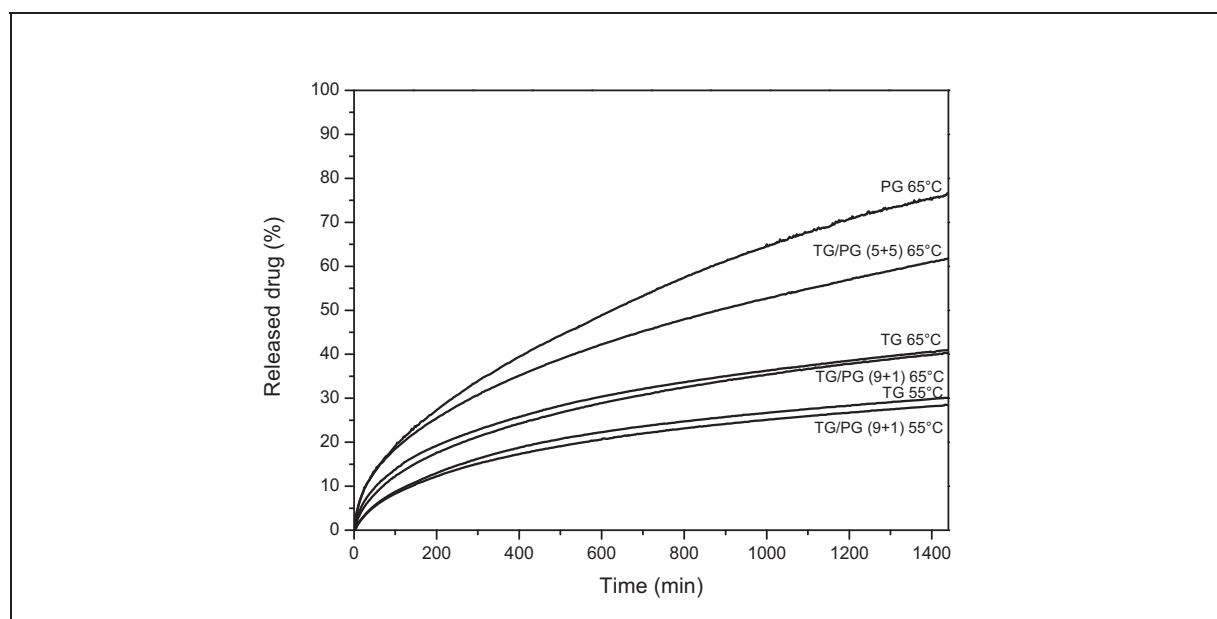


Figure 5: Dissolution curves of different lipids and their mixtures at different extrusion temperatures directly after manufacturing (TG = triglyceride tristearin, PG = partial glyceride glyceryl monostearate) ($n = 3$, mean, $SD < 2\%$, not shown).

The surfactant properties of the pure partial glyceride matrix made of glyceryl monostearate led to the fastest release of the drug compared to the other batches. The 5+5 (w/w) tristearin/glyceryl monostearate matrix exhibited a release rate between those of the pure triglyceride and pure partial glyceride. Even though the partial glyceride portion resulted in a pronounced recrystallization of the tristearin to the unstable α -form during extrusion which was followed by transformation to the β -form, the release of theophylline anhydrate was faster than from the pure tristearin extrudate due to the surfactant properties of the partial glyceride. By comparing the pure tristearin matrices produced at different extrusion temperatures with the 9+1 (w/w) tristearin/glyceryl monostearate mixture produced at the same temperatures two key factors can be identified. On the one hand the batches produced at 55 °C exhibited a significantly slower drug release than the batches produced at 65 °C. On the other hand the drug dissolution from the 9+1 (w/w) mixtures was slower than from the pure tristearin matrix which is unexpected on first glance regardless of extrusion temperature. The mixed matrix would be expected to show a faster release due to the

surfactant properties of the partial glyceride. In this case these surfactant properties are overcome by the β -form recrystallising as fractal structures on the surface of the extrudate that impair the wettability of the extrudate by the dissolution medium and hence reduce the release of the drug.

Storage experiments in two different climatic conditions (ambient and 40 °C/75 %RH) for 12 months revealed that the temperature has a strong impact on the transformation to the more stable polymorphic form as all lipids stored in accelerated conditions only contain the tristearin β -form after one year. In ambient conditions small amounts of the tristearin α -form are remained except in the 5+5 (w/w) mixture of tristearin/glyceryl monostearate. A higher molecular mobility of the partial glyceride exhibiting two hydroxyl groups might facilitate the transformation to the stable β -form.

In conclusion, the chemical composition of the glycerides used for solid lipid extrusion is of great importance as it affects the solid-state behaviour of the lipid and the consequently the dissolution of the drug. Due to its surfactant properties the partial glyceride exhibits a faster release of the drug compared to the triglyceride. In different mixtures of both lipids the partial glyceride led to increased incidence of the unstable α -form of the triglyceride leading to recrystallization of the stable β -form over time. This leads to fractal structures on the extrudate surface slowing down the dissolution rate. Storage experiments under accelerated and ambient conditions revealed a strong influence of temperature on the recrystallization kinetics. The results of this study help to elucidate the complex solid-state behaviour of solid lipid extrudates with different compositions which facilitates the development of suitable lipid based oral dosage forms with desired dissolution characteristics.

4.2. Investigating and understanding the principles of lipid solid-state behaviour during processing and storage

4.2.1. Introduction

As the previous studies revealed, different polymorphic forms after processing of lipids or unpredictable interactions can occur and be detected. Therefore, there is a strong need to perform systematic investigations on different influences which can affect these changes. This section features a systematic study in which different lipids

and their mixtures are investigated with respect to their solid-state behaviour. The results can be correlated to the solid-state behaviour of lipid-based dosage forms and should help to gain deeper insight into the principles of recrystallization processes which often occur unpredicted and hinder the manufacturing of reproducible and reliable dosage form quality.

Corresponding article: 3.

4.2.2. Investigating the principles of recrystallization from glyceride melts

Different powdered glycerides and mixtures were melted above their melting points and resolidified in Teflon moulds to produce thin lipid layers of reproducible appearance (2 mm thick), which served as model systems for the investigation of recrystallization processes. The layers were stored in different climatic conditions (room temperature and 40 °C) and solid-state analysis was performed at certain time points using a combination of DSC and XRPD. The influence of chain length, storage temperature, chemical substitution and interactions between different glycerides on solid-state behaviour were systematically investigated.

Experiments with three monoacid triglycerides of different fatty acid chain lengths revealed the effect of fatty acid chain length on the recrystallization behaviour. Trilaurin, the glyceride with the shortest fatty acids in the study (12 C-atoms), crystallized in a mixture of β' - and β -forms. The α -form, having its melting point at 14 °C, is not stable at room temperature (Hagemann, 1988). After one day of storage only pure β -form was detected using XRPD (figure 6 a and b). The storage conditions made no difference in this case.

Tripalmitin exhibiting 16 C-atoms for each fatty acid crystallized purely in the α -form after solidification. In this context, DSC thermograms exhibit some shortcomings as the sample which had originally been in the α -form is able to recrystallize in other polymorphic forms after less stable forms melt during the measurement. Therefore, a non-destructive complementary analysis was needed. No solid-state changes to other polymorphic forms were detected during storage at room temperature with XRPD (figure 6c) (Hongisto et al, 1996). In this case, the storage temperature plays an important role as the samples stored in 40 °C (figure 6d) completely transformed to the β -form after storage for 24 hours.

Tristearin, the glyceride with the longest fatty acids in this study (18 C-atoms), exhibited a similar behaviour to tripalmitin. The freshly resolidified sample existed completely in its α -form (figure 6e). Storage temperature had a great effect as the XRPD pattern of the samples stored in 40 °C depict (figure 6f). After 4 days of storage peaks due to the β -form appeared and after 48 days of storage only the β -form was detected.

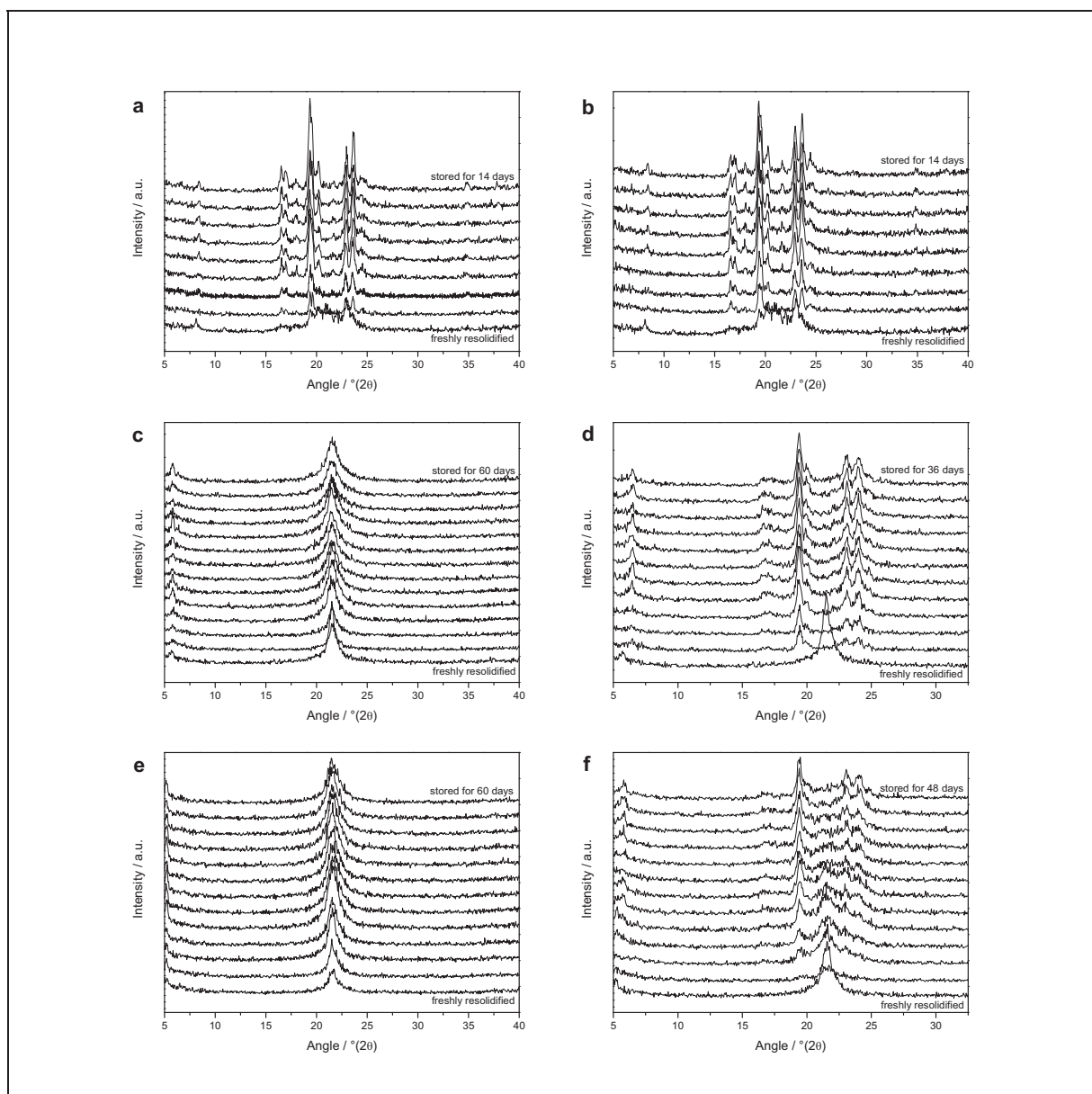


Figure 6: XRPD patterns of resolidified triglyceride melts during storage. Trilaurin (a) at room temperature, (b) at 40 °C, tripalmitin (c) at room temperature, (d) at 40 °C, tristearin (e) at room temperature and (f) at 40 °C.

In conclusion, fatty acid chain length, storage temperature and storage time affect the recrystallization behaviour of lipids from resolidified melts. The chain length of the fatty acids which are esterified with glycerol in a triglyceride molecule affected the recrystallization as the transformation rate from unstable to stable polymorphic forms decreased with increasing chain length at the storage temperatures used in this study. The second variable, storage temperature, had a pronounced effect on recrystallization to more stable polymorphic forms. Increasing the temperature greatly accelerated the recrystallization to the stable form.

For investigating the influence of chemical substitution on recrystallization, two partial glycerides were melted and resolidified as already described above. The monoglyceride, glyceryl monostearate, and the partial glyceride, glyceryl stearate, consisting of approximately equal fractions of monoglycerides and diglycerides are both esterified with stearic acid. Since partial glycerides are less homogenous and different melting endotherms tend to overlap, proper peak assignment is very difficult (Hagemann, 1988). Again, temperature plays an important role for the rate of recrystallization as shifting of the melting endotherms in the DSC thermograms happened faster at storage at 40 °C than at room temperature storage.

Two different mixtures of the monoacid triglyceride tristearin and the monoglyceride glyceryl monostearate were prepared in order to investigate the influence of possible interactions on the solid-state behaviour of the two components. One mixture consisted of 90% tristearin and 10% glyceryl monostearate (w/w), the other contained 50% tristearin and 50% glyceryl monostearate (w/w). The combination of 10% partial glyceride with 90% triglyceride led to interesting results as an interaction could be revealed. In the freshly resolidified sample only the tristearin α -form was detected. Due to the small amount of glyceryl monostearate no information about its crystal form can be made based on the analytical results. During storage at room temperature the sample remained in the same crystal structure for the whole time whereas during storage at 40 °C recrystallization to the stable tristearin β -form was observed. After 24 days of storage recrystallization to the β -form was complete. A comparison of DSC thermograms of the pure tristearin sample and the 90%/10% mixture was interesting (figure 7). During the DSC measurement the tristearin α -form melts (endotherm onset 53 °C) and hence the recrystallization of more stable polymorphs can occur. In the mixture, glyceryl monostearate was able to prevent or delay the transformation to the

stable tristearin β -form (figure 7a) as can be seen from the reduced intensity of the melting endotherm of the tristearin β -form (onset 65 °C) compared to the pure tristearin sample (figure 7b). The tristearin α -form is probably stabilised by combined structures of tristearin and glyceryl monostearate on an intermolecular level. The ability to hinder another lipid transforming into its stable polymorph has been previously reported (Garti, 1988, Garti et al, 1988).

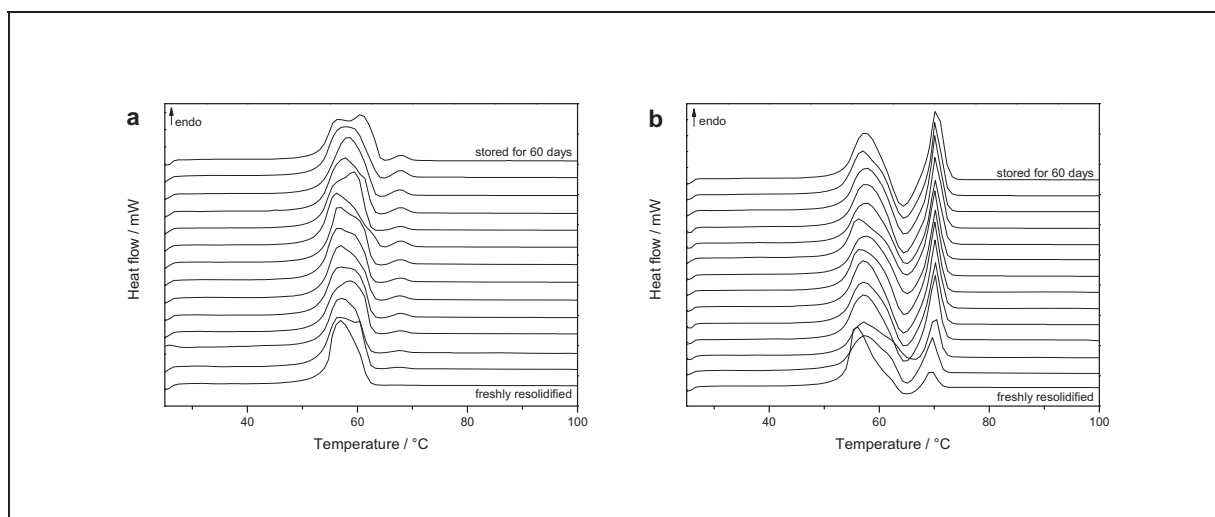


Figure 7: DSC thermograms of resolidified melts during storage. (a) 90% tristearin/10% glyceryl monostearate and (b) tristearin at room temperature.

Comparison of the pure tristearin sample with the mixed sample containing 10% partial glyceride during storage at 40 °C revealed the strong influence of temperature on recrystallization. Even though the presence of glyceryl monostearate hinders the formation of the tristearin β -form during the DSC measurement, complete transformation to the tristearin β -form was faster and more pronounced for the mixture than for the pure tristearin sample. This phenomenon is probably associated with a less organised and energetically favourable packing and higher molecular mobility in the resolidified melt of the combined lipids due to the different structures of the two lipids which are mixing. This might affect the mixed melt in terms of recrystallization rate at higher temperatures.

The extent of interactions between the partial glyceride and the triglyceride was investigated further in the lipid mixture containing 50% tristearin and 50% glyceryl monostearate (w/w). The increased amount of unstable α -form of the triglyceride compared to that of a pure tristearin melt was also observed for the mixture containing

50% partial glyceride. Comparing the two different mixing ratios suggests the ability of the solid-state form of the triglyceride to incorporate different amounts of the partial glyceride molecules affects the transformation rate to a large extent. The mixture containing 10% glyceryl monostearate exhibits the tristearin α -form for 16 days whereas the mixture containing 50% glyceryl monostearate features the tristearin α -form just for 10 days.

In conclusion, solid-state analysis of thin glyceride layers of different glycerides or mixtures of a triglyceride and a partial glyceride as model systems for lipid-based dosage forms led to a deeper insight into the principles of recrystallization from melts and during storage. The combination of DSC and XRPD measurements provided a reasonably comprehensive overview of the recrystallization from the melts. Generally, temperature was shown to have a pronounced impact on the rate of recrystallization with the higher temperature accelerating the recrystallization. Based on these results changes in solid dosage forms based on glycerides during processing and storage can be better understood and such knowledge is mandatory to avoid unpredictable and undesirable changes in a glyceride based dosage forms during processing and storage.

4.3. Combining lipid and hydrophilic polymer in one matrix

4.3.1. Introduction

Even though solid lipid extrudates in various compositions have been shown to provide a versatile basis for the formulation of pharmaceutical dosage forms they are mainly restricted to sustained release for the incorporated drug. To overcome these limitations mixed matrices were formulated containing a lipid and a hydrophilic polymer to accelerate the release of the drug. In this section mixtures of different triglycerides with polyethylene glycols varying in their molecular weights were extruded, and investigated with respect to their solid-state behaviour, their stability in different conditions and their dissolution profiles.

Corresponding articles: 4 and 5.

4.3.2. Tailor-made dissolution profiles by extruded matrices based on lipid polyethylene glycol mixtures

The monoacid triglyceride tripalmitin was extruded in different ratios with the hydrophilic polymer polyethylene glycol exhibiting a mean molecular weight of 10000 to form mixed matrices. By varying the ratio of hydrophobic and hydrophilic component tailor-made dissolution profiles over a wide range should be achievable.

The triglyceride tripalmitin was already established as a good matrix former for the solid lipid extrusion process in former studies (4.1.2) providing long term stability and predictable dissolution profiles. Polyethylene glycol has been used as a matrix for controlled release and as a tablet binder and coating agent (Rowe et al, 2003). In addition, polyethylene glycol has also been used in small quantities as a pore former and release modifier (Schmidt and Prochazka, 1979; Herrmann et al, 2007a; Cleek et al, 1997). In general, the formulation of dosage forms with polyethylene glycol involves melting of the polymer and resolidification with an API (Craig and Newton, 1991). Unfortunately, this approach can lead to unpredictable degeneration of the polymer (Crowley et al, 2002).

In this study, the suitability of polyethylene glycol for extrusion below its melting point was investigated with the pure polymer and with 50% theophylline anhydrate as a model drug. Well-formed extrudates were obtained and solid-state analysis with DSC and XRPD did not reveal any solid-state changes for either the polymer and or drug (Craig and Newton, 1991; Chen et al, 1997). A limited interaction occurred between theophylline and polyethylene glycol above the melting point of the polymer, as theophylline is able to partially dissolve into the polymer.

For the manufacturing of mixed matrices, tripalmitin and polyethylene glycol were extruded without drug below their melting ranges in the ratios 9+1 and 5+5 tripalmitin to polyethylene glycol (w/w). Solid-state analysis of powders and extrudates proved that both substances remained in their stable crystalline form and there was no evidence of any interactions. In a second step, extrudates were produced which contained 50% theophylline anhydrate. The amount of polyethylene glycol in the matrix (excluding drug) was varied from 5% up to 50% (w/w). For each composition, acceptable extrudates could be obtained providing the same crystal stability as described for the extrudates above.

Dissolution studies were performed on the extrudates. The results are depicted in figure 8. Pure tripalmitin matrices exhibited the slowest release of the drug as the dissolution is purely diffusion controlled and the pores were only due to the drug dissolving (Reitz et al, 2008). This could also be visualized with SEM before and after dissolution (figure 9a and b), where only small holes due to the former presence of the drug were visible on the surface of the extrudate after dissolution for 24 hours.

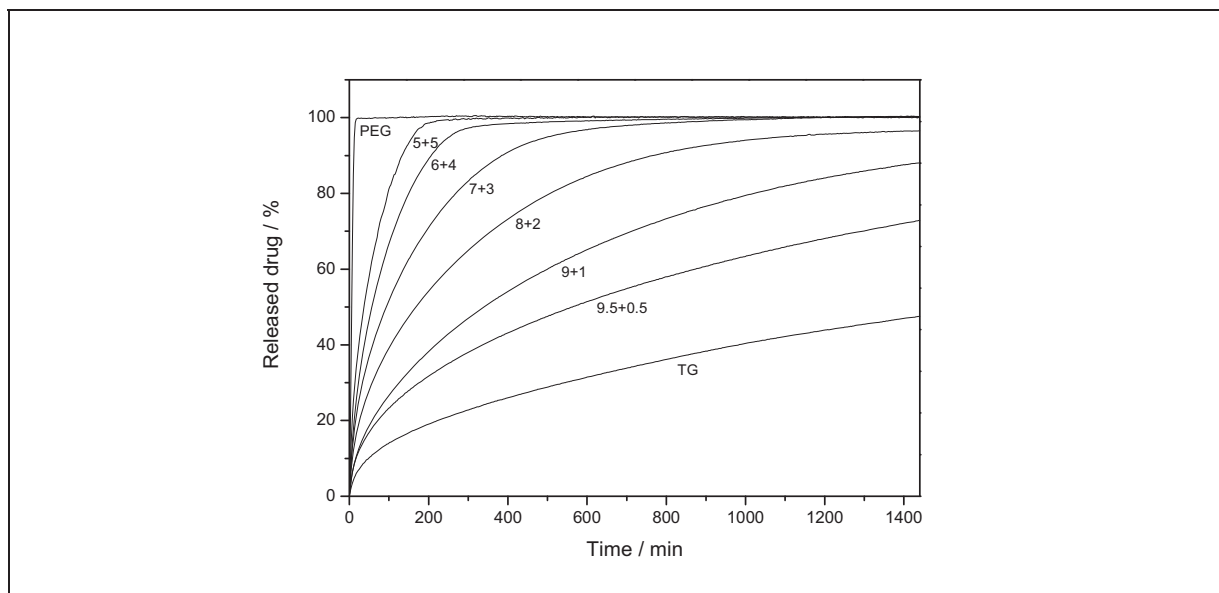


Figure 8: Dissolution curves of extrudates (TG = triglyceride tripalmitin, PEG = polyethylene glycol, $n = 3$, mean, $SD < 4\%$, not shown).

Within 24 hours the drug could not be completely released from the pure lipid matrix. At the other extreme, pure polyethylene glycol matrices released the drug very rapidly by dissolving completely (figure 8). The desired tailor-made dissolution profiles were obtained with mixed matrices of tripalmitin and polyethylene glycol. Polyethylene glycol as a hydrophilic polymer increases the dissolution rate from the matrix by dissolving and hence forming an interconnected pore network facilitating the release of the drug (Herrmann et al, 2007b). By varying the amount of polyethylene glycol in the matrix, release of the drug could be controlled over a broad range of dissolution profiles (figure 8). Even small amounts resulted in a significant increase of the release of the drug. The medium penetrated into the matrix and drug as well as polyethylene glycol particles dissolve. Pores of different sizes are formed depending on the amount of polyethylene glycol in the matrix. As examples, the SEM picture of the 5+5 and the

9+1 (w/w) tripalmitin and polyethylene glycol extrudates are depicted in figure 9 c-f before and after dissolution testing for 24 hours.

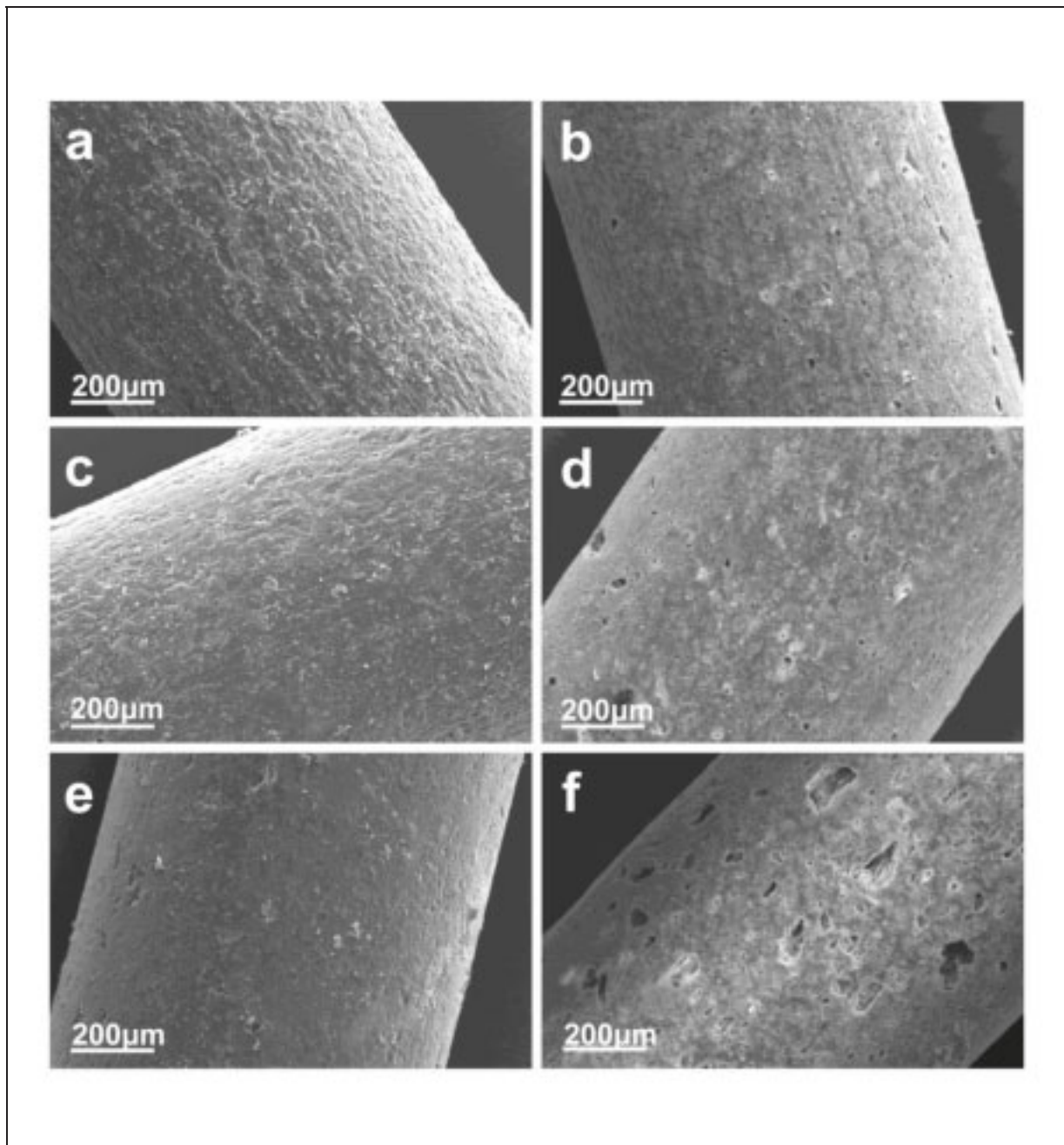


Figure 9: SEM images of extrudates before and after dissolution (a) tripalmitin before dissolution, (b) tripalmitin after dissolution, (c) tripalmitin/polyethylene glycol (9+1 w/w) before dissolution, (d) tripalmitin/polyethylene glycol (9+1 w/w) after dissolution, (e) tripalmitin/polyethylene glycol (5+5 w/w) before dissolution and (f) tripalmitin/polyethylene glycol (5+5 w/w) after dissolution.

In addition, the contact angle of the extrudate surfaces was determined. The pure tripalmitin extrudate exhibited poor wettability (contact angle 115°) due to its hydrophobic properties. A linear decrease of contact angle was detected with increasing polyethylene glycol amount in the matrix which correlates to the dissolution profiles.

Storage stability testing was performed at accelerated conditions ($40^\circ\text{C}/75\% \text{RH}$) for one year. The crystalline structure of the components was unchanged. Furthermore, as polyethylene glycol is a hydrophilic polymer possible interactions with water vapour were investigated. Karl Fischer titrimetry was performed on the extrudates before and after storage. The pure polyethylene glycol extrudates exhibited the highest water content with 1.2% (w/w) after storage in accelerated conditions, while the other extrudates possessed values of below 0.2% (w/w). In addition, a dynamic vapour sorption analyzer was used to expose the samples to different relative humidities ranging from 0 % to 80 %. The results were in good agreement with those obtained by Karl Fischer titrimetry. Therefore, the produced extrudates are stable against humidity.

In conclusion, tailor-made dissolution profiles were obtained by extrusion of a combination of a triglyceride and polyethylene glycol in extruded matrices below their melting point. The extrudates exhibited no evidence of solid-state changes or interactions. Storage experiments for one year in accelerated conditions and moisture sorption testing revealed the physical stability of these dosage forms was appropriate for oral dosage forms.

4.3.3. Influence of structural variations on drug release from lipid/polyethylene glycol matrices

As the combination of a triglyceride and polyethylene glycol was successfully introduced in extrudates produced below their melting points as a suitable oral dosage form this study was aiming to vary the composition of these mixed matrices. In a first step, the triglyceride tripalmitin was extruded with polyethylene glycol of different molecular weights in order to investigate the influence of molecular weight of the hydrophilic polymer in the range of 10000–7000000 on the dissolution characteristics. In a second step, triglycerides of different fatty acid chain lengths and hence different optimal extrusion temperatures were extruded in combination with polyethylene glycol 10000. It should be investigated whether different extrusion temperatures can be used

to extrude the mixed matrices consisting of a suitable triglyceride and polyethylene glycol in order to broaden the possible manufacturing temperatures with respect to temperature sensitive drugs.

It is necessary for extrudates to have a good external appearance with a smooth surface. This was achieved for each of the prepared formulations. For the extrusion studies with mixtures of tripalmitin and polyethylene glycol of different molecular weights the temperature was always kept at 55 °C which is below the reported melting points for tripalmitin (Hagemann, 1988) and polyethylene glycol (Craig and Newton, 1991). For the formulations containing trilaurin the extrusion temperature was adjusted to 40 °C as the melting point of the substance is 46 °C (Hagemann, 1988). For formulations containing tristearin with a melting point of 73 °C (Hagemann, 1988) the melting point of polyethylene glycol was the limiting factor, so that these formulations were extruded at 55 °C.

Solid-state analysis with DSC and XRPD of the extrudates containing tripalmitin in combination with polyethylene glycol of different mean molecular weights did not reveal any interactions or solid-state changes. During dissolution testing the effect of the molecular weight of the polyethylene glycol in the matrix was investigated (figure 10). The dissolution curve for extrudates containing only tripalmitin as matrix material is added for comparison. The acceleration of the dissolution depended on the molecular weight of polyethylene glycol.

Polyethylene glycol 10000 led to the largest increase in dissolution rate, and all the other polyethylene glycols in the matrices had approximately the same influence on the dissolution rate. The particle size of the different polyethylene glycol powders was determined with laser diffraction. All powders exhibit the mean of the 90 % percentile in the range of 300-500 µm. Therefore, phenomena depending on particle size differences could be excluded. Scanning electron microscopy was performed on the samples before and after dissolution to investigate surface transformations. Irrespective of mean molecular weight of polyethylene glycol the different formulations led to the same outer appearance after 24 h of dissolution. As there are no morphologic differences on the surface the results should depend on the swelling and dissolution behaviour of the polyethylene glycol molecules in the matrix. The swelling of polyethylene glycol is a phenomenon which depends on the molecular weight as higher molecular weights tend to swell more but more slowly than lower molecular

weights (Apicella et al, 1993; Maggi et al, 2001). In addition, the larger molecules dissolve more slowly. Based on these assumptions, the similar drug dissolution behaviour for all molecular weights of polyethylene glycol except 10000 is unexpected and requires further investigations. In addition, contact angle measurements were performed to investigate the wetting abilities of the different extrudate surfaces before dissolution. The contact angle increased with increasing mean molecular weight of the polyethylene glycol in the matrix within the range of 100-113°. Therefore, during dissolution testing the extrudates containing polyethylene glycol 10000 provided the best contact surface for the dissolution medium.

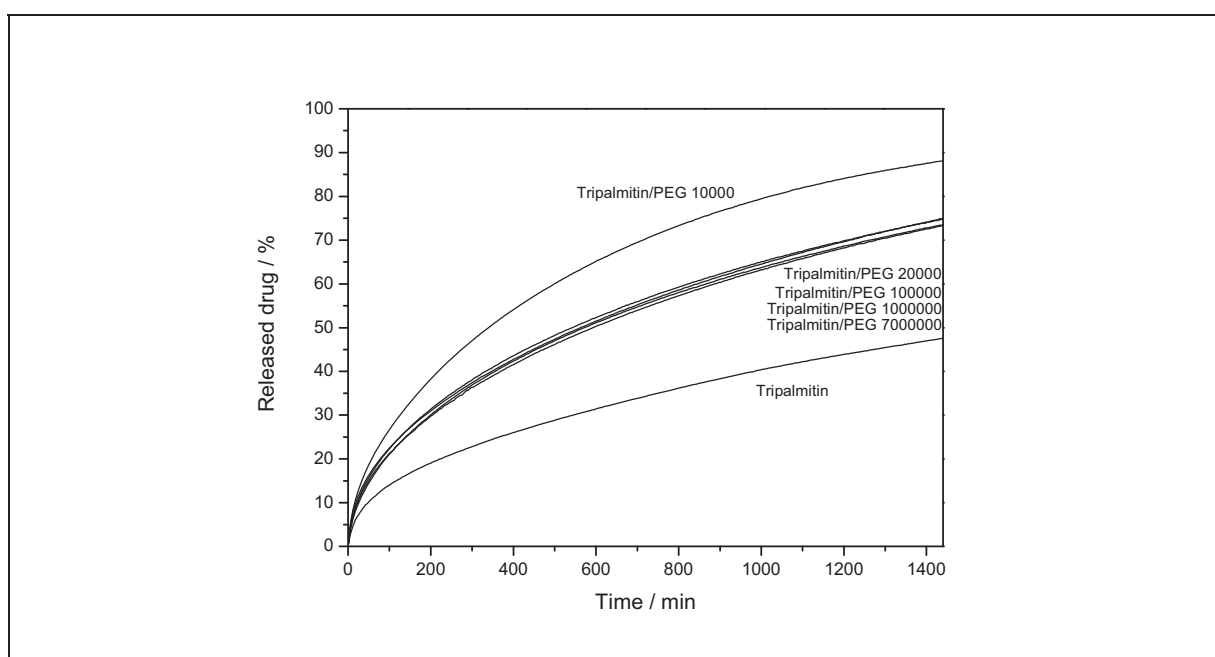


Figure 10: Dissolution curves of extrudates containing different matrix compositions based on tripalmitin and polyethylene glycol (PEG) (9+1 w/w) (mean, $n = 3$, $SD < 3\%$, not shown).

The extrudates consisting of different triglycerides and polyethylene glycol 10000 were also subjected to solid-state analysis. The triglyceride with shorter fatty acids (trilaurin) resulted in stable mixed matrices with no detectable solid-state changes whereas the triglyceride with longer fatty acids (tristearin) exhibited polymorphic transitions. In pure tristearin extrudates, depending on the extrusion temperature, a mixture of α - and β -forms (extrusion temperature 55 °C) or the pure desirable β -form (extrusion temperature 65 °C) of the lipid was present in the extrudate (4.1.2). In this

study the extrusion temperature of the extrudate containing tristearin was limited to 55 °C by the melting point of the polyethylene glycol.

Dissolution testing was performed to investigate the effect of the chain length of the different monoacid triglycerides on the dissolution behaviour. The release rate depended on the chain length of the fatty acids in case of the mixed extrudates. The longer they were the slower is the release (figure 11). Compared to the respective pure triglyceride matrices release of the drug could always be accelerated by the addition of polyethylene glycol.

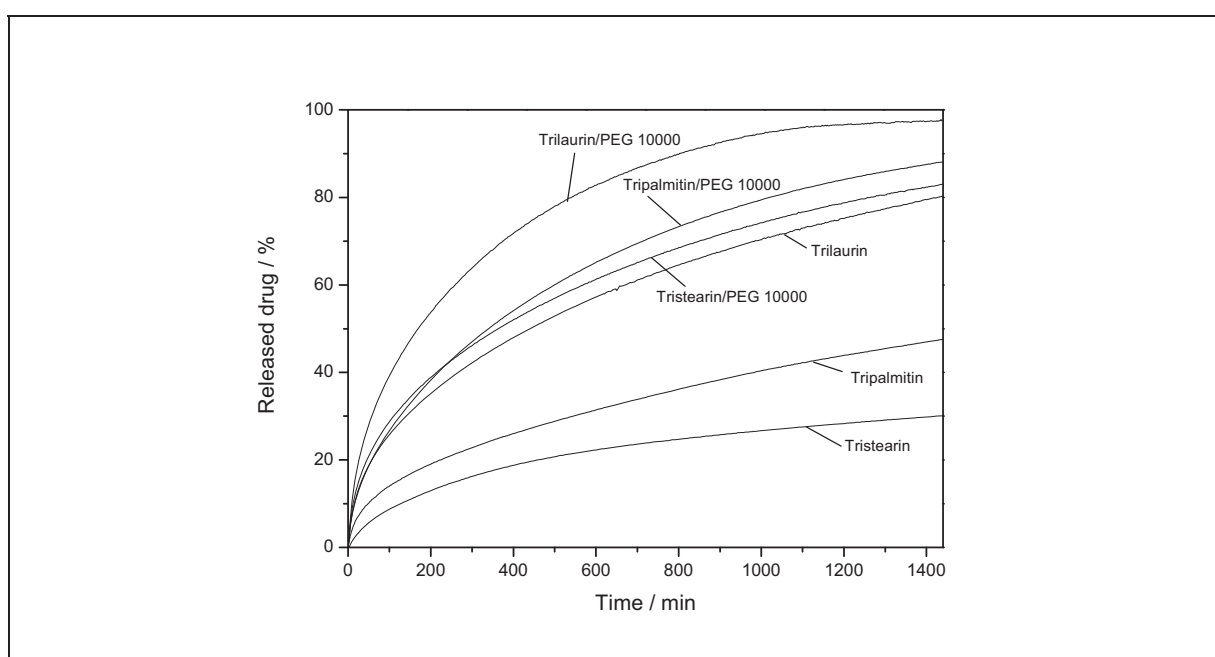


Figure 11: Dissolution profiles of extrudates based on different triglycerides and PEG 10000 (9+1 w/w) (mean, $n = 3$, $SD < 4\%$, not shown).

In conclusion, different combinations of monoacid triglycerides and polyethylene glycols could successfully be extruded below their melting temperatures. Variation of the mean molecular weight of polyethylene glycol showed that each of these polymers was able to accelerate the dissolution rate but a mean molecular weight of 10000 had the largest effect. Therefore, the addition of polyethylene glycol with a mean molecular weight exceeding 10000 provides no additional advantage. The variation of the fatty acid chain length in the lipid component of the extrudate broadened the range of possible processing temperatures, and in the case of trilaurin the extrusion temperature of 40 °C was suitable which is advantageous for temperature sensitive

APIs. The extrusion temperature for tristearin could not be increased to the suitable temperature at which this lipid remains its most stable β -form as polyethylene glycol melted. Therefore, lipid polymorphic transitions occurred which can have a pronounced effect on the dissolution characteristics and are uncontrollable. The results of this study helped to gain a deeper understanding of the variables that may influence drug dissolution behaviour from these oral dosage forms. Such knowledge broadens the potential applications of solid lipid extrudates through the ability to provide tailor-made dissolution profiles.

4.4. Development and establishing of novel dissolution methods with focus on *in situ* monitoring of drug release and solid-state behaviour

4.4.1. Introduction

Dissolution testing is a crucial part of pharmaceutical dosage form investigations and is generally performed by analyzing the concentration of the released drug in a defined volume of flowing dissolution medium. As solid-state properties of the components affect dissolution behaviour to a large and sometimes even unpredictable extent there is a strong need for monitoring and especially visualizing solid-state properties during dissolution testing. Furthermore, as there is evidence that the release of APIs from matrix dosage forms as solid lipid extrudates is largely a function of drug distribution the distribution at the surface and in the core should be mapped and correlated to dissolution profiles. In this section, lipid matrices as tablets and extrudates were investigated with Raman mapping before and after dissolution and with *in situ* Raman spectroscopy during dissolution testing. In addition, coherent anti-Stokes Raman scattering microscopy was used for *in situ* visualization of distribution and release characteristics of the API within the solid lipid extrudates with a self-built dissolution setup.

Corresponding articles: 6, 7 and 8.

4.4.2. Investigating the relationship between drug distribution in solid lipid extrudates and dissolution behaviour using Raman spectroscopy and mapping

In this study, the structural aspects of solid lipid extrudates that influence drug release behaviour were investigated using Raman mapping and spectroscopy. The influence of drug distribution on the solid-state behaviour of the model drug during dissolution was investigated using *in situ* Raman spectroscopy. Furthermore, Raman microscopy was used for chemical mapping of the components at the surface and in the core of the dosage forms before and after dissolution testing (Breitenbach et al, 1999). The drug distribution was then related to the drug dissolution behaviour.

Intrinsic dissolution testing with tablets compressed from a physical powder mixture containing 50% tripalmitin and 50% theophylline anhydrate was performed. In addition, extrudates were compressed to tablets containing 50% tripalmitin and 50% theophylline anhydrate as well as 25% tripalmitin, 25% polyethylene glycol and 50% theophylline anhydrate. The tablets ensured the same surface exposure of each of the different formulations. The dissolution curve of a tablet compressed from extrudates depicts a release which is a magnitude slower than the corresponding curve for the tablet compressed from the physical powder mixture. Since both samples initially had approximately the same surface area exposed to dissolution medium, the different dissolution rates must result from structural differences between the two samples. The release rate of the drug was also dramatically enhanced by the presence of polyethylene glycol.

The distribution of the components in an extrudate containing lipid and API is depicted in figures 12 and 13. For each substance a unique peak was determined which was mapped and the signal intensity was used as a basis for the construction of Raman maps. The graduated colour scales used to construct the maps represent the percentages of the maximum observed peak areas across the sampled area which is marked in the optical microscope images (figures 12e and 13e). The cross section of the extrudate is shown in figure 12. In the majority of regions the signal for only one component is evident suggesting that the particle size in these regions is larger than the sampling volume of the Raman microscope. In a few areas the spectra represent both components, and these regions are probably due to intimately mixed particles smaller

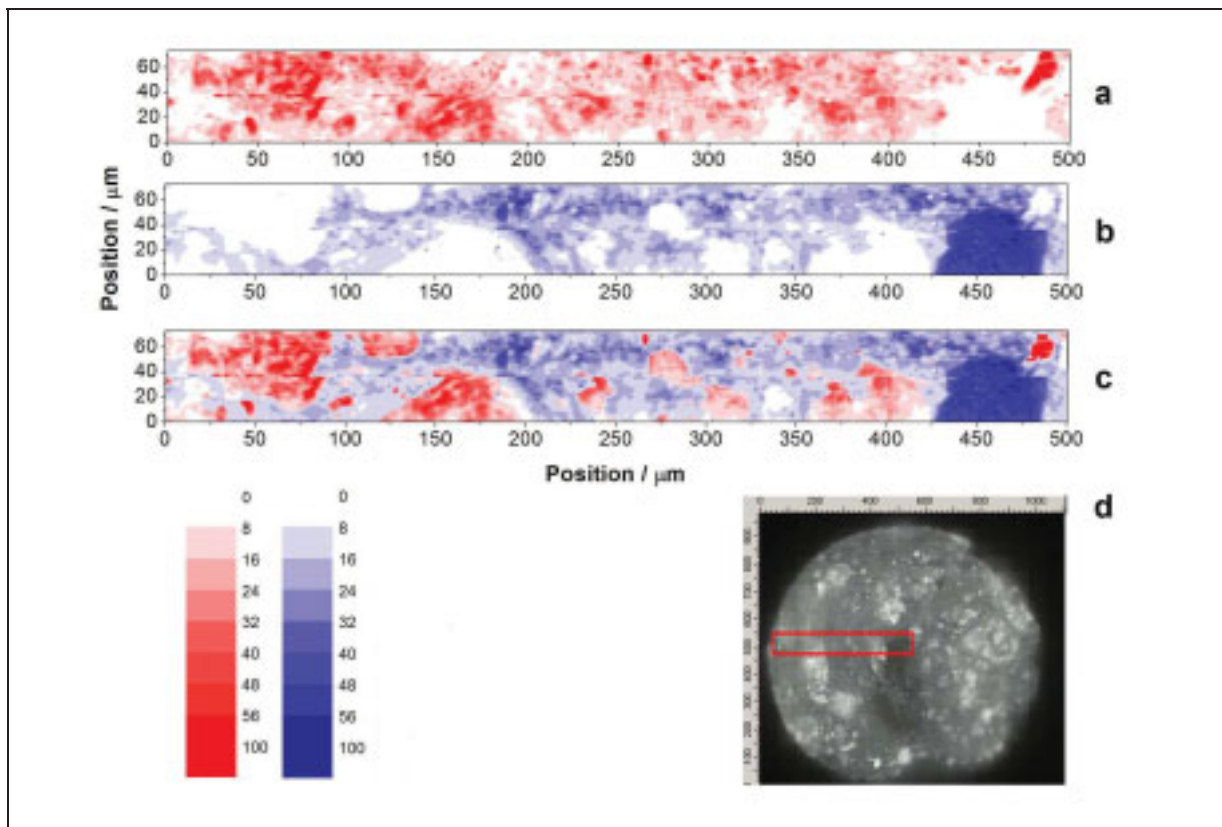


Figure 12: Cross section of an extrudate. Raman maps of (a) theophylline anhydrate, (b) tripalmitin, (c) both components and (e) optical image of the area mapped.

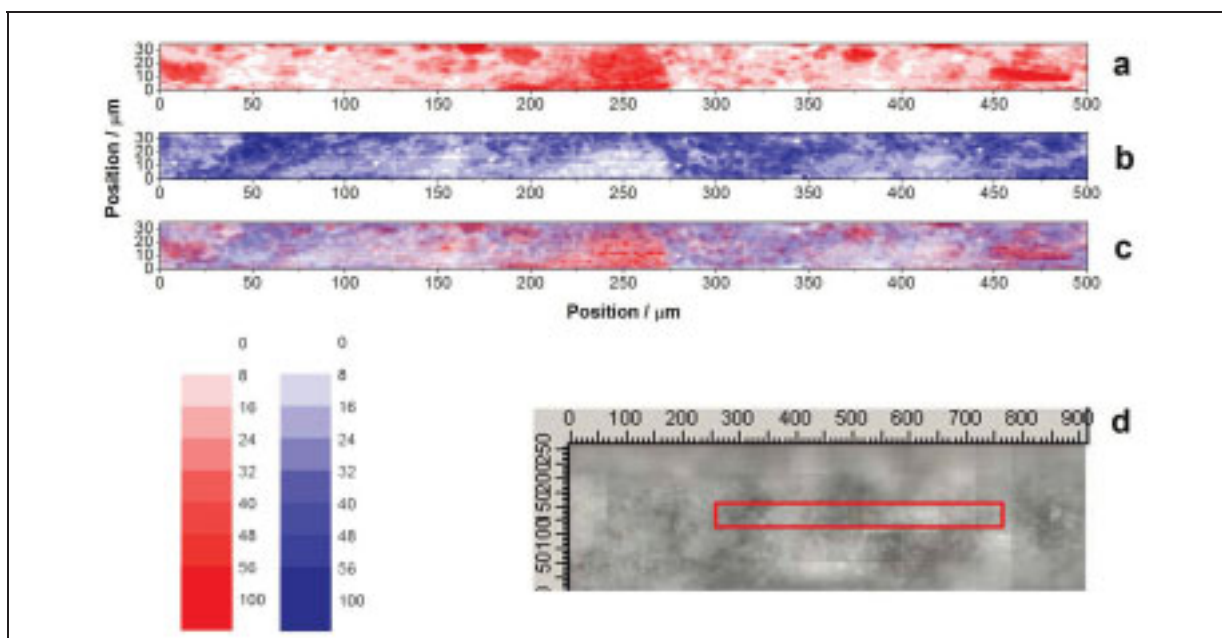


Figure 13: Surface of an extrudate. Raman maps of (a) theophylline anhydrate, (b) tripalmitin, (c) both components and (e) optical image of the area mapped.

than the sampling volume of the microscope or interfaces between larger particles of both components. Within the region sampled there is a wide range in particle size of theophylline, and the lipid appears to be the continuous phase. The distribution at the surface of the same extrudate is depicted in figure 13. In contrast to the image of the cross-section, a larger proportion of the spectra from the surface represent both theophylline and tripalmitin. This shows up as purple in the map representing both components. This suggests a more intimate degree of mixing at the extrudate surface than core, at a level that is below the sampling volume of Raman microscope.

Since the lipid matrix remains intact during drug release in the dissolution media used, the initial drug release rate must be largely determined by the surface area of the drug exposed to dissolution medium. The extrudate exhibited a much slower initial release than the physical mixture. Therefore, there is some evidence that the drug exposed at the surface of the extrudate is disproportionately low. This is supported by previously recorded scanning electron microscope images of solid lipid extrudate samples after dissolution, where the voids created by drug release are less numerous and generally smaller at the surface than the core of the extrudate (Reitz et al, 2008). The Raman mapping is not inconsistent with the presence of a thin lipid layer and a low concentration of drug at the surface of the extrudate. Such a lipid layer is consistent with the 'wall depletion' effect that has been observed during extrusion of slurries with a high concentration of the disperse phase (Barns, 1995; Suwardie et al, 1998). In this case, the lower melting lipid in contact with die walls is known to melt during extrusion due to shear stress and it is expected that it fills the voids created by the solid and irregular-shaped drug particles against the die walls.

In the extrudate containing polyethylene glycol as additional matrix component, all three components were found to be present at the surface. In the core there was no evidence of any component preferentially associating with another in the investigated regions.

Mapping was also performed after certain times of dissolution testing. The results suggest a uniformly receding drug boundary does not exist. Such behaviour can be expected for two reasons. In the matrices, non percolating drug particles may be completely surrounded by lipid, and since the lipid remains intact, these drug particles are never released. Secondly, the tortuosity of the channels in the matrix through which the drug must diffuse during release will differ greatly since the drug is

randomly distributed and particle size varies greatly. Larger areas must be mapped to better investigate this phenomenon. Nevertheless, these studies show the potential for Raman microscopy for spatially resolved analysis of drug loss from matrix dosage forms.

The *in situ* Raman spectra obtained from the tablets during intrinsic dissolution testing to monitor the solid-state form of the model drug are depicted in figure 14.

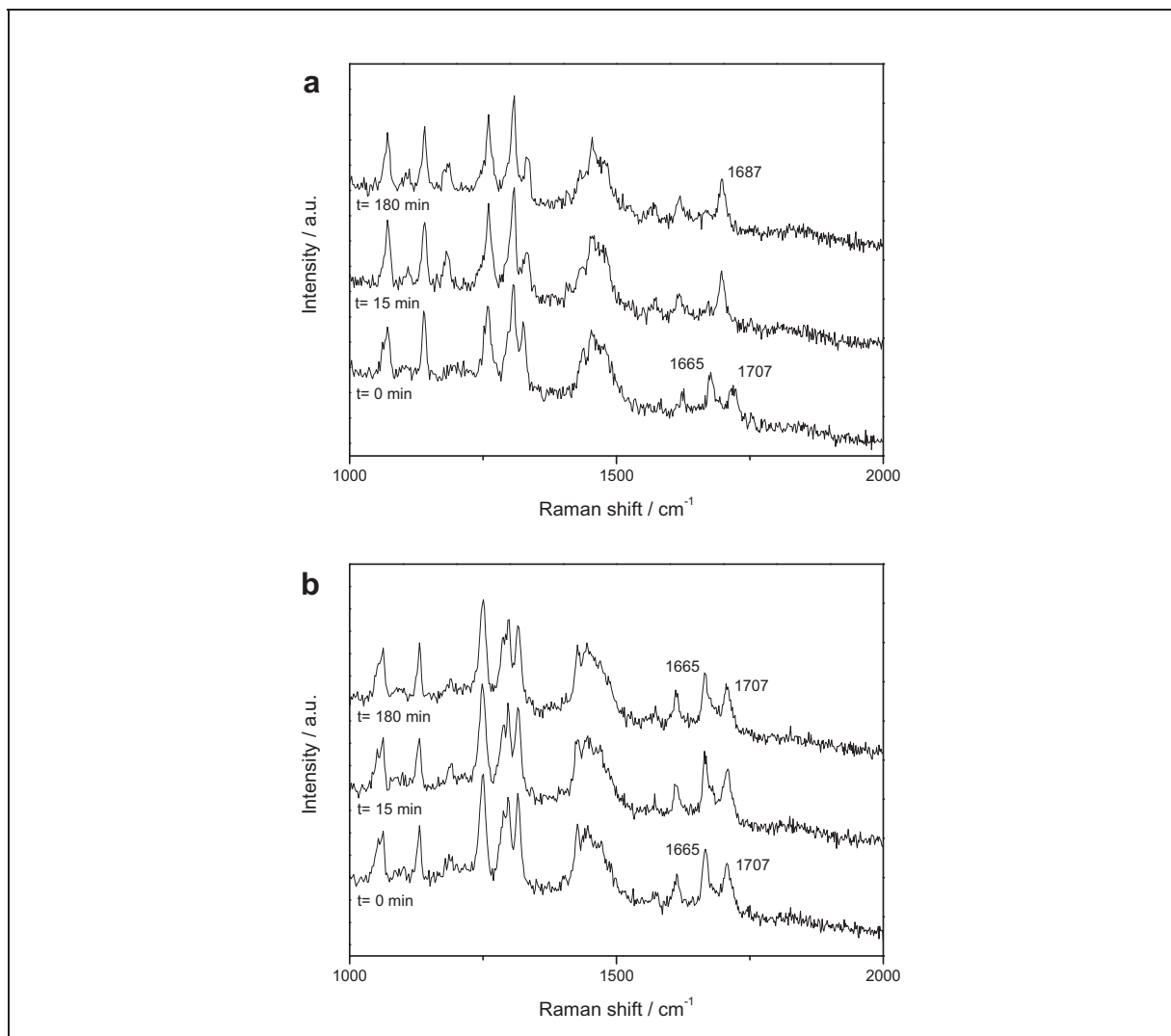


Figure 14: Raman spectra from *in situ* analysis during intrinsic dissolution testing of tablets compressed from physical mixture (a) and extrudate (b) containing tripalmitin and theophylline anhydrate.

The Raman peaks used to differentiate the anhydrate from the monohydrate form were 1687 cm⁻¹ (monohydrate), and 1665 cm⁻¹ and 1707 cm⁻¹ (anhydrate) (Nolasco et al,

2006; Amado et al, 2007). In the sample compressed from a powder mixture of theophylline anhydrate and tripalmitin, transformation of the drug to monohydrate was observed (Figure 14a), and the conversion was virtually complete after 15 minutes. The monohydrate remained after 180 minutes, when the Raman analysis was stopped. In comparison, the spectra of the tablet compressed from extrudates suggested that there was no conversion at any stage up to 180 min (Figure 14b). This shows that the drug distribution was found to have a pronounced effect on the solid-state behaviour of theophylline monohydrate during intrinsic dissolution testing. The results observed using Raman spectroscopy are supported by SEM images taken of each formulation after different times of immersion in water. After immersion for 30 min, needle-like structures are present on the surface of the tablet compressed of the powder mixture. Such structures have previously been associated with theophylline monohydrate formation (Aaltonen et al, 2006). After 180 min of immersion all needles on the surface had dissolved. Such needles were never observed on the tablet compressed from extrudates of the same composition. Since the conversion to the monohydrate is solution mediated, different solid-state behaviour between the compressed extrudate and physical mixture must be related to the drug concentration in solution at the extrudate-dissolution medium interface. The drug exposure at the surface of the tablet prepared from the physical mixture, leads to a higher initial dissolution rate, and a sufficiently supersaturated solution to initiate monohydrate crystallization. As the anhydrate at the surface is depleted, the monohydrate also dissolves. Presumably, because less anhydrate is exposed at the surface of the extrudate sample, the solution does not become sufficiently supersaturated to induce crystallization of the monohydrate form.

While such solid-state analysis reveals that spatial distribution of the drug can have a pronounced effect on solid-state behaviour of the drug, the formation of the less soluble monohydrate appears to have a minor role, compared to the direct effect of spatial distribution of the drug on drug release.

This study showed that Raman mapping can be used for chemically-resolved high-resolution imaging of multi-component sustained release matrices as a means to better understand their drug release behaviour. Although, in this study, Raman microscopy did not have sufficient spatial resolution to determine the exact component distribution at the very surface of the extrudates, it was shown that micrometer scale differences in

surface structure can have a pronounced effect on dissolution behaviour. The technique has also shown potential for chemically resolved imaging of drug distribution after dissolution, and a uniformly receding drug boundary was not observed. Solid-state changes of the drug during dissolution testing were also investigated using *in situ* Raman spectroscopy. This study has emphasised the importance of drug distribution on the release behaviour from sustained release dosage forms, and Raman mapping is potentially a very useful tool to understand drug distribution in such dosage forms and physical changes during drug release.

4.4.3. Chemical imaging of oral solid dosage forms and changes upon dissolution using coherent anti-Stokes Raman scattering microscopy and

Coherent anti-Stokes Raman scattering microscopy to monitor drug dissolution in different oral pharmaceutical tablets

In situ chemically selective imaging of dosage forms during dissolution testing is a challenging task as it involves several requirements. These include an absence of both analysis-related destruction and interference of the dissolution medium flow. Furthermore, the data acquisition time has to be sufficiently fast and data have to be obtained in the presence of the dissolution medium. Each of the imaging methods that have been used so far for chemically selective imaging of dosage forms, including Raman microscopy, exhibit shortcomings in this respect.

Coherent anti-Stokes Raman scattering microscopy (CARS) is able to fulfil all the stated requirements. This method is based on two laser beams of which one is tunable in wavelength. These two beams are collinearly overlapped and focussed into the sample. If the wavelength difference between the two input laser beams coincides with a Raman active vibrational mode an anti-Stokes wavelength (blue shifted compared to the input wavelengths) is created. When there are differences in the vibrational spectra of the molecules in the sample, chemically selective imaging is possible with this technique at sub-micron resolution in three dimensions (Cheng and Xie, 2004; Jurna et al, 2006). CARS has been used for imaging polymer films (Kee and Cicerone, 2004) as well as living cells (Nan et al, 2003) and tissues (Evans et al, 2006). Additionally, the technique has recently been used to monitor drug distribution and release from stent coating material (Kang et al, 2006 and 2007).

Suitable vibrational bands for selective analysis were found by analyzing the Raman spectra of the respective substances as Raman and CARS spectra are not identical but uniquely related to each other (Jurna et al, 2008). The distribution of drug and lipid were rapidly visualised with a spatial resolution of 1.5 μm . Figure 15 depicts false colour images of the surfaces of different lipid-based tablets. The drug is encoded in green (signal at 3109 cm^{-1}) whereas the lipid is encoded in red (signal at 2880 cm^{-1}) (Nolasco et al, 2006; Bresson et al, 2005). The three different tablets were immersed into 500 mL of purified water and investigated with CARS microscopy after 30 min and after 180 min. Figure 15a-c depicts a tablet compressed of a powder mixture containing 50% theophylline monohydrate and 50% tripalmitin powder (w/w).

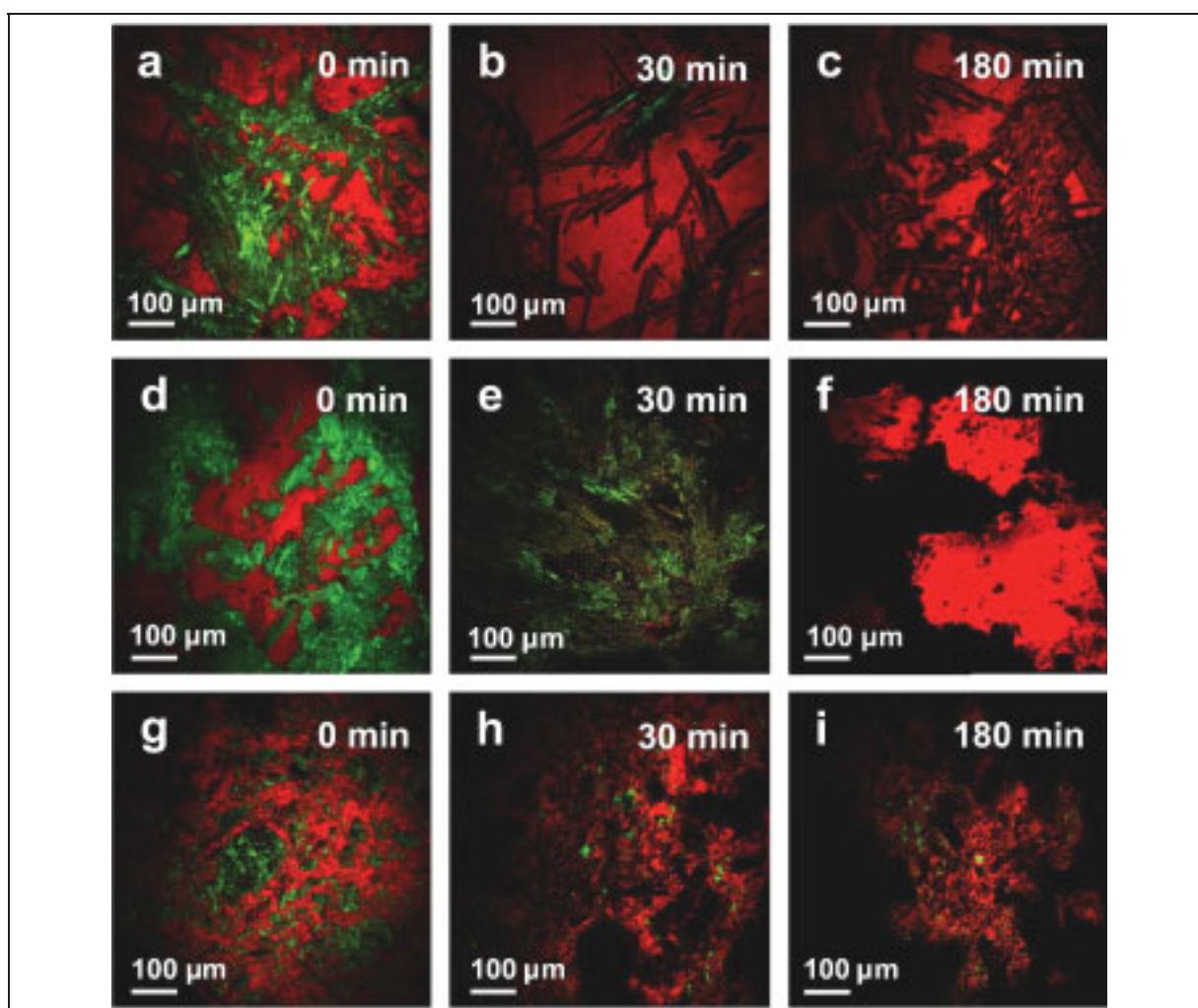


Figure 15: Solid dosage forms consisting of lipid (red) and drug (green) after different immersion times in dissolution medium. (a-c) tablet of tripalmitin/theophylline monohydrate, (d-f) tablet of tripalmitin/theophylline anhydrate and (g-i) tablet of extrudates of tripalmitin/theophylline anhydrate.

The drug was heterogeneously distributed and a gradual loss of the green colour over time represents the release of the drug from the matrix. After release of the drug dark areas represent the pores in the lipid matrix where drug particles were located before. In comparison, several phenomena could be observed on a tablet compressed of the physical mixture of 50% theophylline anhydrate and 50% tripalmitin (w/w) (figure 15d-f). Before immersion the anisometric drug particles were homogeneously distributed within the lipid matrix. After 30 min of immersion the complete surface of the tablet was covered with fine green needles representing theophylline monohydrate which had recrystallized on the tablet surface. This can be attributed to a solution-mediated transformation as the monohydrate form, being less soluble, is able to recrystallize from a supersaturated solution which has been formed from the released anhydrate particles (Ando et al, 1992; De Smidt et al, 1986). After 180 min the drug is completely dissolved leaving the empty lipid matrix. To investigate the influence of the extrusion process on the release profile a tablet was compressed of the extrudates (figures 15g-i). For this tablet release was observed but no monohydrate formation could be detected. These results correlate with the results obtained by *in situ* Raman spectroscopy (4.4.2). In addition, the pure extrudates consisting of 50% tripalmitin and 50% theophylline (w/w) were also subjected to the same dissolution study. There was also no evidence of needle formation due to the monohydrate on the extrudate surface. A depth scan was performed in the pores of the extrudates (depth 50 μm). Very few monohydrate needles can be found inside the pores.

In a further step, the transformation from theophylline anhydrate to theophylline monohydrate should be monitored in real time. Therefore, tablets consisting of powder mixtures of tripalmitin and theophylline anhydrate were placed directly on the microscope stage in a small container which was mounted on a thin glass slide. The container was filled with purified water so that a thin layer of water was located between the sample and the microscope objective. Figure 16 depicts several frames of the recorded images which realized the real time visualization of the transformation from theophylline anhydrate to monohydrate for the first time.

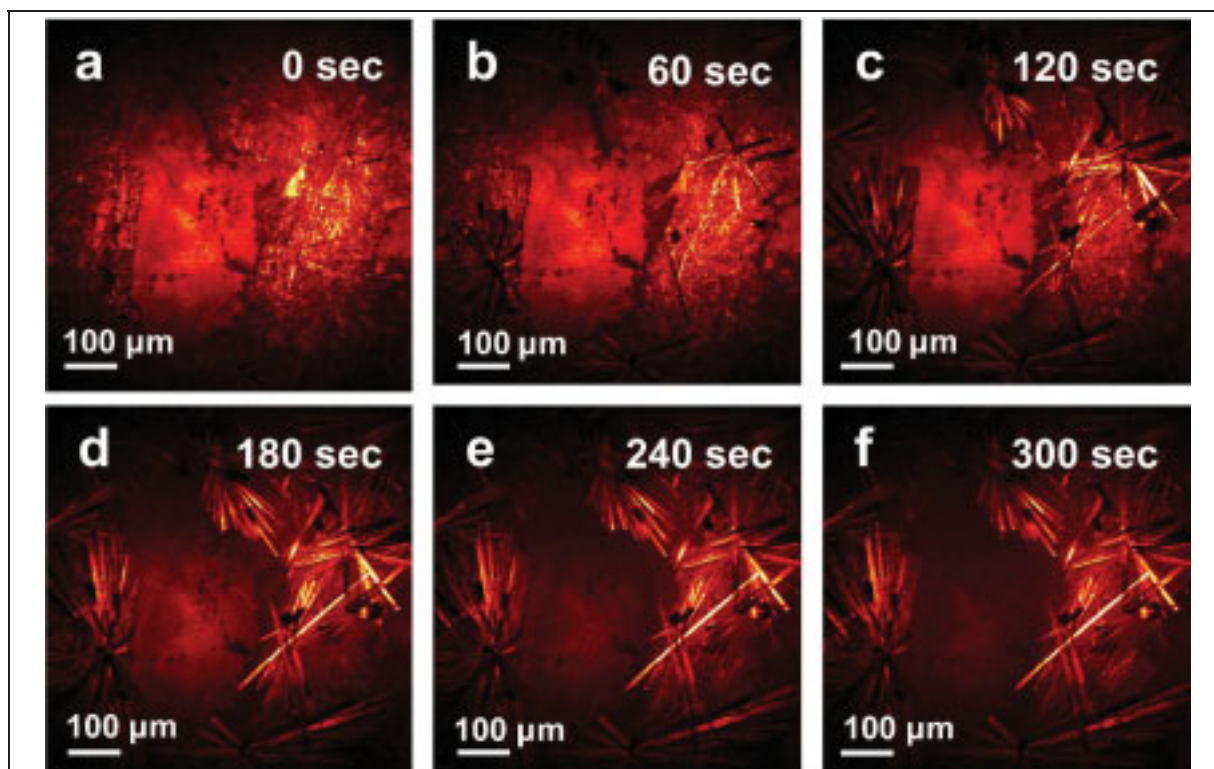


Figure 16: In-line visualization of theophylline monohydrate crystal growth on the surface of a tablet in water consisting originally of tripalmitin/theophylline anhydrate.

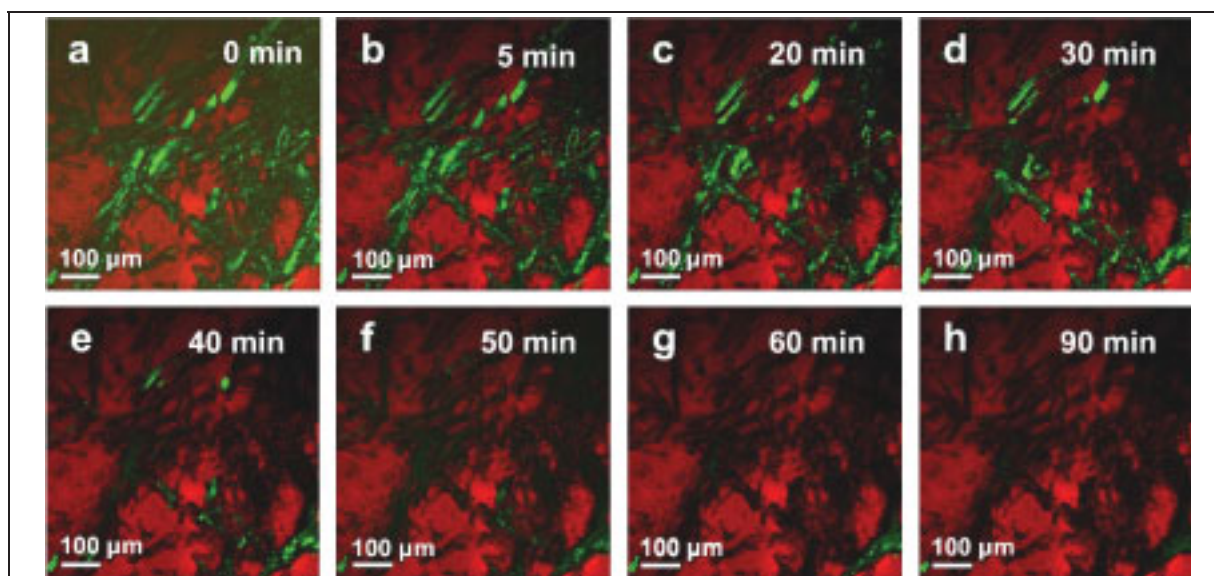


Figure 17: In-line visualization of drug release from a tablet of tripalmitin (red) and theophylline monohydrate (green) during dissolution testing.

Based on these results, the setup was modified to provide a dissolution setup for oral dosage forms with pharmaceutically acceptable dissolution medium flow (Peltonen et

al, 2003). A self-built dissolution flow-through cell allowed the dosage form (either tablet or extrudate) to be fixed in a constant fluid-flow bed which was covered by a microscope cover glass facing the microscope objective. The dissolution medium was continuously pumped through the cell surrounding the sample. A good CARS signal intensity could be obtained from the tablet through the flowing dissolution medium. Several frames are depicted in figure 17. The tablet consisting of tripalmitin and theophylline monohydrate powder proved that release of the drug could be visualized in real time.

These studies demonstrated that, with CARS microscopy, it is possible to achieve temporally and spatially resolved visualization of the distribution of dosage form components in matrix systems during dissolution. In addition, solid-state changes could be visualized. The combination of CARS microscopy with a suitable flow-through cell setup is a means to gaining a deeper understanding of the physicochemical behaviour of oral dosage forms during dissolution and is likely to impact future applications of different kinds of dosage forms.

5. Summary and conclusions

Solid lipid extrudates were produced by the extrusion of lipid powders and drug below their melting points to form coherent matrices in which the drug is embedded. Systematic investigations with a combination of novel and established characterization methods led to a significantly increased process understanding and improved dosage form quality.

The combination of extrusion temperature and friction was identified as a key factor for the polymorphic behaviour of lipids during extrusion. As polymorphic transitions had a strong influence on the dissolution behaviour due to crystallization of the stable polymorphic form on the extrudate surface it is of high importance to avoid those changes. To obtain extrudates containing purely the stable β -form of the lipid the process temperature has to be adjusted above the melting point of any unstable polymorphic form to ensure that the thin lipid fraction on the extrudate surface which is molten due to friction directly recrystallizes in the most stable form after processing.

The dissolution behaviour from lipid-based matrices depended on the chain length of the fatty acids and the degree of esterification of the individual lipid. The longer the chains were and the higher the degree of esterification was the slower was the dissolution rate. In addition, interactions between different glycerides led to unpredictable solid-state changes as a partial glyceride was able to stabilize the metastable α -form of the triglyceride which affected the surface structure of the extrudates as the contact angle was increased due to recrystallization of the stable β -form on the surface. This 'blooming effect' significantly decreased the dissolution rate. The recrystallization behaviour of resolidified lipid melts as model systems showed the great influence of storage temperature on the rate of recrystallization.

Tailor-made dissolution profiles were obtained from extrudates consisting of various ratios of a triglyceride and the hydrophilic polymer polyethylene glycol. There was no evidence of solid-state changes in the matrix components and drug. Polyethylene glycol powders with different mean molecular weights were tested in combination with a triglyceride and a mean molecular weight of 10000 resulted in the fastest dissolution. Varying the chain lengths of the fatty acids in the glyceride in combination

with polyethylene glycol allowed the extrusion temperature to be varied, which is beneficial for temperature sensitive drugs.

During storage testing in accelerated conditions all processed formulations remained stable protecting the humidity-sensitive model drug against hydration.

The distribution of drug and matrix material in the core and at the surface of the extrudates was mapped with Raman microscopy. The results emphasized the importance of drug distribution on the release behaviour of matrix dosage forms as the spatial distribution due to the manufacturing technique had a higher impact on dissolution than solid-state changes of the drug. Raman mapping of extrudate cross sections after certain times of dissolution suggested that a uniformly receding drug boundary does not exist.

Intrinsic dissolution testing comprising simultaneous measurement of the drug concentration in the dissolution medium (UV-VIS spectrometry) and the solid-state form of the sample (*in situ* Raman spectroscopy) offered deeper insight into the release characteristics from lipid-based matrices. Compacts were prepared consisting of either powder mixtures or the extrudates. The dissolution of theophylline anhydrate is usually accompanied by a relatively fast transformation to the monohydrate leading to a slower dissolution rate. This transformation was observed for compacts produced of powder mixtures but not for those produced from extrudates suggesting that the extruded lipid matrix inhibits monohydrate formation during dissolution due to surface differences.

For the first time, *in situ* high-resolution visualization of solid-state characteristics and drug release of a solid dosage form was realized during dissolution testing with coherent anti-Stokes Raman scattering (CARS) microscopy and is likely to impact future applications for different kinds of solid dosage forms.

6. Zusammenfassung der Arbeit

Im Rahmen dieser Arbeit wurden Festfettextrudate durch die Extrusion von Lipidpulvern und Arzneistoff unterhalb ihrer Schmelzpunkte zu kohärenten Matrizes mit eingebettetem Arzneistoff verarbeitet. Systematische Untersuchungen mit einer Kombination aus neuen und etablierten Charakterisierungsmethoden führten zu einem signifikant gesteigerten Prozessverständnis und verbesserter Produktqualität.

Die Kombination von Friktion und Extrusionstemperatur konnte als Schlüsselfaktor für das polymorphe Verhalten der Lipide nach der Extrusion identifiziert werden. Da polymorphe Transformationen einen starken Einfluss auf das Freisetzungsverhalten hatten, welcher durch die Kristallisation der stabilen polymorphen Form auf der Oberfläche der Extrudate bedingt war, ist es von großer Wichtigkeit, diese Veränderungen zu vermeiden. Um Extrudate zu erhalten, die nur die stabile β -Form des Lipids enthalten, sollte die Prozesstemperatur oberhalb der Schmelzpunkte der unstabilen polymorphen Formen eingestellt werden. So wird gewährleistet, dass die dünne Lipidfraktion auf der Extrudat-Oberfläche, welche durch Friktion schmilzt, nach der Herstellung direkt in der stabilsten Form rekristallisiert.

Das Freisetzungsverhalten aus Lipid-basierten Matrizes hängt von der Kettenlänge der Fettsäuren und dem Grad der Veresterung des individuellen Lipides ab. Je länger die Ketten und je höher der Veresterungsgrad war, desto langsamer war die Freisetzungsrates. Interaktionen zwischen verschiedenen Glyceriden führten zu unvorhersehbaren Solid-State Veränderungen. Ein Partialglycerid war in der Lage, die metastabile α -Form eines Triglycerides zu stabilisieren, was die Oberflächenstruktur der Extrudate beeinflusste. Der Kontaktwinkel wurde durch die Rekristallisation der stabilen β -Form auf der Oberfläche vergrößert. Dieser 'Ausblüh-Effekt' verringerte die Freisetzungsrates signifikant. Das Rekristallisationsverhalten von wieder erstarrten Lipid-Schmelzen als Modellsysteme zeigte den großen Einfluss der Lagerungstemperatur auf die Rekristallisierungsrate.

Maßgeschneiderte Freisetzungsprofile konnten mit Extrudaten erzielt werden, welche aus verschiedenen Anteilen von Triglycerid und dem hydrophilen Polymer Polyethylenglykol bestanden. Es gab keine Hinweise auf Solid-State Veränderungen der Matrixbestandteile oder des Arzneistoffes. Polyethylenglykol-Pulver mit

7. References

- Aaltonen J, Heinänen P, Peltonen L, Kortejärvi H, Tanninen VP, Christiansen L, Hirvonen J, Yliruusi J and Rantanen J. In situ measurement of solvent-mediated phase transformations during dissolution testing. *J Pharm Sci* 95 (2006) 2730-2737.
- Amado MM, Nolasco AM and Ribeiro-Claro PJA. Computationally-assisted approach to the vibrational spectra of molecular crystals: study of hydrogen-bonding and pseudo-polymorphism. *Chem Phys Chem* 7 (2006) 2150-2161.
- Amidon GL, Lennernäs H, Shah VP and Crison JR. A theoretical basis for a biopharmaceutical drug classification – the correlation of in-vitro drug product dissolution and in-vivo bioavailability. *Pharm Res* 12 (1995) 413-420.
- Ando H, Ishii M and Kayano M. Effect of moisture on crystallization of theophylline in tablets. *Drug Dev Ind Pharm* 18 (1992) 453-467.
- Apicella A, Capello B, Del Nobile MA, La Rotonda MI, Mensitieri G and Nicolais L. Poly(ethylene oxide) (PEO) and different molecular weight PEO blends monolithic devices for drug release. *Biomaterials* 14 (1993) 83-90.
- Barnes HA. A review of the slip (wall depletion) of polymer solutions, emulsions and particle suspensions in viscometers: its cause, character and cure. *J Non-Newtonian Fluid Mech* 56 (1995) 221-251.
- Barthelemy P, Laforet JP, Farah N and Joachim J. Compritol (R) 888 ATO: an innovative hot-melt coating agent for prolonged-release drug formulations. *Eur J Pharm Biopharm* 47 (1999) 87-90.
- Belu AM, Davies MC, Newton JM and Patel N. TOF-SIMS characterization and imaging of controlled-release drug delivery systems. *Anal Chem* 72 (2000) 5625-5638.
- Bowtle WJ. Materials, process, and manufacturing considerations for lipid-based hard-capsule formats. In: *Oral Lipid-Based Formulations - Enhancing the Bioavailability of Poorly Water-Soluble Drugs*. Hauss DJ. Ed. Informa Healthcare, New York (2007) 79-106.
- Breitenbach J. Melt extrusion: from process to drug delivery technology. *Eur J Pharm Biopharm*. 54 (2002) 107-117.

- Breitenbach J, Schrof W and Neumann J. Confocal Raman spectroscopy: analytical approach to solid dispersions and mapping of drugs. *Pharm Res* 16 (1999) 1109-1113.
- Breitkreutz J, El Saleh F, Kiera C, Kleinebudde P and Wiedey W. Pediatric drug formulations of sodium benzoate: II. Coated granules with a lipophilic binder. *Eur J Pharm Biopharm* 56 (2003) 255-260.
- Bresson S, El Marssi M and Khelifa B. Raman spectroscopy investigation of various saturated monoacid triglycerides. *Chem Phys Lipids* 134 (2005) 119-129.
- Brittain HG, Bogdanowich SJ, Bugay DE, DeVincendis J, Lewen G and Newman AW. Physical characterization for pharmaceutical solids. *Pharm Res.* 8 (1991) 963-73.
- Brittain HG and Grant DJW. Effect of polymorphism and solid-state solvation on solubility and dissolution rate. In: *Polymorphism in pharmaceutical solids*. Brittain HG. Ed. Marcel Dekker, New York (1999) 279-330.
- Bugay DE. Characterization of the solid state: spectroscopic techniques. *Adv Drug Deliv Rev* 48 (2001) 43-65.
- Bunjes H, Westensen K and Koch MHJ. Crystallization tendency and polymorphic transitions in triglyceride nanoparticles. *Int J Pharm* 129 (1996) 159-173.
- Cavallari C, Rodriguez L, Albertini B, Passerini N, Rosetti F and Fini A. Thermal and fractal analysis of diclofenac/Gelucire 50/13 microparticles obtained by ultrasound-assisted atomization. *J Pharm Sci* 94 (2005) 1124-1134.
- Chauhan B, Shimpi S and Paradkar A. Preparation and characterization of etoricoxib solid dispersions using lipid carriers by spray drying technique. *AAPS Pharm Sci Tech* 6 (2005) E405-412.
- Chen ML. Lipid excipients and delivery systems for pharmaceutical development: A regulatory perspective. *Adv Drug Del Rev* 60 (2008) 768-777.
- Chen W, Zhang X, Shan B and You X. Methylxanthines. I. Anhydrous Theophylline. *Acta Cryst C* 53 (1997) 777-779.

- Cheng JX and Xie XS. Coherent anti-Stokes Raman scattering microscopy: instrumentation, theory, and applications. *J Phys Chem B* 108 (2004) 827-840.
- Choy YW, Khan N and Yuen KH. Significance of lipid matrix aging on in vitro release and in vitro bioavailability. *Int J Pharm* 299 (2005) 55-64.
- Cleek RL, Ting KC, Eskin SG and Mikos AG. Microparticles of poly (DL-lactic-co-glycolic-acid)/poly(ethylene glycol) blends for controlled drug delivery. *J Control Release* 48 (1997) 259-268.
- Cole ET. Liquid-filled hard-gelatin capsules. *Pharm Technol* 13 (1989) 124-140.
- Costa P and Lobo JMS. Modeling and comparison of dissolution profiles. *Eur J Pharm Sci* 13 (2001) 123-133.
- Coutts-Lendon CA, Wright NA, Mieso EV and Koenig JL. The use of FT-IR imaging as an analytical tool for the characterization of drug delivery systems. *J Control Release* 93 (2003) 223-248.
- Craig DQM and Newton JM. Characterisation of polyethylene glycol solid dispersions using differential scanning calorimetry and solution calorimetry. *Int J Pharm* 76 (1991) 17-24.
- Crowley MM, Zhang F, Koleng JJ and McGinity JW. Stability of polyethylene oxide in matrix tablets prepared by hot-melt extrusion. *Biomaterials* 23 (2002) 4241-4248.
- Debnath S, Predecki P and Suryanarayanan R. Use of glancing angle X-Ray powder diffractometry to depth-profile phase transformations during dissolution of indomethacin and theophylline tablets. *Pharm Res* 21 (2004) 149-159.
- De Smidt JH, Fokkens JG, Grjseels H and Crommelin JA. Dissolution of theophylline monohydrate and anhydrous theophylline in buffer solutions. *J Pharm Sci* 75 (1986) 497-501.
- Erni W, Zeller M and Piot N. Die Eignung von Fettpellets als Zwischenform für perorale Depotarzneiformen. *Acta Pharm Technol* 26 (1980) 165-171.

- Evans CL, Potma EO, Puoris'haag M, Côté D, Lin CP and Xie XS. Chemical imaging of tissue in vivo with video-rate coherent anti-Stokes Raman scattering microscopy. *Proc Natl Acad Sci USA* 102 (2005) 16807-16812.
- Evrard B, Amighi K, Beten D, Delattre L and Moës AJ. Influence of melting and rheological properties of fatty binders on the melt granulation process in a high-shear mixer. *Drug Dev Ind Pharm* 25 (1999) 1177-1184.
- Fang W, Mayama H and Tsujii K. Spontaneous formation of fractal structures on triglyceride surfaces with reference to their water-repellent properties. *J Phys Chem B* 111 (2007) 564-571.
- Garti N. Effects of surfactants on crystallization and polymorphic transformation of fats and fatty acids. In: *Crystallization and polymorphism of fats and fatty acids*. Garti N and Sato K. Eds. Marcel Dekker, New York (1988) 267-303.
- Garti N, Schlichter S and Sarig S. DSC studies concerning polymorphism of saturated monoacid triglycerides in the presence of food emulsifiers. *Fat Sci Technol* 90 (1988) 295-299.
- Gowen AA, O'Donnell CP, Cullen PJ and Bell SEJ. Recent applications of chemical imaging to pharmaceutical process monitoring and quality control. *Eur J Pharm Biopharm* 69 (2008) 10-22.
- Hagemann JW. Thermal behaviour and polymorphism of acylglycerides. In: *Crystallization and polymorphism of fats and fatty acids*. Garti N and Sato K. Eds. Marcel Dekker, New York (1988) 9-95.
- Hamdani J, Moes, AJ and Amighi K. Development and evaluation of prolonged release pellets obtained by the melt pelletization process. *Int J Pharm* 245 (2002) 167-177.
- Hamdani J, Moes AJ and Amighi K. Physical and thermal characterisation of Precirol[®] and Compritol[®] as lipophilic glycerides used for the preparation of controlled-release matrix pellets. *Int J Pharm* 260 (2003) 47-57.
- Herrmann S, Mohl S, Siepmann F, Siepmann J and Winter G. New insights into the role of polyethylene glycol acting as protein release modifier in lipidic implants. *Pharm Res* 8 (2007a) 1527-1537.

- Herrmann S, Winter G, Mohl S, Siepmann F and Siepmann J. Mechanisms controlling protein release from lipidic implants: Effect of PEG addition. *J Contr Release* 118 (2007b) 161-168.
- Hongisto V, Lehto, VP and Laine E. X-Ray diffraction and microcalorimetry study of the $\alpha \rightarrow \beta$ transformation of tripalmitin. *Thermochim Acta* 276 (1996) 229-242.
- Humberstone AJ and Charman WN. Lipid based vehicles for the oral delivery of poorly water soluble drugs. *Adv Drug Deliv Rev* 25 (1997) 103-128.
- Jannin V, Musakhanian J and Marchaud D. Approaches for the development of solid and semi-solid lipid-based formulations. *Adv Drug Del Rev* 60 (2008) 734-746.
- Jurna M, Korterik JP, Offerhaus HL and Otto C. Noncritical phase-matched lithium triborate optical parametric oscillator for high resolution coherent anti-Stokes Raman scattering spectroscopy and microscopy. *Appl Phys Lett* 89 (2006) 2511-2516.
- Jurna M, Korterik JP, Otto C, Herek JL and Offerhaus HL. Background free CARS imaging by phase sensitive heterodyne CARS. *Opt Express* 16 (2008) 15863-15869.
- Kang E, Robinson J, Park K and Cheng JX. Paclitaxel distribution in poly(ethylene glycol)/poly(lactide-co-glycolic acid) blends and its release visualized by coherent anti-Stokes Raman scattering microscopy. *J Control Release* 122 (2007) 261-268.
- Kang E, Wang H, Kwon IK, Robinson J, Park K and Cheng JX. In situ visualization of paclitaxel distribution and release by coherent anti-stokes Raman scattering microscopy. *Anal Chem* 78 (2006) 8036-8043.
- Kee TW and Cicerone MT. Simple approach to one-laser, broadband coherent anti-Stokes Raman scattering microscopy. *Opt Lett* 29 (2004) 2701-2703.
- Kellens M, Meeussen W, Gehrke R and Reynaers H. Synchrotron radiation investigations of the polymorphic transitions of saturated monoacid triglycerides. Part 1: Tripalmitin and tristearin. *Chem Phys Lipids* 58 (1991) 131-144.
- Kerns EH. High throughput physicochemical profiling for drug discovery. *J Pharm Sci* 90 (2001) 1838-1858.

- Khan N and Craig DQM. Role of blooming in determining the storage stability of lipid-based dosage forms. *J Pharm Sci* 93 (2004) 2962-2971.
- Kleinebudde, P. Pharmazeutische Pellets durch Extrudieren/Sphäronisieren. Habilitationsschrift (1997) Christian-Albrechts-University Kiel.
- Kobayashi M. Vibrational spectroscopic aspects of polymorphism and phase transition of fats and fatty acids. In: *Crystallization and polymorphism of fats and fatty acids*. Garti N and Sato K. Eds. Marcel Dekker, New York (1988) 139-187.
- Krause J, Thommes M and Breitzkreutz J. Immediate release pellets with lipid binders obtained by solvent-free cold extrusion. *Eur J Pharm Biopharm* 71 (2009) 138-144.
- Larsson K. Classification of glyceride crystal forms. *Acta Chem Scand* 20 (1996) 2255-2260.
- Li FQ, Hu JH, Deng JX, Su H, Xu S and Liu, JY. In vitro controlled release of sodium ferulate from Compritol 888 ATO-based matrix tablets. *Int J Pharm* 324 (2006) 152-157.
- Ling J, Weitman SD, Miller MA, Moore RV and Bovic AC. Direct Raman imaging techniques for study of the subcellular distribution of a drug. *Appl Opt* 41 (2002) 6006-6017.
- Liu J, Zhang F, and McGinity JW. Properties of lipophilic matrix tablets containing phenylpropanolamine hydrochloride prepared by hot-melt extrusion. *Eur J Pharm Biopharm* 52 (2001) 181-190.
- Löbenberg R and Amidon GL. Modern bioavailability, bioequivalence and biopharmaceutics classification system. New scientific approaches to international regulatory standards. *Eur J Pharm Biopharm* 50 (2000) 3-12.
- MacNaughtan W, Farhat IA, Himawan C, Starov VM and Stapley AGF. A differential scanning calorimetry study of the crystallization kinetics of tristearin-tripalmitin mixtures. *J Am Oil Chem Soc* 83 (2006) 1-9.
- Maggi L, Segale L, Torre ML, Ochoa Machiste E and Conte U. Dissolution behaviour of hydrophilic matrix tablets containing different polyethylene oxides (PEOs) for the

- controlled release of a water-soluble drug. Dimensional study. *Biomaterials* 23 (2001) 1113-1119.
- Mahoney CM, Roberson SV and Gillen G. Depth profiling of 4-acetaminophenol-doped polylactic acid) films using cluster secondary ion mass spectrometry. *Anal Chem* 76 (2004) 3199-3207.
- Mehnert W and Mäder K. Solid lipid nanoparticles – Production, characterization and applications. *Adv Drug Deliv Rev* 47 (2001) 165-196.
- Michalk A, Kanikanti VR, Hamann HJ and Kleinebudde P. Controlled release of active as a consequence of the die diameter in solid lipid extrusion *J Control Release* 132 (2008) 35-41.
- Nan X, Cheng JX and Xie XS. Vibrational imaging of lipid droplets in live fibroblast cells using coherent anti-Stokes Raman microscopy. *J Lipid Res* 40 (2003) 2202-2208.
- Nolasco MM, Amado AM and Ribeiro-Claro PJA. Computationally-assisted approach to the vibrational spectra of molecular crystals: study of hydrogen-bonding and pseudo-polymorphism. *Chem Phys Chem* 7 (2006) 2150-2161.
- Ozdemir AN and Agabeyoglu IT. Studies on sustained-release. 11. Lipid granules of sulfamethizole. *Drug Dev Ind Pharm* 16 (1990) 1805-1814.
- Pajander J, Soikkeli AM, Korhonen A, Forbes R, and Ketolainen J. Drug release phenomena within a hydrophobic starch acetate matrix: FTIR mapping of tablets after in vitro dissolution testing. *J Pharm Sci* 97 (2008) 3367-3378.
- Pallagi E, Vass K, Pintye-Hódi K, Kása Jr P, Falkay G, Eros I, Szabó-Révész P. Iron(II) sulphate release from drop-formed lipophilic matrices developed by special hot-melt technology. *Eur J Pharm Biopharm* 57 (2004) 287-294.
- Peltonen L, Liljeroth P, Heikkilä T, Kontturi K and Hirvonen J. Dissolution testing of acetylsalicylic acid by a channel flow method-correlation to USP basket and intrinsic dissolution methods. *Eur J Pharm Sci* 19 (2003) 395-401.
- Phadnis, NV and Suryanarayanan R. Polymorphism in anhydrous theophylline – implications on the dissolution rate of theophylline tablets. *J Pharm Sci* 86 (1997) 1256-1263.

- Pinto JF and Silverio NP. Assessment of the extrudability of three different mixtures of saturated polyglycolysed glycerides by determination of the 'specific work of extrusion' and by capillary rheometry. *Pharm Dev Tech* 6 (2001) 117-128.
- Pouton CW and Porter CJH. Formulation of lipid-based delivery systems for oral administration. *Adv Drug Del Rev* 60 (2008) 625-637.
- Prabhu S, Ortega M and Ma C. Novel lipid-based formulations enhancing the in vitro dissolution and permeability characteristics of a poorly water-soluble model drug, piroxicam. *Int J Pharm* 301 (2005) 209-216.
- Prapaitrakul W, Sprockel OL and Shivan P. Release of chlorpheniramine maleate from fatty acid disks prepared by melt-extrusion. *J Pharm Pharmacol* 43 (1991) 377-381.
- Qi S, Deutsch D and Craig DQM. An investigation into the mechanisms of drug release from taste-masking fatty acid microspheres. *J Pharm Sci* 97 (2008), 3842-3854.
- Reich G. Near-infrared spectroscopy and imaging: Basic principles and pharmaceutical applications. *Adv Drug Deliv Rev* 57 (2005) 1109-1143.
- Reitz C and Kleinebudde P. Solid lipid extrusion of sustained release dosage forms. *Eur J Pharm Biopharm* 67 (2007) 440-448.
- Reitz C, Strachan C and Kleinebudde P. Solid lipid extrudates as sustained-release matrices: The effect of surface structure on drug release properties. *Eur J Pharm Sci* 35 (2008) 335-343.
- Ricci M, Puglia C, Bonina F, Di Giovanni CD, Giovagnoli S and Rossi C. Evaluation of indomethacin percutaneous absorption from nanostructured lipid carriers (NLC): in vitro and in vivo studies. *J Pharm Sci* 94 (2005) 1149-1159.
- Rowe RC, Sheskey PJ and Weller PJ, Eds. *Handbook of pharmaceutical excipients*, 4th ed. Pharmaceutical Press, London (2003), 460-461.
- San Vicente A, Hernandez RM, Gascon AR, Calvo MB and Pedraz, JP. Effect of aging on the release of salbutamol sulphate from lipid based matrices. *Int J Pharm* 208 (2000) 13-21.

- Šašić S. An in-depth analysis of Raman and near-infrared chemical images of common pharmaceutical tablets. *Appl Spectrosc* 61 (2007) 239-250.
- Sato K. Crystallization behaviour of fats and lipids – a review. *Chem Eng Sci* 56 (2001) 2255-2265.
- Sato K, Ueno S, Yano J. Molecular interactions and kinetic properties of fats. *Prog Lipid Res* 38 (1999) 91-116.
- Savolainen M, Kogermann K, Heinz A, Aaltonen J, Peltonen L, Strachan CJ and Yliruusi J. Better understanding of dissolution behaviour of amorphous drugs by in situ solid-state analysis using Raman spectroscopy. *Eur J Pharm Biopharm* 71 (2009) 71-79.
- Schlichter-Aronhime J and Garti N. Solidification and polymorphism in cacao butter and the blooming problems In: *Crystallization and polymorphism of fats and fatty acids*. Garti N and Sato K. Eds. Marcel Dekker, New York (1988) 363-393.
- Schmidt P. and Prochazka J. Über die Entwicklung von Retardgranulaten durch Granulatformung. *Pharm Ind* 38 (1976) 921-926.
- Sutananta W, Craig DQM and Newton JM. The effects of ageing on the thermal behaviour and mechanical properties of pharmaceutical glycerides. *Int J Pharm* 111 (1994) 51-62.
- Suardie H, Yazici R, Kalyon DM and Kovenklioglu S. Capillary flow behaviour of microcrystalline wax and silicon carbide suspension. *J Mater Sci* 33 (1998) 5059-5067.
- Thoma K and Serno P. Thermoanalytischer Nachweis der Polymorphie der Suppositoriengrundlage Hartfett. *Pharmazeutische Industrie* 45 (1983) 990-994.
- Ticehurst MD, Storey, RA and Watt C. Application of slurry bridging experiments at controlled water activities to predict the solid-state conversion between anhydrous and hydrated forms using theophylline as a model drug. *Int J Pharm* 247 (2002) 1-10.
- Timms RE. Phase behaviour of fats and their mixtures. *Prog Lipid Res* 23 (1984) 1-38.
- Uzunbajakava N, Lenferink A, Kraan Y, Volokhina E, Vrensen G, Greve J and Otto C. Nonresonant confocal Raman imaging of DNA and protein distribution in apoptotic cells. *Biophys J* 84 (2003) 3968-3981.

- Van der Weerd J, Chan KLA and Kazarian SG. An innovative design of compaction cell for in situ FT-IR imaging of tablet dissolution. *Vib. Spectrosc* 35 (2004) 9-13.
- Van der Weerd J and Kazarian SG. Combined approach of FTIR imaging and conventional dissolution tests applied to drug release. *J Control Release* 98 (2004) 295-305.
- Van der Weerd J and Kazarian SG. Release of poorly soluble drugs from HPMC tablets studied by FTIR imaging and flow-through dissolution tests. *J Pharm Sci* 94 (2005) 2096-2109.
- Van Langevelde A, Peschar R and Schenk H. Structure of β -trimyristin and β -tristearin from high-resolution X-ray powder diffraction data. *Acta Cryst. B*57 (2001) 372-77.
- Wagner B and Schneider GM. Investigations of phase transitions in pure and gas-saturated triglycerides up to 20 MPa by thermal analysis according to Smit. *Thermochim Acta* 274 (1996) 179-186.
- Whittam JH and Rosano HL. Physical aging of even saturated monoacid triglycerides. *J Am Oil Chem Soc* 52 (1975) 128-133.
- Yajima T, Itai S, Takeuchi H and Kawashima Y. Determination of optimum processing temperature for transformation of glyceryl monostearate. *Chem Pharm Bull* 50 (2002) 1430-1433.
- Yano J and Sato K. FT-IR studies on polymorphism of fats: molecular structures and interactions. *Food Research Intern* 32 (1999) 249-259.
- Zeitler JA, Taday PF, Newnham DA, Pepper M, Gordon KC and Rades T. Terahertz-pulsed spectroscopy and imaging in pharmaceutical setting. *J Pharm Pharmacol* 59 (2007) 209-223.
- Zhang YE and Schwartz JB. Melt granulation and heat treatment for wax matrix-controlled drug release. *Drug Dev Ind Pharm* 29 (2003) 131-138.

8. Acknowledgements

The work for this thesis was performed in many different international institutions and would not have been possible without the contributions of many persons.

First of all I would like to thank my main supervisor Prof. Dr. Peter Kleinebudde for the possibility to join his working group. His professional guidance and support throughout my work at the Institute of Pharmaceutics and Biopharmaceutics in Düsseldorf and also hundreds of kilometres away has enabled me to successfully conduct my research. I deeply appreciated his open-door policy and his trust in me to provide space for my own research ideas.

I thank Prof. Dr. Jörg Breitzkreutz and Prof. Dr. Thomas Rades for their attendance to assume the review of my thesis and for many fruitful discussions.

Furthermore, I would like to thank all my colleagues in Düsseldorf for their support, technical assistance and friendship during work and numerous social activities. A lot of conference trips and shared experiences will make this time unforgettable for me.

My deepest thanks go to Dr. Clare Strachan for her encouraging supervision and constant support during my whole PhD time and for her friendship.

I would also like to express my gratitude to Prof. Dr. Arto Urtti (Centre for Drug Research, Helsinki) and Prof. Dr. Jouko Yliruusi (Division of Pharmaceutical Technology, University of Helsinki) for providing excellent research facilities during my year in Finland. Special acknowledgements go to the whole research group in Helsinki. Thank you for your warm welcome in Finland, for sharing your knowledge with me, for your support and friendship. Kiitos paljon ihanasta ajasta!

In addition, thank goes to Martin Jurna and Dr. Herman Offerhaus (MESA⁺ Institute for Nanotechnology, University of Twente) for an excellent multidisciplinary cooperation, for their enthusiasm and professional scientific work during my stays at Twente as well as in many emails and telephone conferences.

Miriam Haaser, Dr. Cushla McGoverin and Prof. Dr. Keith Gordon (School of Pharmacy and Department of Chemistry, University of Otago, New Zealand) are

gratefully acknowledged for their excellent contributions and scientific work during our cooperative research project.

I am very thankful to the Marie Curie Fellowship and the Galenos Network for generous funding of my research and for giving me the chance to participate in their Euro PhD programme which enabled me to conduct excellent research in many different places. Thanks go to my whole ‘Galenos family’ who enriched my scientific journey during many conferences, scientific courses and social events.

In addition, thank goes to the University of Helsinki for funding of conference trips.

I am grateful to Sasol, Clariant, BASF and the Dow Chemical Company for generous provision of their substances for my research.

My deepest appreciation goes to my family for their unconditional support and encouragement throughout my whole education.

Last but not least my thanks go to my husband Thomas who gave me the love and strength to go my way and who always stood beside me no matter what I did.

9. Original publications

Reprints with the permission of the publishers.

9.1. Article 1: Understanding the solid-state behaviour of triglyceride solid lipid extrudates and its influence on dissolution



Contents lists available at ScienceDirect

European Journal of Pharmaceutics and Biopharmaceutics

journal homepage: www.elsevier.com/locate/ejpb

Research paper

Understanding the solid-state behaviour of triglyceride solid lipid extrudates and its influence on dissolution

Maike Windbergs^{a,b,c}, Clare J. Strachan^{b,*}, Peter Kleinebudde^a^a Institute of Pharmaceutics and Biopharmaceutics, Heinrich-Heine-University, Düsseldorf, Germany^b Centre for Drug Research, University of Helsinki, Helsinki, Finland^c Division of Pharmaceutical Technology, University of Helsinki, Helsinki, Finland

ARTICLE INFO

Article history:

Received 29 February 2008

Accepted in revised form 21 May 2008

Available online 6 June 2008

Keywords:

Solid lipid extrusion

Triglycerides

Polymorphism

Dissolution

Solid-state behaviour

Physical stability

ABSTRACT

Three monoacid triglycerides differing in their fatty acid chain lengths were extruded below their melting temperatures. Physical characterization was conducted on the powders as well as the extrudates with a combination of DSC, XRPD and vibrational spectroscopy to get a deeper insight into the complex solid-state behaviour of lipids and solid lipid extrudates during processing and storage. The combination of extrusion temperature and friction was a key factor for the lipid polymorphic behaviour after extrusion. Polymorphic transitions had a strong influence on the dissolution behaviour due to crystallization of the stable β -form from the unstable α -form on the surface of the extrudate. These correlations help to understand the solid-state behaviour of lipids and to avoid process conditions which lead to unstable dosage forms. Tailor-made dissolution profiles for a model drug could be achieved using triglycerides of different fatty acid chain lengths as the dissolution rate is chain-length dependent. The solid-state form of the drug was unchanged after storage in accelerated conditions over 10 months. These studies demonstrate that although triglycerides are a promising basis for oral dosage forms, a good understanding and monitoring of the solid-state behaviour is mandatory to obtain reliable and reproducible dosage forms.

© 2008 Elsevier B.V. All rights reserved.

1. Introduction

Lipids are a group of excipients that have recently generated substantial interest for the production of oral dosage forms. They show a high variability in their physico-chemical properties which offer various possibilities for different types of pharmaceutical formulations. In particular, they have shown a high potential for the development of controlled release systems. On the one hand, lipids can be used for prolonged release [1]. In addition, they are able to enhance the solubility and permeability of drugs with poor oral bioavailability [2], a fact that is increasingly important since a large proportion of the newly developed APIs have low solubility and permeability (Bioclassification System Class 4). Furthermore, taste masking is also feasible with the help of lipids [3]. In addition, a specific advantage of lipids is that they are biodegradable and physiologically non-toxic.

Various preparation techniques have been used to produce lipid-based oral dosage forms. The most common approach involves melting the lipid and then resolidification with the solid API to form a matrix [4–7]. One relatively new technique is solid lipid

extrusion [8,9]. Using this technique, glycerides which are available as pharmaceutical excipients in powdered form such as Dymasan[®] for instance are blended with a specific amount of an API and extruded through an extruder below their melting temperatures avoiding melting of the whole lipid mass. The resulting extrudates are spherulized to pellets or cut into cylinders of suitable size, depending on the applicable dosage form. Although the lipid pellet or extrudate provides a lot of advantages, the formulation is quite difficult.

Due to their chemical and physical structures, lipids exhibit complex solid-state behaviour including melting, crystallization and physical modifications during processing and even storage [10]. They usually exhibit three different polymorphic forms (α , β' and β). The relationship is monotropic in most cases: the α -form is the least thermodynamically stable form, β' is metastable and β is stable, exhibiting the densest packing mode for a lipid [11,12]. Since the polymorphic behaviour is typically monotropic, each polymorph has its unique melting point. The lipid polymorphic behaviour is quite difficult to predict. Thus, for example, a dosage form produced with a metastable lipid modification and the desired properties may subsequently transform to a more stable one [13,14]. The result is usually a deterioration of the product's quality and its desired properties including drug release profiles. Moreover, the physical "ageing" effects during storage must be well understood to avoid any further drug release alteration during storage [15].

* Corresponding author. Centre for Drug Research, Faculty of Pharmacy, University of Helsinki, Viikinkaari 5E, P.O. Box 56, FI-00014 Helsinki, Finland. Tel.: +358 9 191 59074.

E-mail address: clare.strachan@helsinki.fi (C.J. Strachan).

At present, there is a lack of understanding of the physico-chemical behaviour at the core and on the surface of solid lipid extrudates during processing and storage. The aim of this study was to better understand the solid-state behaviour of triglycerides during solid lipid extrusion and relate this to the drug-dissolution behaviour from the extrudates. This should allow the production of stable dosage forms with reproducible and advantageous performance characteristics (e.g. dissolution). Three pure monoacid triglycerides differing only in their fatty acid chain lengths were extruded below their melting temperature. Physical characterization was conducted on the powders as well as on the extrudates with a combination of DSC, XRPD and vibrational spectroscopy [16]. Dissolution tests and storage experiments were also performed and the results interpreted in light of the physical characterization results.

2. Materials and methods

2.1. Materials

The pure powdered monoacid triglycerides trilaurin (Dynasan 112[®]), tripalmitin (Dynasan 116[®]) and tristearin (Dynasan 118[®]) provided by Sasol (Witten, Germany) were used as received. The model drug theophylline anhydrate (BASF, Ludwigshafen, Germany) was used in powdered form as supplied. Theophylline monohydrate was prepared by recrystallization of theophylline anhydrate from purified water. All crystal forms were verified by X-ray powder diffraction and compared to the theoretical patterns available from the Cambridge Structural Database (Cambridge Crystallographic Data Centre (CCDC), Cambridge, United Kingdom), using the associated Mercury software (v. 1.5). The reference codes for the crystal structures used were: BAPLOT01 (theophylline anhydrate), THEOPH01 (theophylline monohydrate), BTRILA05 (trilaurin β -form), SUWMAY (tripalmitin β -form), and QOYK1Y (tristearin β -form). Resolidified melts for variable X-ray powder diffraction measurements were produced by heating the powdered lipids up above their individual melting temperature and holding the melt for at least 3 min to erase structural memory. The melts were poured into the X-ray diffraction sample holders, resolidified rapidly on ice and measured directly afterwards.

2.2. Methods

2.2.1. Extrusion

The powdered glycerides were used in pure form or were weighed in a 1:1 ratio with theophylline anhydrate and then blended in a laboratory mixer (LM20 Bohle, Ennigerloh, Germany) for 15 min at 25 rpm. The powders were fed from a gravimetric dosing device (KT20K-Tron Soder, Lenzhard, Switzerland) into the barrel of a co-rotating twin-screw extruder (Mikro 27GL-28D, Leistritz, Nürnberg, Germany) and extruded with a constant screw speed of 30 rpm and a feeding rate of 40 g min⁻¹. The processing temperature was individually chosen depending on the melting temperature of the lipid. The extruder die plate contained 23 holes of 1 mm diameter and 2.5 mm length.

2.2.2. Differential scanning calorimetry (DSC)

Differential scanning calorimetry was performed using a DSC 821e calorimeter (Mettler-Toledo, Gießen, Germany). The samples were heated from 20 to 300 °C with a heating rate of 10 °C min⁻¹. All experiments were conducted twice using hermetically sealed aluminium pans (40 μ l) containing approximately 5 mg of sample.

2.2.3. X-ray powder diffraction (XRPD)

The samples were measured using a theta-theta X-ray powder diffractometer (D8 Advance, Bruker AXS GmbH, Karlsruhe,

Germany). Measurements were done in symmetrical reflection mode with CuK α radiation ($\lambda = 1.54 \text{ \AA}$) using Göbel mirror bent multilayer optics. The angular range measured was 5–40° (2 θ), with a step size of 0.05° (2 θ). The measuring time was 1 s per step. The samples were put in the sample holder and gently compressed to smooth the surface. All experiments were conducted in triplicate. Variable temperature measurements were also done with the same diffractometer with resolidified melts of the lipids (see above) in the temperature range of 25 °C up to the individual melting temperatures of the lipids.

2.2.4. Attenuated total reflectance infrared (ATR-IR) spectroscopy

Samples were measured using an FTIR spectrometer (Bruker FTIR Vertex 70, Bruker, Ettlingen, Germany) with an ATR accessory fitted with a single reflection diamond/ZnSe crystal plate (MIRacle ATR, PIKE Technologies, Madison, WI, USA). The samples were placed in the ATR device without any preparation and measured using 64 scans for each spectrum. Spectra were collected between 4000 and 650 cm⁻¹. All experiments were conducted in triplicate.

2.2.5. Near infrared (NIR) spectroscopy

For NIR measurements, a NIR spectrometer (NIR-256L-2.2T2, Control Development Inc., South Bend, IN, USA) with a thermoelectrically cooled 256 element InGaAs array detector, tungsten light source and a fiber optic reflectance probe (six illuminating optical fibers around one signal collecting fiber) was used. A reference spectrum was recorded with a Teflon background. The spectra were collected from 1100 to 2200 nm with 30 ms integration time and 500 scans per spectrum. All experiments were conducted in triplicate.

2.2.6. Dissolution

Dissolution studies were performed according to the USP29 Method 2 with a paddle apparatus (Sotax AT7 smart, Sotax, Lörrach, Germany). Extrudates were cut to lengths of approximately 1 cm, and a sample size of 140 mg was used in each vessel. Experiments were conducted in purified water containing 0.001% polysorbate 20 at 37 \pm 0.5 °C with a stirring speed of 50 rpm. The absorption of the medium was measured at 5 min intervals using a UV-vis spectrometer with an absorption wavelength of 242 nm (Lambda 40, Perkin-Elmer, Rodgau-Juegesheim, Germany) in a continuous flow-through cuvette. The experiments were conducted in triplicate taking the mean for the dissolution curve. The standard deviation was below 3% in all cases.

2.2.7. Storage

Samples were stored for 10 months in a climate chamber (KBF 240, Binder, Tuttlingen, Germany). The extrudates were placed in open Petri dishes and exposed to accelerated and constant climatic conditions (40 °C/75% RH).

2.2.8. Scanning electron microscopy (SEM)

SEM micrographs were recorded on samples mounted on aluminium stubs using double-sided carbon tape and sputter coated with platinum for 20 s. They were viewed using a DSM 962 scanning electron microscope (Carl Zeiss, Oberkochen, Germany).

3. Results and discussion

3.1. Obtaining extrudates with acceptable external appearance

During extrusion the equipment variables as well as the process variables can be modified. In these experiments all equipment variables, e.g. the screw configuration and the design of the die plate, were kept constant so that different runs were comparable.

Among the process variables one can distinguish between screw speed, feed rate and temperature. The screw speed and the feed rate were adjusted to obtain a continuous product flow and then retained unchanged for all the experiments. The only parameter which was chosen individually for each powder mixture was the barrel temperature.

The lipids used differ in their melting temperature depending on the chain length of the fatty acids esterified with the glycerol molecule. The aim of the extrusion experiments was to obtain reproducible cylindrical extrudates with a smooth surface and a high mechanical stability. Experiments were performed at different temperatures that were below the melting point of each lipid but sufficiently high to form intact extrudates. The best results were achieved at extrusion temperatures just a few degrees below the melting temperature of the individual lipid. In trilaurin, the glycerol molecule is esterified with three relatively short fatty acids (12 C atoms). The melting point in the literature is 46 °C [17]. The most suitable extrudates for formulation were obtained with a processing temperature of 40 °C. Elongating the fatty acid chain lengths with four C atoms each (compared to trilaurin) to form tripalmitin leads to a higher melting point of 66 °C [17]. It was possible to produce good extrudates at 55 °C and at 60 °C. The smoothest extrudates were obtained with a processing temperature of 60 °C. In the tristearin molecule, glycerol is esterified with three stearic acids (18 C atoms). The melting point is 73 °C [17]. Suitable extrudates could be obtained with processing temperatures of 55 and 65 °C.

The external appearance of all triglyceride extrudates was similar for the best processing temperatures for each individual lipid mentioned above. Fig. 1 shows two SEM images of two representative extrudate surfaces: pure tripalmitin (Fig. 1a) and a combination of tripalmitin and theophylline (50% w/w lipid/drug) (Fig. 1b). Both extrudates show a continuous and rather smooth surface. The mixture of lipid and drug results in a rougher surface than the pure lipid due to the fact that the lipid partly melts on the surface during processing, whereas the drug remains completely solid.

3.2. Solid-state structure analysis of extrudates

As previously stated, lipids can exhibit quite complex polymorphic behaviour during processing and storage. Monitoring the pure triglycerides individually should show the influence of the lipid structure in combination with temperature on the solid-state behaviour of the extrudates. Using DSC, XRPD and ATR-IR spectroscopy as complementary methods the powders of the different substances, the pure lipid extrudates and the mixed extrudates of 50% lipid/drug (w/w) were examined.

3.2.1. Trilaurin

The results of the physical characterization of this triglyceride with the shortest fatty acid chains (12 C atoms) of the processed lipids are shown in Fig. 2. The DSC thermograms of powder, extrudate (100% lipid) and extrudate with drug (50% w/w lipid/drug) (Fig. 2a) do not show significant changes in the onset of the lipid melting peaks. The stable β -form can be identified in each thermogram by its melting peak with an onset at 45 °C [17]. There is no evidence of an interaction between lipid and drug, since theophylline shows a sharp melting peak onset at 270.8 °C (the melting temperature of the stable anhydrate form of theophylline in the literature is 275.8 °C [18]) and there are no other thermal events. In addition, in the XRPD patterns (Fig. 2b) the trilaurin β -form is indicated by three strong reflections at 19.4° (2 θ), 23.1° (2 θ) and 24.05° (2 θ) [19] in the lipid powder and extrudate. The peak positions of the drug, for example, at 7.1° (2 θ) and 12.6° (2 θ), are the same as those for the powder indicating that no polymorphic change has occurred in the drug. In addition, no solid-state changes or interactions were observed using ATR-IR spectra, with the peak positions

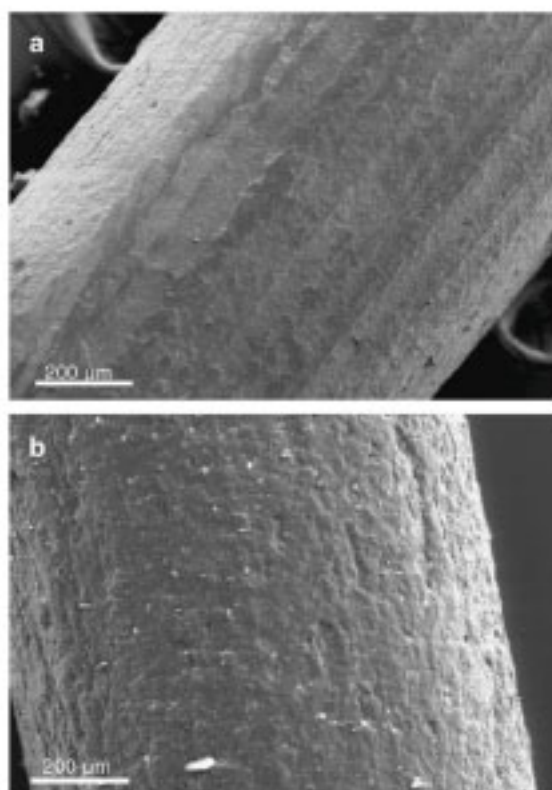


Fig. 1. SEM images of extrudate surfaces (a) 100% tripalmitin and (b) 50% tripalmitin/50% theophylline (w/w).

and relative intensities of trilaurin and theophylline unchanged (Fig. 2c). For trilaurin the following peaks can be identified: CH₂ scissoring (1473 cm⁻¹), C=O stretch (1735 cm⁻¹), CH₂ symmetric stretch (2851 cm⁻¹) and CH₂ antisymmetric stretch (2919 cm⁻¹) [20,21]. Theophylline anhydrate shows specific peaks like C=O stretches (1665 and 1713 cm⁻¹) and the CH stretch (3122 cm⁻¹) [22]. In summary, none of the analytical methods used in this context was able to detect any solid-state changes of the glyceride or interactions with the drug before and after processing. Trilaurin remained in its stable β -form, and the crystal structure of theophylline anhydrate was unchanged.

3.2.2. Tripalmitin

Tripalmitin contains the intermediate fatty acid chains length in these studies (16 C atoms). Extrudates produced at 55 °C and at 60 °C did not exhibit differences according to the solid-state analysis, so only the 60 °C results are shown. Analysis using DSC, XRPD and ATR-IR spectroscopy revealed the lipid remained crystalline in the most stable β -form after processing (Fig. 3). No interactions between drug and lipid could be observed. The DSC thermograms (Fig. 3a) depict clearly separated melting peaks of lipid (onset 63.6 °C) and drug (onset 270.7 °C) [17,18], and the peak positions in the XRPD patterns (Fig. 3b) [19,23] and ATR-IR (Fig. 3c) spectra remain unchanged after extrusion [20,21].

3.2.3. Tristearin

Tristearin is the triglyceride with the longest fatty acids used in these studies (18 C atoms). Extrudates were produced at 55 °C and at 65 °C, and in this case obvious differences can be observed be-

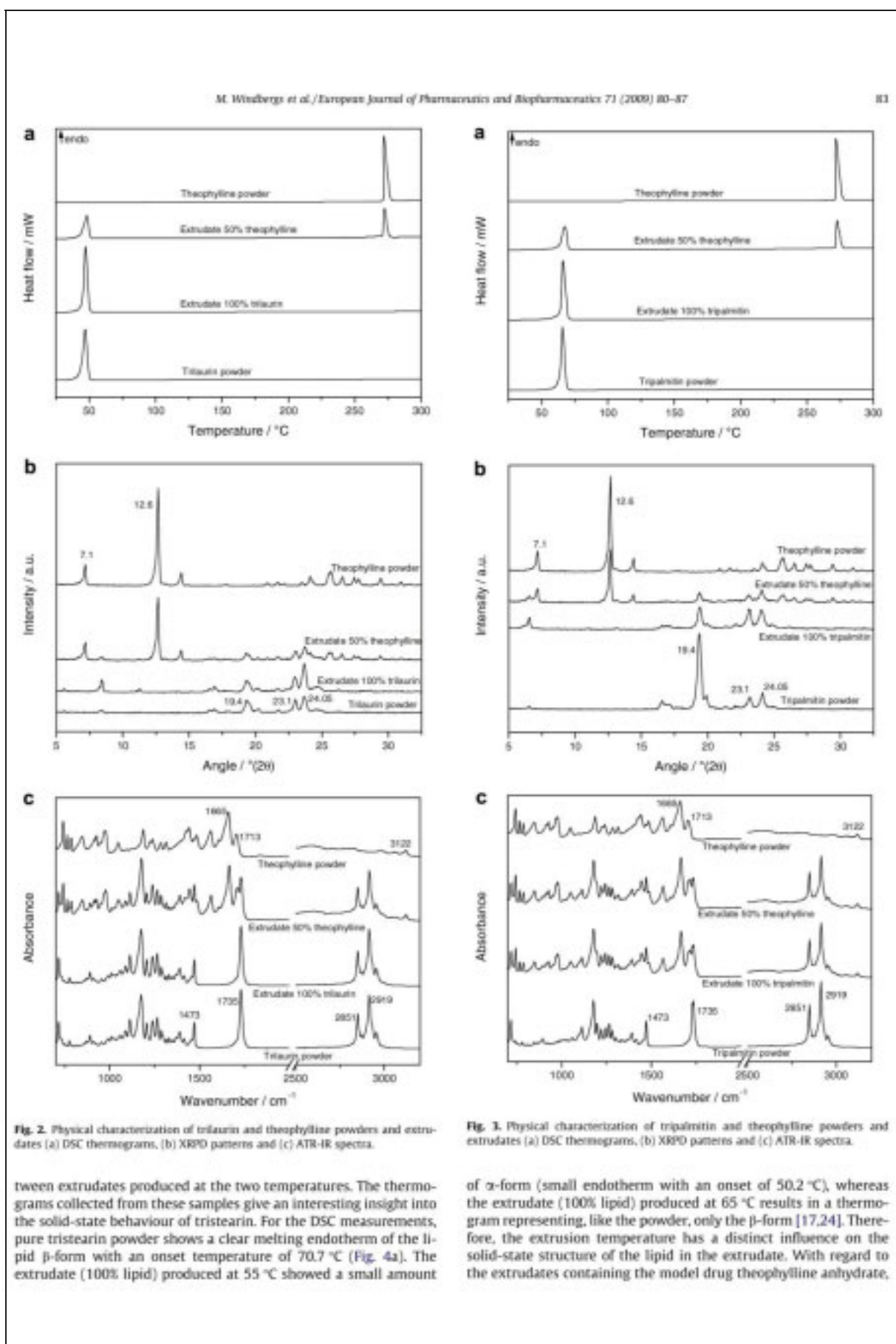


Fig. 4a reveals the same behaviour as that seen for the 100% lipid extrudates. The extrudate produced at 55 °C shows the presence of a small amount of the α -form, while the extrudate produced at 65 °C shows the same thermal events as the pure lipid powder with the additional drug-melting peak (onset 271.1 °C).

ATR-IR spectra of the lipid powder (pure β -form) and the pure lipid extrudates produced at different temperatures corroborate these observations [Fig. 4b]. In the region around 1300–1400 cm^{-1} (highlighted), the differences in the peak shape between the 100% tristearin extrudate produced at 55 °C and the powder and the extrudate produced at 65 °C (pure β -form) can be observed [20,21]. Diffractograms were taken of powders, extrudate (100% lipid) and extrudate with drug (50% w/w lipid/drug). The temperature dependant behaviour revealed with DSC measurements (see above) can also be monitored with XRPD [Fig. 5]. The pure lipid extrudates produced at different temperatures were compared to the pure powders in the different polymorphic forms (Fig. 5a). In the region around 20.0–23.0° (2 θ) (highlighted), the extrudate produced at 55 °C shows some α -form with the characteristic peak at 21.4° (2 θ), whereas extrudates produced at 65 °C only show β -form indicated by the peaks at 19.4° (2 θ), 23.1° (2 θ) and 24.05° (2 θ) as the powder [19,24]. Addition of the model drug does not change the solid-state behaviour of the lipid (Fig. 5b). Extrudates produced at 55 °C contain the α -form (21.4° (2 θ)), while extrudates produced at 65 °C do not.

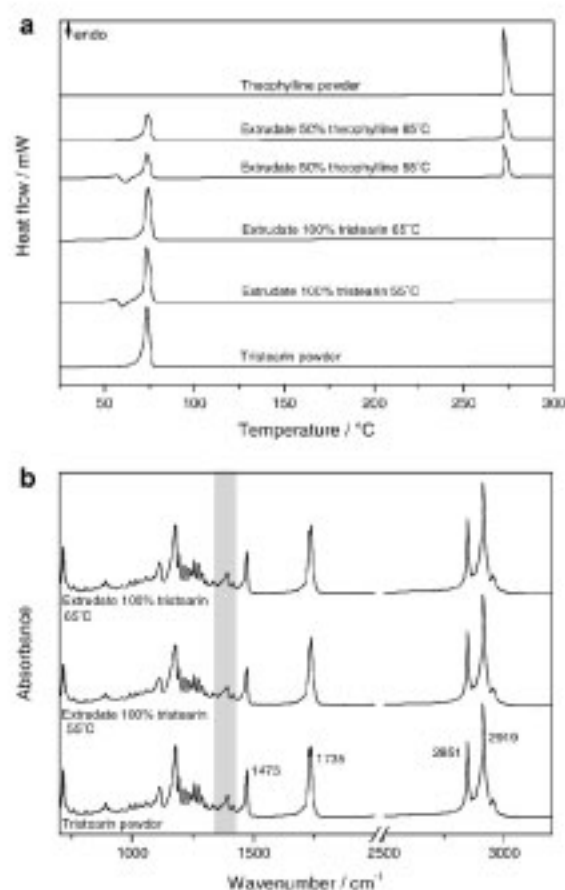


Fig. 4. Physical characterization of tristearin (a) DSC thermograms and (b) ATR-IR spectra.

3.3. Interpreting the solid-state behaviour of the triglycerides during extrusion

To further understand the solid-state behaviour of tristearin, diffractograms of the powder were also taken while heating the

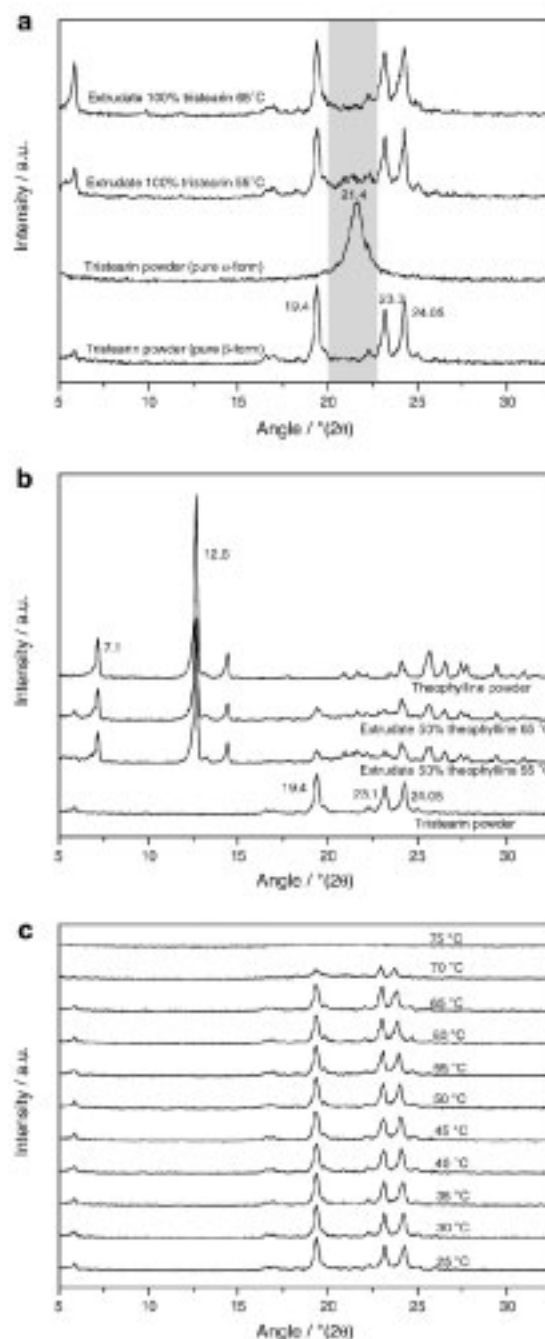


Fig. 5. XRPD patterns of (a) tristearin powder and extrudates, (b) tristearin and theophylline powders and extrudates and (c) variable temperature XRPD patterns of tristearin powder.

sample from 25 to 75 °C in 5 °C steps (Fig. 5c). Interestingly, there was no incidence of any structural changes until melting. This is in agreement with the monotropic relationship between the three polymorphs of the triglycerides, and thus the observed α -form must be created via the melt [11,12]. Therefore, the α -form monitored in the extrudates produced at 55 °C cannot exclusively be attributed to the influence of the processing temperature.

The phase behaviour of monoacid triglycerides at different pressures has been studied [25]. The pressure was found to have an influence on the lipid polymorphic transition behaviour depending on the pressure range which is applied to the lipids. During extrusion, the pressure was monitored simultaneously never exceeding 0.7 MPa. According to the study, this pressure is below that required to have an influence on the lipid transition behaviour.

A combination of temperature and friction during extrusion seems to be the factor influencing the solid-state structure of tristearin during extrusion. Friction causes the temperature to rise and some melting at the edges of the lipid mass is induced inside the extruder barrel. This happens at both extrusion temperatures. The difference in the polymorphic form which can be found in the extrudate after processing is due to the temperature at which the extrudate mass leaves the extruder. After leaving the die plate hole, the molten portion of the lipid at the surface directly solidifies. The α -form is supposed to crystallize after melting up to the temperature of 54.5 °C, according to a study by MacNaughtan *et al.* [26] using DSC. Hence, at an extrusion temperature of 55 °C the molten part of the extrudate mass appears to partly crystallize in α -form.

The temperature at which the extrudate leaves the die plate seems to be a key factor determining the crystallization behaviour from the molten component of the extruded lipid. To prove this hypothesis variable temperature XRPD measurements were done with the lipid powders. They were completely melted and resolidified again. Tripalmitin and tristearin resolidified in the α -form, while trilaurin only crystallized into the β -form as the α -form is unstable at room temperature due to its low melting point of 14 °C [17]. The resolidified samples were heated up in the X-ray diffractometer to monitor the physical structure at each temperature step. The results of these measurements were in agreement with the extrusion results (Fig. 6). Trilaurin (Fig. 6a) forms the stable β -form before melting at 45 °C [17]. Tripalmitin (Fig. 6b) exhibits pure α -form in the lower temperature region (up to 40 °C). Around the melting point of the α -form (46 °C) [17] and above the transformation the more stable β -form can be observed. At the extrusion temperatures of these experiments (55 and 60 °C), only β -form can be observed. Tristearin (Fig. 6c) shows in general the same solid-state behaviour, but at slightly different temperatures. Up to 55 °C, pure α -form can be monitored exclusively as the melting point of the α -form for tristearin is 55 °C [17], and above this temperature the β -form crystallizes. So as seen in the extrusion experiments, partial α -form is obtained at 55 °C while at 65 °C only the β -form appears.

3.4. Storage stability

All extrudates in stable β -form were stored for 10 months in accelerated conditions (40 °C/75% RH). Physical characterization was performed using XRPD and NIR spectroscopy to detect water absorption. There was no evidence of any solid-state changes in the lipid or the drug (tripalmitin extrudates are shown in Fig. 7 as an example). For all triglycerides, the β -form is thermodynamically stable at 40 °C as evidenced by the XRPD patterns in Fig. 7a, and increased water activity is likely to have a minimal effect on the thermodynamically stable form since the lipids are hydrophobic. Despite there being some evidence that theophylline monohydrate is the thermodynamically stable form in these conditions

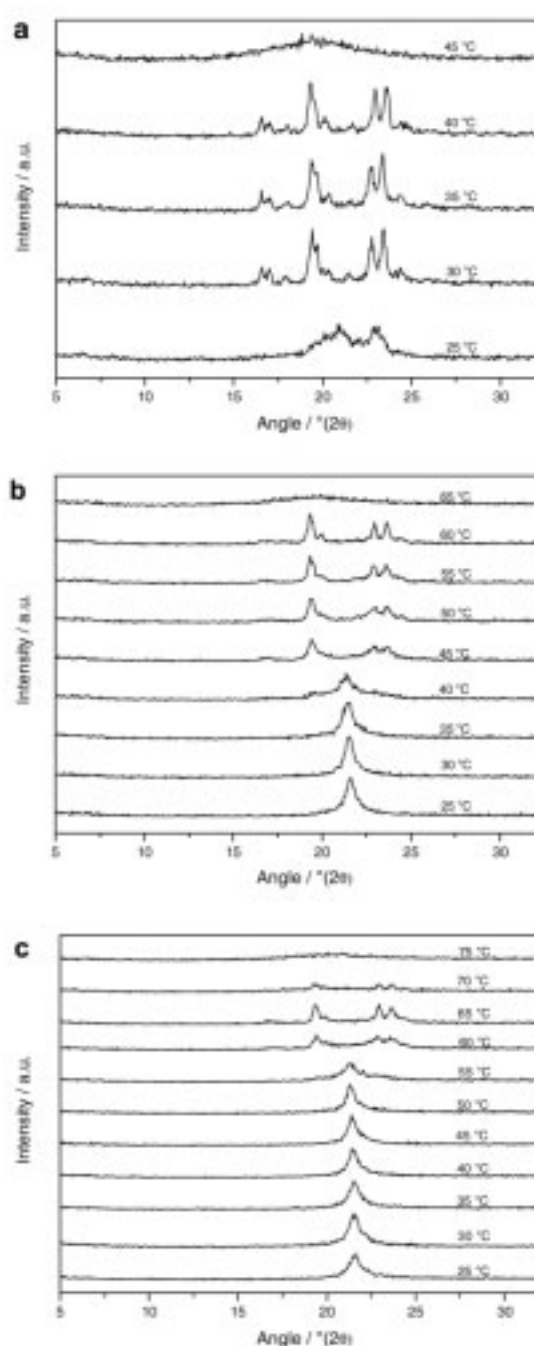


Fig. 6. Variable temperature XRPD patterns of resolidified melts of (a) trilaurin, (b) tripalmitin and (c) tristearin.

[27], the drug remained in the anhydrate form as the XRPD patterns depict. NIR spectra in Fig. 7b support these results as the main peaks for the monohydrate form, specifically the OH overtone (1490 cm^{-1}) and the OH combination (1970 cm^{-1}) bands associated with water, are not observed for the extrudates. The lack of

transformation of theophylline anhydrate to the monohydrate is likely to be due to two factors: an intrinsically slow transformation rate and the hydrophobic barrier provided by the lipid matrix.

3.5. Dissolution from triglyceride matrices

Dissolution from triglyceride matrices is completely diffusion controlled since the matrix stays intact after the release of the drug. Comparison of the three triglycerides revealed a chain-length dependent dissolution behaviour: the longer the fatty acid chains the slower the dissolution of the drug (Fig. 8a).

Fig. 8b depicts how polymorphism of a lipid during processing can influence the dissolution rate of the dosage form after storage. Tristearin extrudates produced at 55 °C exhibited a slower release of the drug than tristearin extrudates produced at 65 °C. This observation is unintuitive at first glance because the dissolution is purely diffusion controlled. A less dense packing mode of the matrix due to formation of the less ordered α -form in case of the extrudate produced at 55 °C as stated before should lead to an equal or higher dissolution rate. The explanation for this apparent anomaly can be found with a closer look at the surface of the extrudates. The surface of a tristearin extrudate produced at 65 °C consists of a rather smooth structure (Fig. 9a), while the surface of an extrudate produced at 55 °C is covered by sharp fractal structures

(Fig. 9b). The presence of these sharp fractal structures has been described in the literature and is known as the "blooming effect" [28]. When the extrudate leaves the extruder die plate and the molten parts of the lipid recrystallize as the unstable α -form, a transformation to the stable β -form results. The formation of β -form results in the flowery fractal structures on the surface of the extrudate. The fractal structures increase the contact angle to water [29], which would be expected to decrease wetting, and hence the dissolution rate of the drug in the dissolution medium.

4. Conclusions

The solid-state behaviour of triglyceride solid lipid extrudates is influenced by different factors during processing and has to be well understood and monitored to obtain reproducible dosage forms of high quality. The combination of temperature and friction was found to be a key point for the lipid polymorphic composition after extrusion. As some lipid melting always occurs while extruding triglycerides, the temperature of the extruder die plate should always be above the melting point of the unstable α -form of the extruded triglyceride to avoid subsequent alteration of the product which could be shown to strongly affect the dissolution rate. Tailor-made dissolution profiles can be achieved using triglycerides of different fatty acid chain lengths as the dissolution rate is chain-length

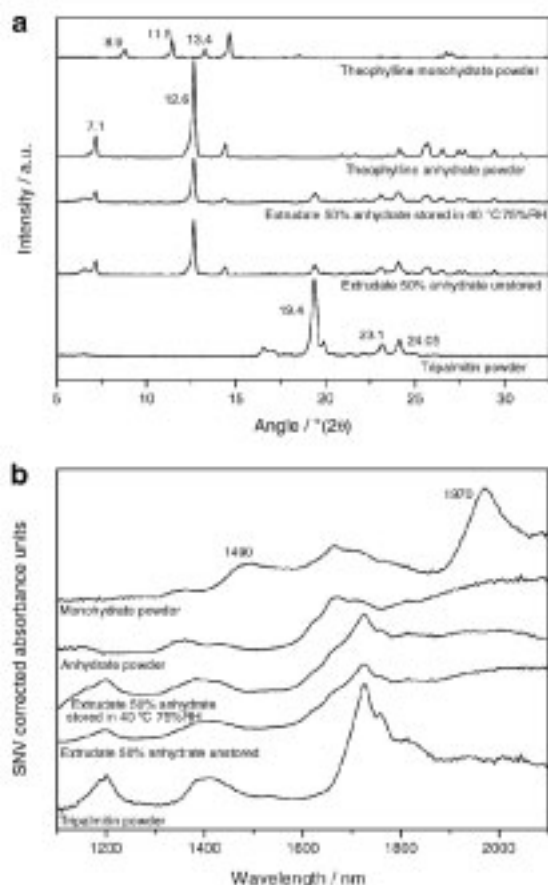


Fig. 7. Storage of tripalmitin extrudates for 10 months (a) XRPD patterns and (b) IR spectra.

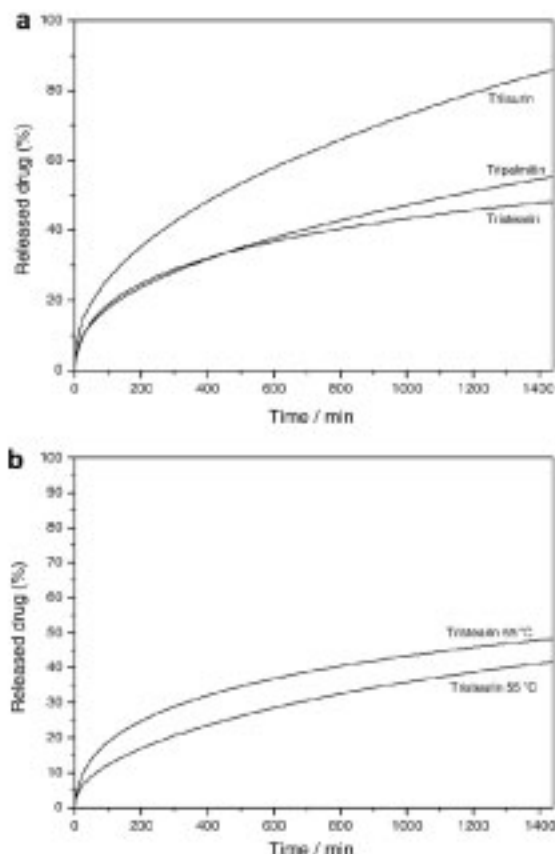


Fig. 8. Dissolution curves of triglyceride extrudates (a) comparison of different triglycerides and (b) comparison of tristearin extrudates produced at different temperatures ($n = 3$, mean, $cv < 15$ not shown).

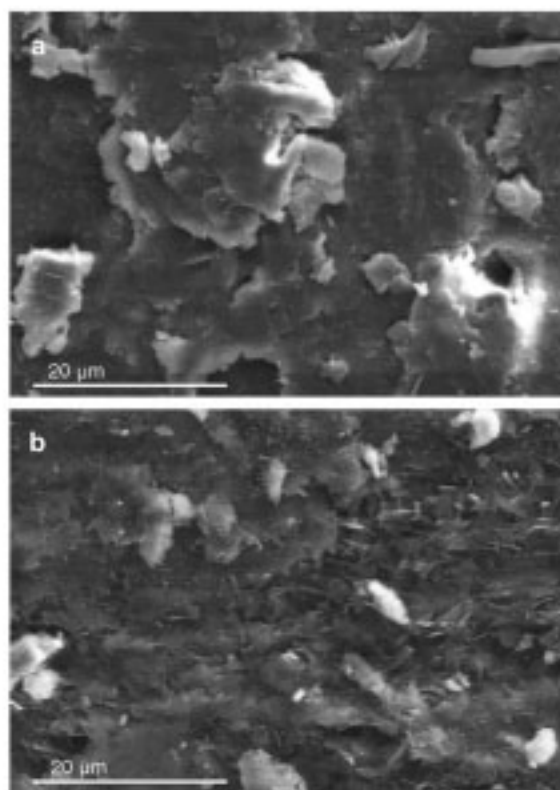


Fig. 9. SEM images of the surface of tristearin extrudates produced at (a) 65 °C and (b) 55 °C.

dependent. Storage experiments in accelerated conditions also suggested that the anhydrate form of the drug was stable over 10 months with the hydrophobic barrier of the lipid helping to protect the drug against any hydrate formation. The understanding of polymorphic behaviour of triglyceride solid lipid extrudates and its effect on dissolution will help in the development of solid lipid extrudates with desired and predictable dissolution behaviour.

Acknowledgements

The Marie Curie Fellowship and the Galenus Network are acknowledged for financial support (MEST-CT-2004-404902). Mrs. Karin Mattheé is acknowledged for help with the DSC measurements. Sasol GmbH is acknowledged for generous provision of the lipids.

References

- [1] J. Hamdani, A.J. Moes, K. Amighi, Development and evaluation of prolonged release pellets obtained by the melt pelletization process, *Int. J. Pharm.* 245 (1–2) (2002) 167–177.
- [2] S. Prabhu, M. Ortega, C. Ma, Novel lipid-based formulations enhancing the in vitro dissolution and permeability characteristics of a poorly water-insoluble model drug, piroxicam, *Int. J. Pharm.* 301 (1–2) (2005) 209–216.
- [3] S. Qi, D. Deutsch, D.Q. Craig, An investigation into the mechanisms of drug release from taste-masking fatty acid microspheres, *J. Pharm. Sci.* (2008) 1–13.
- [4] H. Bunjes, K. Westersen, M.J.J. Koch, Crystallization tendency and polymorphic transitions in triglyceride nanoparticles, *Int. J. Pharm.* 129 (1996) 159–173.
- [5] Y.E. Zhang, J.B. Schwartz, Melt granulation and heat treatment for wax matrix-controlled drug release, *Drug Dev. Ind. Pharm.* 29 (2) (2003) 131–138.
- [6] B. Chauhan, S. Shimpi, A. Parashkar, Preparation and characterization of atorvastatin solid dispersions using lipid carriers by spray drying technique, *AAPS PharmSciTech* 6 (3) (2005) E405–E412.
- [7] J. Liu, F. Zhang, J.W. McGinity, Properties of lipophilic matrix tablets containing phenylpropanolamine hydrochloride prepared by hot-melt extrusion, *Eur. J. Pharm. Biopharm.* 52 (2) (2001) 181–190.
- [8] J. Bretkreutz, F. El Saleh, C. Kiera, P. Kleinbudda, W. Wiedey, Pediatric drug formulations of sodium benzoate: II. Coated granules with a lipophilic binder, *Eur. J. Pharm. Biopharm.* 56 (2003) 255–260.
- [9] J.F. Pinto, N.P. Silverio, Assessment of the extrudability of three different mixtures of saturated polyglycolysed glycerides by determination of the “specific work of extrusion” and capillary rheometry, *Pharm. Dev. Technol.* 6 (2001) 117–128.
- [10] J. Hamdani, A.J. Moes, K. Amighi, Physical and thermal characterisation of Precirol[®] and Compritol[®] as lipophilic glycerides used for the preparation of controlled-release matrix pellets, *Int. J. Pharm.* 260 (2003) 47–57.
- [11] K. Sato, Crystallization behaviour of fats and lipids – a review, *Chem. Eng. Sci.* 56 (2001) 2255–2265.
- [12] K. Sato, S. Ueno, J. Yano, Molecular interactions and kinetic properties of fats, *Prog. Lipid Res.* 38 (1999) 91–116.
- [13] J.H. Whittam, H.L. Rosano, Physical aging of even saturated monoacid triglycerides, *J. Am. Oil Chem. Soc.* 52 (1975) 128–133.
- [14] W. Sutananta, D.Q.M. Craig, J.M. Newton, The effects of aging on the thermal behaviour and mechanical properties of pharmaceutical glycerides, *Int. J. Pharm.* 111 (1994) 51–62.
- [15] Y.W. Choy, N. Khan, K.H. Yuen, Significance of lipid matrix aging on in vitro release and in vitro bioavailability, *Int. J. Pharm.* 290 (2005) 55–64.
- [16] D.E. Bugay, Characterization of the solid state: spectroscopic techniques, *Adv. Drug Deliv. Rev.* 48 (2001) 43–65.
- [17] J.W. Hagemann, Thermal behaviour and polymorphism of acylglycerides, in: N. Garti, K. Sato (Eds.), *Crystallization and Polymorphism of Fats and Fatty Acids*, Marcel Dekker, New York, 1988, pp. 9–95.
- [18] W. Chen, X. Zhang, B. Sihan, X. You, Methylxanthines. I. Anhydrous theophylline, *Acta Crystallogr C* 53 (1997) 777–779.
- [19] M. Kellers, W. Meussen, R. Gehrke, H. Reynaers, Synchrotron radiation investigations of the polymorphic transitions of saturated monoacid triglycerides. Part 1: Tripalmitin and tristearin, *Chem. Phys. Lipids* 58 (1991) 131–144.
- [20] M. Kobayashi, Vibrational spectroscopic aspects of polymorphism and phase transition of fats and fatty acids, in: N. Garti, K. Sato (Eds.), *Crystallization and Polymorphism of Fats and Fatty Acids*, Marcel Dekker, New York, 1988, pp. 139–187.
- [21] J. Yano, K. Sato, FT-IR studies on polymorphism of fats: molecular structures and interactions, *Food Res. Intern.* 32 (1999) 249–259.
- [22] M.M. Nolasco, A.M. Amado, P.J.A. Ribeiro-Claro, Computationally-assisted approach to the vibrational spectra of molecular crystals: study of hydrogen-bonding and pseudo-polymorphism, *Chem. Phys. Chem.* 7 (2006) 2150–2161.
- [23] V. Hongisto, V.-P. Lehto, E. Laine, X-ray diffraction and microcalorimetry study of the $\alpha \rightarrow \beta$ transformation of tripalmitin, *Thermochim. Acta* 276 (1996) 229–242.
- [24] A. van Langeveld, R. Peschar, H. Scherik, Structure of β -tristearin and β -tristearin from high-resolution X-ray powder diffraction data, *Acta Crystallogr B* 57 (2001) 372–377.
- [25] B. Wagner, G.M. Schneider, Investigations of phase transitions in pure and gas-saturated triglycerides up to 20 MPa by thermal analysis according to Smit, *Thermochim. Acta* 274 (1996) 179–186.
- [26] W. MacNaughtan, L.A. Farhat, C. Hirawan, V.M. Starov, A.G.F. Stapley, A differential scanning calorimetry study of the crystallization kinetics of tristearin–tripalmitin mixtures, *J. Am. Oil Chem. Soc.* 83 (2006) 1–9.
- [27] M.D. Ticehurst, R.A. Storey, C. Watt, Application of slurry bridging experiments at controlled water activities to predict the solid-state conversion between anhydrous and hydrated forms using theophylline as a model drug, *Int. J. Pharm.* 247 (2002) 1–10.
- [28] N. Khan, D.Q.M. Craig, Role of blooming in determining the storage stability of lipid-based dosage forms, *J. Pharm. Sci.* 93 (12) (2004) 2962–2971.
- [29] W. Fang, H. Mayama, K. Tsujii, Spontaneous formation of fractal structures on triglyceride surfaces with reference to their water-repellent properties, *J. Phys. Chem. B* 111 (2007) 564–571.

9.2. Article 2: Influence of the composition of glycerides on the solid-state behaviour and the dissolution profiles of solid lipid extrudates

G Model
 JP-10549; No. of Pages 8

ARTICLE IN PRESS

International Journal of Pharmaceutics xxx (2009) xxx–xxx



Contents lists available at ScienceDirect

International Journal of Pharmaceutics

journal homepage: www.elsevier.com/locate/ijpharm



Influence of the composition of glycerides on the solid-state behaviour and the dissolution profiles of solid lipid extrudates

Maike Windbergs^{a,b,c}, Clare J. Strachan^{b,d}, Peter Kleinebudde^{a,*}

^a Institute of Pharmaceutics and Biopharmaceutics, Heinrich-Heine-University Düsseldorf, Germany

^b Centre for Drug Research, Faculty of Pharmacy, University of Helsinki, Finland

^c Division of Pharmaceutical Technology, Faculty of Pharmacy, University of Helsinki, Finland

^d School of Pharmacy, University of Otago, New Zealand

ARTICLE INFO

Article history:

Received 16 October 2008

Received in revised form 20 February 2009

Accepted 6 March 2009

Available online xxx

Keywords:

Solid lipid extrusion

Glycerides

Polymorphism

Dissolution

Physical stability

Solid-state behaviour

ABSTRACT

A monoacid triglyceride and a partial glyceride were extruded below their melting ranges alone and together in different mixture ratios to investigate the influence of the chemical composition of the lipid matrix on the solid-state properties and dissolution characteristics. The partial glyceride exhibits a faster release of the drug compared to the triglyceride due to its surfactant properties. The lipid mixtures show rather complex solid-state behaviour and hence unexpected dissolution characteristics. Adding 10% (w/w) partial glyceride to a triglyceride matrix led to increased incidence of the unstable α -form of the triglyceride leading to recrystallization of the stable β -form over time which causes fractal structures on the extrudate surface which decrease the dissolution rate. Adding 50% (w/w) partial glyceride to the triglyceride matrix also results in tristearin α -formation subsequently followed by recrystallization to the β -form. But as 50% of the matrix consists of the partial glyceride the dissolution rate was faster than the rate obtained by pure triglyceride or the 9 + 1 (w/w) mixture of triglyceride and partial glyceride. The results of this study help in understanding the complex solid-state behaviour of solid lipid extrudates with different composition and to manufacture suitable lipid-based oral dosage forms.

© 2009 Elsevier B.V. All rights reserved.

1. Introduction

The application of lipids as excipients for the processing of oral dosage forms is widespread in the field of pharmaceutical sciences. Due to their versatile structural appearance they offer a wide range of different possibilities for pharmaceutical formulation purposes. Furthermore, these substances are biodegradable and physiologically non-toxic. Lipids can be used to enhance solubility and permeability of drugs exhibiting poor bioavailability (Humberstone and Charman, 1997; Prabhu et al., 2005; Porter and Charman, 2001) to realize prolonged release (Hamdani et al., 2002) and to achieve taste masking (Qi et al., 2008).

Several techniques are established for processing lipid-based dosage forms and they are solvent free and do not involve drying steps. Either thermal or mechanical energy or a combination of both is used to produce the dosage form (Zhang and Schwartz, 2003; Liu et al., 2001; Chauhan et al., 2005). Generally, the production of lipid dosage forms involves melting the lipid and resolidification in combination with a solid active pharmaceutical ingredient (API) to form a coherent matrix in which the API is embedded. A relatively new

approach to process lipid-based dosage forms is solid lipid extrusion (Pinto and Silverio, 2001; Breitzkreutz et al., 2003; Windbergs et al., 2009). This technique uses lipids in powdered form available as pharmaceutical excipients like Dynasan[®] which are blended with the API and extruded through an extruder below the lipid melting temperature, thus avoiding melting of the complete lipid mass. In a further step the extrudates are either spheronized to pellets or cut into cylindrical pieces of suitable size (Reitz and Kleinebudde, 2007). The choice of manufacturing technology strongly influences the subsequent properties of the dosage form as surface structure, crystallinity, stability and reproducibility.

There are some difficulties in the processing of lipid-based dosage forms. Due to their versatile structure, they exhibit rather complex solid-state behaviour. Usually lipids exhibit three different polymorphic modifications: the thermodynamic least stable α -form, the metastable β' -form and the stable β -form (Sato, 2001; Sato et al., 1999). Each of these forms is defined by a specific packing mode of the fatty acid chains, with the stable β -form exhibiting the densest packing mode. Transformations from a less stable to a more stable form can occur. Therefore, the processing of lipid-based dosage forms is often accompanied by transformations, melting events and recrystallization. Furthermore, the processed dosage forms often show transformations during storage, which finally affect the dissolution behaviour (Choy et al., 2005). This effect in

* Corresponding author.

E-mail address: kleinebudde@uni-duesseldorf.de (P. Kleinebudde).

the literature often called "aging" is mostly due to the appearance of a metastable lipid modification during processing which eventually transforms to a more stable modification during storage (Whittam and Rosano, 1975; Sutananta et al., 1994). These effects might result in alterations of the drug release. Therefore, the solid-state behaviour of lipids during processing and its relationship to drug release and storage is quite difficult to predict.

The aim of this study is to modify the composition of a lipid matrix under controlled conditions in order to develop solid lipid extrudates with tailor-made dissolution profiles. Furthermore, the solid-state behaviour of the glycerides that are used should be understood for the production of dosage forms according to the Quality by Design approach. Based on the results of studies done on pure triglycerides (Windbergs et al., 2009) a partial glyceride was extruded alone and in different ratios with a triglyceride to evaluate the effect of the lipid matrix composition and possible interactions between either the lipids or matrix components and API. Solid-state analysis was conducted on the powders and on the extrudates using a combination of DSC, XRPD, contact angle measurements and ATR-IR spectroscopy. In addition, dissolution testing and storage experiments were performed.

2. Materials and methods

2.1. Materials

The following powdered glycerides were provided by Sasol (Witten, Germany) and were used as received: tristearin (Dynasan 118®) and glyceryl monostearate (Imwitor 491®). Tristearin is a monoacid triglyceride which is 98% pure, whereas glyceryl monostearate is a partial glyceride consisting of 96% monoglycerides. Theophylline anhydrate (BASF, Ludwigshafen, Germany) was used as a model drug in powdered form as supplied. Each of the crystal forms was verified by X-ray powder diffraction and where possible compared to the theoretical patterns provided by the Cambridge Structural Database (Cambridge Crystallographic Data Centre (CCDC), Cambridge, United Kingdom) with the associated software Mercury (v. 1.5). The ref codes for the crystal structures used were: BAPLOT01 (theophylline anhydrate) and QOYKIY (tristearin β -form). All lipid powders were in their stable β -form before processing. The particle sizes were determined with laser diffraction and the following results were obtained: tristearin $x^{50} = 27 \mu\text{m}$, $x^{90} = 90 \mu\text{m}$; glyceryl monostearate $x^{50} = 316 \mu\text{m}$, $x^{90} = 556 \mu\text{m}$; theophylline anhydrate $x^{50} = 94 \mu\text{m}$, $x^{90} = 288 \mu\text{m}$ taking the mean of three measurements.

2.2. Methods

2.2.1. Extrusion

The powdered glycerides in different ratios were weighed in a 1:1 ratio with theophylline anhydrate and then blended in a laboratory mixer (LM20 Bohle, Ennigerloh, Germany) for 15 min at 25 rpm. A gravimetric dosing device (KT20 K-Tron Soder, Lenzhard, Switzerland) fed the powder mixtures into the barrel of a co-rotating twin-screw extruder (Mikro 27GL-28D, Leistritz, Nürnberg, Germany). Extrusion was performed with a constant screw speed of 30 rpm and a feeding rate of 40 g min⁻¹. The processing temperature was either 55 °C or 65 °C with both temperatures below the melting temperature of the excipients. The extruder die plate contained 23 holes of 1 mm diameter and 2.5 mm length.

2.2.2. Differential scanning calorimetry (DSC)

For DSC experiments a DSC 821e calorimeter (Mettler-Toledo, Gießen, Germany) was used. The heating rate was

10 °C min⁻¹ within a temperature range of 20–300 °C. Hermetically sealed aluminium pans (40 μl) were used containing samples of approximately 5 mg each. All experiments were conducted twice.

2.2.3. X-ray powder diffraction (XRPD)

A theta-theta X-ray powder diffractometer (D8 Advance, Bruker AXS GmbH, Karlsruhe, Germany) was used for XRPD analysis. The measurements were performed in symmetrical reflection mode with CuK α radiation ($\lambda = 1.54 \text{ \AA}$) using Göbel mirror bent multilayer optics. The angular range measured was 5–40° (2 θ), with a step size of 0.05° (2 θ) and a measuring time of 1 s per step. The samples were gently compressed in the sample holders to obtain a smooth and flat surface. All experiments were conducted in triplicate. With the same diffractometer variable temperature measurements were performed in the temperature range of 25 °C up to the melting temperatures of the individual lipids.

2.2.4. Attenuated total reflectance infrared (ATR-IR) spectroscopy

For these experiments an FTIR spectrometer (Bruker FTIR Vertex 70, Bruker, Ettlingen, Germany) with an ATR accessory fitted with a single reflection diamond/ZnSe crystal plate (MIRacle ATR, PIKE Technologies, Madison, WI, USA) was used. Spectra were collected of powder or extrudate between 4000 and 650 cm⁻¹ at a resolution of 4 cm⁻¹ and using an average of 64 scans for each spectrum. All experiments were conducted in triplicate.

2.2.5. Dissolution

A basket apparatus (Sotax AT7 smart, Sotax, Lörrach, Germany) in accordance with the USP29 Method 1 was used for dissolution experiments. For each vessel a sample size of 140 mg was used consisting of extrudates cut to approximately 1 cm. Experiments were performed in purified water containing 0.001% polysorbate 20 as a dissolution medium. The temperature was kept at 37 \pm 0.5 °C and the stirring speed was 50 rpm. The absorption of the dissolution medium was measured using the absorption wavelength of 242 nm in 2.5 min intervals using a UV-Vis spectrometer (Lambda 40, Perkin-Elmer, Rodgau-Juegesheim, Germany) in a continuous flow-through cuvette. Each experiment was conducted in triplicate and for the dissolution curve the mean was calculated. The standard deviation of the replicates was below 2%.

2.2.6. Storage

Samples were placed in open Petri dishes and exposed to accelerated constant climatic conditions (40 °C/75%RH) for 12 months in a climate chamber (KBF 240, Binder, Tuttlingen, Germany).

2.2.7. Scanning electron microscopy (SEM)

SEM micrographs were recorded with a working voltage of 20 kV using a scanning electron microscope (Leo 1430VP, Leo Elektron Microscopy, Cambridge, UK). Samples were mounted on aluminium stubs using double-sided carbon tape and sputter-coated with gold for 150 s (Agar Manual Sputter Coater B7340, Agar Scientific, Stansted, UK).

2.2.8. Contact angle measurements

Contact angle measurements were performed with an optical contact angle meter (Drop shape analysis system DSA100, Krüss, Hamburg, Germany). A 0.8 μl drop of distilled water was placed on the extrudate surface and the contact angle was directly determined by using the associated software (Drop shape analysis DSA1 v 1.90, Hamburg, Germany). For each sample eight measurements were performed and the mean was calculated.

3. Results and discussion

3.1. Extrusion and solid-state characterization of triglycerides

As shown in a previous paper (Windbergs et al., 2009) triglycerides provide a suitable matrix for oral dosage forms. However, a good understanding and appropriate monitoring of the solid-state formation is mandatory to obtain reliable dosage forms. The solid-state behaviour during processing and storage is quite complex and difficult to predict. The combination of friction and temperature during the extrusion process was found to influence the solid-state formation to a large extent. Tristearin, for instance, partly forms the metastable α -form at a processing temperature of 55 °C, whereas at a production temperature of 65 °C only the stable β -form is obtained. In the thermogram depicted in Fig. 1 relevant melting endotherms can be found at 70.7 °C (onset tristearin β -form) and at 50.2 °C (onset tristearin α -form) (Hagemann, 1988). Interaction with the model drug theophylline anhydrate was not observed as the endotherms in the DSC thermograms depict. Lipid as well as drug (onset melting endotherm 271.1 °C) provide sharp and clearly defined melting peaks (Chen et al., 1997).

3.2. Extrusion and solid-state characterization of partial glycerides

A partial glyceride was investigated with respect to its suitability as matrix material for solid lipid extrudates. For the solid-state characterization a combination of DSC, XRPD and ATR-IR spectroscopy was used to monitor solid-state changes in powders and extrudates. The partial glyceride glyceryl monostearate consists of 96% monoglycerides exhibiting a reported melting temperature of 77–83 °C for the stable β -form (Hagemann, 1988). Extrudates were obtained with processing temperatures of 50, 55, 62 and 65 °C. The smoothest extrudates were achieved at 65 °C. Fig. 2 depicts the analytical results obtained for the powder compared to extrudates produced at different temperatures. XRPD diffractograms suggest that the powder exists in the β -form as their peak positions (Fig. 2) did not change irrespective of extrusion temperatures. The stable β -form of the lipid was maintained (Yajima et al., 2002). Minor differences in peak intensity are due to orientation effects of the crystals. Therefore the lipid remains in a stable conformation after processing.

Adding 50% (w/w) theophylline anhydrate as a model drug led to interesting results. The DSC thermograms of the pure powders and the extrudate consisting of lipid and drug (50% w/w) (Fig. 3a) show

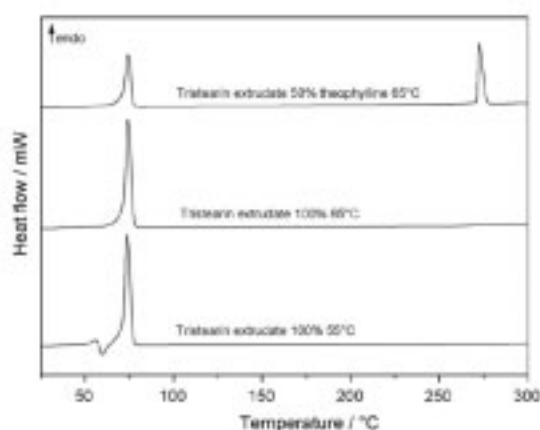


Fig. 1. DSC thermograms of tristearin extrudates.

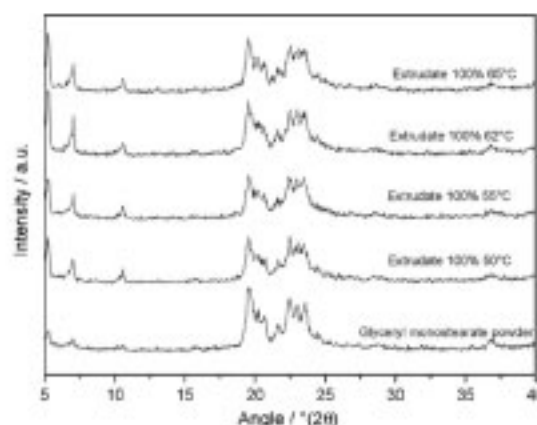


Fig. 2. XRPD patterns of glyceryl monostearate powders and extrudates.

a limited interaction between lipid and drug. In the thermogram depicting the results for the extrudate the lipid is characterized by its clear melting peak (onset 76 °C) whereas the drug shows a broad endotherm (onset 250 °C) instead of the sharp melting peak observed for the pure drug powder (onset 270.7 °C). Due to the surfactant properties of glyceryl monostearate the drug is able to partially dissolve into the molten lipid when the melting temperature of the lipid is exceeded during the measurement. The XRPD and ATR-IR spectra indicate that the crystalline structures of lipid and drug in the extrudate remain intact (Fig. 3b,c). In the XRPD pattern the drug in the extrudate exhibits the same peak positions (at 7.1° (2 θ) and 12.6° (2 θ)) as in the powder, and therefore one can conclude that no polymorphic changes have occurred. Furthermore, the ATR-IR spectra suggest no solid-state changes as the peaks specific to theophylline anhydrate, such as the C=O stretching (1665 and 1713 cm^{-1}) and CH stretching (3122 cm^{-1}), remain unchanged (Nolasco et al., 2006; Kobayashi, 1988). The lipid exhibits several characteristic peaks such as those due to CH₂ scissoring (1473 cm^{-1}) and C=O stretching (1735 cm^{-1}) (Yano and Sato, 1999).

From these results it can be summarised that extrudates could be produced in the chosen temperature range without undergoing solid-state transformations as a result of processing. The crystal structure of the drug was unchanged, but DSC thermograms were able to indicate a limited interaction between drug and lipid during the measurement.

3.3. Extrusion and solid-state characterization of mixtures of a triglyceride and a partial glyceride

To investigate the impact of composition of the lipid matrix structure powder mixtures of tristearin and glyceryl monostearate were prepared in two different weight ratios (9+1 and 5+5 w/w). The 9+1 mixture was extruded at 55 and 65 °C. As the results of the solid-state analysis at the different temperatures led to the same results the 5+5 (w/w) mixture was only extruded at 65 °C.

Fig. 4a depicts the DSC thermograms of the lipid powders and the extrudates of the mixture tristearin/glyceryl monostearate (9+1 w/w) at two different processing temperatures. As the melting peaks of the pure powders (both β -form) are quite close to each other, they only form one melting peak due to the β -form in the extruded mixture (onset 70 °C). In addition, there is a small melting peak at 50.2° in the extrudates which is due to the metastable α -form of tristearin (Hagemann, 1988). At a processing temperature of 55 °C this phenomenon can also be found for the pure tristearin extrudate (Fig. 1) as this extrusion temperature leads

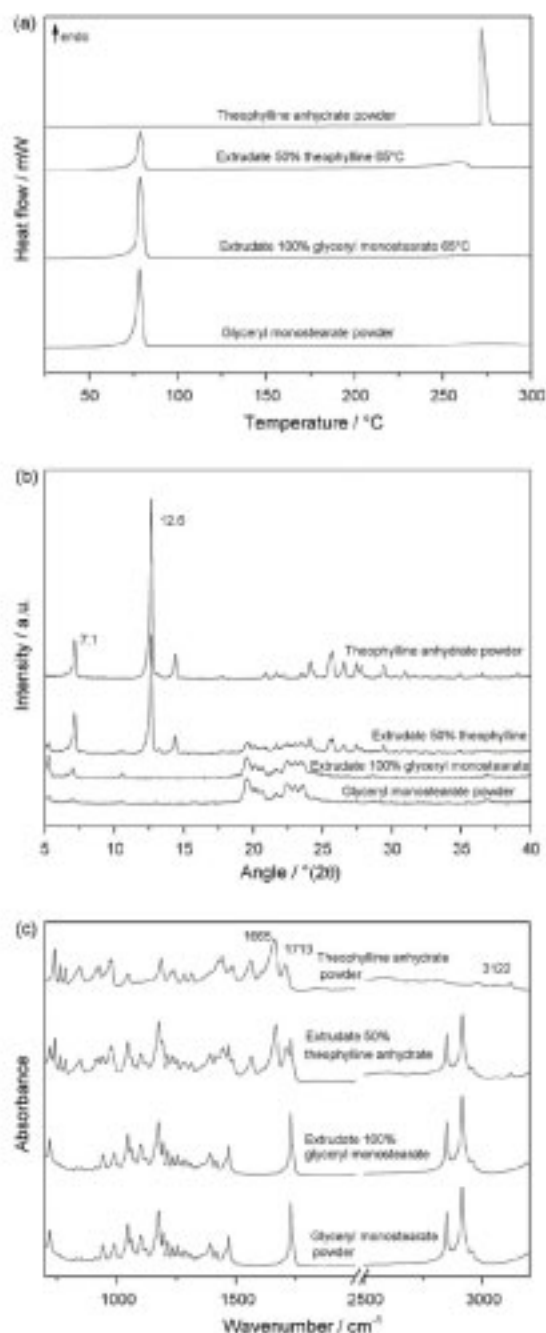


Fig. 3. Physical characterization of glyceryl monostearate and theophylline powder and extrudates (a) DSC thermograms, (b) XRPD patterns and (c) ATR-IR spectra.

to a partial solid-state transformation of tristearin (Windbergs et al., 2009). Small parts of the lipid mass melt during the extrusion process induced by a combination of friction and temperature. The temperature at which the extrudate leaves the extruder determines whether the molten parts recrystallize in the metastable α -form or directly in the stable β -form. For pure tristearin extru-

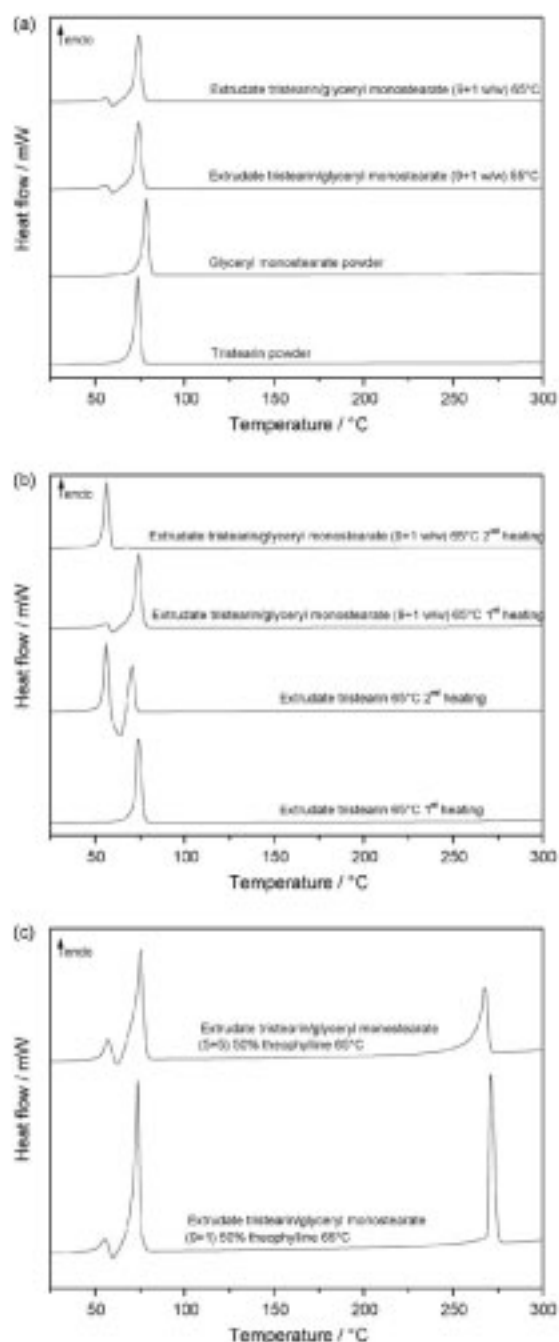


Fig. 4. DSC thermograms of tristearin and glyceryl monostearate (a) powders and extrudates, (b) different heating schemes and (c) mixed extrudates with drug.

dates only the β -form is obtained at a processing temperature of 65 °C [Fig. 1].

When the tristearin is extruded with glyceryl monostearate, the α -form is also obtained at a processing temperature of 65 °C. Modifying the DSC measurements led to a deeper insight into these solid-state phenomena. The DSC samples were measured once (1st

heating), then stored for 24 h in ambient conditions and measured again (2nd heating). The results are shown in Fig. 4b. During the first measurement the samples melt completely, and therefore the results of the second measurements depict the thermograms of the recrystallized melts. By comparing the pure tristearin to the mixed sample it becomes quite obvious that the presence of the partial glyceride, glyceryl monostearate, hinders the formation of the tristearin β -form, which is consistent with previous findings (Garti et al., 1988). Glyceryl monostearate is able to stabilize the α -form of tristearin and prevent or delay the transformation to the stable β -form.

The chemical structure of glyceryl monostearate exhibits some comparability with the tristearin structure and therefore it is likely that some formation of structures that combine both tristearin and glyceryl monostearate occurs, which appears to promote the formation of the α -form (Garti, 1988). In the food industry especially in the chocolate manufacturing this effect is deliberately used to prevent crystallization of cocoa butter to the stable polymorph of cocoa butter as it lacks gloss and is aesthetically unappealing (Schlichter-Aronhime and Garti, 1988). The melt of the pure tristearin extrudate recrystallizes in a mixture of α - (onset 53.5 °C) and β -forms (onset 67 °C). The two melting endotherms are connected by a recrystallization exotherm (onset 58.8 °C) which is due to the metastable β -form. Unfortunately, melting of the β -form cannot be detected

properly as it is severely suppressed by the recrystallization to the stable β -form (Kellens et al., 1991). The second measurement of the mixed matrix sample depicts almost completely the α -form of tristearin (onset 53.5 °C). To test the observed correlation between the presence of the partial glyceride and the effect on solid-state behaviour, two mixing ratios of the lipids were compared (Fig. 5c). As can be seen from the thermogram the quantity of tristearin α -form in the extrudate and the intensity of the interaction with the drug can both be correlated to the amount of glyceryl monostearate in the mixture. The comparison of the two tristearin α -form endotherms (onset 52.8 °C) shows that even though the amount of tristearin is lower in the 5+5 mixture, the intensity of the α -form peak is higher than in the 9+1 mixture. The extent of the interaction between glyceryl monostearate and drug can be seen in the intensity of the drug melting endotherm. In the 9+1 mixture the peak is sharp and clear (onset 269.3 °C) whereas the peak in the 5+5 mixture is much broader and less defined (onset 263.7 °C) indicating the increased interaction with glyceryl monostearate.

To test the hypothesis that the tristearin α -form in the lipid mixture is only formed via the melt powder mixtures of tristearin and glyceryl monostearate (9+1 and 5+5) were prepared and diffractograms were taken while heating the samples up from 25 to 75 °C in 5 °C steps (Fig. 5a and b). There was no evidence of any solid-state changes until the sample melted completely as can be seen from the diffractograms.

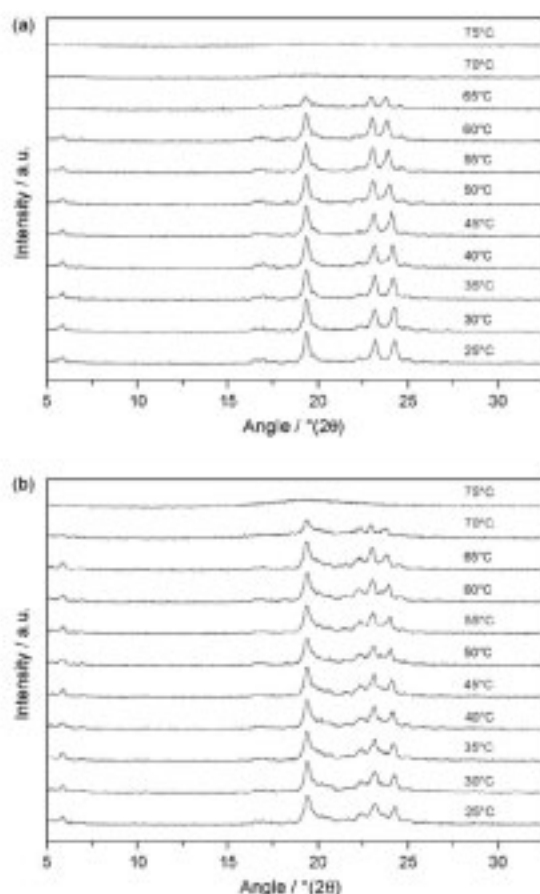


Fig. 5. Variable temperature XRPD patterns of physical powder mixtures (a) tristearin/glyceryl monostearate (9+1 w/w) and (b) tristearin/glyceryl monostearate (5+5 w/w).

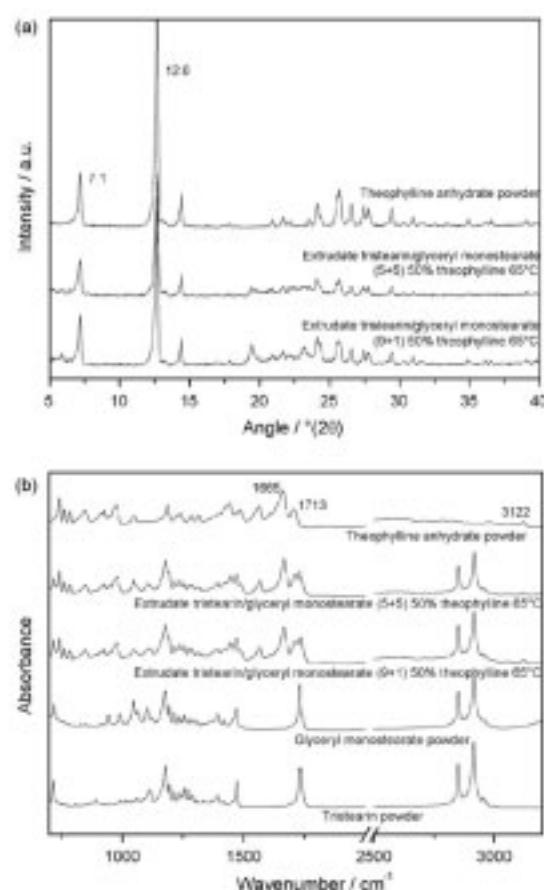


Fig. 6. Physicochemical characterization of powders and mixed extrudates of tristearin and glyceryl monostearate (a) XRPD patterns and (b) ATR-IR spectra.

Fig. 6 displays the results obtained with XRPD and ATR-IR measurements. For both mixing ratios of the two lipids in the extrudates the XRPD peaks for the drug and lipid are obvious (Fig. 6a). ATR-IR spectra (Fig. 6b) support the XRPD results. The crystalline structure of the lipids and the drug is maintained.

3.4. Surface characterization

The surface of solid lipid extrudates is very important with regard to the dissolution behaviour as the dissolution from glyceride matrices is completely diffusion controlled. Thus, the matrix stays intact and no erosion occurs. The surface of the processed extrudates was investigated using SEM and contact angle measurements.

The SEM images (Fig. 7) provide visual support for the results already obtained with solid-state analysis. The surface of extrudates containing 50% (w/w) theophylline anhydrate was investigated. The extrudates consisting of glyceryl monostearate exhibit a rather smooth surface. The contact angle of 106° is in good agreement with the SEM image (Fig. 7a) (Fang et al., 2007). Fig. 7b depicts the surface of a tristearin/glyceryl monostearate (5+5 w/w) extrudate. The surface is also smooth but the higher contact angle of 116° is due to the triglyceride which reduces the surfactant effect of the partial glyceride glyceryl monostearate. The extrudate consisting of tristearin (manufactured at 65°C) exhibits a contact angle of 121° and a relatively smooth surface (Fig. 7c). As a comparison Fig. 7d depicts an extrudate consisting of tristearin and glyceryl monostearate (9+1 w/w) produced at 65°C which should be expected to possess a reduced contact angle due to the surfactant properties of the partial glyceride glyceryl monostearate. But Fig. 7d depicts

an extrudate surface exhibiting needle-like structures. This phenomenon, sometimes called blooming, is due to the transformation from the unstable tristearin α -form to the stable β -form (Khan and Craig, 2004). This effect is intensified at a processing temperature of 55°C . Fig. 7e depicts the surface of the tristearin extrudates whereas Fig. 7f depicts the surface of the tristearin/glyceryl monostearate (9+1 w/w) mixed extrudate. The surface of both extrudates is completely covered with sharp needles possessing a contact angle of 125° in both cases. As the contact angle is a predictor of the wettability it is quite obvious that the needles at the extrudate surface strongly affect the dissolution behaviour.

3.5. Dissolution

As already stated the dissolution from solid lipid matrices is purely diffusion controlled. Fig. 8 depicts the dissolution characteristics of the processed batches. The surfactant properties of the pure partial glyceride matrix made of glyceryl monostearate lead to the fastest release of the drug compared to the other batches. The 50% tristearin and 50% glyceryl monostearate matrix materials exhibit a release curve between those of the pure triglyceride and pure partial glyceride. Even though the partial glyceride portion results in a pronounced recrystallization of the tristearin to the unstable α -form during extrusion which is followed by transformation to the β -form, the release of theophylline anhydrate is faster than from the pure tristearin extrudate due to the surfactant properties of the partial glyceride. By comparing the pure tristearin matrices produced at different extrusion temperatures with the tristearin (90%) and glyceryl monostearate (10%) mixture produced at the same temperatures two key factors can be identified. On the one

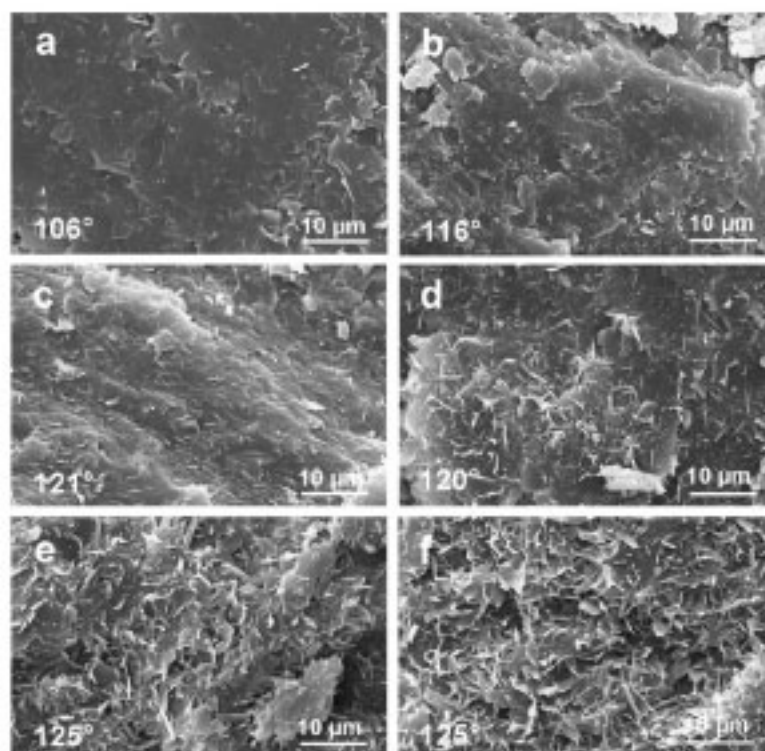


Fig. 7. SEM images of extrudate surfaces containing 50% theophylline anhydrate produced at different temperatures (a) glyceryl monostearate 65°C , (b) tristearin/glyceryl monostearate (5+5 w/w) 65°C , (c) tristearin 65°C , (d) tristearin/glyceryl monostearate (9+1 w/w) 65°C , (e) tristearin 55°C and (f) tristearin/glyceryl monostearate (9+1 w/w) 55°C .

Please cite this article in press as: Windbergs, M., et al., Influence of the composition of glycerides on the solid-state behaviour and the dissolution profiles of solid lipid extrudates. *Int. J. Pharm.* (2009), doi:10.1016/j.ijpharm.2009.03.002

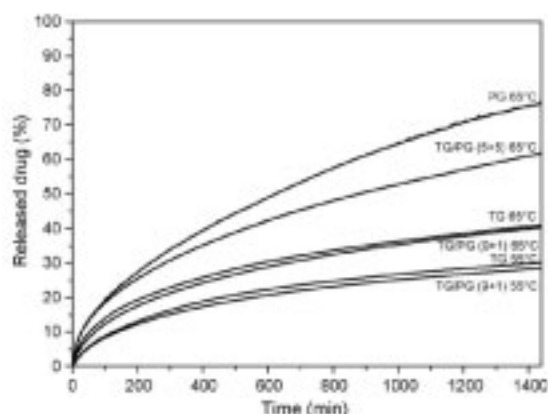


Fig. 8. Dissolution profiles of different lipids and their mixtures at different extrusion temperatures (TG, triglyceride tristearin; PG, partial glyceride glyceryl monostearate) ($n=3$, SD <2% not shown).

hand the batches produced at 55 °C exhibit a significantly slower drug release than the batches produced at 65 °C. On the other hand the drug dissolution from the 9+1 (w/w) mixtures is slower than from the pure tristearin matrix which is unexpected on first glance

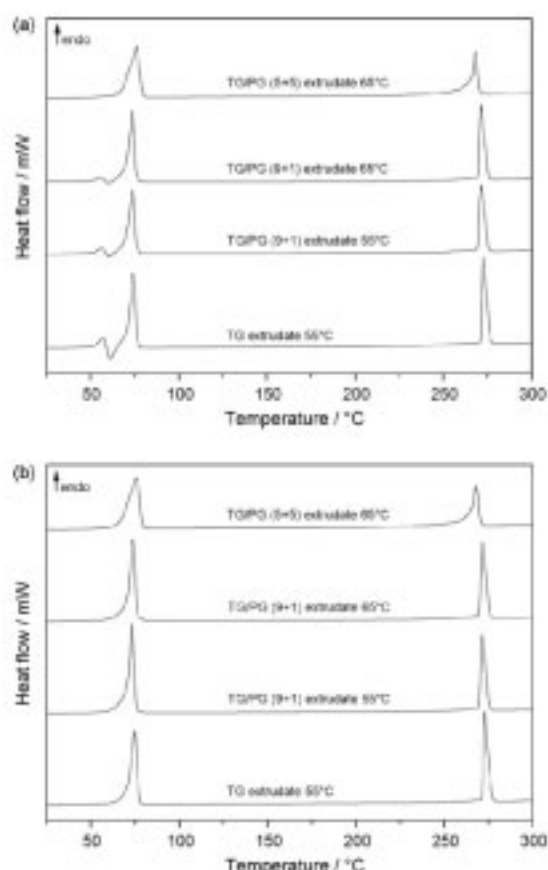


Fig. 9. Storage stability of solid lipid extrudates (a) one year at room conditions and (b) one year at 40 °C/75%RH.

regardless of extrusion temperature. The mixed matrix would be expected to show a faster release due to the surfactant properties of the partial glyceride. In this case these surfactant properties are overcome by the recrystallized β -form creating fractal structures on the surface of the extrudate that impair the wettability of the extrudate by the dissolution medium and hence reduce the release of the drug.

3.6. Storage stability

Storage experiments were performed in two different climate conditions (ambient condition and 40 °C at 75%RH) for 12 months. Samples were investigated using DSC. Fig. 9a depicts the thermograms for the samples stored at ambient conditions. The tristearin extrudate produced at 55 °C and the mixed extrudates 9+1 (w/w) produced at both extrusion temperatures both still contain a small portion of tristearin α -form. In the 5+5 (w/w) mixed extrudates after one year only the tristearin β -form exists, the recrystallization process from the metastable α -form to the stable β -form is already completed. The molecular mobility in this matrix compared to the 9+1 (w/w) matrix is increased which might facilitate the restructuring of the stable β -form. In comparison all the samples stored at 40 °C and 75%RH for one year exhibit only the stable tristearin β -form, and thus the transformation process is already completed. The results show the strong temperature dependency of the transformation from tristearin α -form to β -form.

4. Conclusions

The chemical composition of glycerides used for the manufacturing of solid lipid extrudates was found to have a large influence on the solid-state behaviour and dissolution profiles. Due to its surfactant properties the partial glyceride exhibits a faster release of the drug compared to the triglyceride. In different mixtures of both lipids the partial glyceride led to increased incidence of the unstable α -form of the triglyceride leading to recrystallization of the stable β -form over time which causes fractal structures on the extrudate surface deteriorating the dissolution properties. Storage experiments under accelerated and ambient conditions revealed a strong influence of temperature on the recrystallization kinetics. The results of this study help to elucidate the complex solid-state behaviour of solid lipid extrudates with different compositions which facilitates the development of suitable lipid-based oral dosage forms with desired dissolution characteristics.

Acknowledgements

The Marie Curie Fellowship and the Galenos Network are acknowledged for financial support (MEST-CT-2004-404992). The Sasol GmbH is acknowledged for generous provision of the lipids.

References

- Breitkreutz, J., El Saleh, F., Kiera, C., Kleinschäfer, P., Wiedry, W., 2003. Pediatric drug formulations of sodium benzoate. II. Coated granules with a lipophilic binder. *Eur. J. Pharm. Biopharm.* 56, 255–260.
- Chauhan, B., Shimpi, S., Paradkar, A., 2005. Preparation and characterization of etoricoxib solid dispersions using lipid carriers by spray drying technique. *AAFS Pharm. Sci. Tech.* 6, E405–E412.
- Chen, W., Zhang, X., Shan, B., You, X., 1997. Methylxanthines. I. Anhydrous theophylline. *Acta Cryst.* C53, 777–779.
- Choy, Y.W., Khan, N., Yuen, J.H., 2005. Significance of lipid matrix aging on in vitro release and in vivo bioavailability. *Int. J. Pharm.* 299, 55–64.
- Fang, W., Mayama, H., Tsujii, K., 2007. Spontaneous formation of fractal structures on triglyceride surfaces with reference to their water-repellent properties. *J. Phys. Chem. B* 111, 564–571.
- Garb, N., Schlichter, J., Sarig, S., 1988. DSC studies concerning polymorphism of saturated monacid triglycerides in the presence of food emulsifiers. *Fat Sci. Technol.* 9, 295–298.

G Model

[P-30549; No. of Pages 8]

ARTICLE IN PRESS

8

M. Windbergs et al. / *International Journal of Pharmaceutics* xxx (2009) xxx–xxx

- Garti, N., 1988. Effects of surfactants on crystallization and polymorphic transformation of fats and fatty acids. In: Garti, N., Sato, K. (Eds.), *Crystallization and Polymorphism of Fats and Fatty Acids*. Marcel Dekker, New York, pp. 207–303.
- Hamdani, J., Moes, A.J., Amighi, K., 2002. Development and evaluation of prolonged release pellets obtained by the melt pelletization process. *Int. J. Pharm.* 245, 167–177.
- Hagemann, J.W., 1988. Thermal behaviour and polymorphism of acylglycerides. In: Garti, N., Sato, K. (Eds.), *Crystallization and Polymorphism of Fats and Fatty Acids*. Marcel Dekker, New York, pp. 9–95.
- Humberstone, A.J., Charman, W.N., 1997. Lipid based vehicles for the oral delivery of poorly water soluble drugs. *Adv. Drug Deliv. Rev.* 25, 103–128.
- Kellens, M., Meunier, W., Gebhe, R., Roymaers, H., 1993. Synchrotron radiation investigations of the polymorphic transitions of saturated monoacid triglycerides. Part I: Tripalmitin and tristearin. *Chem. Phys. Lipids* 58, 131–144.
- Khan, N., Craig, D.Q.M., 2004. Role of blooming in determining the storage stability of lipid-based dosage forms. *J. Pharm. Sci.* 93, 2962–2971.
- Kobayashi, M., 1988. Vibrational spectroscopic aspects of polymorphism and phase transition of fats and fatty acids. In: Garti, N., Sato, K. (Eds.), *Crystallization and Polymorphism of Fats and Fatty Acids*. Marcel Dekker, New York, pp. 139–187.
- Liu, J., Zhang, F., McGinity, J.W., 2001. Properties of lipophilic matrix tablets containing phenylpropranolamine hydrochloride prepared by hot-melt extrusion. *Eur. J. Pharm. Biopharm.* 52, 181–190.
- Nolasco, M.M., Amado, A.M., Ribeiro-Claio, P.J.A., 2006. Computationally-assisted approach to the vibrational spectra of molecular crystals: study of hydrogen-bonding and pseudo-polymorphism. *Chem. Phys. Chem.* 7, 2150–2161.
- Prata, J.F., Sanches, N.P., 2001. Assessment of the extrudability of three different mixtures of saturated polyglycerol glycerides by determination of the “specific work of extrusion” and capillary rheometry. *Pharm. Dev. Technol.* 6, 117–128.
- Porter, C.J.H., Charman, W.N., 2001. In vitro assessment of oral lipid based formulations. *Adv. Drug Deliv. Rev.* 50, 127–147.
- Prabha, S., Ortega, M., Ma, C., 2005. Novel lipid-based formulations enhancing the in vitro dissolution and permeability characteristics of a poorly water-soluble model drug, piroxicam. *Int. J. Pharm.* 301, 209–216.
- Qi, S., Deutsch, D., Craig, D.Q., 2008. An investigation into the mechanisms of drug release from taste-masking fatty acid microspheres. *J. Pharm. Sci.* 97, 3842–3854.
- Reitz, C., Kleinbuddie, P., 2007. Solid lipid extrusion of sustained release dosage forms. *Eur. J. Pharm. Biopharm.* 67, 440–448.
- Sato, K., 2001. Crystallization behaviour of fats and lipids—A review. *Chem. Eng. Sci.* 56, 2255–2265.
- Sato, K., Ueno, S., Yano, J., 1990. Molecular interactions and kinetic properties of fats. *Prog. Lipid Res.* 29, 91–136.
- Schlichter-Aronhime, J., Garti, N., 1988. Solidification and polymorphism in cacao butter and the blooming problems. In: Garti, N., Sato, K. (Eds.), *Crystallization and Polymorphism of Fats and Fatty Acids*. Marcel Dekker, New York, pp. 363–383.
- Sutarsanta, W., Craig, D.Q.M., Newton, J.M., 2004. The effects of aging on the thermal behaviour and mechanical properties of pharmaceutical glycerides. *Int. J. Pharm.* 271, 51–62.
- Whitram, J.H., Rosano, H.L., 1975. Physical aging of even saturated monoacid triglycerides. *J. Am. Oil Chem. Soc.* 52, 128–133.
- Windbergs, M., Strachan, C.J., Kleinbuddie, P., 2009. Understanding the solid-state behaviour of triglyceride solid lipid extrudates and its influence on dissolution. *Eur. J. Pharm. Biopharm.* 71, 80–87.
- Yano, J., Sato, K., 1999. FT-IR studies on polymorphism of fats: molecular structures and interactions. *Food Res. Int.* 32, 249–258.
- Yajima, T., Hat, S., Takemichi, H., Kawahara, Y., 2002. Determination of optimum processing temperature for transformation of glyceryl monostearate. *Chem. Pharm. Bull.* 50, 1430–1433.
- Zhang, Y.E., Schwartz, J.B., 2003. Melt granulation and heat treatment for wax matrix-controlled drug release. *Drug Dev. Ind. Pharm.* 29, 131–138.

Please cite this article in press as: Windbergs, M., et al., Influence of the composition of glycerides on the solid-state behaviour and the dissolution profiles of solid lipid extrudates. *Int. J. Pharm.* (2009), doi:10.1016/j.ijpharm.2009.03.002

9.3. Article 3: Investigating the principles of recrystallization from glyceride melts

Investigating the principles of recrystallization from glyceride melts

Maike Windbergs^{a,b,c}, Clare J. Strachan^{b,d}, Peter Kleinebudde^{a*}

^aInstitute of Pharmaceutics and Biopharmaceutics, Heinrich-Heine-University, Düsseldorf, Germany

^bCentre for Drug Research, University of Helsinki, Helsinki, Finland

^cDivision of Pharmaceutical Technology, Faculty of Pharmacy, Helsinki, Finland

^dSchool of Pharmacy, University of Otago, Dunedin, New Zealand

*Corresponding author:

Peter Kleinebudde

Postal address: Institute of Pharmaceutics and Biopharmaceutics, Heinrich-Heine-University, Universitaetsstr. 1, 40225 Duesseldorf, Germany

Telephone: +49 211 81 14220

Fax: +49 211 81 14251

Email: kleinebudde@uni-duesseldorf.de

ABSTRACT

Different lipids were melted and resolidified as model systems to gain deeper insight into the principles of recrystallization processes in lipid-based dosage forms. Solid-state characterization was performed on the samples with differential scanning calorimetry and X-ray powder diffraction. Several recrystallization processes could be identified during storage of the lipid layers. Pure triglycerides that generally crystallize to the metastable α -form from the melt followed by a recrystallization process to the stable β -form with time showed a chain-length dependant behaviour during storage. With increasing chain length the recrystallization to the stable β -form was decelerated. Partial glycerides exhibited a more complex recrystallization behaviour due the fact that these substances are less homogenous. Mixtures of a long-chain triglyceride and a partial glyceride showed evidence of some interaction between the two components as the partial glyceride hindered the recrystallization of the triglyceride to the stable β -form. In addition, the extent of this phenomenon depended on the amount of partial glyceride in the mixture. Based on these results changes in solid dosage forms based on glycerides during processing and storage can be better understood.

KEYWORDS

Lipids, recrystallization, polymorphism, triglycerides, partial glycerides

INTRODUCTION

During the last decade there has been increased interest in lipids for the formulation of pharmaceutical dosage forms¹. The high variability in their structure and therefore versatile physico-chemical properties offer various possibilities for the production of different dosage forms. Several systems for the delivery of drugs have already been introduced into the market, with their characteristics depending on both the choice of lipid and processing technique. As one of the first attempts, capsules were filled with liquid or semi-solid lipid formulations in which the active pharmaceutical ingredient (API) is either suspended or dissolved^{2,3}. Solid particles can be produced with a variety of different methods including melt extrusion⁴, melt granulation^{5,6}, spray cooling⁷ or spray drying⁸. The resulting particles can either be processed into tablets or filled into capsules. Additional established systems are solid lipid nanoparticles⁹ and nanostructured lipid carriers¹⁰ which can be produced by different techniques. In general, each of the techniques mentioned above involves complete or almost complete melting of the lipid followed by resolidification in most cases. There is also a relatively new approach for the formulation of lipid-based dosage forms called solid lipid extrusion, in which the lipid remains mostly solid during processing^{11,12,13}.

The advantages of lipid-based formulations include the possibility of prolonged release¹⁴ as well as enhancement of solubility and permeability for APIs exhibiting poor bioavailability^{15,16}. As the majority of newly developed chemical entities have poor solubility and permeability¹⁷, bioavailability enhancement is increasingly important. Furthermore, taste masking and protection of sensitive APIs is possible with the help of lipids as excipients¹⁸. In addition, lipids are biodegradable and physiologically non-toxic.

Lipid-based dosage forms can exhibit stability problems associated with complex solid-state behaviour¹⁹. In general, three polymorphic forms are characteristic for lipids, in which the fatty acid chains exhibit different packing modes and consequent thermodynamic energies²⁰. The α -form is the highest energy polymorph, the β' -form is intermediate and the β -form is the lowest energy and hence thermodynamically stable form²¹. Furthermore, for some lipids an additional form called the sub- α -form is

known. The relationship between the different forms is monotropic, and thus transformations to more stable forms over time are likely to happen. However, the resulting polymorphic form and transformation rate are influenced by the temperature of the system²².

As previously mentioned, most processing approaches involve the melting of the lipid with the potential for an unstable polymorphic form to crystallize during resolidification. Therefore the processing of dosage forms is often accompanied by undesired solid-state changes^{23,24}. In addition, the polymorphic form of the lipid after processing might undergo a change to another form during storage, often referred to as 'aging' in the literature²⁵. These changes can lead to alteration of the dissolution characteristics of the drug, and possibly bioavailability of the drug in human body^{12,26}.

At present, there is a lack of understanding of the underlying principles of such transformations during the manufacturing of pharmaceutical dosage forms, and hence the formulation of lipid-based dosage forms is often performed based on empirical knowledge. However, for reliable and reproducible dosage forms an understanding of the physico-chemical behaviour is mandatory to prevent potential stability problems.

In previous studies, different triglycerides which were processed to solid lipid extrudates were found to exhibit different polymorphic forms after manufacturing depending on their structure and the extrusion temperature¹². In addition, interactions between triglycerides and partial glycerides were revealed during extrusion which subsequently affected the release of the drug²⁷. Based on these experiences, a systematic investigation of the influence of chain length, storage temperature, substitution and interactions between different lipids was performed. Therefore, different powdered glycerides were melted above their melting points and resolidified in Teflon moulds as thin lipid layers in order to investigate their recrystallization behaviour. Storage experiments were performed using different climatic conditions (room temperature and 40 °C) to examine the influence of temperature on the crystallization processes. In addition, mixtures of different lipid powders were prepared and subjected to the same experiments as the pure powders to elucidate possible interactions between the lipids which might affect the recrystallization behaviour. Based on these studies with the lipid layers serving as model systems, a better understanding of the processes determining the solid-state behaviour of lipid-

based dosage forms should be provided in order to ensure reproducible and stable lipid-based dosage forms.

MATERIALS AND METHODS

Materials

The pure powdered monoacid triglycerides trilaurin (Dynasan 112[®]), tripalmitin (Dynasan 116[®]) and tristearin (Dynasan 118[®]) as well as the partial glycerides glyceryl monostearate (Inwitor 491[®]) and glyceryl stearate (Imwitor 900P[®]) were provided by Sasol (Witten, Germany) and used as received. The crystal structure of the powders was verified with X-Ray powder diffraction before use.

Methods

Preparation of melts

The powdered lipids were completely melted 20 °C above their melting points. Each melt was held for 3 min before they were poured into purpose-built Teflon moulds. The melts resolidified in thin lipid layers (2 mm) in ambient conditions.

Storage

The lipid layers were stored at either room temperature or in a climate chamber at 40 °C (Ehret, Emmendingen, Germany).

Sampling

At certain time points samples of appropriate size of the lipid layer surface were removed with a medical scalpel and investigated. Analysis was performed on the freshly resolidified sample and after 24 and 48 hours. Afterwards, measurements were conducted at 2 day intervals up to 16 days. The following measurements were accomplished after 24, 36, 48 and 60 days.

Differential scanning calorimetry (DSC)

Thermal analysis was performed on the lipids using a DSC 821e calorimeter (Mettler-Toledo, Gießen, Germany). Samples (approximately 5 mg) were weighed into 40 µl aluminium pans which were hermetically sealed. The apparatus was heated from 20-100 °C with a heating rate of 10 °Cmin⁻¹. All experiments were conducted twice.

X-ray powder diffraction (XRPD)

Diffraction patterns were recorded with a theta-theta X-ray diffractometer (D8 Advance, Bruker AXS GmbH, Karlsruhe, Germany). Measurements were performed in

symmetrical reflection mode with CuK α radiation ($\lambda=1.54$ Å) with Göbel mirror bent multilayer optics in the angular range of 5-40° (2 θ). The step size was 0.05° (2 θ) and the measuring time was of 1 s per step. Each experiment was conducted in triplicate compressing the samples into the sample holder hence providing a smooth surface.

Hot-stage microscopy

Thermomicroscopic investigations were performed with a hot-stage FP 900 (Mettler-Toledo, Giessen, Germany) in combination with an optical microscope M 76 (Leica, Wetzlar, Germany). The powdered lipids were heated up to 10 °C above their melting points and the melt was held for at least three minutes at this temperature before monitoring the resolidification at room temperature.

RESULTS AND DISCUSSION

Monoacid triglycerides and the influence of fatty acid chain lengths

Three monoacid triglycerides differing in their fatty acid chain length were investigated with respect to their recrystallization behaviour from the corresponding melts. The resolidified melts were stored either at room temperature or 40 °C and investigated after certain time intervals with a combination of DSC and XRPD measurements.

Trilaurin, a monoacid triglyceride containing 12 C-atoms for each fatty acid esterified with the glycerol molecule, exhibits two melting endotherms for the freshly solidified sample with the onsets at 34 °C and at 44 °C (figure 1 a and b). The first endotherm is due to the melting of the unstable β' -form whereas the second endotherm indicates the melting of the stable β -form of trilaurin. Both onsets are in good agreement with the reported melting points of the two forms²⁸. As thermal events observed using DSC may be associated with physical and/or chemical forms which have not been present in the original sample, XRPD patterns were recorded as complimentary data (figure 2 a and b). The freshly resolidified sample of trilaurin exhibits several peaks which can be related to different polymorphic forms. Peaks at 19.4° and 23.1° are due to the β -form whereas the peak at 21.1° corresponds to the β' -form²⁹. After 24 hours of storage at room temperature only the stable β -form can be detected using both DSC and XRPD (figure 1 a and 2 a). The same result is obtained for those samples stored at 40 °C (figure 1 b and 2 b). The unstable α -form is not observed in these studies due to the fact that its reported melting point of 14 °C is below room temperature²⁸. In conclusion, for trilaurin the storage temperature of the resolidified melt is of minor

importance as the samples stored at different temperatures exhibit the same thermal behaviour irrespective of storage conditions.

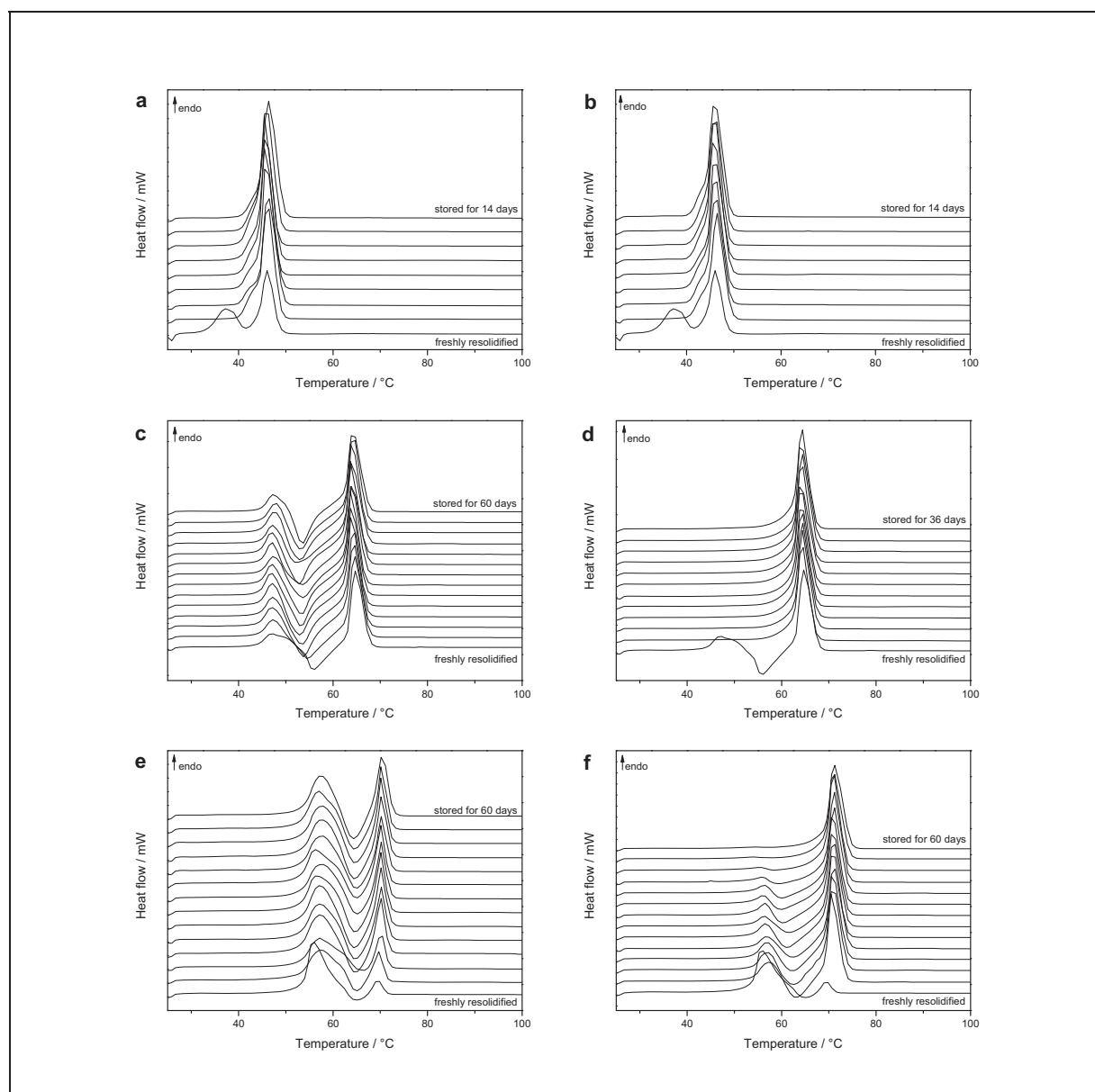


Figure 1. DSC thermograms of resolidified triglycerides during storage. Trilaurin (a) at room conditions, (b) at 40 °C, tripalmitin (c) at room conditions, (d) at 40 °C, tristearin (e) at room conditions and (f) at 40 °C.

The recrystallization from the melt was visualized by hot-stage microscopy (figure 3 a). The appearance of the β -form is associated with flower-like morphology.

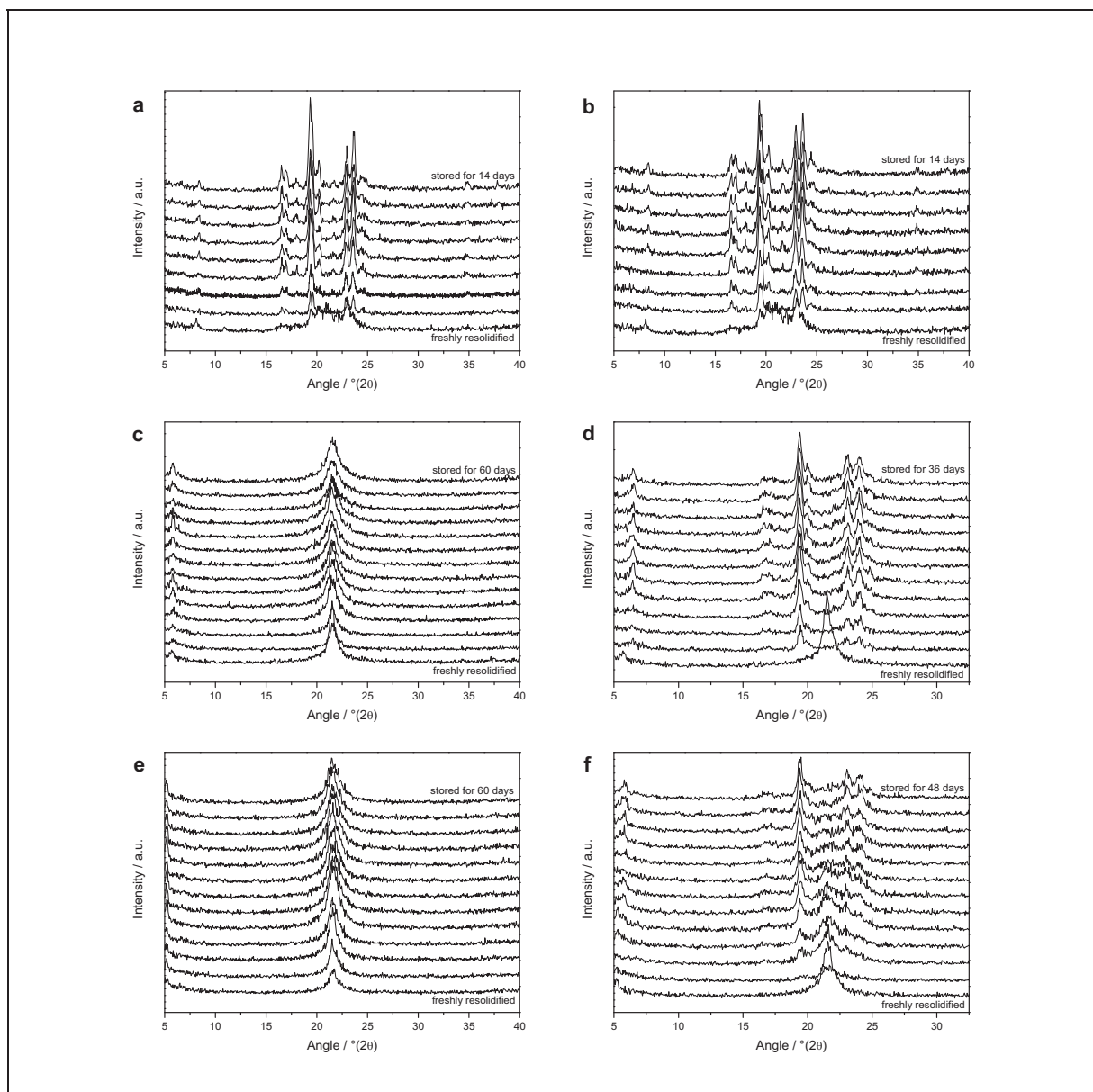


Figure 2. XRPD patterns of resolidified triglycerides during storage. Trilaurin (a) at room conditions, (b) at 40 °C, tripalmitin (c) at room conditions, (d) at 40 °C, tristearin (e) at room conditions and (f) at 40 °C.

Tripalmitin is a triglyceride with the fatty acids each containing 16 C-atoms. The corresponding thermograms are depicted in figure 1 c and d. Different polymorphic forms as can be identified in the figures for the freshly resolidified sample. The endothermic melting peak of the unstable α -form is depicted with its onset at 44 °C directly followed by the recrystallization exotherm of the metastable β' -form (onset 51 °C)²⁸. This peak is formed through the resolidification of the molten α -form during DSC measurement. The stable β -form can be identified by its melting endotherm (onset 63 °C). The melting points in the literature are in good agreement with those in

this study²⁸. The XRPD patterns of the sample samples are depicted in figure 2 c and d. The freshly resolidified sample exhibits only the pure α -form, as indicated by the peak at 21.4° ²⁹. During the storage at room temperature (figure 2 c) the α -form of the triglyceride remains the only polymorphic form which can be detected.

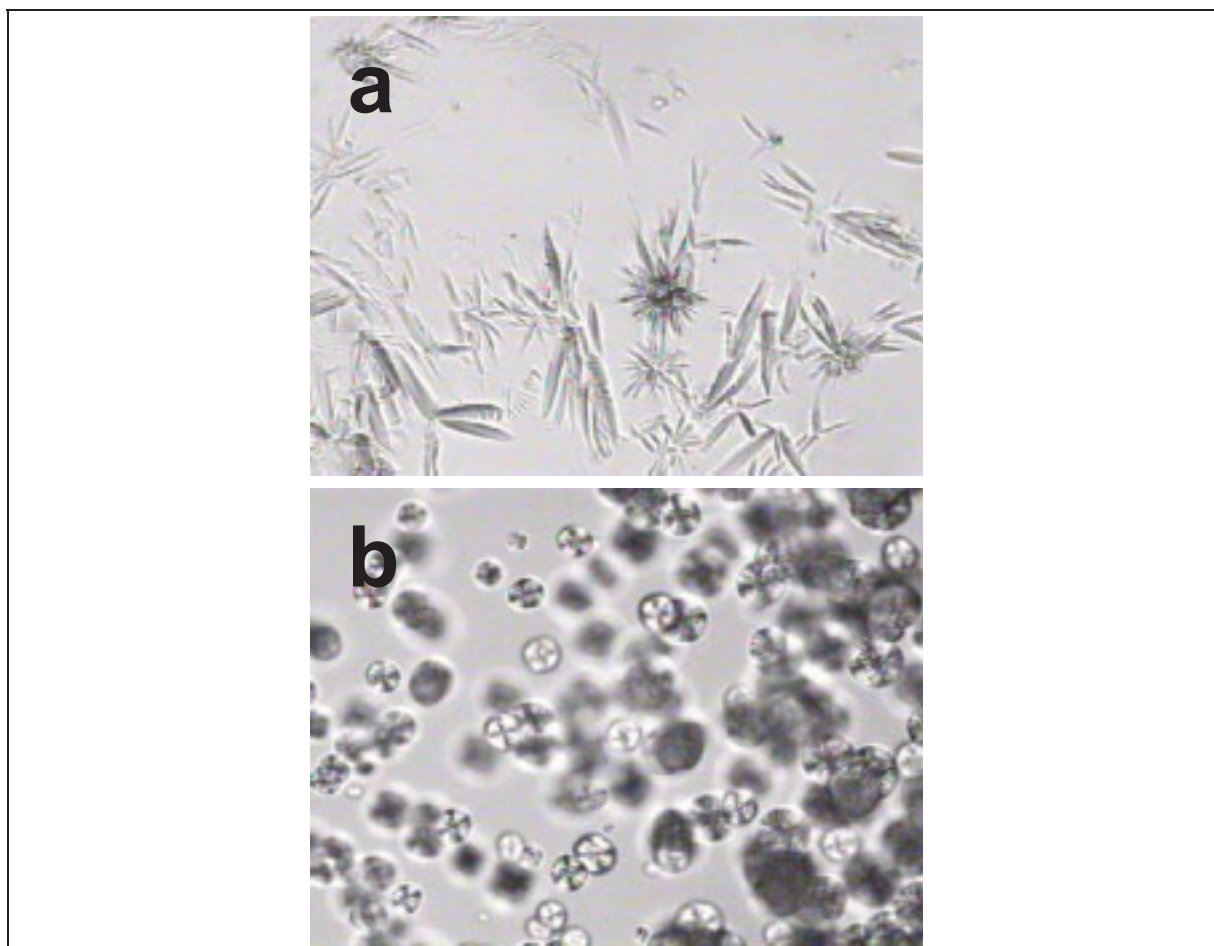


Figure 3. Recrystallization of triglycerides from the melt. (a) trilaurin and (b) tripalmitin.

DSC measurements exhibit some shortcomings in this context as the sample which had originally been in the α -form is able to recrystallize in other polymorphic forms after less stable forms melt during the measurements. This example shows the importance of choosing suitable analytical methods as DSC must be complemented by a method such as XRPD to definitively determine the crystal form(s) of the sample. The same solid-state behaviour was observed with both DSC (figure 1 d) and XRPD (figure 2 d) for the sample stored at 40°C . After 24 hours of storage only the β -form of the lipid can be detected. Interestingly, the β' -form cannot be detected, a fact which is in

accordance with the literature²⁹. Two reasons have been proposed for this: on the one hand the melting of the β' -form is strongly suppressed by the recrystallization of the β -form which hinders its detection, and on the other hand there is evidence that the α -form can directly transform to the β -form.

In conclusion, tripalmitin crystallizes in its α -form after melting. During storage the temperature plays an important role and affects the rate of recrystallization to a more stable form. During storage at 40 °C the stable β -form was obtained after 24 hours whereas at room temperature no recrystallization had occurred after 60 days. The crystallization of the α -form from the melt could be visualized with hot-stage microscopy (figure 3 b).

Tristearin is the triglyceride with the longest fatty acids (chain length 18 C-atoms) and hence the highest melting point. It also showed different solid-state behaviour in different storage conditions. The freshly resolidified samples (figures 1 e and f) exhibit the following thermal events during DSC measurements: a melting endotherm of the unstable α -form (onset 54 °C), a recrystallization exotherm of the metastable β' -form (onset 63 °C) and a melting endotherm of the stable β -form (onset 69 °C)²⁸. Tristearin samples stored at room temperature exhibit all three forms in the DSC thermograms during the investigation period of 60 days (figure 1 e). With respect to the storage at 40 °C the effect of temperature on the recrystallization is clearly visible (figure 1 f). Already after one day of storage the α -form melting endotherm has decreased in intensity while the β -form melting endotherm peak has increased in intensity. After 48 days the α - and β' -forms cannot be detected in the thermogram. Therefore the recrystallization to the stable β -form was complete.

The data recorded with DSC and XRPD revealed a behaviour that was similar to that of tripalmitin. The XRPD patterns of tristearin are depicted in figure 2 e and f. The freshly resolidified sample exhibited only the α -form of the lipid, as indicated by the sole peak at 21.4°²⁹. The same results could be found for the samples stored at room temperature over 48 days. Samples stored at 40 °C exhibited solid-state transformations during storage. As for tripalmitin, no peaks indicating the β' -form (peaks at 21.1° and 23.3°) can be observed as discussed above²⁹. After four days of storage peaks indicating the β -form appear (19.4° and 23.1°). The DSC thermograms and XRPD patterns are in good accordance with respect to when only the β -form is observed for the tristearin samples. Both methods suggest that the α -form is not

present after 48 days of storage. Prior to this a mixture of peaks correlating to α - and β -form can be found.

The influence of chain length on recrystallization rate was evident upon comparison of tripalmitin and tristearin, with tristearin, which consists of longer fatty acids, exhibiting a slower recrystallization to the stable form. This fact should be interpreted in light of the temperature difference between the storage and melting temperatures of the β -form of the two lipids. For tristearin this difference is 33 °C, while for tripalmitin it is 26 °C.

In conclusion, fatty acid chain length, storage temperature and storage time were found to affect the recrystallization behaviour of lipids from resolidified melts. The chain length of the fatty acids which are esterified with glycerol in a triglyceride molecule affected the recrystallization as the transformation rate from unstable to stable polymorphic forms decreased with increasing chain length at the temperatures used for storage experiments in this study. The second variable, storage temperature, had a pronounced effect on recrystallization to more stable polymorphic forms. Increasing the temperature greatly accelerated the recrystallization to the stable form.

Partial glycerides and the influence of degree of esterification

In contrast to the triglycerides in which each moiety of the glycerol molecule is esterified with a fatty acid, partial glycerides contain only one or two esterified glycerol moieties. In this study, a monoglyceride and a mixed partial glyceride consisting of approximately equal proportions of monoglycerides and diglycerides containing stearic acid were investigated.

The DSC thermograms of the monoglyceride glyceryl monostearate are depicted in figure 4 a and b. The freshly resolidified sample exhibits two endothermic melting peaks with onsets at 37 °C and 71 °C. The lower melting endotherm could be identified as the sub α -form of the partial glyceride²⁸. The endotherm with the onset at 71 °C is due to the melting of the α -form²⁸. The XRPD diffractograms (figure 5 a and b) show a significant peak for the α -form at 21.3°³⁰. The sub α -form could not be identified with this method in this study. During storage at room temperature the sub α -form can be detected up to 36 days with DSC. The α -form can be detected up to 16 days. Subsequently, the peak shifts slightly towards higher temperatures to reach a melting endotherm with an onset of 75 °C after 36 days of storage. This peak

corresponds to the stable β -form of the lipid³⁰. The results are in good agreement with the XRPD patterns (figure 5 a) as they also show evidence of the β -form after 24 days of storage (19.5° and 22.5°)³⁰. After 36 days of storage the peak indicating the α -form disappears. In comparison, the samples stored at 40°C only exhibit the sub α -form for the freshly resolidified sample (onset 37°C) as well as the α -form (onset 71°C) (figure 4 b)²⁸. After 24 hours of storage these peaks can no longer be detected. With respect to other polymorphic forms the peak with an onset of 75°C indicating the stable β -form is observed after 1 day of storage at 40°C . These findings correspond to the data obtained by XRPD (figure 5 b).

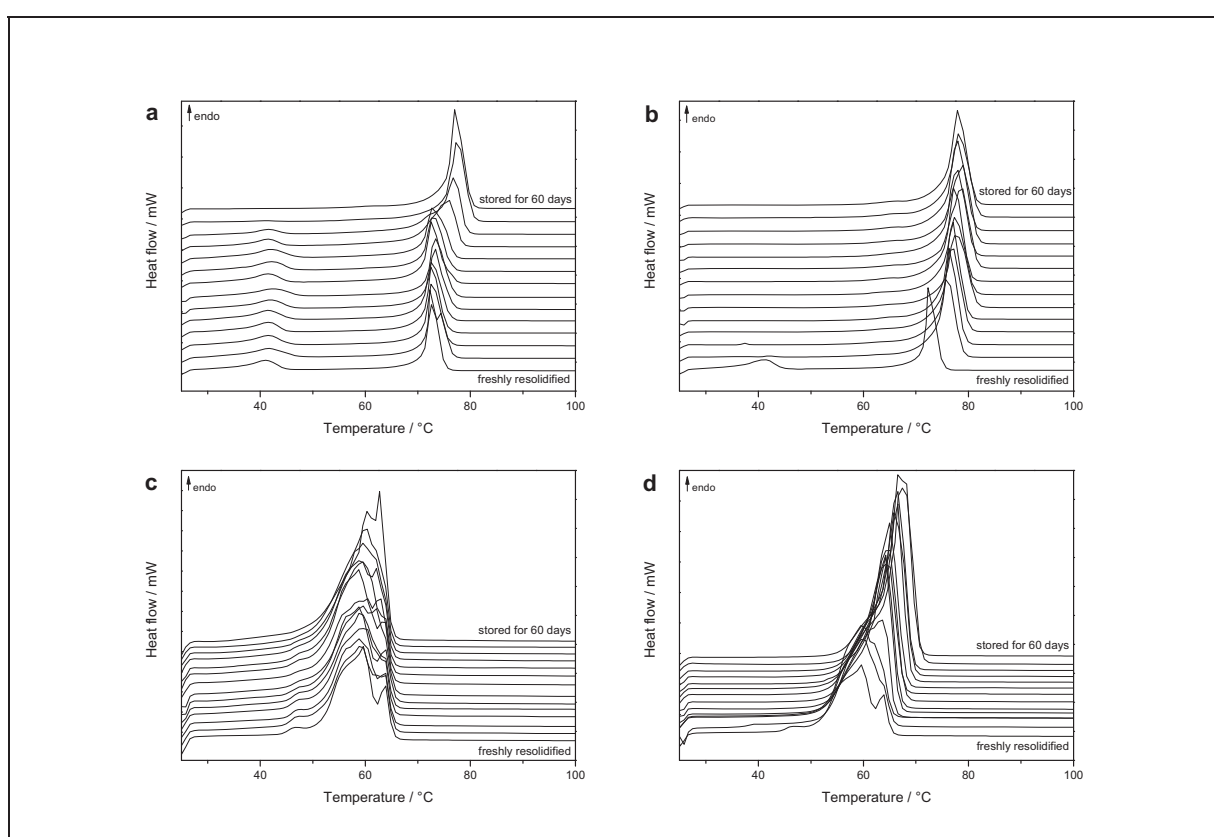


Figure 4. DSC thermograms of resolidified partial glycerides during storage. Glyceryl monostearate (a) at room conditions, (b) at 40°C and glyceryl stearate (c) at room conditions (c) and (d) at 40°C .

In conclusion, the peak assignment in case of the partial glycerides is more complex than for triglycerides. Temperature plays an important role during storage as increased temperature increases the velocity of recrystallization.

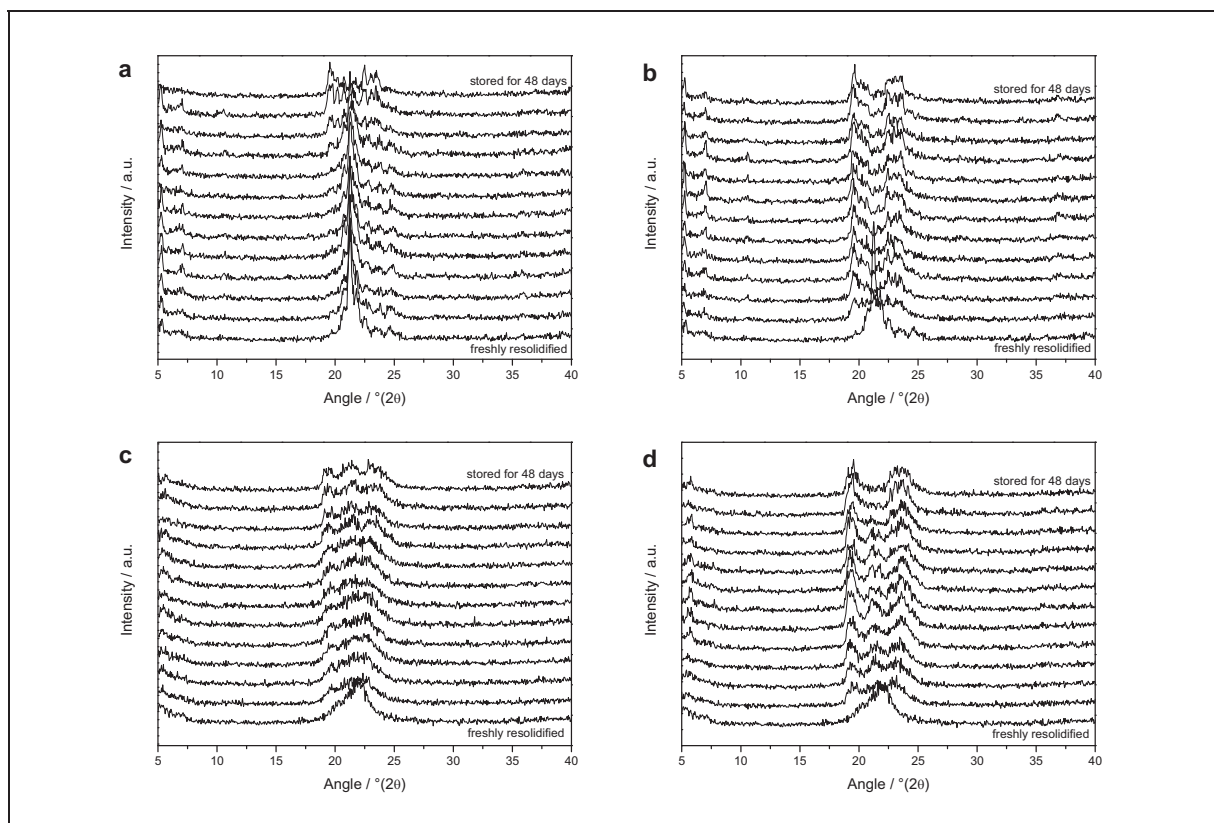


Figure 5. XRPD diffractograms of resolidified partial glycerides during storage. Glyceryl monostearate (a) at room conditions, (b) at 40 °C and glyceryl stearate (c) at room conditions (c) and (d) at 40 °C.

The results for the second partial glyceride glyceryl stearate which was investigated are depicted in figure 4 c and d and 5 c and d. As the substance is rather chemically inhomogeneous the assignment of melting or crystallization events in the thermograms is very difficult, with the different thermal events overlapping²⁸. It can thus only be stated that the melting endotherm during storage at room temperature shifts to higher temperatures over time indicating transformations to more stable and less energetic forms. During storage at 40 °C this shift occurs faster and the peaks are more defined as the higher temperature facilitates such transformations. The peak at 22° in the XRPD pattern (figure 5 c and d) suggests the α -form of the glycerides for the freshly resolidified sample²⁸. During storage at room temperature a broader pattern occurs which cannot be definitively assigned (figure 5 c). In comparison, at 40 °C storage the peaks become more resolved (figure 5 d).

In conclusion, the peak assignment of the partial glycerides is more complex than for triglycerides. Temperature plays an important role during storage as increased temperature increases the velocity of recrystallization.

Mixtures of a triglyceride and a partial glyceride and the impact of interactions

Two different mixtures of tristearin and glyceryl monostearate powders were prepared to investigate the impact of possible interactions between the two lipids on their solid-state behaviour. The mixing ratios were: 90% tristearin / 10% glyceryl monostearate and 50% tristearin / 50% glyceryl monostearate (w/w).

After mixing for 15 min the powder mixtures were melted as described in the Materials and Methods section and resolidified. The DSC thermograms are depicted in figure 6. The 90% / 10% mixture of tristearin and glyceryl monostearate (figure 6 a and b) exhibits only one melting endotherm with an onset of 53 °C for the freshly resolidified sample which corresponds to the tristearin α -form²⁸. As there are no further melting peaks it can be assumed that glyceryl monostearate is in a crystal form which melts within the temperature range of the tristearin α -form. For the samples stored at room temperature this melting endotherm remains essentially the same for 60 days of storage. In addition, after 24 hours of storage a tiny melting endotherm (onset 65 °C) appears which becomes more intense over time. This peak is due to the recrystallization of the tristearin β -form from the molten sample during DSC measurement²⁸. The XRPD patterns (figure 7 a) only depict the tristearin α -form peak (21.4°) during the whole storage time²⁹.

The samples stored at 40 °C exhibit substantially different thermal behaviour (figure 6 b). After storage for 24 hours a large endotherm (onset 66 °C) can be detected corresponding to the stable β -form of tristearin²⁸. In addition, up to a storage duration of 16 days a small melting endotherm with an onset at 53 °C is present and corresponds to the α -form of tristearin²⁸. Since glyceryl monostearate is only present in a very low concentration and the melting ranges of tristearin and glyceryl monostearate overlap, it is very difficult to make a statement about the polymorphic forms of the partial glyceride. The XRPD patterns (figure 7 b) correspond to the results obtained by DSC measurements. The freshly resolidified sample contains tristearin in its α -form (peak 21.4°) which transforms to a mixture of α - and β -forms (peaks at 19.4°, 23.1° and 24.05°) over time²⁹. After 24 days of storage only the the tristearin β -form is evident.

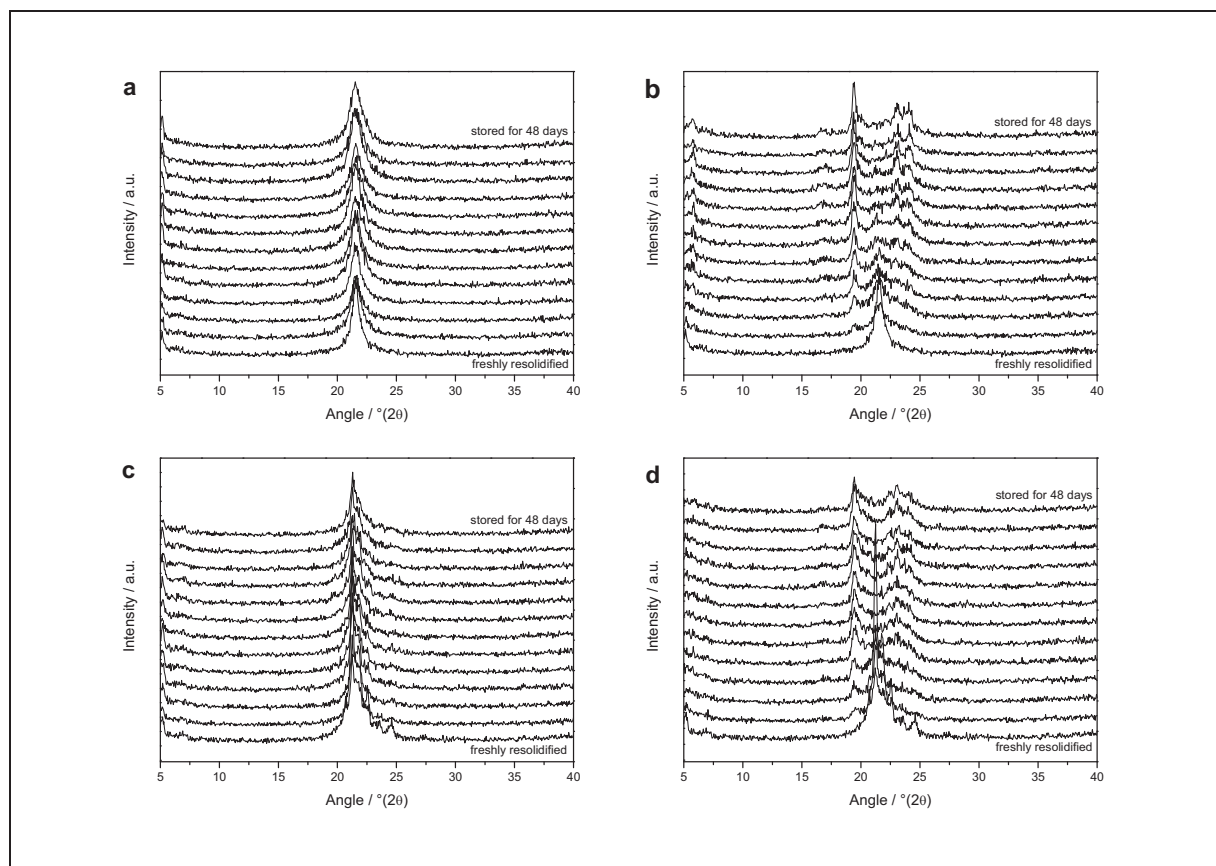


Figure 6. DSC thermograms of resolidified lipid mixtures during storage. 90% tristearin/10% glyceryl monostearate (w/w) (a) at room conditions, (b) at 40 °C, 50% tristearin/50% glyceryl monostearate (w/w) (c) at room conditions, (d) at 40 °C.

It is interesting to compare the recrystallization behaviour of pure tristearin melts with melts consisting of 90% tristearin and 10% glyceryl monostearate. The XRPD patterns (figure 2 e and f, figure 7 a and b) do not show any significant differences. In this case DSC measurements are the method of choice to investigate solid-state differences (figure 1 e and f, figure 6 a and b). For samples stored in room temperature (figure 1 e and 6 a) an increased incidence of the unstable tristearin α -form can be detected for the sample containing the mixture in comparison to the pure tristearin melt. During the DSC measurement the tristearin α -form melts and hence recrystallization of more stable polymorphs can occur. In the mixture it appears that the glyceryl monostearate is able to prevent or delay the transformation from the tristearin α -form (peak onset 63 °C) to the stable β -form as the β -form peak (onset 69 °C) exhibits a much reduced intensity compared to the pure tristearin sample²⁸.

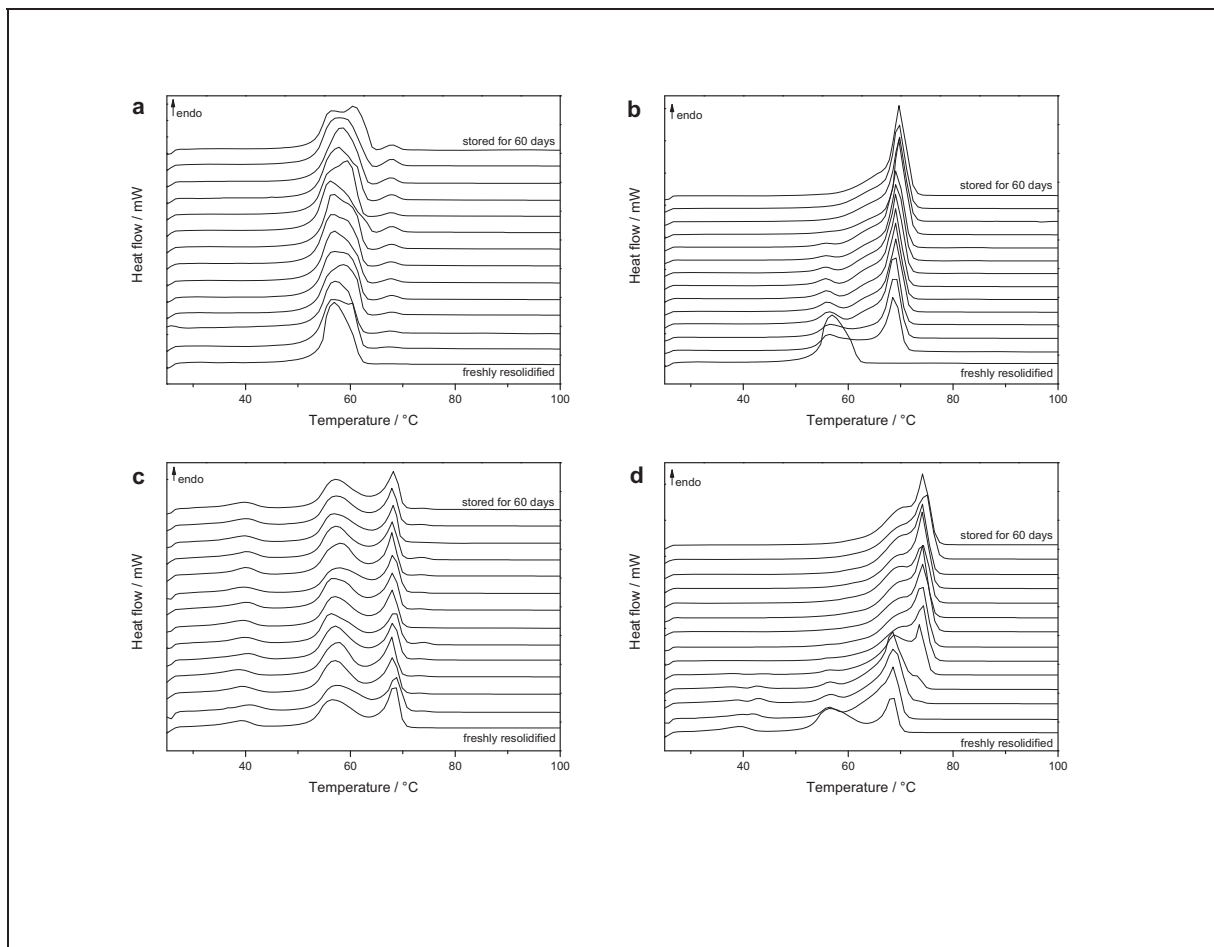


Figure 7. XRPD diffractograms of resolidified lipid mixtures during storage. 90% tristearin/10% glyceryl monostearate (w/w) (a) at room conditions, (b) at 40 °C, 50% tristearin/50% glyceryl monostearate (w/w) (c) at room conditions, (d) at 40 °C.

The α -form is probably stabilized by combined structures of tristearin and glyceryl monostearate on the intermolecular level. The ability of a partial glyceride to hinder another lipid transforming into its stable polymorph has been previously reported^{31,32}. In the chocolate industry this specific effect is used to maintain an unstable polymorph of cocoa butter which appears more glossy than the recrystallized stable polymorph³³.

It is also interesting to compare the DSC pattern of the tristearin and the mixed samples stored at 40 °C (figures 1 f and 6 b). Even though the presence of the partial glyceride, glyceryl monostearate, hinders the formation of the β -form during the DSC measurement, complete transformation to the tristearin β -form is faster and more pronounced than in case of pure tristearin during storage. For the pure tristearin sample (figure 1 f) the melting peak of the α -form can be observed for up to 48 days of storage

whereas in the thermogram of the mixed sample the melting endotherm of the α -form is absent after only 24 days of storage²⁸. This phenomenon is probably associated with a less organised and energetically favourable packing and higher molecular mobility in the resolidified melt of the combined lipids due to the different structures of the two lipids which are mixing. This might affect the mixed melt in terms of recrystallization rate at higher temperatures.

The extent of interactions between the partial glyceride and the triglyceride was investigated further in the lipid mixture containing 50% tristearin and 50% glyceryl monostearate (w/w). The DSC thermograms are depicted in figure 6 c and d. The freshly resolidified sample exhibits three melting endotherms. Their onsets can be detected at 37 °C, 53 °C and 66 °C respectively²⁸. The first peak is likely to be due to the unstable sub α -form of glyceryl monostearate. The melting endotherm having its onset at 53 °C corresponds to the α -form of tristearin whereas the last endotherm (onset 66 °C) is a mixture of melting events of both lipids which is difficult to assign to the exact polymorphic forms of the lipids²⁸. During storage at room temperature the sub α -form of glyceryl monostearate as well as the α -form of tristearin remain in the resolidified sample for the whole storage time. The melting endotherm with an onset at 66 °C also persists. After six days of storage a tiny melting endotherm (onset 72 °C) occurs corresponding to the tristearin β -form. In contrast in the sample stored at 40 °C the sub α -form is only detected up to six days of storage with the peak onset shifting from 37 °C up to 41 °C (figure 6 d). The tristearin α -form (onset 54 °C) is detectable up to eight days of storage. The melting endotherm with an onset at 65 °C corresponding to both glycerides in the resolidified melt can be detected for four days. After six days of storage this peak becomes bimodal, and then the peak completely shifts to higher temperatures (onset 71 °C) with a shoulder remaining at lower temperatures. The maximum of this endotherm is likely to be due to a mixture of the stable β -forms of tristearin and glyceryl monostearate²⁸. The XRPD patterns (figure 7 c and d) supported this interpretation.

In conclusion, resolidified melts consisting of mixtures of triglyceride and partial glyceride show diverse solid-state behaviour. Small quantities of partial glyceride (10 %) increased the amount of unstable α -form of the triglyceride compared to that of a pure tristearin melt. This behaviour was also observed for the mixture containing 50% partial glyceride. Nevertheless, the mixtures allow faster recrystallization of the stable

β -form than pure tristearin samples during storage. This becomes obvious upon comparison of the pure tristearin sample (figure 1 f) and the mixtures (figure 6 b, d) after storage in 40 °C. Again, increasing the temperature accelerated the transformation rate to more stable polymorphic forms. Comparing the different mixing ratios suggests the ability of the solid state form of the triglyceride to incorporate different amounts of the partial glyceride molecules which affect the transformation rate to a large extent. The mixture containing 10% glyceryl monostearate exhibits the tristearin α -form for 16 days (figure 6 b) whereas the mixture containing 50% glyceryl monostearate features the tristearin α -form just for 10 days (figure 6 d).

CONCLUSION

Solid-state analysis of thin glyceride layers of pure triglycerides or mixtures of a triglyceride and a partial glyceride as model systems for lipid-based dosage forms led to a deeper insight into the principles of recrystallization from melts and during storage. The combination of DSC and XRPD measurements was found to give a more comprehensive overview of the recrystallization from the melts. It could be shown that the results of only one method can be misleading for the interpretation.

Triglycerides exhibited chain-length dependant recrystallization behaviour. With increasing chain length the recrystallization to the stable polymorph was decelerated at each storage temperature. Partial glycerides exhibited a more complex recrystallization behaviour due to the fact that the melting ranges of their different polymorphs overlap. The combination of a triglyceride and a partial glyceride led to interactions influencing the recrystallization. Generally, temperature was shown to have a pronounced impact on the rate of recrystallization with the higher temperature accelerating the recrystallization. However, storage at elevated temperatures does not necessarily lead to a fast transformation to the stable form of the lipid. Based on these results changes in solid dosage forms based on glycerides during processing and storage can be better understood. A deeper knowledge of the underlying principles of solid-state changes in lipids used in the pharmaceutical setting is mandatory to avoid unpredictable and undesirable changes in a glyceride based dosage forms during processing and storage.

ACKNOWLEDGEMENTS

The Marie Curie Fellowship and the Galenos Network are acknowledged for financial support (MEST-CT-2004-404992). The Sasol GmbH is acknowledged for generous provision of the lipids.

REFERENCES

- (1) C.J.H. Porter and W.N. Charman. In vitro assessment of oral lipid-based formulations. *Adv. Drug Deliv. Rev.* 50: 127-147 (2001).
- (2) E.T. Cole. Liquid-filled hard-gelatin capsules. *Pharm. Technol.* 13: 124-140 (1989).
- (3) W.J. Bowtle. Materials, process, and manufacturing considerations for lipid-based hard-capsule formats. In D.J. Hauss (ed.), *Oral Lipid-Based Formulations - Enhancing the Bioavailability of Poorly Water-Soluble Drugs*, Informa Healthcare, New York, 2007, 79-106.
- (4) J. Liu, F. Zhang and J.W. McGinity. Properties of lipophilic matrix tablets containing phenylpropanolamine hydrochloride prepared by hot-melt extrusion. *Eur. J. Pharm. Biopharm.* 52: 181-190 (2001).
- (5) B. Evrard, K. Amighi, D. Beten, L. Delattre and A.J. Moës. Influence of melting and rheological properties of fatty binders on the melt granulation process in a High-Shear mixer. *Drug Dev. Ind. Pharm.* 25: 1177-1184 (1999).
- (6) Y.E. Zhang, J.B. Schwartz. Melt granulation and heat treatment for wax matrix-controlled drug release. *Drug Dev. Ind. Pharm.* 29: 131-138 (2003).
- (7) C. Cavallari, L. Rodriguez, B. Albertini, N. Passerini, F. Rosetti and A. Fini. Thermal and fractal analysis of diclofenac/Gelucire 50/13 microparticles obtained by ultrasound-assisted atomization. *J. Pharm. Sci.* 94: 1124–1134 (2005).
- (8) B. Chauhan, S. Shimpi and A. Paradkar. Preparation and characterization of etoricoxib solid dispersions using lipid carriers by spray drying technique. *AAPS Pharm. Sci. Tech.* 6: E405-412 (2005).
- (9) H. Bunjes, K. Westensen and M.H.J. Koch. Crystallization tendency and polymorphic transitions in triglyceride nanoparticles. *Int. J. Pharm.* 129: 159-173 (1996).
- (10) M. Ricci, C. Puglia, F. Bonina, C.D. Di Giovanni, S. Giovagnoli and C. Rossi. Evaluation of indomethacin percutaneous absorption from nanostructured lipid carriers (NLC): in vitro and in vivo studies. *J. Pharm. Sci.* 94: 1149–1159 (2005).

- (11) J.F. Pinto and N.P. Silverio. Assessment of the extrudability of three different mixtures of saturated polyglycolysed glycerides by determination of the “specific work of extrusion” and capillar rheometry. *Pharm. Dev. Tech.* 6: 117-128 (2001).
- (12) M. Windbergs, C.J. Strachan and P. Kleinebudde. Understanding the solid-state behaviour of triglyceride solid lipid extrudates and its influence on dissolution. *Eur. J. Pharm. Biopharm.* 71: 80-87 (2009).
- (13) J. Breitzkreutz, F. El Saleh, C. Kiera, P. Kleinebudde and W. Wiedey. Pediatric drug formulation of sodium benzoate: II. Coated granules with a lipophilic binder. *Eur. J. Pharm. Biopharm.* 56: 255-260 (2003).
- (14) J. Hamdani, A.J. Moes and K. Amighi. Development and evaluation of prolonged release pellets obtained by the melt pelletization process. *Int. J. Pharm.* 245: 167-177 (2002).
- (15) S. Prabhu, M. Ortega and C. Ma. Novel lipid-based formulations enhancing the in vitro dissolution and permeability characteristics of a poorly water-soluble model drug, piroxicam. *Int. J. Pharm.* 301, 209-216 (2005).
- (16) A.J. Humberstone and W.N. Charman. Lipid-based vehicles for the oral delivery of poorly water soluble drugs. *Adv. Drug Deliv. Rev.* 25: 103-128 (1997).
- (17) R. Löbenberg and G.L. Amidon. Modern bioavailability, bioequivalence and biopharmaceutics classification system. New scientific approaches to international regulatory standards. *Eur. J. Pharm. Biopharm.* 50: 3-12 (2000).
- (18) S. Qi, D. Deutsch and D.Q. Craig. An investigation into the mechanisms of drug release from taste-masking fatty acid microspheres. *J. Pharm. Sci.* 97, 3842-3854 (2008).
- (19) J. Hamdani, A.J. Moes and K. Amighi. Physical and thermal characterisation of Precirol® and Compritol® as lipophilic glycerides used for the preparation of controlled-release matrix pellets. *Int. J. Pharm.* 260: 47-57 (2003).
- (20) K. Sato. Crystallization behaviour of fats and lipids – a review. *Chem. Eng. Sci.* 56: 2255-2265 (2001).

- (21) K. Sato, S. Ueno and J. Yano. Molecular interactions and kinetic properties of fats. *Prog. Lipid Res.* 38: 91-116 (1999).
- (22) W. MacNaughtan, I.A. Farhat, C. Himawan, V.M. Starov and A.G.F. Stapley. A differential scanning calorimetry study of the crystallization kinetics of the crystallization kinetics of tristearin-tripalmitin mixtures. *J. Am. Oil Chem. Soc.* 83: 1-9 (2006).
- (23) J.H. Whittam and H.L. Rosano. Physical aging of even saturated monoacid triglycerides. *J. Am. Oil Chem. Soc.* 52: 128-133 (1975).
- (24) N. Khan and D.Q.M. Craig. Role of blooming in determining the storage stability of lipid-based dosage forms. *J. Pharm. Sci.* 93: 2962-2971 (2004).
- (25) W. Sutananta, D.Q.M. Craig and J.M. Newton. The effects of ageing on the thermal behaviour and mechanical properties of pharmaceutical glycerides. *Int. J. Pharm.* 111, 51-62 (1994).
- (26) Y.W. Choy, N. Khan and K.H. Yuen. Significance of lipid matrix aging on in vitro release and in vitro bioavailability. *Int. J. Pharm.* 299, 55-64 (2005).
- (27) M. Windbergs, C.J. Strachan and P. Kleinebudde. Influence of the composition of glycerides on the solid-state behaviour and the dissolution profiles of solid lipid extrudates. *Int. J. Pharm.* doi: 10.1016/j.ipharm.2009.03.002.
- (28) J.W. Hagemann. Thermal behaviour and polymorphism of acylglycerides. In: N. Garti and K. Sato (eds.), *Crystallization and polymorphism of fats and fatty acids*, Marcel Dekker, New York, 1988, 9-95.
- (29) M. Kellens, W. Meeussen, R. Gehrke and H. Reynaers. Synchrotron radiation investigations of the polymorphic transitions of saturated monoacid triglycerides. Part 1: Tripalmitin and tristearin, *Chemistry and physics of lipids. Chem. Phys. Lipids* 58: 131-144 (1991).
- (30) T. Yajima, S. Itai, H. Takeuchi and Y. Kawashima. Determination of optimum processing temperature for transformation of glyceryl monostearate. *Chem. Pharm. Bull.* 50: 1430-1433 (2002).

(31) N. Garti, J. Schlichter and S. Sarig. DSC studies concerning polymorphism of saturated monoacid triglycerides in the presence of food emulsifiers. *Fat Sci. Technol.* 90: 295-299 (1988).

(32) N. Garti. Effects of surfactants on crystallization and polymorphic transformation of fats and fatty acids. In: N. Garti and K. Sato (eds.), *Crystallization and polymorphism of fats and fatty acids*, Marcel Dekker, New York, 1988, 267-303.

(33) J. Schlichter-Aronhime and N. Garti. Solidification and polymorphism in cacao butter and the blooming problems, In: N. Garti and K. Sato (eds.), *Crystallization and polymorphism of fats and fatty acids*, Marcel Dekker, New York, 1988, 363-393.

9.4. Article 4: Tailor-made dissolution profiles by extruded matrices based on lipid polyethylene glycol mixtures



Tailor-made dissolution profiles by extruded matrices based on lipid polyethylene glycol mixtures

Maïke Windbergs^{a,b}, Clare J. Strachan^{b,c}, Peter Kleinebudde^{a,*}

^a Institute of Pharmaceutics and Biopharmaceutics, Heinrich-Heine-University, Universitätsstr. 1, 40225 Düsseldorf, Germany

^b Centre for Drug Research, University of Helsinki, Viikinkaari 5E, 00014 University of Helsinki, Finland

^c School of Pharmacy, University of Otago, 18 Frederick Street, Dunedin 9054, New Zealand

ARTICLE INFO

Article history:

Received 16 December 2008

Accepted 2 April 2009

Available online 7 April 2009

Keywords:

Dissolution

Solid lipid extrusion

Controlled release

Polyethylene glycol lipid ratio

Matrix release

ABSTRACT

Extrudates consisting of various ratios of tripalmitin and polyethylene glycol as matrix materials were produced below their melting temperatures. Tailor-made dissolution profiles for the model drug theophylline anhydrate were obtained by varying the matrix composition. The hydrophilic polymer polyethylene glycol increases the dissolution rate of the drug from the extruded matrix by its dissolution and hence formation of an interconnected pore network alleviating the release of the drug.

Even though lipid-based dosage forms often suffer from polymorphic transitions during manufacturing, affecting the dissolution profiles and stability, these extrudates were found to exhibit stable solid-state behaviour. No polymorphic transformations were evident after extrusion. Stability testing was performed by open storage experiments over one year in accelerated conditions (40 °C/75 %RH). Each formulation remained in its stable conformation.

© 2009 Elsevier B.V. All rights reserved.

1. Introduction

Recently, there has been substantial interest in new groups of excipients for the formulation of oral dosage forms. Lipids have shown high potential as the basis for a broad range of different dosage forms due to their versatile physicochemical characteristics [1–4]. Furthermore, they are biodegradable and physiologically non-toxic. Unfortunately, their versatile structure results in complex solid-state behaviour and a good knowledge of this behaviour is required to obtain stable and reproducible lipid based dosage forms [5–7]. Generally, during formulation the lipid excipients are melted and resolidified with the active pharmaceutical ingredient (API) to form a matrix in which the API is embedded [8–10].

Depending on the thermal conditions lipids exhibit different polymorphic forms which are characterized by a particular chain packing and specific thermal stability [11–13]. Solid-state transformations during processing and storage are likely to happen when the lipid is not processed in the most stable form. Due to the lack of understanding and hence control of the processing conditions that result in the formation of metastable forms of lipids, the number of lipid-based formulations on the market is still limited. To circumvent the problems associated with uncontrolled polymorphic forms of lipids during processing a relatively new approach has been introduced for the manufacturing of lipid-based dosage forms – solid lipid extrusion. In this process, powdered glycerides are mixed

with the API and extruded below the melting point of the lipid to avoid melting of the whole matrix material [14–17]. The process conditions can be selected so that the most stable form is exclusively obtained in the dosage form with the result being storage stability and reproducible dissolution profiles. Studies have been performed on using pure monoacid triglycerides to provide stable dosage forms but the extrudates were restricted to sustained release of the API [18]. To broaden the range of dissolution possibilities from solid lipid extrudates partial glycerides and mixtures of triglycerides with partial glycerides have been investigated. Unfortunately, such mixed matrices suffer from interactions between the different glycerides resulting in uncontrolled polymorphic transitions followed by a decreased release rate of the API [19].

In this study, a monoacid triglyceride was extruded in combination with the hydrophilic polymer polyethylene glycol in order to obtain tailor-made dissolution profiles by different mixing ratios of the matrix materials. For the formulation of pharmaceutical solid dosage forms polyethylene glycol is used as a matrix for controlled release and as a tablet binder and coating agent [20]. In addition, polyethylene glycol has also been used in small quantities as a pore former and release modifier [21–23]. In general, the formulation of dosage forms with polyethylene glycol involves melting of the polymer and resolidification with an API [24]. Unfortunately, this approach can lead to unpredictable degeneration of the polymer [25]. In this study a high molecular weight polyethylene glycol (mean molecular weight 10,000) was used. The solid-state behaviour of the starting powdered materials and resulting extrudates was investigated with a combination of differential scanning calorimetry and X-ray powder diffraction,

* Corresponding author.

E-mail address: Kleinebudde@uni-duesseldorf.de (P. Kleinebudde).

as controlling the solid-state behaviour is crucial for predictable release of the drug. Dissolution testing was performed in a basket apparatus and the results were correlated to the results obtained by surface analysis comprising contact angle measurements and scanning electron microscopy. The storage stability was tested in accelerated conditions. In addition, the vapour sorption behaviour of the extrudates was investigated with Karl Fischer titrimetry and moisture sorption analysis.

2. Materials and methods

2.1. Materials

Tripalmitin (Dynasan 116[®]), a monoacid triglyceride, was used in powdered form as received from Sasol (Witten, Germany). Polyethylene glycol with a mean molecular weight of 10,000 was provided by Clariant (Waalwijk, The Netherlands) and was in powdered form (Polyglykol 10000 P[®]). The powdered model drug theophylline anhydrate was produced by BASF (Ludwigshafen, Germany). For comparison, theophylline monohydrate was recrystallized from theophylline anhydrate that had been dissolved in purified water. All crystal forms were verified using X-ray powder diffraction.

2.2. Methods

2.2.1. Extrusion

The powdered matrix materials (tripalmitin, polyethylene glycol) were combined with the model drug theophylline anhydrate in a 1:1 (w/w) ratio of matrix materials to drug. The matrix consisted either of one pure matrix component or a mixture of both excipients in the following ratios: 5+5, 6+4, 7+3, 8+2, 9+1 and 9.5+0.5 (tripalmitin/polyethylene glycol (w/w)). The powders were mixed in a laboratory mixer (LM 20 Bohle, Ennigerloh, Germany) at 25 rpm for 15 min. The mixed powders were filled into the dosing device (KT20K-Tron Soder, Lenzhard, Switzerland) which gravimetrically fed the powder into the barrel of a co-rotating twin-screw extruder (Mikro 27GL-28D, Leistritz, Nürnberg, Germany). Extrusion was performed with a screw speed of 30 rpm and a feeding rate of 40 g min⁻¹. The mass was forced through a die plate equipped with 23 holes exhibiting 1 mm diameter and 2.5 mm length. The processing temperature was 55 °C.

2.2.2. Differential scanning calorimetry (DSC)

Thermograms were recorded with a DSC 821e calorimeter (Mettler-Toledo, Gießen, Germany). The samples (approximately 5 mg) were weighed into hermetically sealed 40 µl aluminium pans. Each experiment was conducted twice using a heating rate of 10 °C min⁻¹ within a temperature range of 20–300 °C.

2.2.3. X-ray powder diffraction (XRPD)

Experiments were performed with the use of a theta-theta X-ray powder diffractometer (D8 Advance, Bruker AXS GmbH, Karlsruhe, Germany). Symmetrical reflection mode with CuK α radiation ($\lambda = 1.54 \text{ \AA}$) with Göbel mirror bent multilayer optics was used in the angular range of 5–40° (2 θ). The step size was 0.05° (2 θ) and the measuring time was of 1 s per step. The samples were compressed into the sample holder to provide a smooth surface. Each experiment was conducted in triplicate.

2.2.4. Dissolution

Dissolution experiments were performed in a basket apparatus (Sotax AT7 smart, Sotax, Lörrach, Germany) in accordance with Method 1 in the USP 29. The extrudates were cut to a uniform length of 1 cm. Each vessel contained 140 mg sample. The dissolution medium consisted of 900 mL purified water containing 0.001% polysorbate 20. Dissolution testing was performed with a

constant stirring speed of 50 rpm and a temperature of 37 ± 0.5 °C. A UV-Vis spectrometer (Lambda 40, Perkin-Elmer, Rodgau-Juegesheim, Germany) was used to measure samples in a continuous flow-through cuvette at 2.5 min intervals. Each experiment was conducted in triplicate. The dissolution curve was drawn based on the calculated mean of the concentration at each time point. The standard deviation at each time point was always below 4% for all extrudate compositions.

2.2.5. Storage

Storage experiments were performed for 12 months in accelerated climatic conditions (40 °C/75 %RH) using a climate chamber (KBF 240, Binder, Tuttlingen, Germany). The samples were stored in open Petri dishes.

2.2.6. Scanning electron microscopy (SEM)

For these experiments a scanning electron microscope (Leo 1430VP, Leo Elektron Microscopy, Cambridge, UK) was used with a working voltage of 20 kV. Samples were attached to aluminium stubs with the help of double-sided carbon tape. Sputter-coating was performed with gold for 150 s (Agar Manual Sputter Coater B7340, Agar Scientific, Stansted, UK).

2.2.7. Contact angle measurements

An optical contact angle meter (Drop shape analysis system DSA100, Krüss, Hamburg, Germany) with the associated software (Drop shape analysis DSA1 v 1.90, Hamburg, Germany) was used to determine the contact angles of the samples. Each experiment was performed eight times by placing a 0.8 µl drop of distilled water on the extrudate surface and calculating the mean result.

2.2.8. Karl Fischer titrimetry

The water content of the extrudates was verified using a Karl Fischer titrator (DL 18, Mettler-Toledo GmbH, Gießen, Germany). The medium consisted of Hydranal[®]-methanol dry and Hydranal[®]-formamide dry combined in equal parts. Hydranal[®]-composite 5 was used as a one-component reagent. Calibration was performed with Hydranal[®] water standard. The mean of three measurements was taken.

2.2.9. Moisture sorption analysis

A dynamic vapor sorption analyzer SPS 11 (Projekt Messtechnik, Ulm, Germany) was used to expose the samples to a specific climate in controlled temperature and humidity. Approximately 1500 mg of the sample was weighed into aluminium cups and the sample weight was monitored at certain time intervals during the measurements. Measurements were performed in duplicate at room temperature in the humidity range between 0% and 80%.

3. Results and discussion

3.1. Extrusion and solid-state characterization of powders and extrudates

3.1.1. Tripalmitin

As already stated in a previous paper tripalmitin provides a good matrix material for the manufacturing of solid lipid extrudates [18]. At a processing temperature of 55 °C extrudates could be produced which consist completely of the stable β -form of the lipid providing long-term stability of the dosage form and predictable dissolution characteristics. Both the lipid and drug remained crystalline and no interaction could be observed. The extrudates exhibited a good external appearance with a smooth and homogenous surface structure (Fig. 1a). Based on these observations [18] tripalmitin was chosen as the lipid matrix component for the present study.

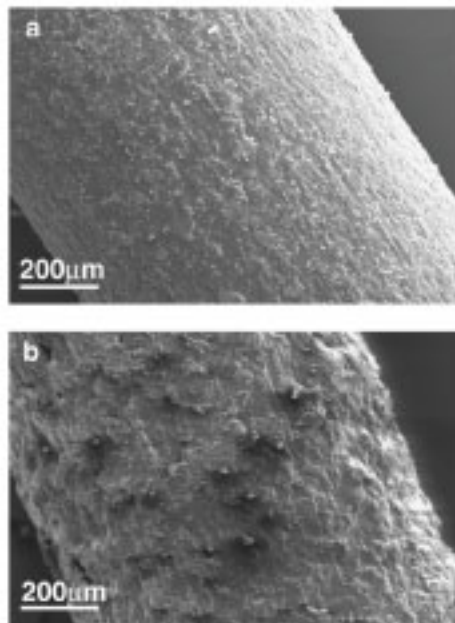


Fig. 1. SEM images of extrudates (a) tripalmitin and (b) polyethylene glycol.

3.1.2. Polyethylene glycol

Polyethylene glycol with a mean molecular weight of 10,000 was investigated with respect to its suitability as a matrix material for extrusion below its melting point of 62 °C [26]. Extrusion was performed at a processing temperature of 55 °C. SEM analysis revealed that the extrudate surfaces were rough (Fig. 1b). Solid-state analysis was performed on the powders and extrudates as a stable solid-state structure is necessary to obtain reliable and controllable release profiles from these kinds of dosage forms. The results are depicted in Fig. 2. Thermal analysis (Fig. 2a) revealed that polyethylene glycol remained in its stable crystalline formation during extrusion as the melting endotherms depict. There was no evidence of any solid-state

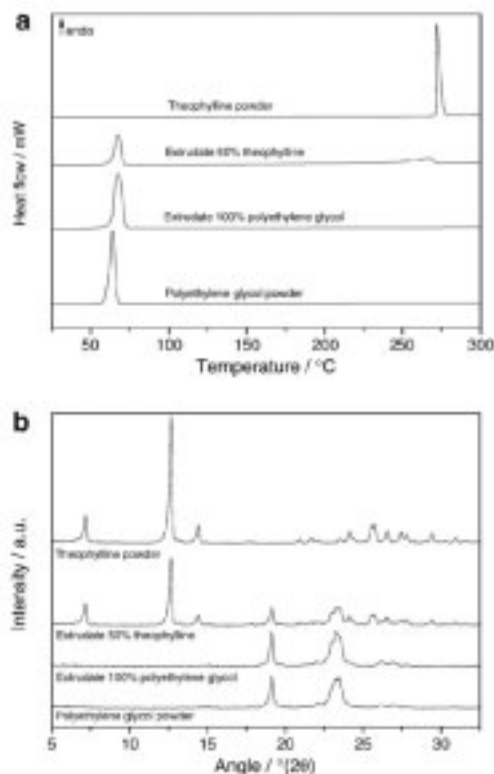
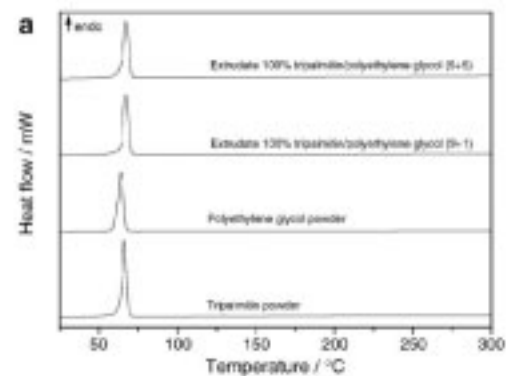


Fig. 2. Physical characterization of polyethylene glycol and theophylline powders and extrudates (a) DSC thermograms and (b) XRPD patterns.

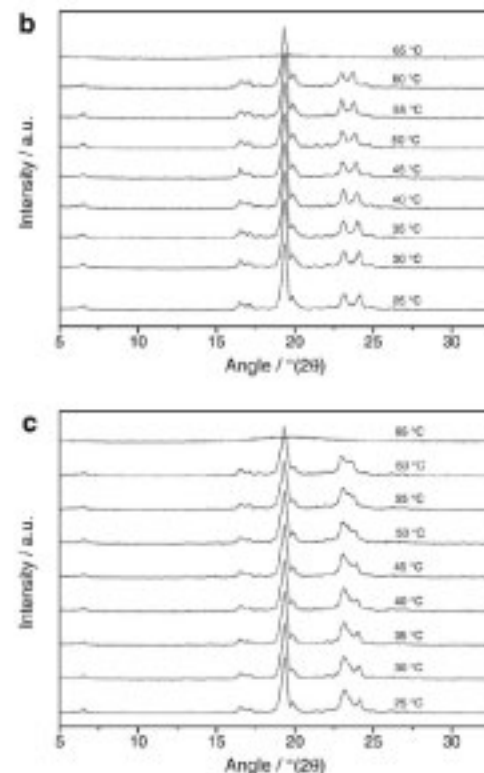


Fig. 3. Physical characterization of mixed extrudates and physical powder mixtures (a) DSC thermograms, variable temperature XRPD patterns of physical mixtures of (b) tripalmitin/polyethylene glycol (5+1) and (c) tripalmitin/polyethylene glycol (5+5).

changes. The powdered substance exhibited a melting endotherm with an onset of 61 °C whereas those for the extrudates were at 63 °C. The melting peak of the extrudate is slightly shifted to higher temperatures and exhibited a broader shape as polyethylene glycol has a rather poor thermal conductivity and the cylindrical extrudate melted slower than the respective powder. Comparison of the sharp melting endotherm of theophylline anhydrate powder (onset 271 °C) and the flatter melting endotherm of the model drug in the extrudate (onset 244 °C) revealed that during the measurements theophylline anhydrate partially dissolved into the molten polyethylene glycol [27]. Results of XRPD measurements reinforce that polyethylene glycol possessed a crystalline structure after extrusion indicated by the peaks at 19.1° (2 θ) and 23.3° (2 θ). The theophylline anhydrate XRPD measurements verified that the model drug also exhibited an unchanged crystalline form in the extrudate. The most significant peaks can be found at 7.1° (2 θ) and 12.6° (2 θ), respectively.

3.1.3. Mixtures of tripalmitin and polyethylene glycol

To obtain a wide range of different dissolution profiles mixed matrices of tripalmitin and polyethylene glycol in various ratios were produced. Initially, mixtures of both substances were extruded at 55 °C in two ratios (tripalmitin/polyethylene glycol 9 + 1 and 5 + 5 w/w) without drug to investigate possible interactions. The thermal analysis results are depicted in Fig. 3a. As the melting endotherms of the pure substances can be found at quite similar temperatures (tripalmitin onset 64 °C, polyethylene glycol onset 61 °C), the mixed extrudates exhibit only one melting endotherm (onset 64 °C) irrespective of mixing ratio. Physical powder mixtures of both ratios were produced and heated in 5 °C steps from 25 °C to 65 °C in the X-ray diffractometer with a diffractogram being

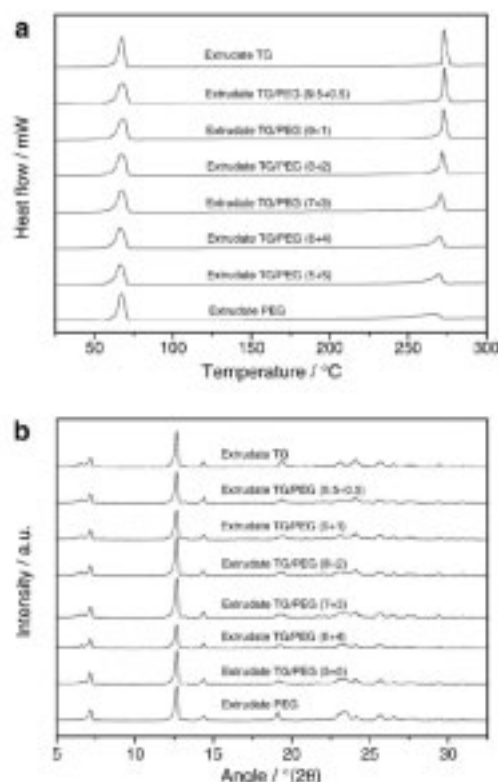


Fig. 4. Physical characterization of mixed extrudates (a) DSC thermograms and (b) XRPD patterns.

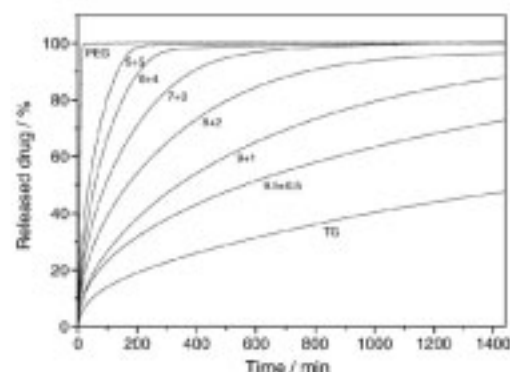


Fig. 5. Dissolution curves of extrudates (PEG = polyethylene glycol, TG = triglyceride), $n = 3$, mean, SD = 4%, not shown.

taken at each temperature step. As the diffractograms for the 9 + 1 (Fig. 3b) and the 5 + 5 mixture (Fig. 3c) depict, both substances remain in the same crystal structures before melting at 65 °C (indicated by an amorphous halo).

In a second step extrudates were produced containing 50% theophylline anhydrate and 50% matrix composed of different ratios (w/w) of lipid and polyethylene glycol. The amount of polyethylene glycol in the matrix (excluding drug) was varied from 5% up to 50% (w/w). Extrudates with acceptable external appearance were obtained for each mixing ratio. Thermal analysis and XRPD analysis were performed on the extrudates. As already seen for the extrudates without drug, one melting endotherm was obtained for the matrix (onset 64 °C) (Fig. 4a). The drug peak was strongly influenced by the amount of polyethylene glycol present. A higher proportion of polyethylene glycol in the matrix led to a less defined and flatter drug melting endotherm. The diffractograms (Fig. 4b) of the different extrudates indicate the crystalline structure of theophylline anhydrate regardless of the matrix composition (peaks at 7.1° and 12.6°). In conclusion, producing extrudates containing different ratios of the matrix materials polyethylene glycol and tripalmitin led to physically stable extrudates, which provides the basis for reproducible release characteristics of drugs.

3.2. Dissolution from extruded matrices

Dissolution testing was performed for 24 hours using a basket apparatus conforming to the USP 29. Fig. 5 depicts the dissolution curves for the pure matrices of tripalmitin and polyethylene glycol as well as the mixed matrices in different ratios. Pure tripalmitin matrices exhibit the slowest release of the drug. The dissolution is purely diffusion controlled, and the drug is released via a pore network formed by the released drug particles [28]. The release of the drug particles is limited in the inert matrix. It is likely that some drug particles are completely surrounded by lipid and hence no release is possible in these cases. At the other extreme, pure polyethylene glycol matrices release the drug very rapid by dissolving completely. Complete drug release is possible with this matrix composition. Tailor-made dissolution profiles could be realized with the mixed matrices. By varying the amount of polyethylene glycol the release of theophylline anhydrate could be controlled over a broad dissolution profile range. The dissolution medium penetrates into the matrix and drug as well as polyethylene glycol dissolve. These processes lead to a porous network in which, depending on the amount of polyethylene glycol, pores of different sizes are formed. Even the addition of small amounts of polyethylene glycol to the tripalmitin matrix results in a significant increase of the release of the drug as observed in Fig. 5.

3.3. Effect of surface characteristics on dissolution behaviour

SEM images were recorded of the extrudate surfaces before and after dissolution testing. Some of these images are depicted in Fig. 6. Before dissolution testing the surfaces are intact without pores. The comparison of the different matrix compositions pure tripalmitin (Fig. 6a), tripalmitin/polyethylene glycol (9+1 w/w) (Fig. 6c) and tripalmitin/polyethylene glycol (5+5 w/w) (Fig. 6e) depicts that the presence of polyethylene glycol leads to smoother surfaces compared to the pure lipid matrix. The pure tripalmitin matrix (Fig. 6a) stays intact after dissolution testing, and only small pores can be found at these positions where drug particles had been located (Fig. 6b). The 9+1 (w/w) mixture matrix exhibits a surface that is similar to that of the pure lipid extrudate before dissolution (Fig. 6c). After dissolution testing some bigger pores can be detected (Fig. 6d) as the drug and polyethylene glycol are simultaneously released. The 5+5 (w/w) mixture shows a differing outer appearance as the surface is smoother (Fig. 6e). After release of the drug large pores can be found all over the surface, where the drug as well as the polyethylene glycol have been released (Fig. 6f) leaving a highly porous tripalmitin matrix. A dense network of pores had been formed during the dissolution process.

As surface characteristics and especially wetting behaviour are important for the dissolution behaviour of a dosage form, contact angle measurements were conducted on the different extrudates. The results are depicted in Fig. 7. Pure tripalmitin extrudates possess poor wettability (contact angle 115°) due to the hydrophobicity of the lipid molecules [29]. The wettability increased linearly ($R^2 = 0.9912$) from the 9.5+0.5 (w/w) mixture with increasing polyethylene glycol in the matrix, which contributes to the increased drug dissolution rates.

3.4. Storage stability

Stability testing was performed on the extrudates with open storage in accelerated conditions (40 °C, 75 %RH) for one year. DSC measurements were performed to determine the solid-state structure

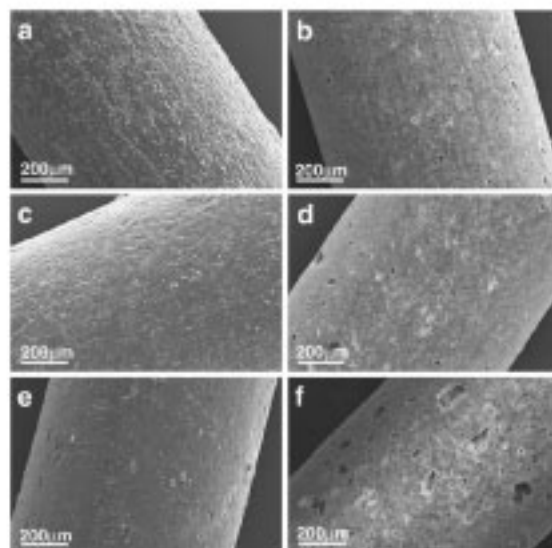


Fig. 6. SEM images of extrudates before and after dissolution [a] tripalmitin before dissolution, [b] tripalmitin after dissolution, [c] tripalmitin/polyethylene glycol (9+1 w/w) before dissolution, [d] tripalmitin/polyethylene glycol (9+1 w/w) after dissolution, [e] tripalmitin/polyethylene glycol (5+5 w/w) before dissolution and [f] tripalmitin/polyethylene glycol (5+5 w/w) after dissolution.

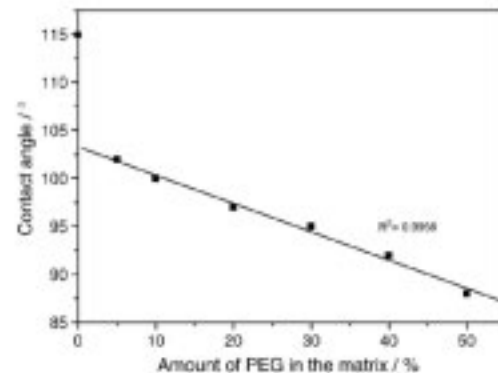


Fig. 7. Contact angle measurements on extrudate surfaces.

of the components. The data in Fig. 8a suggests each of the substances remains in its stable crystalline form over time. Even though polyethylene glycol is a hydrophilic polymer the extrudate remained stable during the stability testing. To investigate the interactions between water vapour and the extrudates during storage Karl Fischer titrimetry was performed before and after storage for one year. Both the pure tripalmitin extrudates and the tripalmitin/polyethylene glycol 9+1 (w/w) mixture extrudates contained less than 0.1% water before and after storage. The tripalmitin/polyethylene glycol 5+5 (w/w) mixture contained less than 0.1% water before storage, and

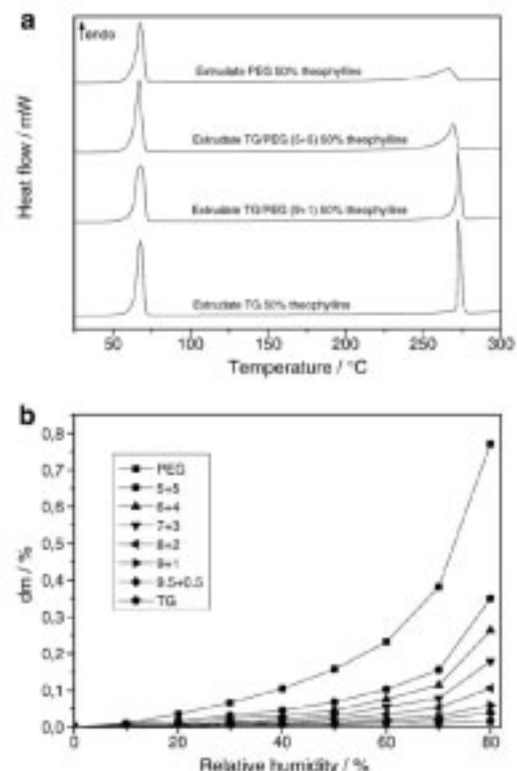


Fig. 8. Storage stability of extrudates [a] DSC thermograms after storage for one year at 40 °C/75%RH and [b] vapour sorption analysis.

after storage the water content increased to 0.16%. The pure polyethylene glycol extrudate possessed an initial water content of 0.11% which increased to 1.19% after storage. In conclusion, all different batches were found to be very stable in accelerated conditions over one year.

In addition, vapour sorption analysis was performed with a dynamic vapor sorption analyzer which exposed the samples to a specific climate. Measurements were performed at room temperature in a humidity range between 0% and 80%. The results were in good agreement with those obtained by Karl Fischer titrimetry (Fig. 8b).

4. Conclusion

Tailor-made dissolution profiles were obtained from matrices consisting of different ratios of triglyceride and the hydrophilic polymer polyethylene glycol produced by extrusion below the melting points of the substances. With these dosage forms the advantages of lipid-based formulations can be combined with faster drug dissolution since the additional release of polyethylene glycol during dissolution leads to a more extensive pore network, facilitating release of the drug. Solid-state analysis reveals that the mixture components exhibit neither physical interactions nor polymorphic transitions during processing and storage. These kinds of extrudates provide a suitable basis for stable oral dosage forms with desirable and reproducible release profiles.

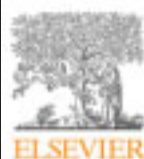
Acknowledgements

The Marie Curie Fellowship and the Galenos Network are acknowledged for financial support (MEST-CT-2004-404992). The work has also been financially supported by the Academy of Finland post-doctoral researcher's project entitled, "Molecular level understanding and control of hydration state changes in pharmaceutical solids", Decision Number 123417.

References

- [1] C.J.H. Porter, W.N. Charman, In vitro assessment of oral lipid based formulations, *Adv. Drug Deliv. Rev.* 50 (2001) 127–147.
- [2] A.J. Humberstone, W.N. Charman, Lipid based vehicles for the oral delivery of poorly water soluble drugs, *Adv. Drug Deliv. Rev.* 25 (1997) 101–128.
- [3] W. Mehnert, K. Müller, Solid lipid nanoparticles – production, characterization and applications, *Adv. Drug Deliv. Rev.* 47 (2001) 165–196.
- [4] S. Prabhu, M. Ortega, C. Ma, Novel lipid-based formulations enhancing the in vitro dissolution and permeability characteristics of a poorly water-soluble model drug, pimecicam, *Int. J. Pharm.* 301 (1–2) (2005) 209–216.
- [5] K. Sato, Crystallization behaviour of fats and lipids – a review, *Chem. Eng. Sci.* 56 (2001) 2255–2265.
- [6] K. Sato, S. Ueno, J. Yano, Molecular interactions and kinetic properties of fats, *Prog. Lipid Res.* 38 (1999) 91–116.
- [7] J.W. Hagemann, Thermal behaviour and polymorphism of acylglycerides, in: N. Garti, K. Sato (Eds.), *Crystallization and Polymorphism of Fats and Fatty Acids*, Marcel Dekker, New York, 1988, pp. 9–95.
- [8] J. Hamdani, A.J. Moes, K. Amighi, Development and evaluation of prolonged release pellets obtained by the melt pelletization process, *Int. J. Pharm.* 245 (1–2) (2002) 167–177.
- [9] Y.E. Zhang, J.B. Schwartz, Melt granulation and heat treatment for wax matrix-controlled drug release, *Drug Dev. Ind. Pharm.* 29 (2) (2003) 131–138.
- [10] B. Chaudhan, S. Shimpi, A. Paradiak, Preparation and characterization of erofenonil solid dispersions using lipid carriers by spray drying technique, *AAPS PharmSciTech* 6 (3) (2005) 1405–12.
- [11] H. Banjes, K. Westemien, M.H. Koch, Crystallization tendency and polymorphic transitions in triglyceride nanoparticles, *Int. J. Pharm.* 129 (1996) 159–173.
- [12] Y.W. Choy, N. Khan, K.H. Yuen, Significance of lipid matrix aging on in vitro release and in vitro bioavailability, *Int. J. Pharm.* 299 (2005) 55–64.
- [13] N. Khan, D.Q.M. Craig, Role of blooming in determining the storage stability of lipid-based dosage forms, *J. Pharm. Sci.* 93 (12) (2004) 2962–2971.
- [14] J. Breitkreutz, F. El Saleh, C. Kiera, P. Kleinbuddé, W. Wiedey, Pediatric drug formulations of sodium benzoate: II. Coated granules with a lipophilic binder, *Eur. J. Pharm. Biopharm.* 56 (2003) 295–299.
- [15] J.F. Pinto, N.P. Silveiro, Assessment of the extrudability of three different mixtures of saturated polyglycolised glycerides by determination of the "specific work of extrusion" and capillary rheometry, *Pharm. Dev. Technol.* 6 (2001) 117–128.
- [16] A. Michalek, V.-R. Kanikani, H.-J. Hamann, P. Kleinbuddé, Controlled release of active as a consequence of the die diameter in solid lipid extrusion, *J. Control. Release* 132 (2008) 35–41.
- [17] C. Reitz, P. Kleinbuddé, Solid lipid extrusion of sustained release dosage forms, *Eur. J. Pharm. Biopharm.* 67 (2007) 440–448.
- [18] M. Windbergs, C.J. Strachan, P. Kleinbuddé, Understanding the solid-state behaviour of triglyceride solid lipid extrudates and its influence on dissolution, *Eur. J. Pharm. Biopharm.* 71 (2009) 80–87.
- [19] M. Windbergs, C.J. Strachan, P. Kleinbuddé, Influence of the composition of glycerides on the solid-state behaviour and the dissolution profiles of solid lipid extrudates, *Int. J. Pharm.* (in press), doi:10.1016/j.ijpharm.2009.03.002.
- [20] R.C. Rowe, F.J. Sheskey, P.J. Weller (Eds.), *Handbook of Pharmaceutical Excipients*, 4th ed., Pharmaceutical press, London, UK, 2003, pp. 460–461.
- [21] P. Schmitt, J. Prochazka, Über die Entwicklung von Retardgranulaten durch Granulatformung, *Pharm. Ind.* 38 (9) (1976) 921–926.
- [22] S. Herrmann, G. Winter, S. Mohl, F. Siepmann, J. Siepmann, Mechanisms controlling protein release from lipidic implants: effect of PEG addition, *J. Control. Release* 118 (2007) 161–168.
- [23] S. Herrmann, S. Mohl, F. Siepmann, J. Siepmann, G. Winter, New insight into the role of polyethylene glycol acting as protein release modifier in lipidic implants, *Pharm. Res.* 24 (8) (2007) 1527–1537.
- [24] D.Q.M. Craig, J.M. Newton, Characterisation of polyethylene glycol solid dispersions using differential scanning calorimetry and solution calorimetry, *Int. J. Pharm.* 76 (1991) 17–24.
- [25] M.M. Crowley, F. Zhang, J.J. Koleg, J.W. McGinity, Stability of polyethylene oxide in matrix tablets prepared by hot-melt extrusion, *Biomaterials* 23 (2002) 4241–4248.
- [26] D.Q.M. Craig, J.M. Newton, Characterisation of polyethylene glycols using differential scanning calorimetry, *Int. J. Pharm.* 74 (1991) 33–41.
- [27] W. Chen, X. Zhang, B. Shan, X. You, Methylxanthines. I. Anhydrous theophylline, *Acta Crystallogr. C53* (1997) 777–779.
- [28] M. Windbergs, M. Juma, H.L. Offenhaus, J.L. Herek, P. Kleinbuddé, C.J. Strachan, Chemical imaging of oral solid dosage forms and changes upon dissolution using coherent anti-Stokes Raman scattering microscopy, *Anal. Chem.* 81 (2009) 2085–2091.
- [29] W. Fang, H. Mayama, K. Tsujii, Spontaneous formation of fractal structures on triglyceride surfaces with reference to their water-repellent properties, *J. Phys. Chem. B* 111 (2007) 564–571.

9.5. Article 5: Influence of structural variations on drug release from lipid/polyethylene glycol matrices



Contents lists available at ScienceDirect

European Journal of Pharmaceutical Sciences

journal homepage: www.elsevier.com/locate/ejps

Influence of structural variations on drug release from lipid/polyethylene glycol matrices

Maïke Windbergs^{a,b}, Clare Joanna Strachan^{b,c}, Peter Kleinebudde^{a,*}^a Institute of Pharmaceutics and Biopharmaceutics, Heinrich-Heine-University, Universitätsstr. 1, 40225 Düsseldorf, Germany^b Centre for Drug Research, University of Helsinki, Viikinkaari 5E, 00014 University of Helsinki, Finland^c School of Pharmacy, University of Otago, 38 Frederick Street, Dunedin 9054, New Zealand

ARTICLE INFO

Article history:

Received 27 January 2009

Received in revised form 14 April 2009

Accepted 17 April 2009

Available online 3 May 2009

Keywords:

Solid lipid extrusion

Dissolution

Polyethylene glycol

Triglyceride

Chain length

Molecular weight

ABSTRACT

Different combinations of monoacid triglycerides and polyethylene glycol powders of different molecular weights were successfully extruded below their melting temperatures as a basis for oral dosage forms. The incorporated polyethylene glycols exhibiting different mean molecular weights were compared with respect to their effect on the dissolution rate for a model drug, and a mean molecular weight of 10,000 resulted in the most advantageous characteristics (fastest dissolution). Triglycerides with different fatty acid chain lengths provided additional options for the extrusion temperature which is beneficial for temperature sensitive active pharmaceutical ingredients. To obtain stable extrudates with desirable and reproducible dissolution characteristics a good understanding of the underlying processes during processing and storage is mandatory.

© 2009 Elsevier B.V. All rights reserved.

1. Introduction

In the course of investigating new groups of excipients as a basis for oral dosage forms lipids have recently generated substantial interest (Prabhu et al., 2005; Porter and Charman, 2001; Liu et al., 2001; Humberstone and Charman, 1997; Qi et al., 2008). Lipid-based dosage forms include solid dispersions (Chauhan et al., 2005) and solid lipid nanoparticles (Bunjes et al., 1996; Mehnert and Mäder, 2001) which involve the melting of the lipid. Solid lipid extrusion, in which the solid structure of the lipid is maintained, has been shown to be a suitable manufacturing process to obtain dosage forms with reproducible and stable dissolution profiles (Windbergs et al., 2009a; Breitzkreutz et al., 2003; Pinto and Silverio, 2001; Michalk et al., 2008; Reitz and Kleinebudde, 2007). In this process, the powdered lipid is mixed with the active pharmaceutical ingredient and the powder mixture is extruded below the melting point of the lipid with the crystal form of the lipid being retained. The process conditions can be adjusted to the melting temperature of a specific lipid so that different lipids can be used for the process. As lipids are a rather versatile and diverse group of substances, a broad range of extruded matrix compositions

is possible. Solid lipid extrusion experiments have already been performed on pure monoacid triglycerides with different chain lengths (Windbergs et al., 2009a). The combination of extrusion temperature and friction inside the extruder was identified as a key factor for the polymorphic behaviour of the glycerides during processing and storage. A thin molten lipid layer on the surface of the extrudate is always obtained during extrusion due to the effect of temperature and friction. This layer directly resolidifies after leaving the die plate. When the extrusion temperature does not exceed the melting points of any unstable polymorphic form during extrusion the thin lipid layer on the surface of the extrudate recrystallizes in the unstable α -form of the lipid. Rapidly, transformation to the stable β -form takes place which appears in the form of fine needles covering the surface of the extrudate. Hence, the wetting of this extrudate is impeded and therefore we obtain decreased dissolution rates. When the temperature of the extruder is adjusted according to these findings only the stable β -form of the lipid is obtained on the extrudate surface and polymorphic transformations can be avoided (Windbergs et al., 2009a). Furthermore, the chain length was found to have a significant influence on the release rate of the drug. The release profile could be varied by selecting the appropriate lipid, but the release was always rather slow. To extend the range of dissolution possibilities, mixed matrices of a triglyceride and a partial glyceride were produced (Windbergs et al., 2009b). Unfortunately, some of

* Corresponding author. Tel.: +49 211 811 4220; fax: +49 211 811 4251.
E-mail address: kleinebudde@uni-duesseldorf.de (P. Kleinebudde).

those formulations were accompanied by interactions between the two excipients leading to undesirable polymorphic transitions influencing the release of the active pharmaceutical ingredient (API). The polymorphic behaviour of these mixtures is more complex to apprehend and control due to the different polymorphic natures of mono-, di- and triglycerides. As polyethylene glycol has already successfully been used as a pore former in controlled release dosage forms (Cleek et al., 1997; Herrmann et al., 2007a) a further approach involved combining triglyceride and polyethylene glycol with a mean molecular weight of 10,000 (Windbergs et al., 2009c). Despite the fact that polyethylene glycol can undergo polymorphic changes this could not be observed for those formulations (Craig, 1995). By varying the proportions of the two excipients, tailor-made dissolution profiles could be obtained. In addition, those formulations were physically stable in accelerated conditions.

In this study, tripalmitin, a monoacid triglyceride, was extruded below its melting point in combination with 10% polyethylene glycol of different mean molecular weights in the range of 10,000–7,000,000 in order to investigate the influence of molecular weight of the hydrophilic polymer on the drug dissolution behaviour. In addition, three monoacid triglycerides of different fatty acid chain lengths were extruded with 10% polyethylene glycol with a mean molecular weight of 10,000 to vary the formulation for these matrices. The extrusion temperature was varied in these cases due to the different requirements of the chosen lipids. For the formulation of dosage forms based on substances such as lipids which tend to form different polymorphic forms during processing and storage careful monitoring of the solid-state behaviour is mandatory to obtain reliable and reproducible dosage forms, as solid-state changes of the components might change desirable characteristics of the dosage form, especially dissolution behaviour (Choy et al., 2005; Khan and Craig, 2004). In this study, the solid-state behaviour of powders and extrudates was investigated using a combination of differential scanning calorimetry and X-ray powder diffraction. Dissolution testing was performed with a basket apparatus following the USP 29 method 1. The dissolution profiles were correlated to the results of solid-state analysis. The stability of the extrudates was tested over time in room conditions and accelerated conditions (40 °C/75% RH). In addition, moisture sorption analysis experiments were performed to investigate the vapour sorption behaviour of the extrudates.

2. Materials and methods

2.1. Materials

Three monoacid triglycerides in powdered form were used as received: trilaurin (Dynasan 112®), tripalmitin (Dynasan 116®) and tristearin (Dynasan 118®). Each of these substances was produced by Sasol (Witten, Germany). The average of the batches which were used contained 98% pure triglycerides. The hydrophilic polymer polyethylene glycol was used in different mean molecular weights. Powdered polyethylene glycols with a mean molecular weight of 10,000 (Polyglykol 10000 P®) and with a mean molecular weight of 20,000 (Polyglykol 20000 P®) were provided by Clariant (Waalwijk, The Netherlands). Polyethylene glycols of mean molecular weights 100,000 (Polyox WSR N10®), 1,000,000 (Polyox WSR N12K®) and 7,000,000 (Polyox WSR 303®) were provided by Dow Chemical (New Milford, CT, USA). The powdered model drug theophylline anhydrate was produced by BASF (Ludwigshafen, Germany). All crystal forms were verified with X-ray powder diffraction measurements and differential scanning calorimetry.

2.2. Methods

2.2.1. Extrusion

The excipients (triglycerides and polyethylene glycol of different mean molecular weights) and the model drug theophylline anhydrate were weighed in a 1:1 ratio and mixed in a laboratory mixer (LM 20 Bohle, Ennigerloh, Germany) at 25 rpm for 15 min. The powder mixture was gravimetrically fed by a dosing device (KT20K-Tron Soder, Lenzhard, Switzerland) into the barrel of a co-rotating twin-screw extruder (Mikro 27GL-28D, Leistritz, Nürnberg, Germany). The die plate contained 23 holes exhibiting 1 mm diameter and 2.5 mm length. The temperature of the extruder barrel was adjusted as described in the individual experiment. A constant screw speed was kept at 30 rpm with a fixed feeding rate of 40 g min⁻¹.

2.2.2. Differential scanning calorimetry (DSC)

Thermograms were recorded using a DSC 821e calorimeter (Mettler-Toledo, Gießen, Germany). Hermetically sealed aluminium pans (40 µl) contained weighed samples of approximately 5 mg. Experiments were conducted twice with a heating rate of 10 °C min⁻¹ within a temperature range of 20–300 °C.

2.2.3. X-ray powder diffraction (XRPD)

Diffraction patterns were recorded with a theta-theta X-ray powder diffractometer (DS Advance, Bruker AXS GmbH, Karlsruhe, Germany) in symmetrical reflection mode with CuK α radiation ($\lambda = 1.54 \text{ \AA}$) and Göbel mirror bent multilayer optics. The angular range of 5–40 °(2 θ) was used with a step size of 0.05° (2 θ) and the measuring time of 1 s per step. The samples were gently compressed into the sample holders to obtain a smooth surface. Each experiment was conducted in triplicate.

2.2.4. Dissolution

According to USP 29 method 1 dissolution experiments were performed in a basket apparatus (Sotax AT7 smart, Sotax, Lörrach, Germany). Extrudates with a diameter of 1 mm were cut into cylinders of 1 cm length and weighed into the baskets (total 140 mg in each basket). Dissolution testing was performed in a medium consisting of 900 mL purified water containing 0.001% (w/v) polysorbate 20. The stirring speed was kept constant at 50 rpm and the temperature was 37 ± 0.5 °C. The drug concentration in solution was determined at 2.5 min intervals at 242 nm with a UV-Vis spectrometer (Lambda 40, Perkin-Elmer, Rodgau-Juergesheim, Germany) and a continuous flow-through cuvette. Each experiment was conducted in triplicate. The mean for the dissolution curve was used and the standard deviation at each time point was always below 4%.

2.2.5. Storage

The samples were stored in open Petri dishes for 12 months in a climate chamber (KBF 240, Binder, Tuttlingen, Germany) at 40 °C and 75% RH.

2.2.6. Scanning electron microscopy (SEM)

Images were recorded with a scanning electron microscope (Leo 1430VP, Leo Elektron Microscopy, Cambridge, UK) at a working voltage of 20 kV. After attaching the samples to aluminium stubs with double-sided carbon tape the samples were sputter-coated with gold for 180 s (Agar Manual Sputter Coater B73-40, Agar Scientific, Stansted, UK).

2.2.7. Contact angle measurements

An optical contact angle meter (Drop shape analysis system DSA100, Krüss, Hamburg, Germany) with the associated software (Drop shape analysis DSA1 v 1.90, Hamburg, Germany) was used to

determine the contact angles of the samples. Each experiment was performed eight times by placing a 0.8 μL drop of distilled water on the extrudate surface and calculating the mean result.

2.2.8. Laser diffraction

The particle size of the powders was determined with a laser diffractometer (Helos, KF-Magic, Clausthal-Zellerfeld, Germany) using the dry dispersion method. The median and the 90% quantile were determined three times. The mean was calculated for each material.

2.2.9. Moisture sorption analysis

The samples were exposed to a specific climate composed of controlled temperature and humidity in a dynamic vapour sorption analyzer SPS 11 (Projekt Messtechnik, Ulm, Germany). The sample weight was continuously monitored to detect mass changes. Aluminium cups contained the samples of approximately 1500 mg. Measurements were performed twice at room temperature in the humidity range of 0–80% with steps of 10% each.

3. Results and discussion

3.1. Extrusion of matrices consisting of lipids and polyethylene glycols

Based on previous experience, the critical process variable for the extrusion of lipid-based matrices is the extrusion temperature (Windberg *et al.*, 2009a). All other process variables were kept constant as described in Section 2. The extrusion temperature affects the crystallization behaviour of the lipid. Triglycerides exhibit different polymorphic forms that are characterized by specific thermal stabilities. Therefore, a lipid produced in a metastable polymorphic form might transform to a more stable one during storage.

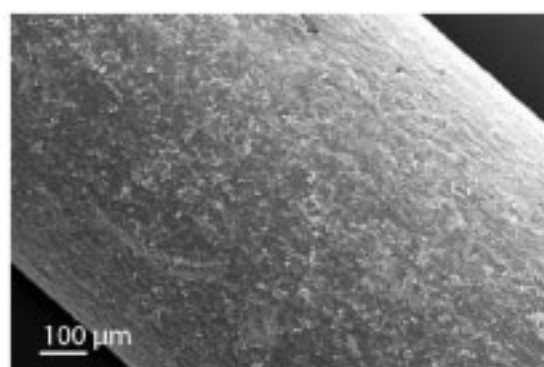


Fig. 1. SEM image of an extrudate containing tripalmitin/polyethylene glycol 100000 (9+1, w/w).

Hence, suitable temperatures for each formulation had to be found to maintain the stable form of the lipid. In addition, a minimum requirement for a successful extrusion process is extrudates with a good external appearance providing a homogenous and smooth surface (Fig. 1). This aim could be reached for each of the prepared formulations. For the extrusion studies with mixtures of tripalmitin and polyethylene glycol of different molecular weights the temperature was always kept at 55 °C which is below the reported melting points of 66 °C for tripalmitin (Hagemann, 1988) and 62–66 °C for polyethylene glycol (Craig and Newton, 1991). For the formulations containing trilaurin the extrusion temperature was adjusted to 40 °C as the melting point of the substance is 46 °C (Hagemann, 1988). For formulations containing tristearin with a melting point of 73 °C (Hagemann, 1988) the melting point of polyethylene glycol

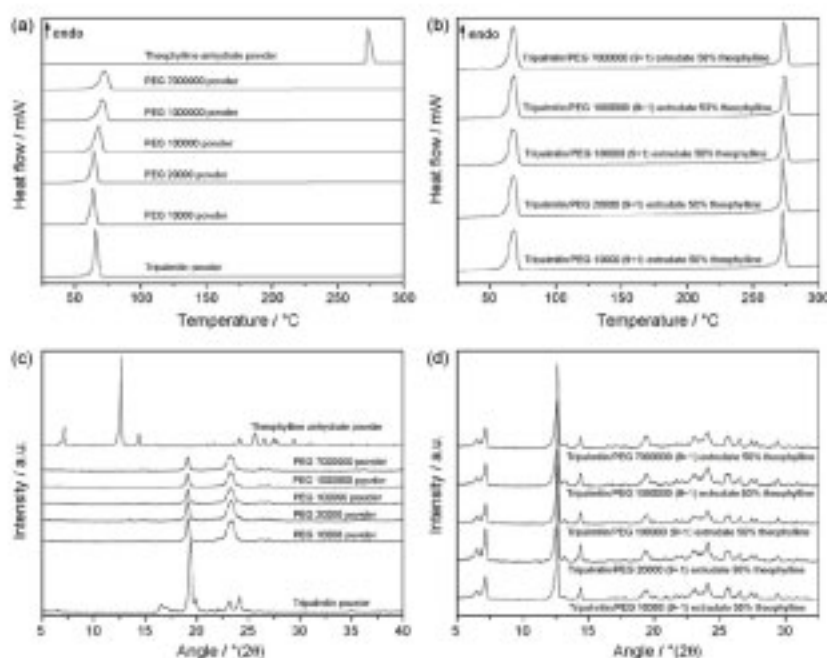


Fig. 2. Physical characterization of powders and extrudates (a) DSC thermograms of powders, (b) DSC thermograms of extrudates, (c) XRPD patterns of powders and (d) XRPD patterns of extrudates.

was the limiting factor, so that these formulations were extruded at 55 °C.

3.2. Solid-state characterization of tripalmitin matrices containing polyethylene glycol with different molecular weights

Extrudates containing 50% model drug theophylline anhydrate and 50% matrix (w/w) were produced with a matrix consisting of tripalmitin and polyethylene glycol (9+1, w/w). The mean molecular weight of polyethylene glycol in the formulation was varied from 10,000 up to 7,000,000. Solid-state analysis was performed on the powders and extrudates with a combination of DSC and XRPD. The results are presented in Fig. 2. The DSC thermograms of the powders (Fig. 2a) depict the melting peaks of the individual substances. Tripalmitin is represented with the peak of the most stable β -form (onset 63.6 °C) (Hagemann, 1988). The polyethylene powders show a slight shift of the melting peak to higher temperatures and peak broadening with increasing mean molecular weight (onset 60.7–65.6 °C) (Craig and Newton, 1991). The model drug theophylline anhydrate is present with a melting peak at 271.1 °C (Chen et al., 1997). Fig. 2b displays the thermograms of the extrudates. Irrespective of polyethylene glycol molecular weight the matrix is represented by one combined melting peak with an onset at about 63 °C for both excipients as the melting points of the individual substances are quite close to each other whereas the drug shows a narrow melting peak with the onset of 270.9 °C. No interactions or solid-state changes could be detected. The diffractograms obtained by XRPD for powders (Fig. 2c) and extrudates (Fig. 2d) also do not provide any evidence of solid-state changes. The significant peaks for theophylline can be detected at 7.1° and 12.6° indicating that theophylline remained in its stable crystalline form.

3.3. Dissolution from extruded matrices based on tripalmitin and different polyethylene glycols

To investigate the effect of the molecular weight of polyethylene glycol on the release characteristics of the model drug, dissolution

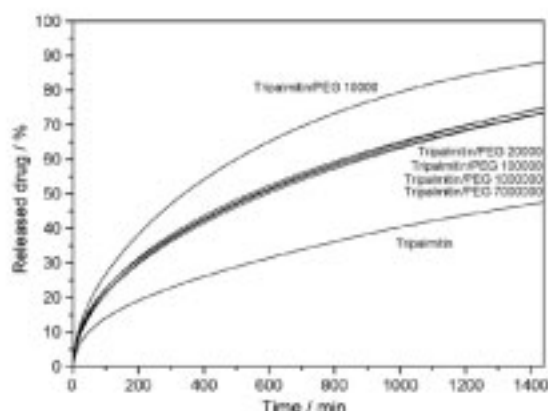


Fig. 3. Dissolution profiles of extrudates containing different matrix compositions based on tripalmitin and polyethylene glycol, PEG (9+1, w/w) (mean, $n=3$, SD \pm 3%, not shown).

studies were performed using a basket apparatus conform to the method 1 in the USP 29. The results are depicted in Fig. 3. The dissolution curve for extrudates containing only tripalmitin as matrix material is added for comparison. The release in the latter case is controlled by diffusion and dissolution of the drug in the water filled pores of the matrix. The drug is liberated through a network created by pores formed by drug particles which have already been released. In contrast, polyethylene glycol as a water soluble polymer increases the dissolution rate of the drug. As water penetrates into the matrix polyethylene glycol is dissolved as well as the drug leaving bigger pores and increasing the pore network within the matrix (Herrmann et al., 2007a,b). The acceleration of the dissolution depended on the molecular weight of polyethylene glycol. Polyethylene glycol 10000 leads to the largest increase in dissolution rate, and all the other polyethylene glycols in the matrices had approximately the same influence on the dissolution rate. The particle size of the different polyethylene glycol powders

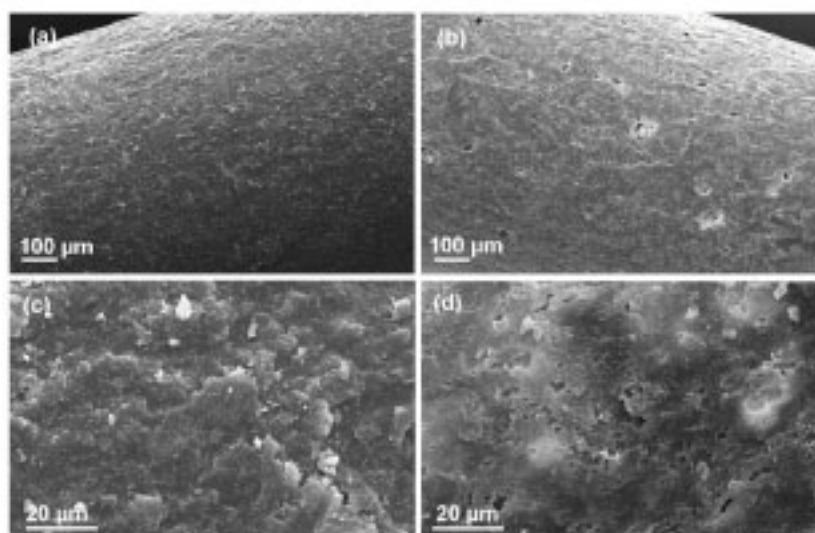


Fig. 4. SEM images of extrudates containing tripalmitin/polyethylene glycol 100000 (9+1, w/w) in different magnifications (a and c) before and (b and d) after dissolution.

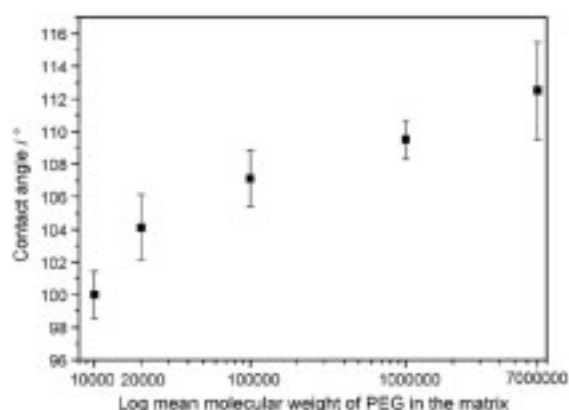


Fig. 5. Contact angles on the surface of different extrudates ($n=8$, mean \pm CI 95%).

was determined with laser diffraction. All powders exhibit the mean of the 90% percentile in the range of 300–500 μm . Therefore, phenomena depending on particle size differences could be excluded. Scanning electron microscopy was performed with the samples before and after dissolution to investigate surface transformations. Irrespective of mean molecular weight of polyethylene glycol the different formulations led to the same outer appearance after 24 h of dissolution. As an example, the surface of an extrudate containing tripalmitin/polyethylene glycol 100000 is depicted in Fig. 4a–d. After dissolution (Fig. 4b and d) the smooth surface is disrupted by pores created by the release of drug and polyethylene glycol. As there are no morphologic differences on the surface the results should depend on the swelling and dissolution behaviour of the polyethylene glycol molecules in the matrix. It is known that the swelling of polyethylene glycol is a phenomenon which depends on the molecular weight as higher molecular weights tend to swell more but more slowly than lower molecular weights (Apicella et al., 1993; Maggi et al., 2001). In addition, the bigger molecules dissolve more slowly. Based on these assumptions, the similar drug dissolution behaviour for all molecular weights of polyethylene glycol except 10,000 is unexpected and requires further explanation. In addition, contact angle measurements were performed to investigate the wetting abilities of the different extrudate surfaces before dissolution. The results are depicted in Fig. 5. The contact angle is increasing with increasing mean molecular weight of the polyethylene glycol in the matrix. Therefore, during dissolution testing the extrudates containing polyethylene glycol 10000 provide the best contact surface for the dissolution medium.

3.4. Solid-state characterization of matrices containing different triglycerides and polyethylene glycol 10000

In addition to the combination of tripalmitin and polyethylene glycol 10000 (9+1, w/w), trilaurin as a monoacid triglyceride with shorter fatty acids and tristearin as a monoacid triglyceride with longer fatty acids were extruded with polyethylene glycol 10000 (9+1, w/w). Each of the formulations consisted of 50% matrix and 50% API (w/w). Solid-state analysis was performed on the extrudates with DSC and XRPD. The results are depicted in Fig. 6. The DSC thermograms suggest that the combined matrix containing trilaurin and polyethylene glycol 10000 resulted in a stable system (Fig. 6a). For comparison also the thermograms of the pure matrices with API are depicted. The mixed matrix extrudate exhibits three

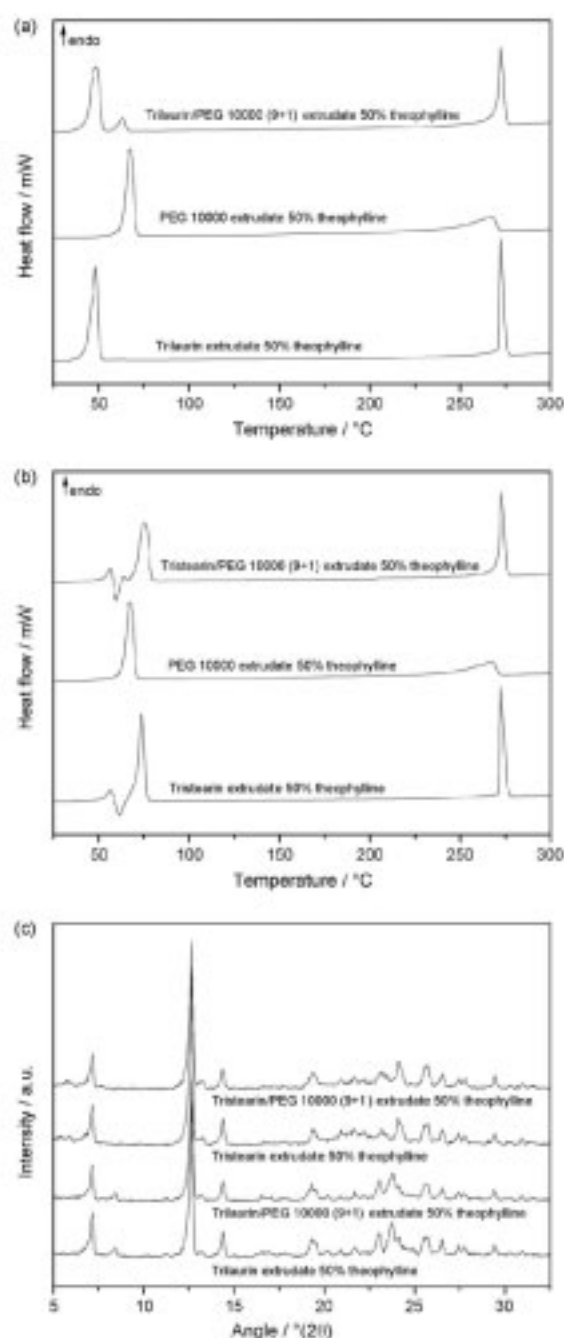


Fig. 6. Physical characterization of extrudates (a) DSC thermograms of extrudates containing trilaurin. (b) DSC thermograms of extrudates containing tristearin and (c) XRPD patterns of extrudates containing trilaurin and tristearin.

peaks, one for each component. Trilaurin is represented by its melting endotherm with the onset at 43.5 $^{\circ}\text{C}$ indicating the most stable β -form of the lipid (Hagemann, 1988). Polyethylene glycol 10000 shows a small peak (onset 58.6 $^{\circ}\text{C}$) due to the small quantity used in the extrudate (Craig and Newton, 1991). The API theophylline

anhydrate can be identified by its melting endotherm with an onset at 270.7 °C (Chen et al., 1997). The different shape of the peak in the different matrices is due to the theophylline anhydrate being able to partly dissolve in the molten polyethylene glycol during the measurement. In conclusion, the combination of trilaurin and polyethylene glycol 10000 led to a stable extrudate as there was no evidence of any of the substances changing their crystal structures during extrusion, which is the basis for a reproducible and reliable dissolution behaviour.

The results of the thermal analysis of the combination of tristearin and polyethylene glycol are depicted in Fig. 6b. For comparison the thermograms of the pure matrix extrudates with API are also represented. The extrusion was performed at 55 °C which was the highest temperature at which polyethylene glycol could be extruded without melting. Tristearin exhibited polymorphic transitions at this extrusion temperature, which is consistent with previous study on tristearin and theophylline extrudates (Windbergs et al., 2009a). Depending on the extrusion temperature a mixture of α - and β -forms [extrusion temperature 55 °C] or the pure desirable β -form (extrusion temperature 65 °C) of the lipid can be obtained in the extrudate. The thermogram of the pure tristearin matrix (extrusion performed at 55 °C) contains three thermal events for the lipid and the melting endotherm of the drug (onset 271.1 °C). The metastable α -form of the lipid can be found as a melting endotherm (onset 52.0 °C). The molten part of the sample recrystallizes to the metastable β -form during the measurement visible through its recrystallization exotherm of (onset 58.6 °C) (Hagemann, 1988). The stable β -form is indicated by the melting endotherm with an onset at 70.7 °C. The combined matrix exhibits the following thermal events: melting endotherm (onset 52.2 °C) of the tristearin α -form, recrystallization exotherm of the tristearin β -form (onset 58 °C) and melting endotherm of the stable tristearin β -form (onset 70.5 °C). The API theophylline anhydrate is represented by its melting endotherm (onset 271.2 °C) (Chen et al., 1997). XRPD experiments were performed on the extrudates to investigate the crystal structure. The diffractograms are depicted in Fig. 6c. Theophylline anhydrate remains in its stable crystal form in each formulation indicated by the significant peaks at 7.1° and 12.6°.

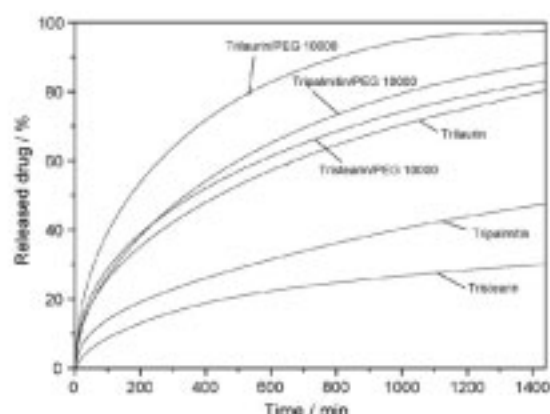


Fig. 7. Dissolution profiles of extrudates based on different triglycerides and polyethylene glycol, PEG 10000 (9+1, w/w) (mean, $n=3$, SD=43, not shown).

3.5. Dissolution from extruded matrices based on different triglycerides and polyethylene glycol 10000

Dissolution testing was performed on the extrudates to investigate the effect of the chain length of the different monoacid triglycerides on the dissolution behaviour. For comparison also the curve of tripalmitin/polyethylene glycol 10000 mixed matrices recorded for a previous study (Windbergs et al., 2009c) is displayed. Release of the drug from pure triglyceride matrices is purely diffusion controlled, as the matrix stays intact. The release rate is dependant on the chain lengths of the fatty acids esterified with the glycerol molecule. The longer they are the slower is the release of the drug (Fig. 7). The contact angle of the extrudate surfaces is increasing with increasing chain length of the lipid leading to decreased wetting ability and hence decreased dissolution rates. Extrudates containing trilaurin exhibited a contact angle of 98°, while extrudates containing tripalmitin possessed a contact angle of 100° and extrudates containing tristearin had a contact angle of

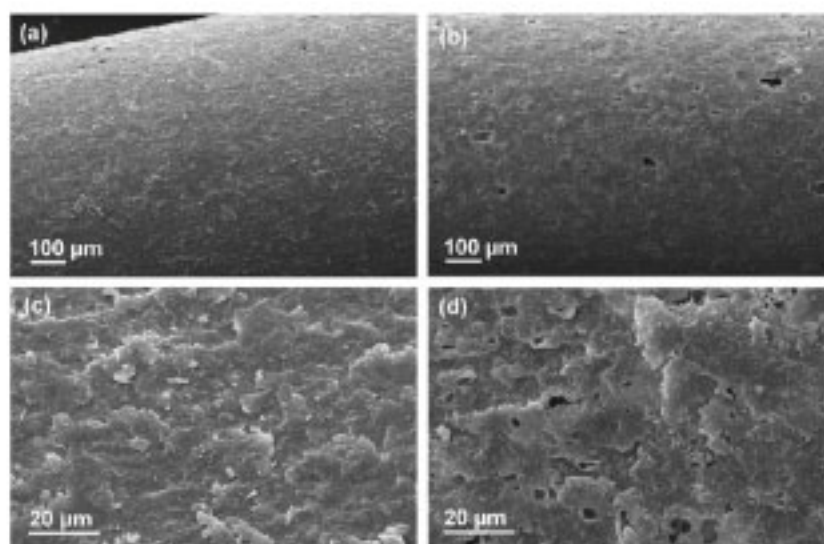


Fig. 8. SEM images of extrudates containing tristearin/polyethylene glycol 10000 (9+1, w/w) in different magnifications (a and c) before and (b and d) after dissolution.

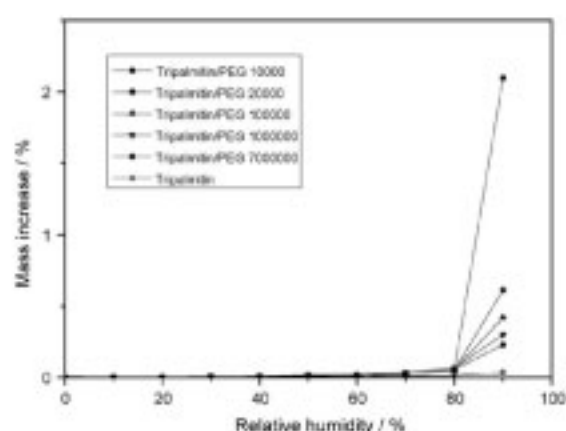


Fig. 9. Vapour sorption analysis of different extrudates.

111°. For each different triglyceride, the dissolution behaviour of the pure lipid matrix and the mixed matrix led to the conclusion that polyethylene glycol could accelerate the dissolution in each case. The surface of the different mixed extrudates was investigated with SEM. Fig. 8a–d depicts the surface of tristearin/polyethylene glycol extrudates before and after dissolution. No general differences were evident in a comparison of the images taken of the mixed extrudate surfaces with different triglycerides (data not shown). The surface of the extrudate before dissolution is homogenous and relatively smooth. After dissolution pores can be found at those places where drug or polyethylene glycol was previously located.

3.6. Vapour sorption analysis

To investigate the interactions between the extrudates and water vapour the samples were exposed to a specific climate. As polyethylene glycol is a relatively hydrophilic polymer this is an important point to address with regard to storage stability. Experiments were performed on extrudates containing different types of polyethylene glycol in the relative humidity range of 0–90%. The results are depicted in Fig. 9. A correlation between the mass increase of the extrudate and the mean molecular weight of the polyethylene glycol in the sample can be established. Increasing the molecular weight of the polyethylene glycol in the formulation leads to a lower mass increase of the sample and hence smaller interaction with water vapour. A substantial mass increase is only observed for a RH of 90%.

4. Conclusion

Different combinations of monoacid triglycerides and polyethylene glycol powders of different molecular weights were successfully extruded below their melting temperatures as a basis for promising oral dosage forms. Variation of the mean molecular weight of polyethylene glycol showed that each of these polymers was able to accelerate the dissolution rate but a mean molecular weight of 10,000 had the best effect. The higher molecular weights ranging from 20,000 to 7,000,000 had a less pronounced effect and were similar among themselves. Therefore, the addition of polyethylene glycol with a mean molecular weight exceeding 10,000 provides no additional advantage. The variation of the fatty acid chain length in the lipid component of the extrudate broadened the range of possible processing temperatures, and in the case of trilaurin the extrusion temperature of 40 °C was suitable

which is advantageous for temperature sensitive APIs. In case of tristearin the extrusion temperature could not be increased to the suitable temperature at which this lipid remains its most stable β -form as polyethylene glycol melted. Therefore, lipid polymorphic transitions occurred which can have a pronounced effect on the dissolution characteristics and are uncontrollable. The results of this study help to gain a deeper understanding of the variables that may influence drug dissolution behaviour from these oral dosage forms. Such knowledge broadens the potential applications of solid lipid extrudates through the ability to provide tailor-made dissolution profiles.

Acknowledgements

The Marie Curie Fellowship and the Galenos Network are acknowledged for the financial support (MEST-CT-2004-404992). The companies Sasol, Clariant and Dow Chemical are acknowledged for providing their substances.

References

- Apicelli, A., Capello, B., Dell'Nobile, M.A., La Rotonda, M.L., Mensitieri, G., Nicolais, L., 1995. Poly(ethylene oxide) (PEO) and different molecular weight PEO blends monolithic devices for drug release. *Biomaterials* 14 (2), 83–90.
- Bretkmeatz, J., El Saleh, F., Kiera, C., Kleinbuecke, F., Wiedey, W., 2003. Pediatric drug formulations of sodium benzoate. II. Coated granules with a lipophilic binder. *Eur. J. Pharm. Biopharm.* 56, 255–260.
- Burjes, H., Westesen, K., Koch, M.H.J., 1996. Crystallization tendency and polymorphic transitions in triglyceride nanoparticles. *Int. J. Pharm.* 129, 159–173.
- Chauhan, B., Shirogi, S., Pasadkar, A., 2005. Preparation and characterization of estradiol solid dispersions using lipid carriers by spray drying technique. *AAPS Pharm. Sci. Tech.* 6 (3), 405–412.
- Chen, W., Zhang, X., Shan, B., You, X., 1997. Methylxanthines. I. Anhydrous theophylline. *Acta Cryst.* C53, 777–779.
- Chey, Y.W., Khan, N., Yuan, K.H., 2005. Significance of lipid matrix aging on in vitro release and in vitro bioavailability. *Int. J. Pharm.* 290, 55–64.
- Cleek, R.L., Ting, K.C., Eskin, S.G., Mikos, A.G., 1997. Microparticles of poly(DL-lactide-co-glycolic acid)/poly(ethylene glycol) blends for controlled drug delivery. *J. Control. Release* 48, 259–268.
- Craig, D.Q.M., 1995. A review of thermal methods used for the analysis of the crystal form, solution thermodynamics and glass transition behaviour of polyethylene glycols. *Thermochim. Acta* 248, 189–203.
- Craig, D.Q.M., Newton, J.M., 1991. Characterization of polyethylene glycols using differential scanning calorimetry. *Int. J. Pharm.* 74, 33–41.
- Hagemann, J.W., 1988. Thermal behaviour and polymorphism of acylglycerides. In: Garti, N., Sato, K. (Eds.), *Crystallization and Polymorphism of Fats and Fatty Acids*. Marcel Dekker, New York, pp. 9–95.
- Herrmann, S., Winter, G., Mohl, S., Siepmann, F., Siepmann, J., 2007a. Mechanisms controlling protein release from lipidic implants: effect of PEG addition. *J. Control. Release* 118, 161–168.
- Herrmann, S., Mohl, S., Siepmann, F., Siepmann, J., Winter, G., 2007b. New insight into the role of polyethylene glycol acting as protein release modifier in lipidic implants. *Pharm. Res.* 24 (8), 1527–1537.
- Humberstone, A.J., Charman, W.N., 1993. Lipid based vehicles for the oral delivery of poorly water soluble drugs. *Adv. Drug Deliv. Rev.* 25, 101–128.
- Khan, N., Craig, D.Q.M., 2004. Role of blooming in determining the storage stability of lipid based dosage forms. *J. Pharm. Sci.* 93 (12), 2962–2971.
- Liu, J., Zhang, F., McGinity, J.W., 2001. Properties of lipophilic matrix tablets containing phenylpropranolamine hydrochloride prepared by hot-melt extrusion. *Eur. J. Pharm. Biopharm.* 52 (2), 181–190.
- Maggi, L., Segale, L., Torre, M.L., Ochoa Machiste, E., Corne, U., 2001. Dissolution behaviour of hydrophilic matrix tablets containing different polyethylene oxides (PEOs) for the controlled release of a water-soluble drug. *Dimensional study*. *Biomaterials* 23, 1103–1119.
- Mehner, W., Mäder, K., 2001. Solid lipid nanoparticles—production, characterization and applications. *Adv. Drug Deliv. Rev.* 47, 165–196.
- Michalek, A., Karikari, V.R., Hamann, H.J., Kleinbuecke, F., 2008. Controlled release of active as a consequence of the die diameter in solid lipid extrusion. *J. Control. Release* 132 (1), 35–41.
- Pinto, J.F., Silverio, N.P., 2001. Assessment of the extrudability of three different mixtures of saturated polyglycolised glycerides by determination of the “specific work of extrusion” and capillary rheometry. *Pharm. Dev. Technol.* 6, 117–128.
- Prabhu, S., Orrega, M., Ma, C., 2005. Novel lipid-based formulations enhancing the in vitro dissolution and permeability characteristics of a poorly water-soluble model drug, piroxicam. *Int. J. Pharm.* 301 (1–2), 209–216.
- Porter, C.J.H., Charman, W.N., 2001. In vitro assessment of oral lipid based formulations. *Adv. Drug Deliv. Rev.* 50, 127–147.

- Qi, S., Deutsch, D., Craig, D.Q., 2008. An investigation into the mechanisms of drug release from taste-masking fatty acid microspheres. *J. Pharm. Sci.* 97 (9), 3842–3854.
- Reitz, C., Kleinebudde, P., 2007. Solid lipid extrusion of sustained release dosage forms. *Eur. J. Pharm. Biopharm.* 67, 440–448.
- Windbergs, M., Strachan, C.J., Kleinebudde, P., 2009a. Understanding the solid-state behaviour of triglyceride solid lipid extrudates and its influence on dissolution. *Eur. J. Pharm. Biopharm.* 71, 89–87.
- Windbergs, M., Strachan, C.J., Kleinebudde, P., 2009b. Influence of the composition of glycerides on the solid-state behaviour and the dissolution profiles of solid lipid extrudates. *Int. J. Pharm.*, doi:10.1016/j.ijpharm.2009.03.002.
- Windbergs, M., Strachan, C.J., Kleinebudde, P., 2009c. Tailor-made dissolution profiles by extruded matrices based on lipid polyethylene glycol mixtures. *J. Control Release*, doi:10.1016/j.jconrel.2009.04.002.

9.6. Article 6: Investigating the relationship between drug distribution in solid lipid matrices and dissolution behaviour using Raman spectroscopy and mapping

Investigating the relationship between drug distribution in solid lipid matrices and dissolution behaviour using Raman spectroscopy and mapping

Maike Windbergs^a, Miriam Haaser^b, Cushla M. McGoverin^c, Keith C. Gordon^c, Peter Kleinebudde^a, Clare J. Strachan^{b,d}

^aInstitute of Pharmaceutics and Biopharmaceutics, Heinrich-Heine-University, Universitaetsstr. 1, 40225 Düsseldorf, Germany

^bSchool of Pharmacy and ^cDepartment of Chemistry and MacDiarmid Institute for Advanced Materials and Nanotechnology, University of Otago, P.O. Box 56, Dunedin 9054, New Zealand

^dCentre for Drug Research, University of Helsinki, Viikinkaari 5E, 00014 University of Helsinki, Finland

ABSTRACT

In this study, *in situ* and mapping Raman spectroscopy measurements were used to investigate the physical structure of solid lipid extrudates and relate the structure to dissolution behaviour. Theophylline anhydrate was extruded with tripalmitin, with and without the water soluble polymer, polyethylene glycol 10000. Raman mapping of the extrudate cores revealed that drug particles of diverse size were dispersed in a continuous lipid phase with or without polyethylene glycol. At the surface, there was evidence of more mixing between the components. Previous characterisation by other methods suggested that the extrudate surface is covered predominantly by lipid, and the Raman mapping suggested that such a layer is in general less than a few micrometres thick. Nevertheless, the lipid layer dramatically reduced the drug dissolution rate. The extrudate cores were also mapped after a period of dissolution testing, and there was no evidence of a uniformly receding drug boundary in the extrudates during drug release. *In situ* Raman spectroscopy analysis during dissolution testing revealed that the drug distribution in the extrudate affected the formation of theophylline monohydrate. However, the drug release rate was primarily determined directly by drug distribution, with the solid state behaviour of the drug having a smaller influence.

KEYWORDS

Raman spectroscopy, Raman mapping, extrusion, lipids, dissolution, solid state, solid lipid extrudates, tripalmitin, theophylline, polyethylene glycol

INTRODUCTION

Sustained drug delivery systems are commonly used to prolong drug release from a dosage form and thereby produce a more sustained therapeutic activity while reducing the required dosing frequency. Such dosage forms are often matrices in which the active pharmaceutical ingredient (API) is dispersed among matrix-forming excipients. The release of the API takes place via diffusion through the matrix or by matrix erosion.¹ One relatively new formulation technique is solid lipid extrusion where drug and lipid are extruded together below the lipid melting point to form a lipid matrix with dispersed drug particles.²⁻⁴ They can be further processed by milling or spheronisation, to incorporate into, for example, tablets. Solid lipid extrudates are promising sustained release matrices because the diverse physicochemical properties of different lipids potentially allow tailor-made drug release profiles, the lipids are physiological and nontoxic, no solvents are used during processing, and the lipids can mask unpleasant tasting drugs.⁵

The release behaviour from matrix dosage forms in general has been extensively studied but is still not completely understood because analysis and modelling is normally based on dissolved drug concentration measurements alone.⁶ In matrices which remain intact during dissolution, such as solid lipid extrudates, there is evidence that the dissolution behaviour is largely a function of drug distribution at the surface and within the core of the matrix, and at present this distribution is not well understood.

Vibrational spectroscopy microscopy has been used to map drug distribution in matrix dosage forms.⁷ Near-infrared (NIR), mid-infrared (IR) and Raman microscopy have been used, and the data acquisition has involved point mapping, line mapping and global imaging. While global imaging has the advantage of speed, the mapping approaches provide rich spectral data which is important when analysing complex or poorly defined systems.⁸ The maximum spatial resolutions possible with NIR and IR radiation are approximately 6 μm ⁸ and 4 μm respectively,⁹ while that of Raman microscopy may approach sub-micron levels.¹⁰ NIR microscopy is characterised by a greater penetration depth than both Raman and IR microscopy (if the IR microscope is fitted with an attenuated total reflection (ATR) setup).⁹ The acquisition of spectroscopic maps using Raman microscopy tends to be slower than the other techniques. Water sensitivity is another important differentiating point, while IR and

NIR show strong bands associated with water this is not the case in Raman microscopy, although moisture changes may be indirectly detected in Raman spectra through band shifts and band shape changes.¹¹ These technique differences make the optimum analysis method for drug distribution analysis sample specific. In a study that directly related drug distribution and release in sustained release matrices, the drug distribution in the matrix before and after dissolution testing was imaged using Fourier transform IR imaging with an ATR sampling set-up.¹² However, the spatial resolution in this study was 100 μm (as defined by the detector pixel size), which is typically larger than the size of drug particles in sustained release matrices, and the high pressure applied to the samples during analysis with an ATR accessory can be destructive. Recently, we have used CARS microscopy to image the drug distribution in lipid matrices before and during dissolution. A significant advantage was that it was sufficiently rapid for *in situ* analysis of the dosage form surface during dissolution testing. While the technique shows much potential for imaging drug release in dosage forms,^{13,14} the set up used was not capable of spectrally resolving different solid-state forms of the model drug, theophylline.¹⁴ In this study, the structural aspects of sustained release matrices that influence drug release behaviour were investigated using high resolution Raman point mapping and spectroscopy. A triglyceride was extruded with the model drug theophylline anhydrate to form solid lipid extrudates. Extrudates containing the watersoluble polyethylene glycol 10000 as a pore-builder were also produced. Raman microscopy was used for chemical mapping of the components at the surface and in the core of the resulting dosage forms before and after dissolution testing. The drug distribution was then related to the drug dissolution behaviour. Furthermore, the influence of drug distribution on the solid-state behaviour of the model drug during dissolution was investigated using *in situ* Raman spectroscopy. with Raman microscopy being less sensitive to water than NIR and IR based methods. These technique differences make the optimum analysis method for drug distribution analysis sample specific.

MATERIALS AND METHODS

Materials

The pure powdered monoacid triglyceride tripalmitin (Dynasan 116[®]) was provided by Sasol GmbH (Witten, Germany). The model drug was theophylline anhydrate (BASF, Ludwigshafen, Germany) in powdered form. For comparison, theophylline monohydrate was recrystallized from theophylline anhydrate which had been

dissolved in purified water. Polyethylene glycol with a mean molecular weight of 10000 was provided by Clariant (Waalwijk, The Netherlands) and was in powdered form (Polyglykol 10000 P[®]).

Particle Sizing

The particle size of the powders was determined with a laser diffractometer (Helos, KF-Magic, Clausthal-Zellerfeld, Germany) using the dry dispersion method. The 10% and 90% quantiles (based on volume distribution, D) were determined three times. The mean was calculated for each material.

Extrusion

Tripalmitin was used either alone or with polyethylene glycol in equal parts as the excipient component. This was then weighed in a 50/50% (w/w) ratio with the model drug and blended in a laboratory mixer (LM20, Bohle, Ennigerloh, Germany) for 15 min at 25 rpm. The powder mixture was fed from a gravimetric dosing device (KT20K-Tron Soder, Lenzhard, Switzerland) into the barrel of a corotating twin-screw extruder (Mikro 27GL-28D, Leistritz, Germany). Extrusion was performed with a constant screw speed of 30 rpm and a feeding rate of 40 gmin⁻¹ at a processing temperature of 55 °C. These extrusion conditions have been shown not to result in solid state differences in each component before and after extrusion.^{2, 15}

Intrinsic dissolution testing

Intrinsic dissolution testing was performed on tablets prepared from extrudates with and without polyethylene glycol, and also from a mixture of equal parts of tripalmitin and theophylline anhydrate blended in a Turbula mixer (Willi A. Bachofen AG, Basel, Switzerland) for 15 min. The extrudates and powder mixture (designated as 'physical mixture' in this study) were compressed on a tableting machine (Korsch EK 0, Erweka Apparatebau, Berlin, Germany) using flat-faced punches (diameter 9 mm). The tablets were inserted into a dissolution flow through cell with a quartz window. The dissolution medium was water at room temperature and sink conditions were maintained. The drug concentration of the dissolution medium was measured in a flow through cuvette with a UV-Vis spectrometer (Ultraspec III, Pharmacia Biotech, Uppsala, Sweden) at 244 nm.

Raman mapping

Surfaces and cross-sections of the extrudates were mapped. Cross-sections were obtained by cutting the extrudates orthogonal to the extrudate surface with a razor blade. The Raman mapping data was collected using a Senterra dispersive Raman microscope (Bruker Optics, Ettlingen, Germany). OPUS version 6.5 was used to control the microscope and collect spectra. Both the Sure_Cal[®] and Spectral shape correction options were implemented within OPUS to ensure wavenumber stability and transferability respectively. An excitation wavelength of 785 nm, with 100 mW power and a 1200 groove per millimetre grating were used. The resulting resolution was 3-5 cm⁻¹ across the spectrum. For the maps, each spectrum was the co-addition of three five second exposures, and collected from 50-1530 cm⁻¹. An Olympus 100x objective (N.A. 0.9) with a 50 µm confocal pinhole was used to collect the Raman signal. The lateral and axial resolution of this experimental setup was determined from the intensity profile of the 520 cm⁻¹ band of silicon; a level of 50% of the maximum intensity was used to define the resolution boundaries. The lateral resolution was approximately 2 µm and the axial resolution 5 µm. The spectra were collected with a step size of 2 µm in both the x- and y directions. Rectangles of 36 µm x 500 µm were mapped, and for the cross-sections two adjacent rectangles were used to construct maps of 72 µm x 500 µm, which constituted 4.6% of the cross-sectional area of the extrudate. Peaks unique to each component were integrated with the integration function in OPUS 6.5, and, for each component, normalised as a percentage of the maximum signal observed for that component in the analysed area. The resulting data were used to construct maps with Origin 7.5 (Origin Lab Corporation, Northampton, MA) which were exported into Adobe Photoshop 7.0 (Adobe Systems Incorporated, San Jose, CA) to create the images as shown.

Mapping of samples after dissolution testing

The dissolution of the extrudate samples used for mapping was performed in a basket apparatus according to USP 29 method 1 (Erweka DT 600, Erweka GmbH, Heusenstamm, Germany). Extrudates were cut into cylinders of 1 cm length and weighed into the baskets (total 140 mg in each basket). Dissolution testing was performed in 900 mL purified water containing 0.001% (w/v) polysorbate 20. The stirring speed was 50 rpm and the temperature 37±0.5 °C. The extrudate sample without polyethylene glycol was removed after 120 min, and the extrudate sample with the polymer was removed for analysis after 10 min. The extrudates were patted

dry using a non-linting tissue and the cross sections were mapped as described above. The drug concentration in solution when the extrudates were removed for mapping was determined using a UV-Vis spectrometer with a detection wavelength of 244 nm (Ultrospec 2000, Pharmacia Biotech, Cambridge, England).

***In situ* Raman analysis during intrinsic dissolution testing**

The intrinsic dissolution testing setup described above was combined with a Raman spectrometer for *in situ* analysis of the tripalmitin and theophylline anhydrate tablets during dissolution testing. A Raman spectrometer (Control Development Inc., South Bend, IN, USA) equipped with a fiber optic probe (Raman Probe RPS785/12-5, InPhotonics, Norwood, MA, USA) was used to record spectra through the quartz window of the flow-through cell. An excitation wavelength of 785 nm was used and the Raman signal was detected using a thermo-electrically cooled CCD detector. Spectra with a spectral resolution of approximately 8 cm^{-1} were recorded at 30 s intervals between 200 and 2200 cm^{-1} . An integration time of 1 s was used and spectra were the average of 3 scans.

Scanning electron microscopy (SEM)

SEM micrographs were recorded with a working voltage of 20 kV (DSM 962, Carl Zeiss, Oberkochen, Germany). Samples were mounted on aluminium stubs using double-sided carbon tape and sputter-coated with platinum for 20 s (Agar Manual Sputter Coater B7340, Agar Scientific, Stansted, UK).

RESULTS AND DISCUSSION

Drug release during intrinsic dissolution testing

The dissolution behaviour of theophylline from the extrudate and physically mixed powder dosage forms was very different (Fig. 1), with the amount released from the extrudate sample after 3 h being 16% of that released from the physical powder mixture. Since both samples initially had approximately the same surface area exposed to the dissolution medium, the different dissolution rates must result from structural differences between the two samples. The release rate of the drug was also dramatically enhanced by the presence of polyethylene glycol. Such differences in dissolution rate would be expected to have therapeutic consequences. In the following sections the component distribution in the solid lipid extrudates before and after dissolution is examined using Raman mapping, and related to the drug release behaviour. Since solid-state changes of theophylline may also affect its dissolution rate

and therapeutic efficacy,^{16,17} the solid-state structure of the drug in the dosage forms during intrinsic dissolution testing was also determined using *in situ* Raman analysis and scanning electron microscopy.

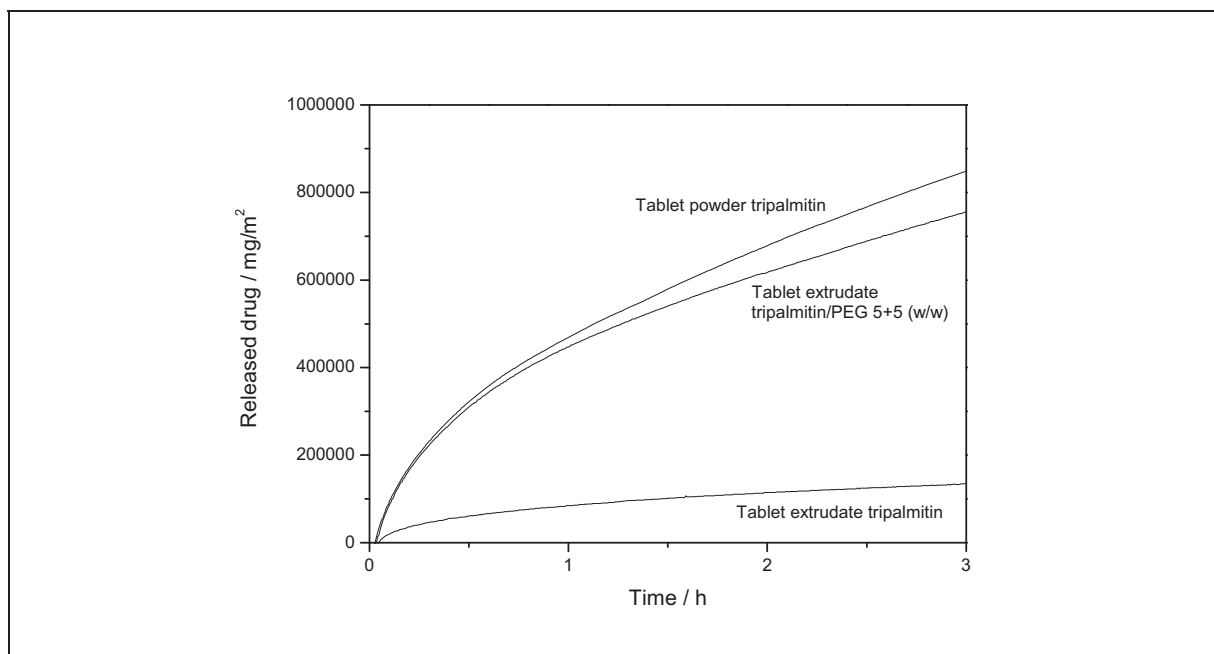


Figure 1: Amount of drug released during intrinsic dissolution testing of theophylline anhydrate and tripalmitin physical mixture and extrudate, and theophylline anhydrate, tripalmitin and polyethylene glycol extrudate.

Distribution of the components in the dosage form

The Raman spectra of tripalmitin, theophylline anhydrate and polyethylene glycol are shown in Fig. 2. The aromatic theophylline was a much stronger Raman scatterer than the aliphatic excipients. Peaks that were unique to each chemical component were used to construct the chemical maps: 1100 cm⁻¹ for tripalmitin, 554 cm⁻¹ for theophylline anhydrate and the combined area for the peaks at 844cm⁻¹ and 860 cm⁻¹ for polyethylene glycol. If polyethylene glycol was not present in the system being investigated, the peak for tripalmitin at 1130 cm⁻¹ was used.¹⁸⁻²⁰ The maximum peak area of each constituent-characteristic band was determined from all 9000 spectra collected from the 72 μm x 500 μm sample region. The constituent-characteristic bands within each spectrum were subsequently quantified as a percentage of the appropriate maximum peak area, and represented using a graduated colour scale. To create Raman maps that are representative of the component distribution it is crucial to use appropriate signal thresholds to define the presence of each component.²¹

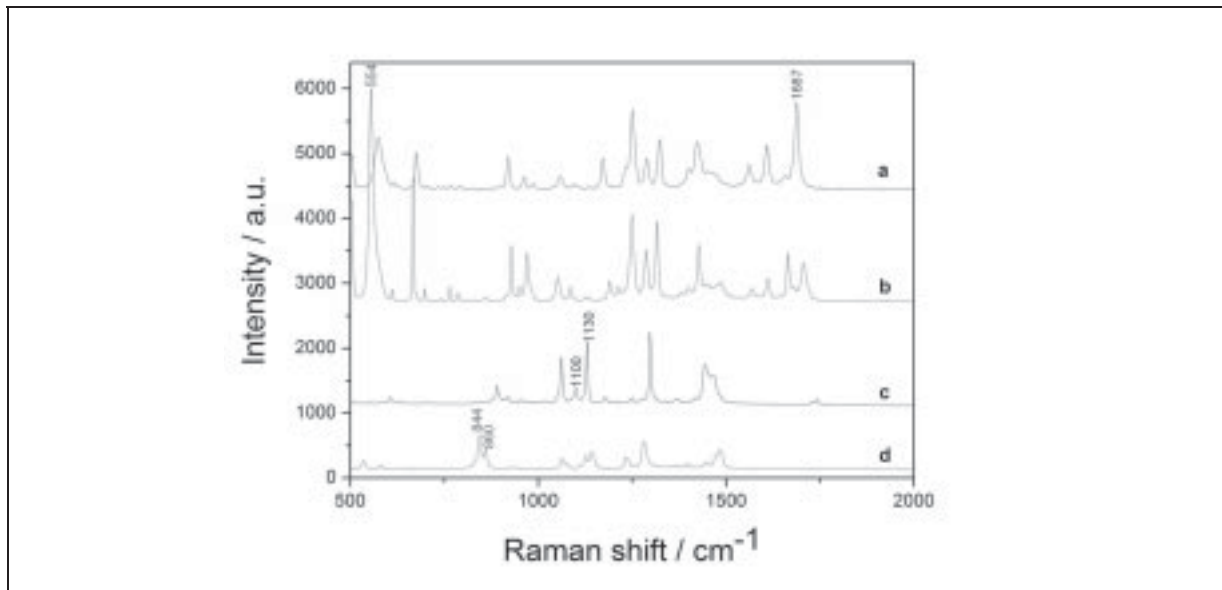


Figure 2: Raman spectra of theophylline monohydrate (a), theophylline anhydrate (b), tripalmitin (c), and polyethylene glycol 10000 (d). Peaks that were integrated and used for constructing the maps are labelled with the peak position.

If the particle sizes are much larger than the sampling volume of the Raman microscope at each point, then a threshold should be adopted such that most pixels are represented by one component. The particle size distributions of the powders (based on volume distribution) before extrusion were as follows: theophylline anhydrate $D_{10} = 12 \mu\text{m}$ and $D_{90} = 288 \mu\text{m}$, tripalmitin $D_{10} = 28 \mu\text{m}$ and $D_{90} = 489 \mu\text{m}$ and polyethylene glycol $D_{10} = 21 \mu\text{m}$ and $D_{90} = 461 \mu\text{m}$. Previous SEM analysis of solid lipid extrudates after dissolution testing suggested that the particle size in the extrudate core after extrusion was still much larger than the Raman microscope sampling volume.⁵ In this study, three different thresholds were investigated: 4%, 8% and 16% of the maximum peak area for each component. When mapping the cross-sections of the extrudates with and without polyethylene glycol, a threshold of 16% resulted in regions in the composite image not being categorised as any component, which was not consistent with the low porosity of the extrudates observed with light and scanning electron microscopy. At a 4% threshold, most of the extrudate was categorised as both tripalmitin and theophylline in the binary systems, and all three components in the extrudates with polyethylene glycol. The 8% threshold resulted in the most complete categorisation of at least one component over the mapped area, and the least overlap. As a result, the 8% threshold was used for all maps.

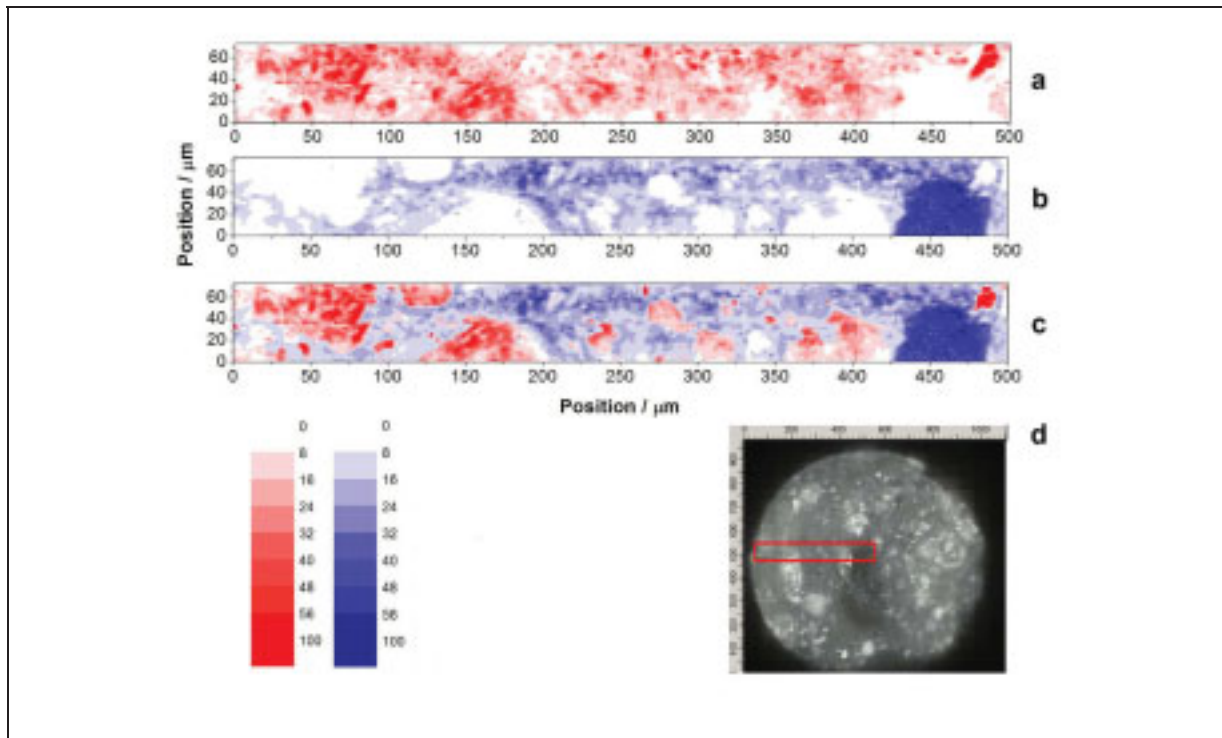


Figure 3: Cross section of theophylline anhydrate and tripalmitin extrudate. Raman map of theophylline anhydrate (a), tripalmitin (b), and both components (c); and optical image of area mapped (d).

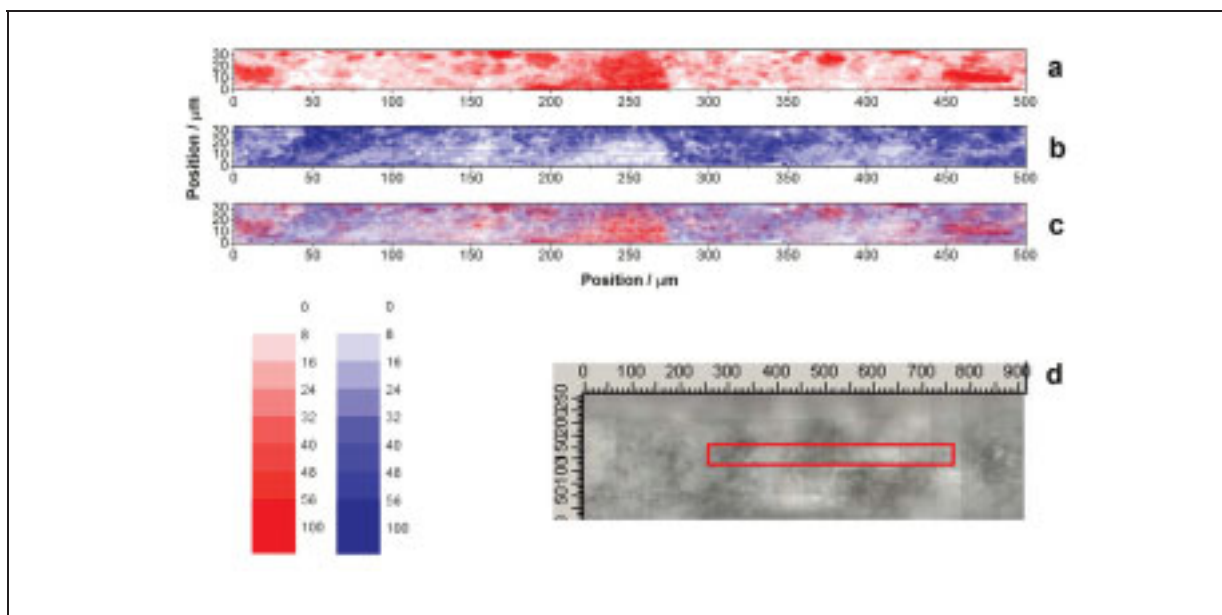


Figure 4: Surface of theophylline anhydrate and tripalmitin extrudate. Raman map of theophylline anhydrate (a), tripalmitin (b), and both components (c); and optical image of area mapped (d).

The chemical map of an extrudate cross-section containing tripalmitin and theophylline anhydrate is shown in Figs. 3 a-c. An optical microscope image of the sampled area is shown in Fig. 3d. The distribution of drug and lipid are separately depicted in Figs. 3a and b. From these two images, it is evident that the cross section is heterogeneous: where a large signal for one component is observed the signal for the other component is either weak or nonexistent. The separate maps of the two components have been overlaid to obtain a chemical map representing both components. In a few areas the spectra represent both components, and these regions are probably due to intimately mixed particles smaller than the sampling volume of the microscope or interfaces between larger particles of both components. The lipid appears to be the continuous phase. The images are consistent with the wide range in particle size of theophylline observed using particle size measurements before extrusion.

The Raman map and optical image of the surface of the same extrudate is shown in Fig. 4. In contrast to the image of the cross-section, a larger proportion of the spectra from the surface represent both theophylline and tripalmitin. This shows up as purple in the map representing both components (Fig. 4c). This suggests a more intimate degree of mixing at the extrudate surface than core, at a level that is below the sampling volume of Raman microscope. Despite theophylline being a much stronger Raman scatterer, there are very few regions where the lipid signal is completely absent. Since the lipid matrix remains intact during drug release in the dissolution media used,^{2,3,22} the initial drug release rate must be largely determined by the surface area of the drug exposed to dissolution medium. The extrudate exhibited a much slower initial release than the physical mixture. Therefore, there is some evidence that the drug exposed at the surface of the extrudate is disproportionately low. This is supported by previously recorded scanning electron microscope images of solid lipid extrudate samples after dissolution, where the voids created by drug release are less numerous and generally smaller at the surface than the core of the extrudate.⁵ The Raman mapping is not inconsistent with the presence of a thin lipid layer and a low concentration of drug at the surface of the extrudate. Such a lipid layer is consistent with the 'wall depletion' effect that has been observed during extrusion of slurries with a high concentration of the disperse phase.^{23,24}

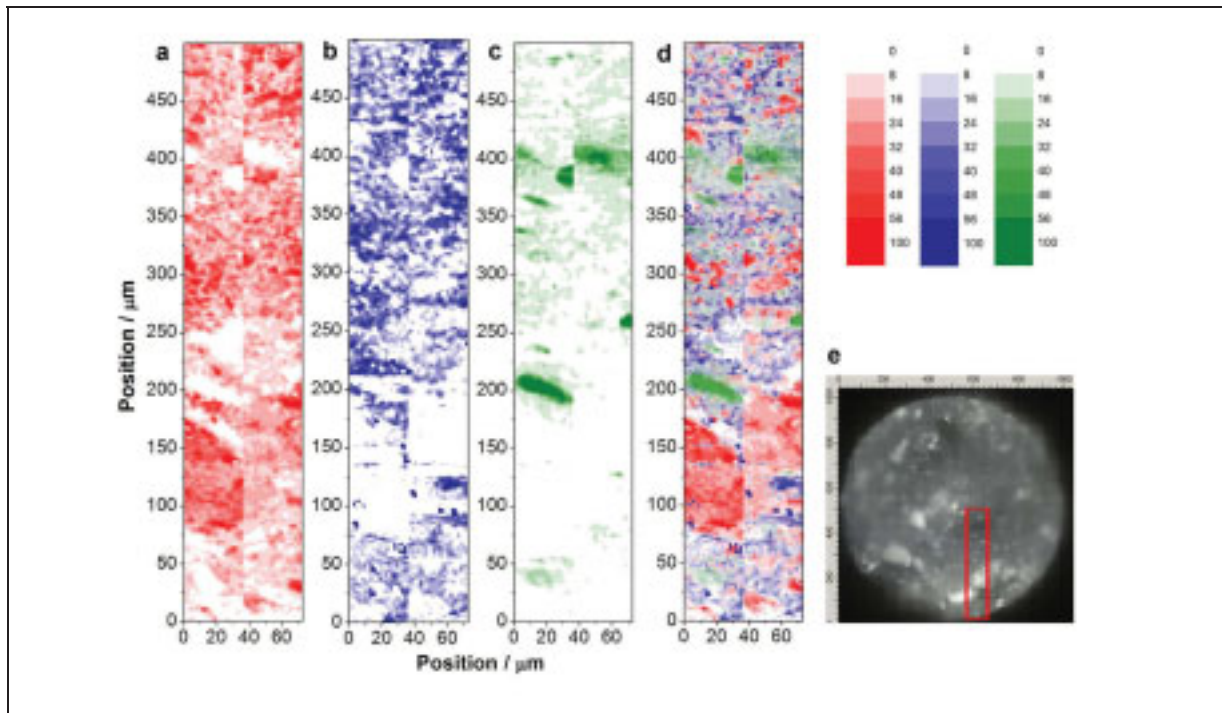


Figure 5: Cross section of theophylline anhydrate, tripalmitin and polyethylene glycol extrudate. Raman map of theophylline anhydrate (a), tripalmitin (b), polyethylene glycol (c), and all three components (d); and optical image of area mapped (e).

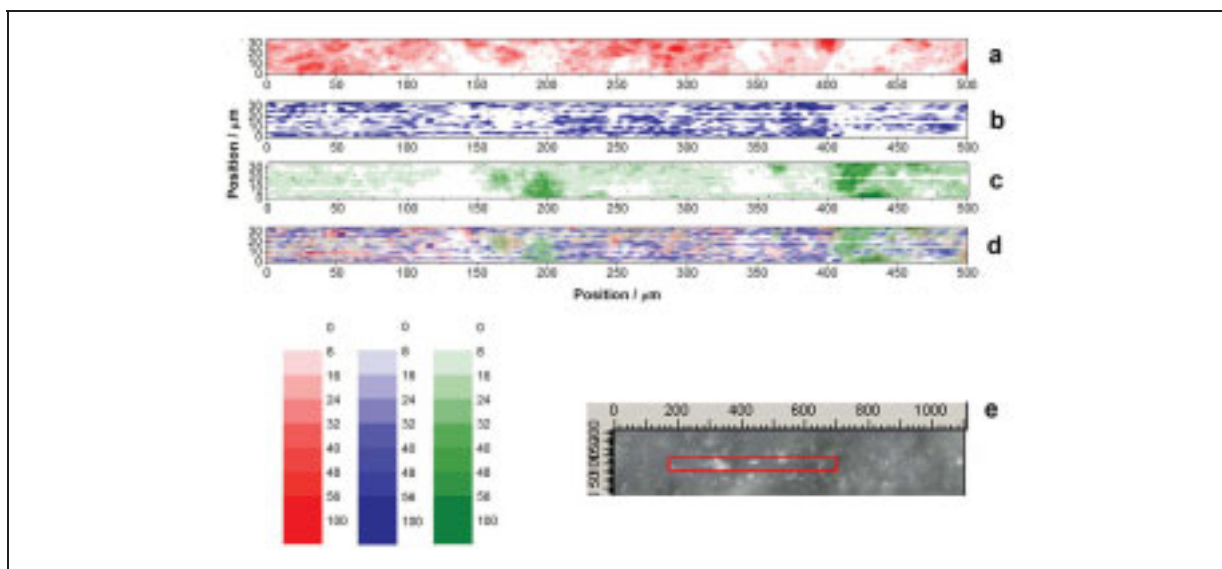


Figure 6: Surface of theophylline anhydrate, tripalmitin and polyethylene glycol extrudate. Raman map of theophylline anhydrate (a), tripalmitin (b), polyethylene glycol (c), and all three components (d); and optical image of area mapped (e).

In this case, the lower melting lipid in contact with die walls is known to melt during extrusion due to shear stress² and it is expected that it fills the voids created by the solid and irregular-shaped drug particles against the die walls.

In the samples containing 25% polyethylene glycol, distinct regions of all three components in the extrudate core were observed (Fig. 5). The maps suggested there was a large particle size range for all components, in particular the drug and polyethylene glycol, and there was no evidence of any component preferentially associating with another in the region studied. The white regions represent those areas of the cross-section where the peak area was less than 8% of the largest peak area in the map for all components. These regions are probably associated with pores or elevations in the prepared cross-section. The Raman image of the extrudate surface suggests that all three components were present at the surface (Fig. 6). In the area imaged, large polyethylene glycol particles are present, and these would rapidly dissolve during dissolution testing, increasing the surface area of drug exposed to the dissolution medium.

Interestingly, longitudinal striations were observed in both the tripalmitin (Fig. 6b) and, to a lesser degree, the polyethylene glycol map of the extrudate surface (Figs. 6c and d). In the extrudates without polyethylene glycol, the lipid also exhibited striations. This was not observed for the drug (Fig. 6a). Elevations of similar width were also observed using scanning electron microscopy.¹⁵ These occur during extrusion if the die hole is not perfectly drilled.

Raman mapping of extrudates after dissolution testing

The drug distribution in the extrudates after dissolution was mapped using Raman microscopy (Figs. 7 and 8). The binary system was mapped after 120 min of dissolution using the basket apparatus, after which 17% (w/w) of the drug had been released according to analysis of the dissolution medium. The system containing polyethylene glycol was mapped after 10 min, with 19% (w/w) of the drug released. If the drug exhibited a uniformly receding boundary, one would expect to observe an absence of drug approximately 45 μm from the extrudate surface for both systems.

In the map of the binary system (Fig. 7), there is almost no signal (above 8% of the maximum observed in the map) for either component up to 15-20 μm from the edge of the map (and extrudate). This area may have been occupied by theophylline, but it is

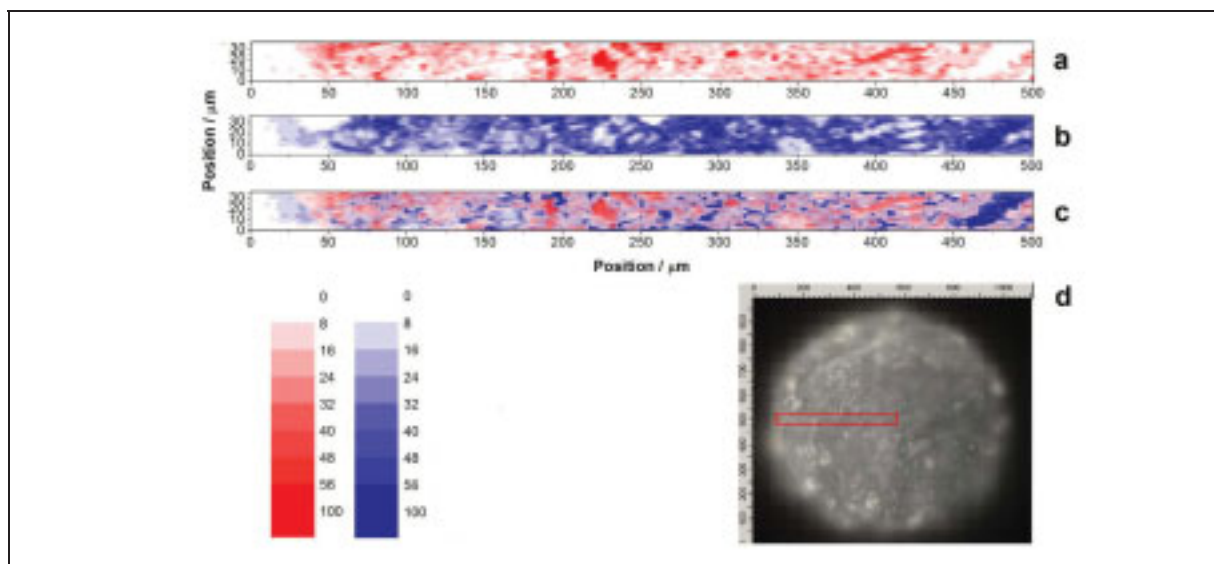


Figure 7: Cross section of theophylline anhydrate and tripalmitin extrudate after 2 h of dissolution testing. Raman map of theophylline anhydrate (a), tripalmitin (b), and both components (c); and optical image of area mapped (d).

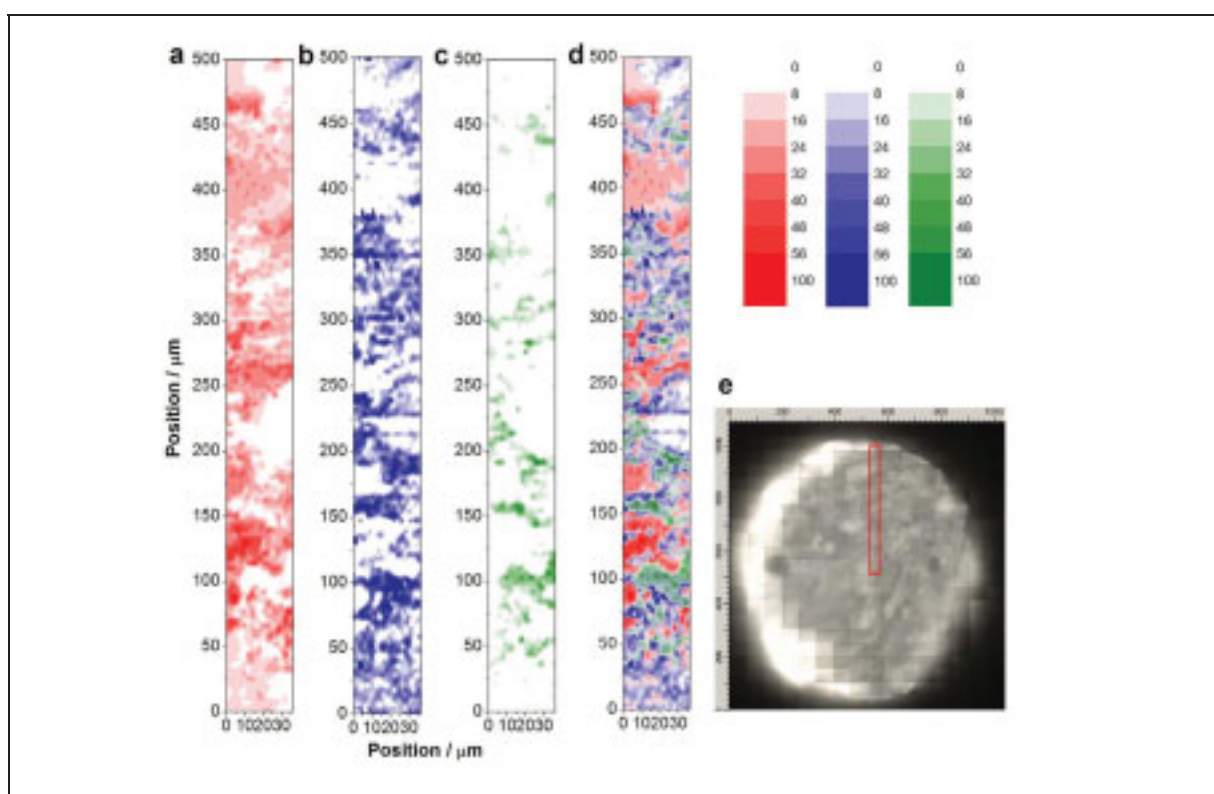


Figure 8: Cross section of theophylline anhydrate, tripalmitin and polyethylene glycol extrudate after 10 min of dissolution testing. Raman map of theophylline anhydrate (a), tripalmitin (b), polyethylene glycol (c), and all three components (d); and optical image of area mapped (e).

also possible that no signal is present because the surface was not completely smooth when the cross-section was prepared. Further into the extrudate tripalmitin is present, and this surrounds a theophylline anhydrate particle 30-70 μm from the edge of the map. In the sample containing polyethylene glycol (Fig. 8), theophylline is present very close to the edge of the extrudate. These results suggest a uniformly receding drug boundary does not exist. Such behaviour can be expected for two reasons. In the matrices, non percolating drug particles may be completely surrounded by lipid, and since the lipid remains intact, these drug particles are never released. Secondly, the tortuosity of the channels in the matrix through which the drug must diffuse during release will differ greatly since the drug is randomly distributed and particle size varies greatly. Larger areas must be mapped to better investigate this phenomenon. Nevertheless, these studies show the potential for Raman microscopy for spatially resolved analysis of drug loss from matrix dosage forms.

The Raman spectra of theophylline anhydrate and monohydrate are distinct (Fig. 2), and there was no evidence of theophylline monohydrate being present after dissolution in any of the spectra used to construct the maps. This supports previous indirect evidence obtained using coherent anti-Stokes Raman scattering (CARS) microscopy,¹⁴ and is interesting because pure theophylline anhydrate is known to undergo solution mediated conversion to the less soluble monohydrate upon contact with water.¹⁶ However, it is possible that the monohydrate could dehydrate before the sample was mapped. To investigate this further, the solid state form of the drug in the binary systems was recorded *in situ* using bulk Raman analysis during intrinsic dissolution testing.

Solid state analysis using *in situ* Raman spectroscopy

Raman spectra obtained from the tablets during intrinsic dissolution testing were used to monitor the solid-state form of the model drug, and are depicted in Fig. 9. The Raman peaks used to differentiate the anhydrate from the monohydrate form were 1687 cm^{-1} (monohydrate), and 1665 cm^{-1} and 1707 cm^{-1} (anhydrate).^{18,20} In the sample compressed from a powder mixture of theophylline anhydrate and tripalmitin, transformation of the drug to monohydrate was observed (Fig. 9a), and the conversion was virtually complete after 15 minutes. The monohydrate remained after 180 minutes, when the Raman analysis was stopped. In comparison, the spectra of the tablet compressed from extrudates suggested that there was no conversion at any stage

up to 180 min (Fig. 9b). This shows that the drug distribution was found to have a pronounced effect on the solid-state behaviour of theophylline monohydrate during intrinsic dissolution.

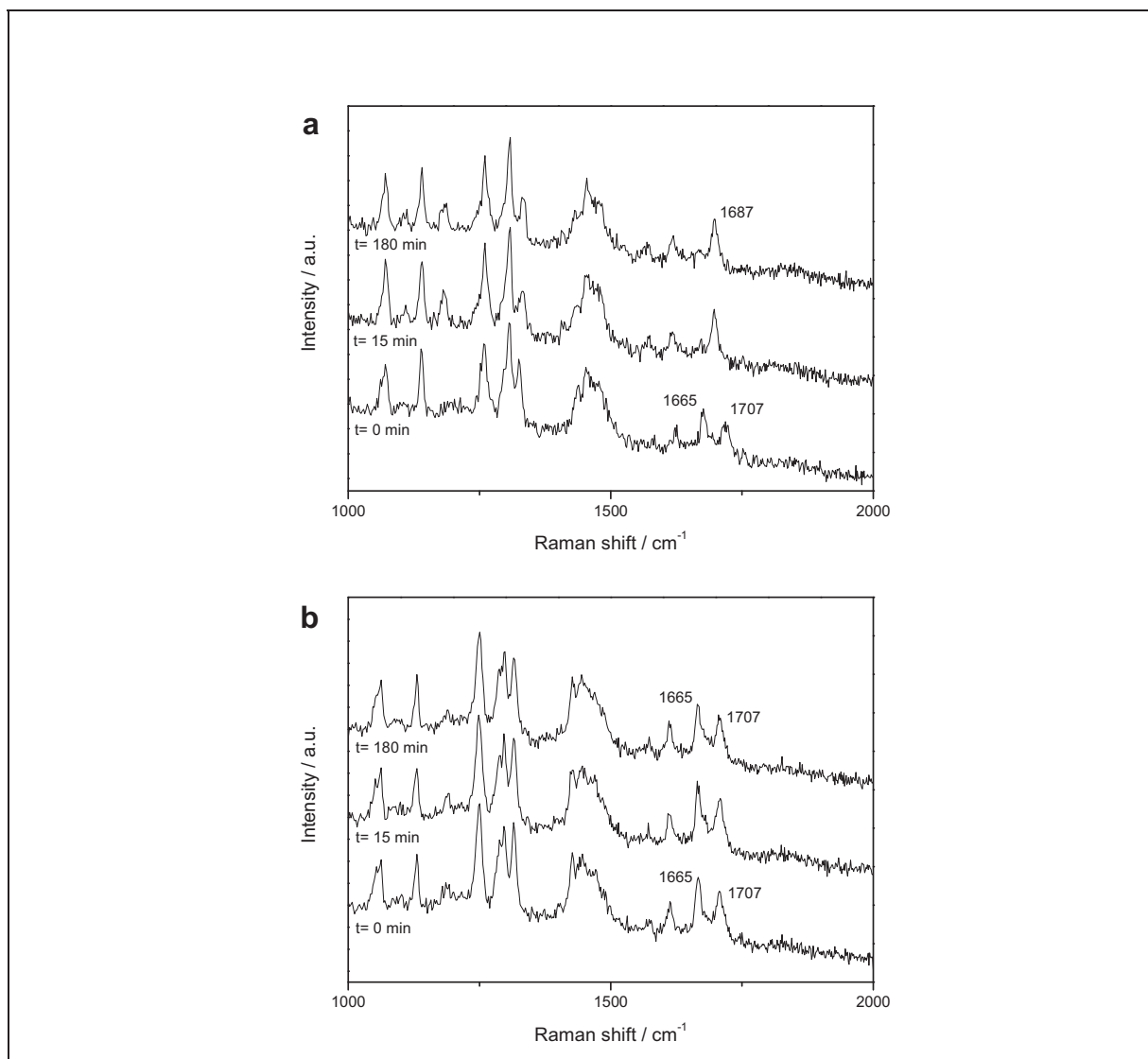


Figure 9: Raman spectra from in situ analysis during intrinsic dissolution testing of physical mixture (a) and extrudate (b) of theophylline anhydrate and tripalmitin.

The results observed using Raman spectroscopy are supported by SEM images taken of each formulation after different times of immersion in water (Fig. 10). After immersion for 30 min, needle-like structures are present on the surface of the tablet compressed of the powder mixture (Fig. 10c). Such structures have previously been associated with theophylline monohydrate formation.¹⁶ After 180 min of immersion all

needles on the surface had dissolved (Fig. 10e). It appears that in the physical mixtures, theophylline monohydrate initially forms on the surface and then in the core of the sample. The theophylline monohydrate on the surface then dissolves before that in the core. Such needles were never observed on the tablet compressed from extrudates of the same composition (Figs. 10 b, d and f).

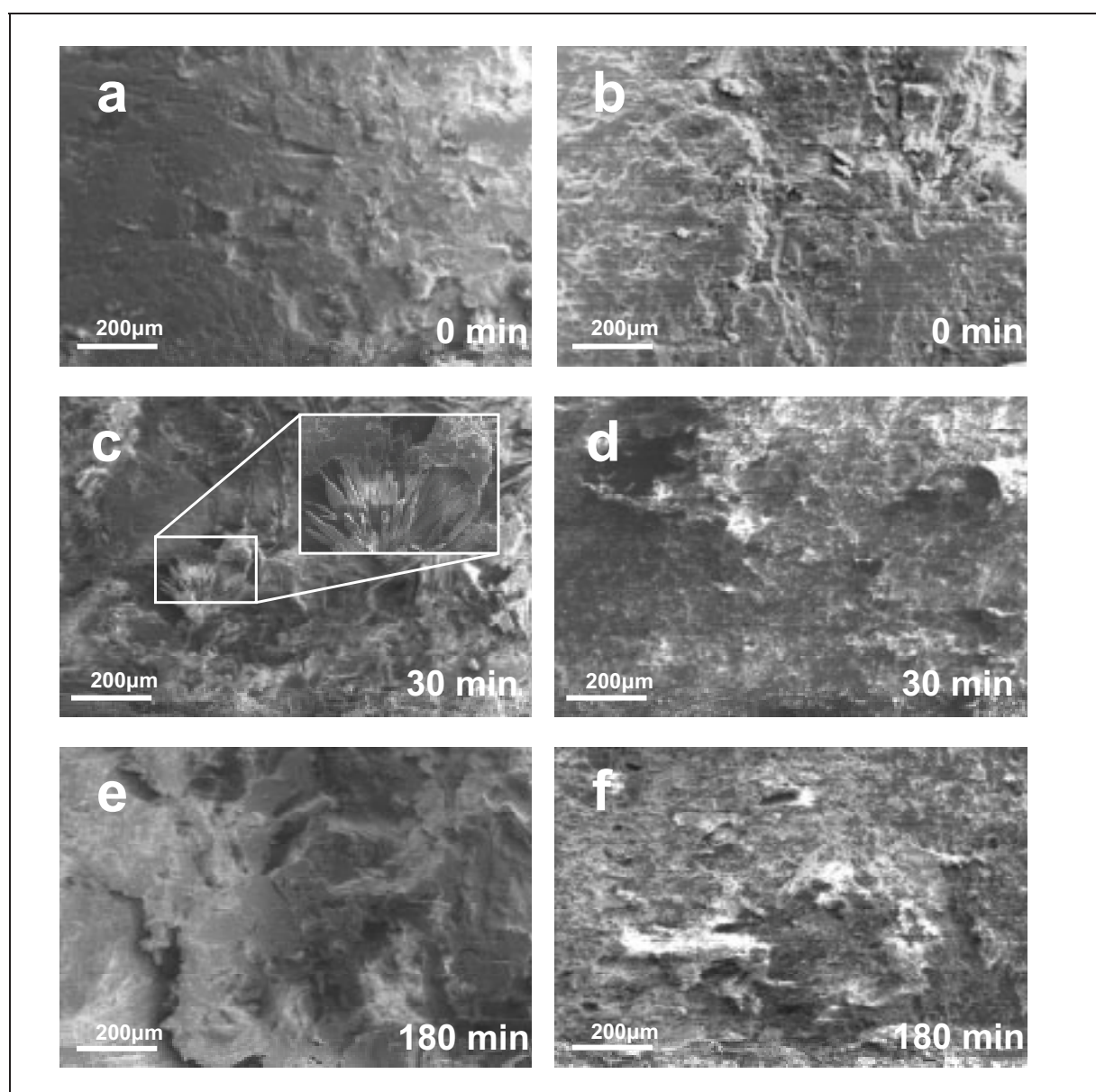


Figure 10: Scanning electron micrographs of theophylline and tripalmitin tablets prepared from a physical mixture (a, c and e) and extrudate (b, d and f), after different immersion times: before immersion (a and b), after 30 min immersion (c and d), and after 180 min immersion (e and f).

Since the conversion to the monohydrate is solution mediated, different solid-state behaviour between the compressed extrudate and physical mixture must be related to the drug concentration in solution at the extrudate-dissolution medium interface. The solubility of the anhydrate in water at 25 °C is 12 mgmL⁻¹, while that of the monohydrate is 6 mgmL⁻¹.²⁵ The drug exposure at the surface of the tablet prepared from the physical mixture, leads to a higher initial dissolution rate, and a sufficiently supersaturated solution to initiate monohydrate crystallisation. As the anhydrate at the surface is depleted, the monohydrate also dissolves (Fig. 10e). Presumably, because less anhydrate is exposed at the surface of the extrudate sample, the solution does not become sufficiently supersaturated to induce crystallisation of the monohydrate form. While such solid state analysis reveals that spatial distribution of the drug can have a pronounced effect on solid-state behaviour of the drug, the formation of the less soluble monohydrate appears to have a minor role, if any, compared to the direct effect of spatial distribution of the drug on drug release.

CONCLUSION

This study showed that Raman mapping can be used for chemically-resolved high-resolution imaging of multi-component sustained release matrices as a means to better understand their drug release behaviour. Although, in this study, Raman microscopy did not have sufficient spatial resolution to determine the exact component distribution at the very surface of the extrudates, it was shown that micrometer scale differences in surface structure can have a pronounced effect on dissolution behaviour. The technique has also shown potential for chemically resolved imaging of drug distribution after dissolution, and in this case a uniformly receding drug boundary was not observed. Solid state changes during dissolution testing can also be analysed. This study has emphasised the importance of drug distribution on the release behaviour from sustained release dosage forms, and Raman mapping is potentially a very useful tool to understand drug distribution in such dosage forms and physical changes during drug release.

ACKNOWLEDGEMENTS

The work has been financially supported by the following grants: a University of Otago Research Grant, entitled 'Microscopic imaging of drug release from delivery systems: testing the uniformly receding drug boundary assumption' (CS, CM, KG, PK); the Marie Curie Fellowship and the Galenos Network (MEST-CT-2004-404992,

MW), and the Academy of Finland postdoctoral researcher's project entitled 'Molecular level understanding and control of hydration state changes in pharmaceutical solids', decision number 123417 (CS). Sasol GmbH is acknowledged for generous provision of the lipids.

REFERENCES

1. Charman SA, and Charman, WN. 2003. Oral modified-release delivery systems. In: M.J. Rathbone, J. Hadgraft, and M.S. Roberts, editors. *Modified-release drug delivery technology*, 1st ed., New York: Marcel Dekker. p. 1-10.
2. Windbergs M, Strachan CJ, Kleinebudde P. 2009. Understanding the solid-state behaviour of triglyceride solid lipid extrudates and its influence on dissolution. *Eur J Pharm Biopharm* 71:80–87.
3. Breitkreutz J, El-Saleh F, Kiera K, Kleinebudde P, Wiedey W. 2003. Pediatric drug formulations of sodium benzoate: II. Coated granules with a lipophilic binder. *Eur J Pharm Biopharm* 56:255–260.
4. Reitz C, Kleinebudde P. 2007. Solid lipid extrusion of sustained release dosage forms. *Eur J Pharm Biopharm* 67:440–448.
5. Reitz C, Strachan C, Kleinebudde P. 2008. Solid lipid extrudates as sustained-release matrices: The effect of surface structure on drug release properties. *Eur J Pharm Sci* 35:335–343.
6. Costa P, Lobo JMS. 2001. Modeling and comparison of dissolution profiles. *Eur J Pharm Sci* 13 (2001) 123–133.
7. Gowen AA, O'Donnell CP, Cullen PJ, Bell SEJ. 2008. Recent applications of chemical imaging to pharmaceutical process monitoring and quality control. *Eur J Pharm Biopharm* 69:10–22.
8. Clark D, Henson M, LaPlant F, Sasic S, Zhang L. 2007. Pharmaceutical applications of mapping and imaging. In: Pivonka DE, Chalmers JM, Griffiths PR, editors. *Applications of vibrational spectroscopy in pharmaceutical research and development*. 1st ed., London: John Wiley & Sons, Ltd, p 309–335.

9. Gendrin C, Roggo Y, Collet C. 2008. Pharmaceutical applications of vibrational chemical imaging and chemometrics: A review. *J Pharm Biomed Anal* 48:533–553.
10. Breitenbach J, Schrof W, Neumann J. 1999. Confocal Raman spectroscopy: Analytical approach to solid dispersions and mapping of drugs. *Pharm Res* 16:1109–1113.
11. Taylor LS, Langkilde FW. 2001. Fourier transform Raman spectroscopic study of the interaction of water vapor with amorphous polymers. *J Pharm Sci* 90:888–901.
12. Pajander J, Soikkeli A-M, Korhonen A, Forbes R, Ketolainen J. 2008. Drug release phenomena within a hydrophobic starch acetate matrix: FTIR mapping of tablets after in vitro dissolution testing. *J Pharm Sci* 97:3367–3378.
13. Jurna M, Windbergs M, Strachan CJ, Hartsuiker L, Otto C, Kleinebudde P, Herek JL, Offerhaus HL. 2009. Coherent anti-Stokes Raman scattering microscopy to monitor drug dissolution in different oral pharmaceutical tablets. *J Innovative Opt Health Sci* 2:37–43.
14. Windbergs M, Jurna M, Offerhaus HL, Herek JL, Kleinebudde P, Strachan CJ. 2009. Chemical imaging of oral solid dosage forms and changes upon dissolution using coherent anti-Stokes Raman scattering microscopy. *Anal Chem* 81:2085–2091.
15. Windbergs M, Strachan CJ, Kleinebudde P. 2009. Tailor-made dissolution profiles by extruded matrices based on lipid polyethylene glycol mixtures. *J Control Release* 137: 210-216.
16. Aaltonen J, Heinänen P, Peltonen L, Kortejaärvä H, Tanninen VP, Christiansen L, Hirvonen J, Yliruusi J, Rantanen J. 2006. In situ measurement of solvent-mediated phase transformations during dissolution testing. *J Pharm Sci* 95:2730–2737.
17. Phadnis NV, Suryanarayanan R. 1997. Polymorphism in anhydrous theophylline - Implications on the dissolution rate of theophylline tablets. *J Pharm Sci* 86:1256–1263.
18. Amado AM, Nolasco MM, Ribeiro-Claro PJA. 2007. Probing pseudopolymorphic transitions in pharmaceutical solids using Raman spectroscopy: Hydration and dehydration of theophylline. *J Pharm Sci* 96:1366–1379.

19. Bresson S, El Marssi M, Khelifa B. 2005. Raman spectroscopy investigation of various saturated monoacid triglycerides. *Chem Phys Lipids* 134: 119–129.
20. Nolasco MN, Amado AM, Ribeiro-Claro PJA. 2006. Computationally-assisted approach to the vibrational spectra of molecular crystals: Study of hydrogen-bonding and pseudo-polymorphism. *Chem Phys Chem* 7:2150–2161.
21. Šašić S. 2007. An in-depth analysis of Raman and near-infrared chemical images of common pharmaceutical tablets. *Appl Spectrosc* 61:239–250.
22. Windbergs M, Strachan CJ, Kleinebudde P. 2009. Influence of the composition of glycerides on the solid state behaviour and the dissolution profiles of solid lipid extrudates. *Int J Pharm* doi: 10.1016/j.jpharm.2009.03.002.
23. Barnes HA. 1995. A review of the slip (wall depletion) of polymer solutions, emulsions and particle suspensions in viscometers: Its cause, character and cure. *J Non-Newtonian Fluid Mech* 56:221– 251.
24. Suryanarayanan R, Phadnis NV. 1997. Polymorphism in anhydrous theophylline - Implications on the dissolution rate of theophylline tablets. *J Pharm Sci* 86:1256–1263.
25. Rodriguez-Hornedo N, Lechuga-Ballesteros D, Wu H. 1992. Phase transition and heterogeneous/epitaxial nucleation of hydrated and anhydrous theophylline crystals. *Int J Pharm* 85:149–162.

9.7. Article 7: Chemical Imaging of Oral Solid Dosage Forms and Changes upon Dissolution Using Coherent Anti-Stokes Raman Scattering Microscopy

Anal. Chem. 2009, 81, 2085–2091

Chemical Imaging of Oral Solid Dosage Forms and Changes upon Dissolution Using Coherent Anti-Stokes Raman Scattering Microscopy

Maïke Windbergs,^{1,2} Martin Jurna,³ Herman L. Offerhaus,³ Jennifer L. Herek,³ Peter Kleinebudde,¹ and Clare J. Strachan^{4,5,6}

Institute of Pharmaceutics and Biopharmaceutics, Heinrich-Heine University, Düsseldorf, Germany, Centre for Drug Research, University of Helsinki, Finland, Optical Sciences Group, MESA+Institute for Nanotechnology, University of Twente, The Netherlands, and School of Pharmacy, University of Otago, New Zealand

Dissolution testing is a crucial part of pharmaceutical dosage form investigations and is generally performed by analyzing the concentration of the released drug in a defined volume of flowing dissolution medium. As solid-state properties of the components affect dissolution behavior to a large and sometimes even unpredictable extent there is a strong need for monitoring and especially visualizing solid-state properties during dissolution testing. In this study coherent anti-Stokes Raman scattering (CARS) microscopy was used to visualize the solid-state properties of lipid-based oral dosage forms containing the model drug theophylline anhydrate during dissolution in real time. The drug release from the dosage form matrix was monitored with a spatial resolution of about 1.5 μm . In addition, as theophylline anhydrate tends to form the less soluble monohydrate during dissolution, CARS microscopy allowed the solid-state transformation of the drug to be spatially visualized. The results obtained by CARS microscopy revealed that the method used to combine lipid and active ingredient into a sustained release dosage form can influence the physicochemical behavior of the drug during dissolution. In this case, formation of theophylline monohydrate on the surface was visualized during dissolution with tablets compressed from powdered mixtures but not with solid lipid extrudates.

The dissolution behavior of drugs is a critical quality attribute for oral solid dosage forms since, in almost all cases, their therapeutic efficacy depends on this very behavior. A combination of chemical and physical properties of both the solid dosage form and the dissolution medium determine the drug dissolution behavior. Important properties of the solid dosage form include the apparent solubility of the drug and the other components, particle size, and drug distribution. These characteristics and hence the dissolution rate change during drug dissolution.¹

Dissolution testing is universally used in the development, production, and quality assurance of oral solid dosage forms. During such testing, the dosage form is immersed in a flowing aqueous medium and the concentration of the released drug in the medium is measured at defined time intervals using techniques such as UV spectroscopy or HPLC. Although valuable, such analysis provides no direct information on the changing dosage form phenomena, and hence the dissolution behavior of drugs cannot be completely understood with such analysis alone. Therefore, there is a need to monitor the changing chemical and physical properties of dosage forms during dissolution.

Initial attempts to characterize dosage form changes involved the bulk characterization of samples *ex situ*, with for example X-ray diffraction.² Recently, Raman spectroscopy has been used to detect solid-state transformations during dissolution *in situ*.^{3,4} However, since drug release from dosage forms is largely dependent on spatial phenomena, it is obviously pertinent to obtain spatially resolved information. Spatially resolved analysis of oral dosage forms has experienced a surge of interest within the past decade,⁵ in part due to much advanced analytical technology. Scanning electron microscopy has been used to characterize dosage form morphology changes after dissolution testing,³ and X-ray powder diffraction has been used to depth-profile dissolution related phase transformations.⁶ Methods exhibiting chemical selectivity that are suitable for imaging dosage forms include near-infrared (NIR), mid-infrared (IR), terahertz and Raman imaging,^{7,8} as well as imaging based on secondary ion mass spectrometry.^{9,10} While these methods are all appropriate for imaging physical and/or

* To whom correspondence should be addressed. Phone: 64 3 4707324. Fax: 64 3 479 7034. E-mail: clare.j.strachan@otago.ac.nz.

¹ Heinrich-Heine University.

² University of Helsinki.

³ University of Twente.

⁴ University of Otago.

(1) Brittain, H. G.; Grant, D. J. W. In *Polyorphism in Pharmaceutical Solids*; Brittain, H. G., Ed.; Marcel Dekker Inc.: New York, 1999; 279–330.

(2) Phadtis, N. V.; Suryanarayana, R. *J. Pharm. Sci.* 1997, 86 (11), 1256–1263.

(3) Aaltonen, J.; Heiskanen, P.; Peltonen, L.; Kortelainen, H.; Tammisen, Y. P.; Christensen, L.; Hirvonen, J.; Ylirasi, J.; Rantanen, J. *J. Pharm. Sci.* 2006, 95 (12), 2730–2737.

(4) Saarelainen, M.; Kogermann, K.; Heinz, A.; Aaltonen, J.; Peltonen, L.; Strachan, C. J.; Ylirasi, J. *Eur. J. Pharm. Biopharm.* 2009, 71 (1), 71–79.

(5) Gowen, A. A.; O'Donnell, C. P.; Cullen, P. J.; Bell, S. E. J. *Eur. J. Pharm. Biopharm.* 2008, 69 (1), 10–22.

(6) Debnath, S.; Pudeckl, P.; Suryanarayana, R. *Pharm. Res.* 2004, 21, 149–159.

(7) Šalić, S. *Appl. Spectrosc.* 2007, 61, 239–250.

(8) Zeller, J. A.; Taday, P. F.; Newsham, D. A.; Pepper, M.; Gordon, K. C.; Rades, T. *J. Pharm. Pharmacol.* 2007, 59, 209–223.

(9) Behl, A. M.; Davies, M. C.; Newton, J. M.; Patel, N. *Anal. Chem.* 2000, 72, 5625–5638.

(10) Mahoney, C. M.; Roberson, S. V.; Gilen, G. *Anal. Chem.* 2004, 76, 3198–3207.

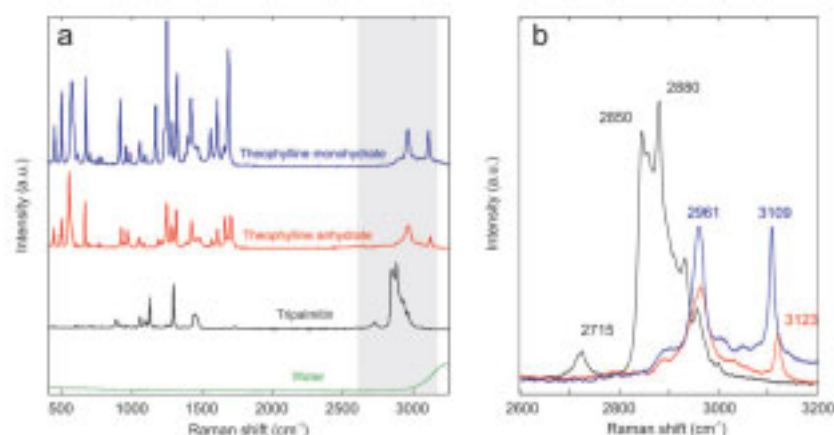


Figure 1. Raman spectra of the powdered substances and water: (a) spectra of water (green), tripalmitin (black), theophylline anhydrate (red), and theophylline monohydrate (blue) and (b) highlighted region of the spectrum.

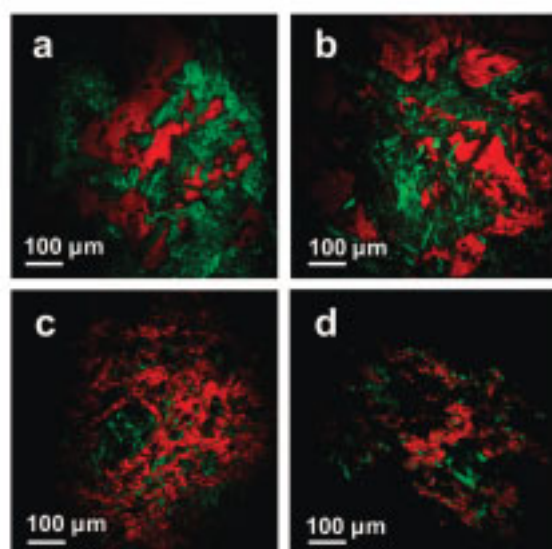


Figure 2. Distribution of lipid (red) and drug (green) in solid dosage forms: (a) tablet of tripalmitin/theophylline anhydrate, (b) tablet of tripalmitin/theophylline monohydrate, (c) tablet of estrudates of tripalmitin/theophylline anhydrate, and (d) extrudate of tripalmitin/theophylline anhydrate.

chemical changes of dosage forms after dissolution testing *ex situ*, they all exhibit serious shortcomings with respect to *in situ* imaging. Demands for *in situ* analysis include an absence of analysis-related dosage form destruction, a sampling setup that does not interfere with the dissolution medium flow, an ability to obtain data in the presence of dissolution media, and sufficient temporal resolution. Secondary ion mass spectrometry cannot be used for sample materials in a dissolution medium. With NIR,¹¹ IR,^{12,13} and terahertz imaging, the radiation used with these techniques is strongly absorbed by water which severely limits

their use in aqueous environments. For IR imaging, this problem has been circumvented by the use of an attenuated total reflectance (ATR) setup, whereby an ATR crystal is interfaced with both a tablet and dissolution medium in a flow through cell dissolution testing setup.^{14,15} However, the requirement for intimate contact between the dosage form and the ATR crystal severely limits sampling setup flexibility making analysis of different kinds of solid dosage forms problematic. Furthermore, commonly observed particle sizes in oral solid dosage forms may be below the spatial resolution of this technique. Raman imaging has potential for *in situ* analysis of solid dosage forms dissolution due to its lack of water sensitivity and relatively high spatial resolution (up to about 1 μm), but potential disadvantages include a typically longer data acquisition time (minutes or hours for 512 by 512 pixels) and possible interference from fluorescence.^{16,17}

Coherent anti-Stokes Raman scattering microscopy is a chemically selective imaging method that appears to fulfill all the requirements listed above for chemically selective *in situ* analysis of dosage forms during dissolution testing. The method is based on two laser beams where one is tunable in wavelength. The two laser beams are collinearly overlapped and focused into the sample of interest. If the wavelength difference between the two input laser beams coincides with a Raman active vibrational mode, an anti-Stokes wavelength (blue-shifted compared to the input wavelengths) is created. When there are differences in the vibrational spectra of the molecules in the sample, chemically selective imaging is possible with this technique with submicrometer resolution in three dimensions. Different configurations and a more complete description can be found in reviews about the technique.^{18,19} CARS has been used for imaging polymer

(11) Reich, G. *Adv. Drug Delivery Rev.* **2005**, *57*, 1109–1143.

(12) Coats-Lendon, C. A.; Wright, N. A.; Mieso, E. V.; Koenig, J. L. *J. Controlled Release* **2003**, *93*, 223–248.

(13) Van der Weerd, J.; Kazarian, S. G. *J. Controlled Release* **2004**, *98*, 295–305.

(14) Van der Weerd, J.; Chan, K. L. A.; Kazarian, S. G. *Vib. Spectrosc.* **2004**, *35* (1–2), 9–15.

(15) Van der Weerd, J.; Kazarian, S. G. *J. Pharm. Sci.* **2005**, *94* (9), 2096–2109.

(16) Umezakura, N.; Lenderink, A.; Kraus, V.; Volkikhin, E.; Vrienen, G.; Greve, J.; Otto, C. *Biophys. J.* **2003**, *84*, 3868–3881.

(17) Ling, J.; Weisman, S. D.; Miller, M. A.; Moore, R. V.; Bovic, A. C. *Appl. Opt.* **2002**, *41*, 6006–6017.

(18) Cheng, J. X.; Xie, X. S. *J. Phys. Chem. B* **2004**, *108*, 827–840.

(19) Jara, M.; Korteik, J. P.; Offerhaus, H. L.; Otto, C. *Appl. Phys. Lett.* **2006**, *88*, 2511–2516.

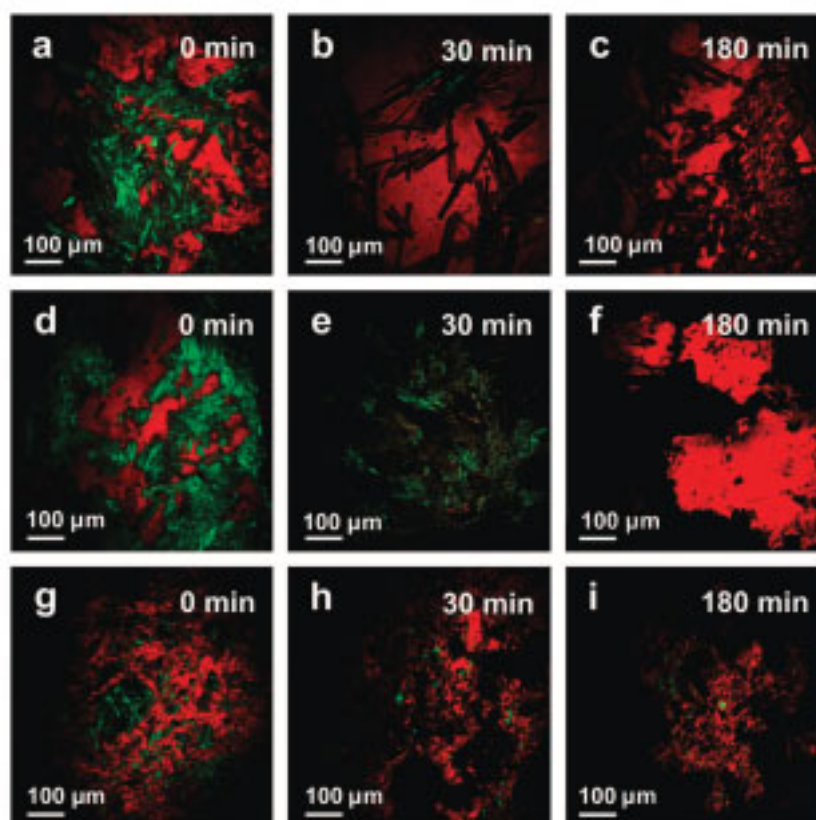


Figure 3. Solid dosage forms consisting of lipid (red) and drug (green) after different immersion times in dissolution medium: (a–c) tablet of tripalmitin/theophylline monohydrate, (d–f) tablet of tripalmitin/theophylline anhydrate, and (g–i) tablet of extrudates of tripalmitin/theophylline anhydrate.

films²⁰ as well as living cells²¹ and tissues.²² Additionally, the technique has recently been used to monitor drug distribution and release from polymer films used in stents.²³ In a subsequent study, drug crystallization during preparation of films was observed for stent coating materials.²⁴ To the best of our knowledge, oral dosage forms and their physicochemical changes during dissolution have not previously been visualized with the use of CARS microscopy.

In these experiments, CARS microscopy was combined with a purpose-built flow-through dissolution cell to visualize physicochemical changes in oral dosage forms during dissolution. The flow-through cell allows the solid dosage form to be fixed in a constant fluid-flow bed which is covered by a microscope cover glass facing the objective of the microscope. The dissolution medium is continuously pumped through the cell surrounding the sample. The two laser beams (of suitable wavelength to coincide with the selected vibrational stretch) are focused onto the sample in the flow cell, creating the anti-Stokes signal. With

CARS it is possible to achieve temporally and spatially resolved visualization of the distribution and the solid-state properties of the sample.

Lipid-based oral dosage forms exhibiting particulate drug dispersion were used as samples. Lipid-based formulations have shown promise as controlled release oral dosage forms as they can effectively control the release rate of drugs, they are physiological and therefore nontoxic, they mask the unpleasant taste of drugs, and no organic solvents are required during dosage form preparation. In these studies different lipid-based oral dosage forms were investigated. Physical powder mixtures of lipid and drug were compressed and compared to extruded matrixes consisting of the same components. In addition, the extruded matrixes were compressed to tablets. The aim of the study was to combine CARS microscopy with a suitable flow-through cell setup as a means to gaining deeper understanding of the physicochemical behaviour of oral dosage forms during dissolution.

EXPERIMENTAL SECTION

Materials. Powdered theophylline anhydrate (BASF, Ludwigshafen, Germany) was used as received. Theophylline monohydrate was obtained by recrystallization of theophylline anhydrate from deionized water. Tripalmitin (Dynasan 116), a pure powdered monoacid triglyceride, provided by Sasol (Witten, Germany) was used as received. The solid state structure of all materials was

(20) Kee, T. W.; Cleerton, M. T. *Opt. Lett.* **2004**, *29*, 2701–2703.

(21) Nan, X.; Cheng, J.-X.; Xie, X. S. *J. Lipid Res.* **2003**, *44*, 2302–2308.

(22) Evans, C. L.; Petrea, E. O.; Phooisuang, M.; Côté, D.; Liu, C. P.; Xie, S. *Proc. Natl. Acad. Sci. U.S.A.* **2005**, *102*, 10807–10812.

(23) Kang, E.; Wang, H.; Kwon, I. K.; Robinson, J.; Park, K.; Cheng, J.-X. *Anal. Chem.* **2006**, *78*, 8036–8043.

(24) Kang, E.; Robinson, J.; Park, K.; Cheng, J.-X. *J. Controlled Release* **2007**, *122*, 261–268.

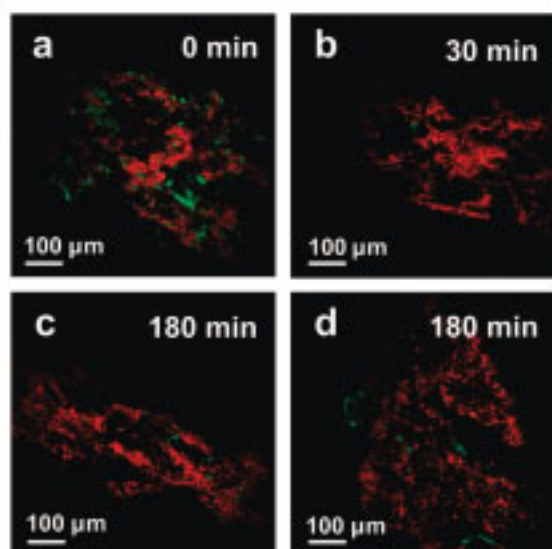


Figure 4. Solid lipid extrudates consisting of lipid (red) and drug (green) after different immersion times in dissolution medium: (a–c) extrudate of tripalmitin/theophylline anhydrate and (d) depth scan (50 μm) of tripalmitin/theophylline anhydrate extrudate.

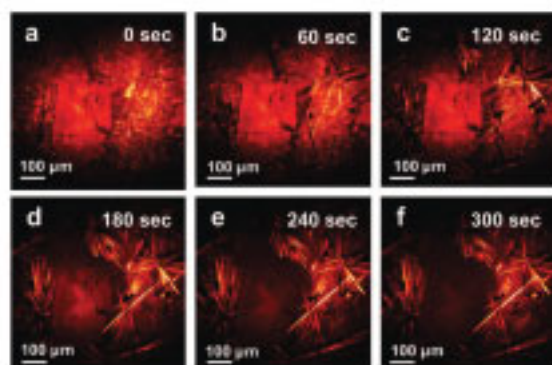


Figure 5. In-line visualization of theophylline monohydrate crystal growth on the surface of a tablet consisting originally of tripalmitin/theophylline anhydrate.

verified using X-ray powder diffraction as detailed in a previous publication.²⁵

Preparation of Tablets. Powdered tripalmitin was weighed in a 50/50% (w/w) mixture with either theophylline anhydrate or with theophylline monohydrate powder and blended in a Turbula mixer (Willi A. Bachofen AG, Basel, Switzerland) for 15 min. The powder mixture (designated as “physical mixture” in this study) was compressed in a tableting machine (Korsch EK 0, Erweka Apparatebau, Berlin, Germany) using flat-faced punches (diameter 9 mm). Tablets were also compressed using extrudates instead of powder mixtures.

Preparation of Extrudates. The powdered tripalmitin and theophylline anhydrate were combined to form a 50/50% (w/w) mixture and blended for 15 min at 25 rpm in a laboratory mixer

(LM 20 Bohle, Ennigerloh, Germany). A gravimetric dosing device (KT20K-Tron Soder, Lenzhard, Switzerland) fed the powder mixture into the barrel of a corotating twin-screw extruder (Mikro 27GL-28D, Leistritz, Nürnberg, Germany). The feeding rate was 40 g min^{-1} , and the screw speed was kept constant at 30 rpm using a processing temperature of $55 \text{ }^\circ\text{C}$. The extruder die plate was equipped with 23 holes (diameter 1 mm, length 2.5 mm). More details about the extrusion process can be found in a previous publication.²⁵

Raman Spectroscopy. Raman spectra were recorded of pure tripalmitin, theophylline anhydrate and monohydrate, and water with a 1600 pix CCD camera (Newton DU-970N, Andor Technology, Belfast, Northern Ireland). The samples were irradiated by a Kr ion Laser (coherent, Innova 90K, Santa Clara, CA) of 30 mW at 647.1 nm and focused by a $40 \times 0.65 \text{ NA}$ microscope objective lens.

CARS. The CARS setup consisted of a coherent Paladin Nd:YAG laser and an APE Levante Emerald optical parametric oscillator (OPO). In this setup, the fundamental (1064 nm, 80 MHz, $> 15 \text{ ps}$) of the laser is used as Stokes, whereas the signal from the OPO (tunable between 700–1000 nm and spectral width of 0.2 nm) is used as the pump and probe. The beams are scanned over the sample by galvano mirrors (Olympus Fluoview 300, IX71) and focused by a $20 \times 0.5 \text{ NA}$ objective lens into the sample. Both beams have a power of several tens of milliwatts at the sample. Because of the highly scattering samples, the forward generated CARS signal is collected in the backward direction.²² The collected signal is filtered and detected by a photomultiplier tube. All images are 512×512 pixels over the full field of view and were obtained in 2 s. Images at different wavelengths require tuning of the OPO but no realignment of the optics. Different images are collected consecutively. For the dissolution testing, the tripalmitin matrix was imaged before and after dissolution to verify the absence of change in the matrix material. During the dissolution, only the theophylline was imaged real time.

Dissolution Testing. The dissolution flow-through cell consisted of a Teflon chamber in which two metal bars were used to fix the dosage form in the middle of a flowing dissolution medium. A hose pump circulated the medium through the chamber via suitable conduits at a constant rate of 5 mL/min. On one side, the cell was equipped with a thin microscope cover glass that was transparent to the incident and scattered radiation. The dissolution medium was purified water, and the measurements were conducted at room temperature. Such a setup allowed the solid-state properties of a solid oral dosage form to be visualized in situ with an appropriate medium flow for dissolution testing of oral solid dosage forms.²⁶

RESULTS AND DISCUSSION

Determination of Suitable Vibrational Bands for Component-Specific Imaging. Raman spectra were recorded of all powdered substances to determine suitable vibrational bands for component-resolved analysis using CARS. Bands that were largely resolved for each component but within a limited spectral range were required. The spectra are shown in Figure 1. Figure 1a depicts the comparison of the three powdered substances, with a region with large spectral differences between the components

(25) Wisdeberg, M.; Strachan, C. J.; Kleinschulte, P. *Eur. J. Pharm. Biopharm.* 2009, 71 (1), 80–87.

(26) Pekonen, L.; Lijeröth, P.; Heikkinen, T.; Koutari, K.; Hirvonen, J. *Eur. J. Pharm. Sci.* 2003, 19, 395–401.

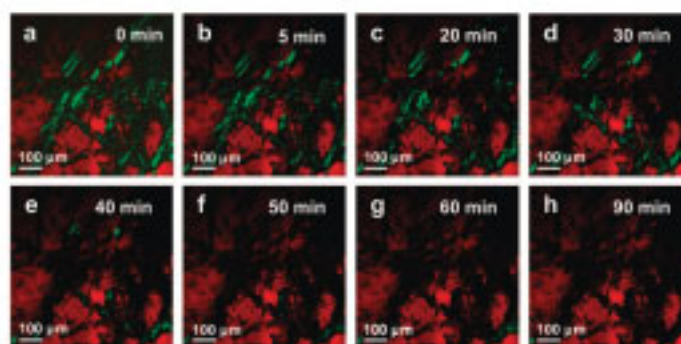


Figure 6. In-line visualization of drug release from a tablet of tripalmitin (red) and theophylline monohydrate (green) during dissolution testing.

highlighted and displayed in Figure 1b. From 1600 to 1800 cm^{-1} , the peaks at 1687 (theophylline monohydrate), 1707 (theophylline anhydrate), and 1728 cm^{-1} (tripalmitin) have been assigned to C=O stretching.^{27–29} All three substances exhibit CH stretching between 2700 and 3200 cm^{-1} . In tripalmitin, the CH stretching associated with the aldehyde function occurs at 2715 cm^{-1} while CH_2 and CH_3 symmetric stretching correspond to peaks at 2850 and 2880 cm^{-1} , respectively.²⁷ Theophylline exhibits CH_3 anti-symmetric stretching at 2961 (theophylline monohydrate) and 2967 cm^{-1} (theophylline anhydrate) and CH stretching associated with the imidazole ring at 3109 (theophylline monohydrate) and at 3123 cm^{-1} (theophylline anhydrate).^{28,29} For component-specific analysis, the 1600–1800 cm^{-1} region with the three components exhibiting highly distinguishable peaks seemed to be favorable. Unfortunately water gives a strong CARS response in the corresponding anti-Stokes region at about 1650 cm^{-1} , which precluded the use of this region. In the 2900–3200 cm^{-1} region, tripalmitin and theophylline can be selectively imaged using the peaks at 2880 (tripalmitin) and 3109 cm^{-1} (theophylline). CARS spectra and Raman spectra are not identical but uniquely related to each other.³⁰ The CARS spectra of the pure samples will be very similar to the Raman spectra due to the relatively weak nonresonant signal from the sample itself. The CARS spectra of the samples dissolved in water will change slightly, due to the mixing of the nonresonant water signal with the resonant signal. This causes the peak positions to shift a few wavenumbers down. On the basis of the Raman spectra, it is clear that a distinction between theophylline anhydrate and monohydrate was not possible with CARS in this region. Nevertheless, the peak at 3109 cm^{-1} can be used to image both forms of theophylline. Around 2880 cm^{-1} , the CARS intensity for tripalmitin exceeds the intensity for the theophylline (both monohydrate and anhydrate). The images obtained at 2880 cm^{-1} can thus be taken to represent the (square of the) tripalmitin density distribution. At 3109 cm^{-1} , the CARS intensity for the monohydrate exceeds that for tripalmitin. The

intensity for the monohydrate is closer to that for the tripalmitin so that the precise ratio is strongly influenced by the amount of nonresonant background. From the images it was clear that the monohydrate exceeded the tripalmitin by a factor larger than 3, based on areas that could be identified to contain only one of the constituents. The images at different wavenumbers can be related to each other by picking a spot that can be seen to contain pure tripalmitin and scaling the intensity in the 3109 cm^{-1} image to reflect the correct ratio. Furthermore (not shown in the graphs), the phase of the tripalmitin signal is between 70 and 90 degrees separated from the signal of the theophylline (monohydrate or anhydrate) so that the total signal from a combination of the substances (the absolute square of the combined amplitude) is almost equal to the addition of the absolute square of both images. The tripalmitin image, once correctly scaled, can then thus be subtracted from the other image to obtain an almost pure image, and this procedure is possible even in regions that contain signals from both substances. For a more precise analysis, the CARS amplitude and phase can be detected locally using heterodyne detection³⁰ to extract the relative components. This paper focuses on the qualitative description; further work will include detailed quantitative measurements. All images in this paper are based on CARS signals only.

Drug Distribution in Different Lipid-Based Oral Dosage

Forms. Tablets and extrudates were analyzed using CARS microscopy to visualize the distribution of lipid and drug in the dosage forms. Figure 2 depicts false-color images of the surface of the dosage forms with a spatial resolution of about 1.5 μm . The images show that the theophylline drug particles (signal at 3109 cm^{-1} , encoded in green) are randomly distributed at the surface of the lipid matrix (signal at 2880 cm^{-1} , encoded in red). A mix of both signals would appear yellow, and since this is not observed, the substances do not mix at this resolution. The comparison of parts a and b of Figure 2 reveals that theophylline monohydrate is characterized by thin needles whereas the anhydrate exhibits anisometric particles. Figure 2c depicts the image of a tablet compressed from extrudates. In this image, the drug particles represent a smaller proportion of the surface signal than is the case for the unextruded samples, which may be

(27) Bresson, S.; El Marssi, M.; Khelifa, B. *Chem. Phys. Lipids* **2005**, *134*, 119–129.

(28) Nolasco, M. M.; Amado, A. M.; Ribeiro-Claro, P. J. A. *Chem. Phys. Chem.* **2006**, *7*, 2150–2161.

(29) Amado, A. M.; Nolasco, M. M.; Ribeiro-Claro, P. J. A. *J. Pharm. Sci.* **2007**, *96*, 1366–1379.

(30) Juma, M.; Korteck, J. P.; Otto, C.; Herck, J. L.; Offerhaus, H. L. *Opt. Express* **2008**, *16*, 15983–15993.

attributed to a depletion of drug adjacent to the extruder barrel wall during processing.²¹ The images of the extrudate itself are depicted in Figure 3d. In the extruded matrixes, the drug particles are homogeneously distributed.

Monitoring Drug Release and Solid-State Transformations during Dissolution Testing. The lipid-based dosage forms were imaged after immersion in 500 mL of purified water and compared with the images of the dosage forms before dissolution. After 30 and 180 min of immersion, they were removed and imaged using CARS microscopy to investigate drug release and solid-state transformations (Figure 3). The release of the drug from a tablet consisting of a physical mixture of tripalmitin and theophylline monohydrate (Figure 3a–c) is evident from a gradual loss of green color representing the drug. After 30 min of immersion, the drug was still visible whereas after 180 min no drug was evident on the surface of the tablet. Instead, pores in the lipid matrix where drug needles were located are represented as dark areas in the false-color image. The lipid (red color) remained after dissolution, demonstrating that the matrix stays completely intact during dissolution. It can thus be concluded that the release of the drug is purely diffusion controlled with the drug initially dissolving at the surface of the matrix and then dissolving within the matrix and diffusing through the resulting pores in the matrix.

Different phenomena were observed in the tablet consisting of tripalmitin and theophylline anhydrate (Figure 3d–f). Figure 3d depicts the tablet surface before immersion with the anhydrous theophylline clearly visible as dispersed particles in the lipid matrix. After 30 min immersion in water, the surface of the tablet was completely green and fine needles could be observed (Figure 3e). This can be attributed to the solution-mediated formation of theophylline monohydrate, a phenomenon which has previously been observed upon immersion of the anhydrate in water.^{1,6,22} In these studies, monohydrate growth in water has always been associated with needle-like morphology. After 180 min of immersion in water, the green color had completely disappeared and the red color of the lipid was once more visible, suggesting that the theophylline monohydrate had completely dissolved. The dissolution process of theophylline anhydrate in this dosage form can therefore be subdivided in several stages. First, the theophylline anhydrate dissolves and, with the monohydrate being less soluble than the anhydrate, a supersaturated solution with respect to theophylline monohydrate is created. This is followed by a transformation phase in which the monohydrate crystallizes.²³ Afterward, dissolution of the two forms takes place.

To investigate the influence of the extrusion process on the release behavior of the drug, a tablet was compressed from tripalmitin and theophylline anhydrate extrudates and subjected to the same dissolution study. For this tablet (Figure 3g–i), release of the anhydrate particles was observed but, strikingly, no monohydrate needle formation on the tablet surface was observed. These observations correlated with results obtained on the same preparations in the same setup using in situ Raman spectroscopy (the Raman spectroscopy setup used has been

published²³), where monohydrate formation was observed for the compressed powder mixtures but not for the extrudate (data not shown).

With the CARS setup, additional studies were conducted using the uncompressed extrudates made of tripalmitin and theophylline anhydrate (results depicted in Figure 4a–d) and in these unmodified extrudate samples there was also no evidence of theophylline monohydrate formation during the dissolution of the anhydrate particles. A scan in the pores of the extrudate at a depth of 50 μm was performed (Figure 4d) to observe physicochemical changes within the matrix in addition to at the surface. At this depth a few very small monohydrate needles can be found inside the pores. The reason for such different solid-state behavior of the unextruded and extruded samples needs further investigation. However, in an attempt to understand such behavior, one can look at the mechanism of crystallization of the monohydrate. The mechanism of conversion is believed to be solution-mediated. First, nucleation from solution must occur followed by crystal growth. Nucleation typically occurs in the presence of a suitable surface and supersaturated solution with respect to the monohydrate, and crystal growth is dictated by the degree of supersaturation. The outer surface of the extrudate may be a poor substrate for nucleation since it is very smooth. In contrast, the surface of the compressed powder mixtures is likely to be rougher. With regard to supersaturation, as already stated it appears that the extrusion process reduces the drug exposure at the surface of the extrudate and hence of the surface of the tablet consisting of extrudates, which may mean that the solution adjacent to the surface is less supersaturated with respect to the monohydrate inhibiting its nucleation and crystal growth. Within the pores, the rougher surface which is left after the release of drug particles in the pores may promote nucleation. In addition, the diffusion within the small pores is likely to be very slow, and therefore through greater supersaturation in these regions crystal formation is more likely to occur. We plan to investigate this issue in future work.

In Situ Imaging of Solid-State Transformations. To monitor the solid-state transformation in real time, tablets consisting of the physical mixture of tripalmitin and theophylline anhydrate were placed directly on the microscope stage in a small container mounted on a thin glass slide which was filled with purified water so that a thin water layer was located between the sample and the microscope objective. Figure 5a–f depicts several frames of the recorded images. In real time, the transformation from theophylline anhydrate to monohydrate could be visualized for the first time on a tablet surface (see Video S-1 in the Supporting Information).

In Situ Monitoring of Solid-State Characteristics during Dissolution Testing. In this part of the study, experiments with the dissolution flow-through cell, which provides a pharmaceutically relevant dissolution setup for oral dosage forms, were performed. It was possible to obtain a good CARS signal intensity from the tablet through the flowing dissolution medium. Figure 6 depicts images recorded during the dissolution testing with a tablet consisting of the physical mixture of tripalmitin and theophylline monohydrate. The release of the drug from the matrix could be visualized in real time. Unfortunately focal drift and wavelength drift prohibited a reliable quantitative analysis for these images at this time.

(31) Reitz, C.; Strachan, C. J.; Kleinbockle, P. *Eur. J. Pharm. Sci.* 2008, 35, 335–343.

(32) Arai, H.; Ishii, M.; Kayano, M. *Drug Dev. Ind. Pharm.* 1992, 18, 453–467.

(33) De Strick, J. H.; Fokkens, J. G.; Geijssels, H.; Crommelin, J. A. J. *J. Pharm. Sci.* 1986, 75, 487–501.

CONCLUSIONS

CARS microscopy was used to visualize the spatial distribution of different components in oral pharmaceutical dosage forms and, by combining the method with a suitable flow-through cell, drug release and physicochemical changes during dissolution testing were monitored in real time. As solid-state properties of pharmaceutical dosage forms affect the dissolution behavior, the visualization of solid-state changes with this method can expand the knowledge about dissolution mechanisms. Such knowledge will help lead to tailor-made dissolution profiles by manufacturing of pharmaceutical dosage forms that exhibit desirable physicochemical properties during dissolution. In the case of solid lipid extrudates, the drug and lipid distribution on the surface of the solid dosage form was rapidly visualized with a spatial resolution of about 1.5 μm every 2 s. CARS was used to monitor the loss of the model drug theophylline from the lipid matrix as well as solution-mediated solid-state transformations (from theophylline anhydrate to the monohydrate form) on the surface of tablets in real time. Solid lipid extrusion prevented theophylline hydrate formation, which was clearly observed with CARS microscopy. On the basis of these results, CARS microscopy may be a valuable characterization method in the future development of different kinds of oral solid dosage forms.

ACKNOWLEDGMENT

The Marie Curie Fellowship and the Galenos Network are acknowledged for financial support (Grant MEST-CT-2004-404992). The Sasol GmbH is acknowledged for generous provision of the lipids. In addition, this research is supported by NanoNed, a nanotechnology programme of the Dutch Ministry of Economic Affairs and partly financed by the "Stichting voor Fundamenteel Onderzoek der Materie (FOM)," which is financially supported by the "Nederlandse Organisatie voor Wetenschappelijk Onderzoek (NWO)". The work has also been supported by the Academy of Finland funded postdoctoral researcher's project entitled, "Molecular level understanding and control of hydration state changes in pharmaceutical solids", Decision Number 123417. Chris Lee is acknowledged for initiating the collaboration that led to this work.

SUPPORTING INFORMATION AVAILABLE

Additional information as noted in text. This material is available free of charge via the Internet at <http://pubs.acs.org>.

Received for review October 3, 2008. Accepted January 16, 2009.

AC8020856

9.8. Article 8: Coherent anti-Stokes Raman scattering microscopy to monitor drug dissolution in different oral pharmaceutical tablets

COHERENT ANTI-STOKES RAMAN SCATTERING MICROSCOPY TO MONITOR DRUG DISSOLUTION IN DIFFERENT ORAL PHARMACEUTICAL TABLETS

M. JURNA*, M. WINDBERGS^{1,5}, C. J. STRACHAN^{5,*},
L. HARTSUIKER², C. OTTO², P. KLEINEBUDDE²,
J. L. HEREK*, and H. L. OFFERHAUS*

**Optical Sciences Group
MESA+ Institute for Nanotechnology
University of Twente, The Netherlands*

*¹Institute of Pharmaceutics and Biopharmaceutics
Heinrich-Heine University of Düsseldorf, Germany*

*²BioPhysical Engineering Group
MESA+ Institute for Nanotechnology
University of Twente, The Netherlands*

*³Centre for Drug Research
University of Helsinki, Finland*

*⁴School of Pharmacy
University of Otago, New Zealand*

Coherent anti-Stokes Raman scattering (CARS) microscopy is used to visualize the release of a model drug (theophylline) from a lipid (tripalmitin) based tablet during dissolution. The effects of transformation and dissolution of the drug are imaged in real time. This study reveals that the manufacturing process causes significant differences in the release process: tablets prepared from powder show formation of theophylline monohydrate on the surface which prevents a controlled drug release, whereas solid lipid extrudates did not show formation of monohydrate. This visualization technique can aid future tablet design.

Keywords: Drug release; coherent anti-Stokes Raman scattering (CARS) microscopy.

1. Introduction

Dissolution of drugs from solid pharmaceutical tablets is a complex process that depends on several properties of the drug and tablet, such as the distribution of the drug in the tablet and the nature and flow of the dissolution medium. One important factor that influences drug dissolution is the solid state

form of the drug. During dissolution, the drug can transform to a less dissolvable hydrate.¹ For this reason, it is crucial that the solid-state properties are monitored during dissolution.

Coherent anti-Stokes Raman scattering (CARS) microscopy has been shown to be a chemically selective method for investigating highly

scattering media² using the Raman active vibrational modes with real-time³ imaging. Hence, we expect that it is a suitable method for probing physicochemical phenomena in tablets, in which the drug is usually dispersed in particulate form, with such dosage forms constituting the majority of medicines currently marketed. The CARS is a four-photon non-linear process, where a pump photon of frequency ω_p , a Stokes photon of frequency ω_s and probe photon of frequency ω_p' (taken the same as the pump frequency) interact with the sample and generate an anti-Stokes photon of frequency $\omega_{as} = \omega_p - \omega_s + \omega_p'$. The CARS signal is resonantly enhanced when the difference frequency $\omega_p - \omega_s$ coincides with a molecular vibrational level transition. With CARS, it is possible to achieve temporally and spatially resolved visualization^{4,5} of the distribution and the solid-state properties of the powders and tablets. This study focuses on the visualization of drug dissolution and solid-state transformations.

2. Experimental System

The CARS set-up is based on a Coherent Paladin Nd:YAG laser and an APE Levante Emerald optical parametric oscillator (OPO). The fundamental (1064 nm) of the laser is used as Stokes, whereas the signal from the OPO (tunable between 700 nm and 1000 nm) is used as the pump and probe. The beams are scanned over the sample by galvanometer mirrors (Olympus Fluoview 300, IX71) and focused by a 20×0.5 NA objective lens into the sample. Both beams have a power of several tens of mW at the sample. Due to the highly scattering samples, the forward-generated CARS signal is collected in the backward direction.² The collected signal is filtered and detected by a photo multiplier tube. All images are 512×512 pixels and obtained in 2 seconds.

To determine suitable vibrational bands for component-specific imaging and analysis, Raman spectra were recorded of pure tripalmitin, theophylline anhydrate, and monohydrate and water with a 1600 pixels CCD camera (Newton DU-970N, Andor Technology) (Fig. 1). The samples were irradiated by a Kr ion Laser (Coherent, Innova 90K) at 647.1 nm of 30 mW and focused by 40×0.65 NA microscope objective lens. Care was taken to ensure that the focal spot was filled with pure material. The spectra are shown in Fig. 2. Figure 2(a) shows the spectra of the three powdered substances. The region exhibiting the large spectral

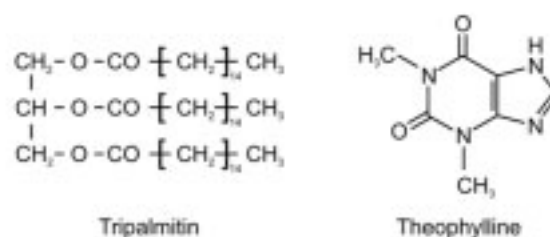


Fig. 1. Molecular structure formula of the lipid tripalmitin and drug theophylline.

differences between the components is highlighted in gray and also featured in Fig. 2(b). Between 2700 cm^{-1} and 3200 cm^{-1} , the CH stretch in the aldehyde function of tripalmitin gives rise to a peak at 2715 cm^{-1} whereas the CH_2 and CH_3 symmetric stretching in the fatty acid chains correspond to peaks at 2850 cm^{-1} and 2880 cm^{-1} , respectively.⁶ Theophylline exhibits CH stretching at 3109 cm^{-1} for the theophylline monohydrate and 3123 cm^{-1} anhydrate.^{7,8} Specific component analysis in the $1600\text{--}1800 \text{ cm}^{-1}$ region is not favorable due to the water vibrational modes around 1650 cm^{-1} and cannot be used for real-time dissolution experiments. In the $2700\text{--}3200 \text{ cm}^{-1}$ region, tripalmitin and theophylline can be imaged selectively using peaks at 2880 cm^{-1} (tripalmitin) and 3109 cm^{-1} (theophylline). Unfortunately, a distinction between theophylline anhydrate and monohydrate is not possible in this region. Nevertheless, the peak at 3109 cm^{-1} can be used to image selectively both forms of theophylline. The interference from water in this region would seem large as well, but these bands are so broad and de-phase so quickly that their influence is limited.

For a qualitative and quantitative monitoring of the drug distribution in the tablet during dissolution, a translation has to be made from the Raman spectra to the CARS images. Using the images at 2880 cm^{-1} and 3109 cm^{-1} , the concentration of theophylline can be related to the concentration of the tripalmitin. Since the tripalmitin stays intact during dissolution, it can serve as the marker for the local theophylline concentration, which is known from the fabrication. The Raman spectra are related to the CARS spectra, but they are not the same. In short, Raman spectra depend linearly on the constituent concentration whereas the CARS spectra depend quadratically on concentration. The Raman spectral intensity can be expressed as the imaginary part of the (resonant) CARS amplitude.⁹

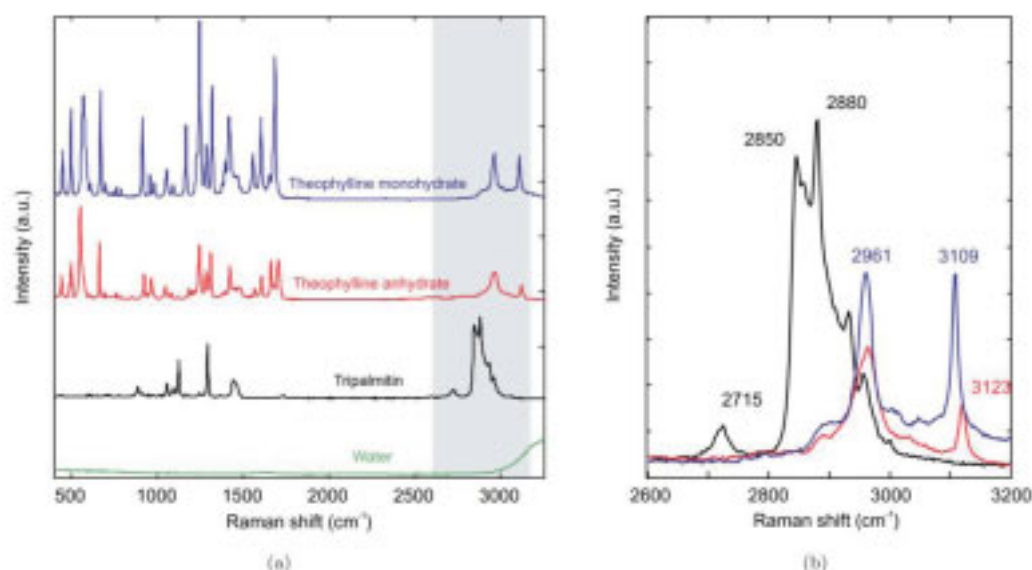


Fig. 2. Raman spectra of the powdered substances and water: (a) full spectra of tripalmitin (black), theophylline anhydrate (red), theophylline monohydrate (blue), and water (green) and (b) highlighted detail of image (a).

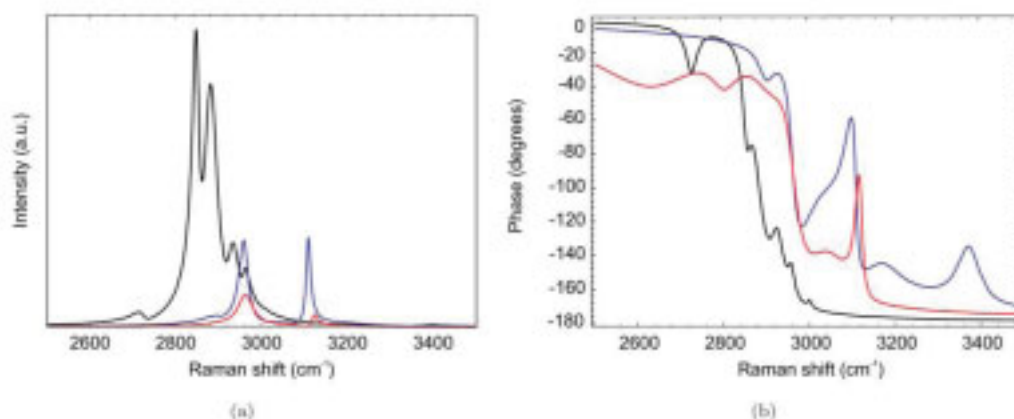


Fig. 3. Simulation on Raman data (Fig. 2) of tripalmitin (black), theophylline anhydrate (red), theophylline monohydrate (blue), to obtain the (a) resonant CARS spectra and (b) CARS phase.

To simulate the CARS spectra, the Raman data were fitted to the imaginary part of multiple complex Lorentzians. The resonant part of the CARS intensity spectra and their phases are depicted in Fig. 3. The full CARS spectra also contain a non-resonant part that cannot be deduced from the Raman measurement. This real part can be effectively described as a constant where the magnitude depends on the excitation pulse lengths and wavelengths. For our experiments, the non-resonant

component can be estimated as somewhere between 1% and 10% of the peak resonant amplitude. This non-resonant contribution has little effect on the signal intensity close to a resonance.

The CARS spectra shown in Fig. 3 reveal that the different powders have partially overlapping spectra. To overlay and compare the CARS images obtained at different vibrational resonances, weight factors have to be found based on the CARS spectra. Around 2880 cm^{-1} , the CARS intensity



Fig. 4. Photograph of the flow cell with tablet (without the cover glass).

for tripalmitin exceeds the intensity for the theophylline (both monohydrate and anhydrate) by a factor of 20. The images obtained at 2880 cm^{-1} can thus be taken to represent the tripalmitin density distribution (absolute squared). At 3109 cm^{-1} , the CARS intensity for the monohydrate exceeds the tripalmitin by a factor of 18. The intensity for the monohydrate is closer to the tripalmitin so that the precise ratio is strongly influenced by the amount of non-resonant background. From the images, it is clear that the monohydrate exceeds the tripalmitin by a factor larger than 3, based on areas that could be identified to contain only one of the constituents.

The images at different wavelengths can be related to each other by picking a spot containing pure tripalmitin and scaling the intensity in the 3109 cm^{-1} image to reflect the correct ratio. Furthermore, the phase of the tripalmitin signal is between 70 and 90 degrees separated from the signal of the theophylline (monohydrate or anhydrate). Therefore, the total signal from a combination of the powders, which is given by the absolute square of the combined amplitude, is almost equal to the addition of the absolute square of the components as is displayed in both images. The tripalmitin image, once correctly scaled, can thus be subtracted from the other image to obtain an almost pure image and this procedure is allowed even for regions that contain signals from both substances. Since the (initial) distribution of substances (Figs. 5(a), (d) and (g)) is coarse on the scale of the images, most pixels can be assigned to contain either tripalmitin or theophylline and the percentage of drug and lipid at the surface can be extracted simply by counting

pixels which yields the coverage percentages mentioned in Fig. 5.

For a more precise analysis, the CARS amplitude and phase can be detected locally using heterodyne detection¹⁰ to extract the relative components. This paper focuses on the qualitative description, further work will include detailed quantitative measurements.

In this study of dissolution from two different types of pharmaceutical tablets, three model systems of a drug (theophylline) in a matrix (tripalmitin) were investigated: (1) tablets of tripalmitin with theophylline *monohydrate*, created by tableting a powder mixture, (2) tablets of tripalmitin with theophylline *anhydrate*, also from a powder mixture, and (3) tablets from an *extrudate* of tripalmitin with theophylline anhydrate. The details of the sample preparation are given elsewhere.¹¹ Two different types of experiments are performed: dissolution by immersion in purified water and dissolution by flowing purified water in a flow cell. The flow cell used for the *in situ* dissolution imaging consisted of a Teflon chamber with two metal bars that fix the tablets in the middle of a flowing water bed (Fig. 4). Purified water was constantly pumped through the cell. The lower side of the cell consists of a thin microscope cover glass that is placed on the microscope stage. This specific set-up allows *in situ* visualization of the solid-state properties of the tablets under pharmaceutically relevant dissolution conditions.

3. Results and Discussion

Figure 5 depicts false-color images of the surface of the three model systems. The drug is always depicted in green, irrespective of its solid-state form. The lipid matrix is depicted in red. The first column depicts the three dry systems. The surface of the theophylline monohydrate 5(a) is characterized by thin needles whereas the anhydrate 5(d) shows anisometric particles. The tablet of compressed extrudates 5(g) shows a smaller proportion of drug signal on the surface, so that the drug can be considered more embedded in the matrix (not observed on an uncompressed extrudate). On the dry tablet, the surface coverage was determined as: 5(a) tablet tripalmitin/theophylline monohydrate (40%/60%), 5(d) tablet tripalmitin/theophylline anhydrate (60%/40%) and 5(g) tablet of extrudates tripalmitin/theophylline anhydrate (20%/80%).

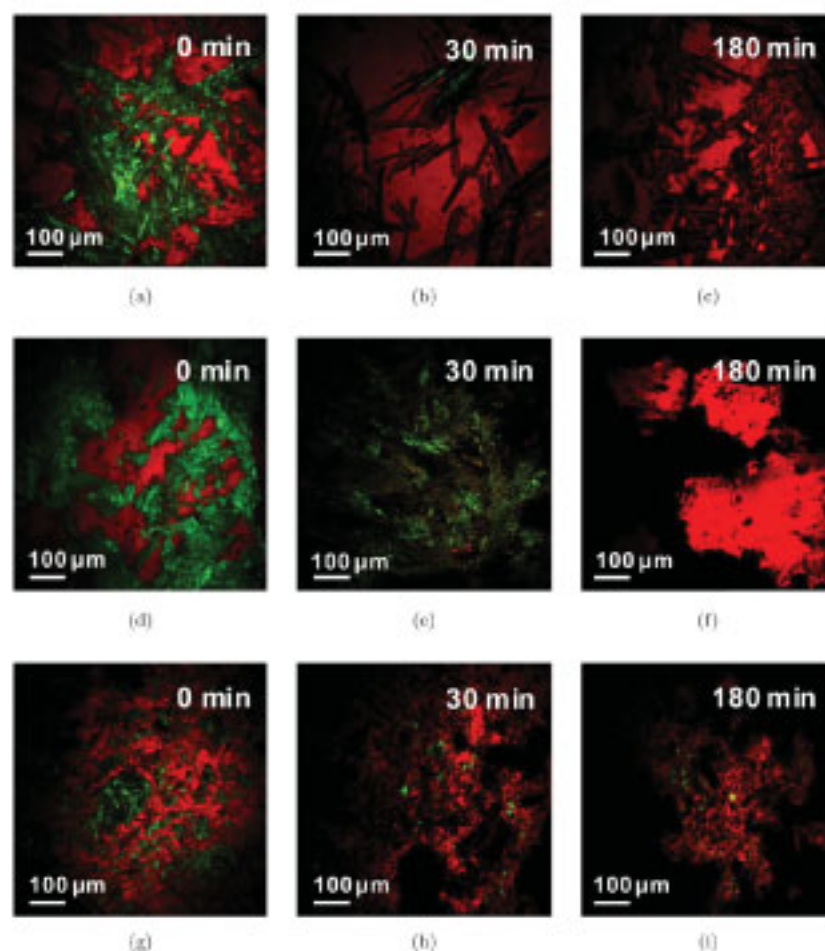


Fig. 5. Images of the lipid tripalmitin (2880 cm^{-1} , red) and drug theophylline (3100 cm^{-1} , green) after different durations of immersion. (a)–(c) tablet tripalmitin/theophylline monohydrate (d)–(f) tablet tripalmitin/theophylline anhydrate (g)–(i) tablet of extrudates tripalmitin/theophylline anhydrate.

The release of drug and changes to the surface were first monitored by imaging after different immersion times. The tablets were immersed in 500 mL of purified water, and after defined time intervals, removed and imaged (Fig. 5). The tablet consisting of tripalmitin and theophylline monohydrate (Fig. 5(a) to (c)) shows the release of the drug from the matrix without significant surface alteration. The lipid matrix stays intact, while the drug dissolves within the matrix and then diffuses through the pores in the matrix. After 30 minutes, a few monohydrate needles are left, while after 180 minutes, no drug is evident on the surface of the tablet. Pores (dark) can be observed where drug needles were

located. The tablet consisting of tripalmitin and theophylline anhydrate (Fig. 5(d) to (f)) shows significant surface effects. After 30 minutes, the surface of the tablet is covered with fine needles (Fig. 5(e)), which are most likely theophylline monohydrate that has a much lower solubility and crystallizes on the surface after transformation from the anhydrate form.^{12–14} After 180 minutes of immersion in water, the needles have completely dissolved.

For the tablet of compressed extrudate (Fig. 5(g) to (i)), release of the anhydrate particles was observed *without* monohydrate needle formation. Additional tests were conducted using the uncompressed extrudates, where the absence

42 M. Jurna et al.

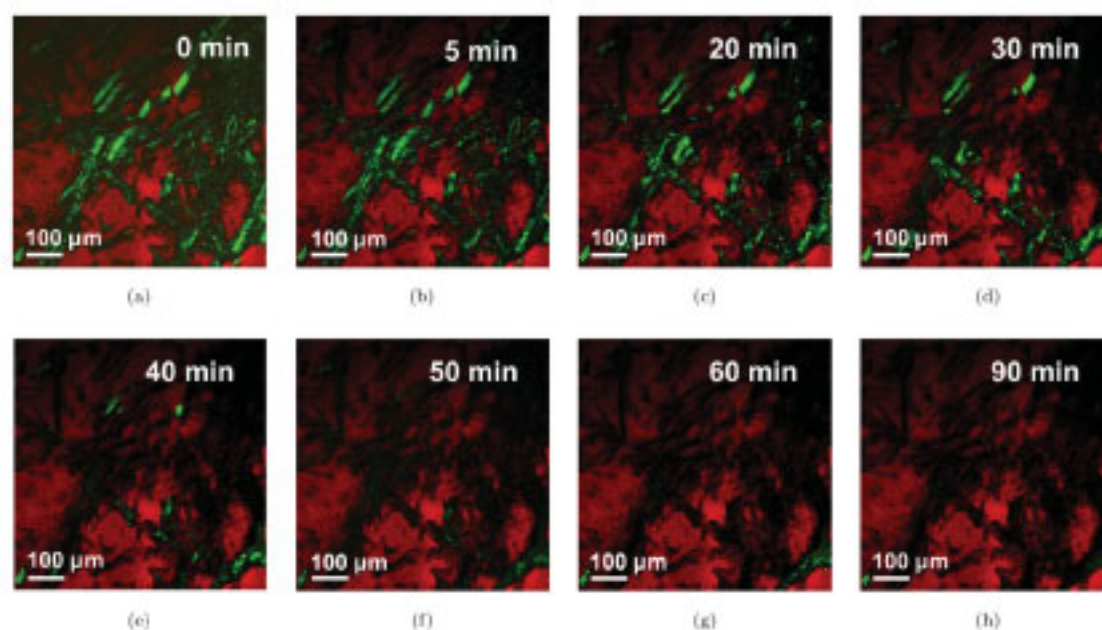


Fig. 6. *In situ* CARS imaging of drug release during dissolution in the flow cell. The lipid tripalmitin (2880 cm^{-1} , red) and drug theophylline monohydrate (3109 cm^{-1} , green).

of needle formation was confirmed. The smoother surface structure of the extrudate appears to prevent monohydrate crystallization. The solid-state transformations and crystal growth on a tablet containing pure theophylline anhydrate was also monitored *in situ*,¹⁵ by placing the tablets in a vessel filled with water directly on the microscope stage. A thin stagnant water layer between the sample and the microscope cover slide promoted the growth of long needles which can be attributed to theophylline monohydrate formation.

For dissolution testing, tablets containing monohydrate were placed in the flow cell and continuously imaged over 90 minutes (Fig. 6). Focal drift and stability issues prevented a direct quantitative analysis of the images, but controlled release of the drug was clearly observed and quantitative analysis should be possible once the stability is improved.

4. Conclusion

CARS microscopy was combined with a pharmaceutically appropriate dissolution set-up and used to visualize the structure and distribution of a model drug in different tablets, as well as the changes

during dissolution in real time. Such results provide valuable information about the physicochemical phenomena that may occur during drug dissolution. Theophylline anhydrate tends to form the monohydrate with a lower solubility during dissolution. The ability of the CARS set-up to distinguish between the different solid-state forms was investigated. Tablets made of lipid-based extrudates did not exhibit theophylline hydrate formation during drug dissolution. The difference between the two dosage forms is probably due to surface differences of the lipid matrix. Based on these results, CARS appears to be well-suited to the imaging of physicochemical changes in oral solid dosage forms during dissolution.

Acknowledgments

This research is supported by NanoNed, a nanotechnology program of the Dutch Ministry of Economic Affairs and partly financed by the Stichting voor Fundamenteel Onderzoek der Materie (FOM), which is financially supported by the Nederlandse Organisatie voor Wetenschappelijk Onderzoek (NWO). The Marie Curie Fellowship and the Galenos Network are acknowledged

for financial support (MEST-CT-2004-404992). The Sasol GmbH is acknowledged for generous provision of the lipids. We also acknowledge Coherent Inc. for the use of the Paladin laser and APE Berlin for the collaboration and use of a Levante Emerald OPO. Last but not least, we would like to acknowledge Chris Lee for bringing this collaboration possibility to our attention.

References

1. Brittain, H. G., *Polymorphism in Pharmaceutical Solids* (Marcel Dekker Inc., New York, 1999), pp. 279–330.
2. Cheng, J. X., Volkmer, A. and Xie, X. S., "Theoretical and experimental characterization of coherent anti-Stokes Raman scattering microscopy," *J. Opt. Soc. Am. B* **19**, 1363–1375 (2002).
3. Evans, C. L., Potma, E. O., Puoris'haag, M., Cote, D., Lin, C. P. and Xie, X. S., "Chemical imaging of tissue *in vivo* with video-rate coherent anti-Stokes Raman scattering microscopy," *Proc. Natl. Acad. Sci. USA* **102**, 16807–16812 (2005).
4. Kang, E., Wang, H., Keun Kwon, I., Robinson, J., Park, K. and Cheng, J. X., "In situ visualization of Paclitaxel distribution and release by coherent anti-Stokes Raman scattering microscopy," *Anal. Chem.* **78**, 8036–8043 (2006).
5. Wang, H., Bao, N., Le, T. L., Lu, C. and Cheng, J. X., "Microfluidic CARS cytometry," *Opt. Express* **16**, 5782–5789 (2008).
6. De Smidt, J. H., Fokkens, J. G., Grjseels, H. and Crommelin, J. A., "Dissolution of theophylline monohydrate and anhydrous theophylline in buffer solutions," *J. Pharm. Sci.* **75**, 497–501 (1986).
7. Nolasco, M. M., Amado, A. M. and Ribeiro-Claro, P. J. A., "Computationally-assisted approach to the vibrational spectra of molecular crystals: Study of hydrogen-bonding and pseudo polymorphism," *Chem. Phys. Chem.* **7**, 2150–2161 (2006).
8. Amado, A. M., Nolasco, M. M. and Ribeiro-Claro, P. J. A., "Effect of moisture on crystallization of theophylline in tablets," *J. Pharm. Sci.* **96**, 1366–1379 (2007).
9. Potma, E. O., Evans, C. L., Xie, X. S., "Heterodyne coherent anti-Stokes Raman scattering (CARS) imaging," *Opt. Lett.* **31**, 241–243 (2006).
10. Jurna, M., Korterik, J. P., Otto, C. and Offerhaus, H. L., "Shot noise limited heterodyne detection of CARS signals," *Opt. Express* **15**(23), 15207–15213 (2007).
11. Windbergs, M., Strachan, C. J. and Kleinebudde, P., "Understanding the solid-state behaviour of triglyceride solid lipid extrudates and its influence on dissolution," to appear in *Eur. J. Pharm. Biopharm.*, available online June 2008.
12. Aaltonen, J., Heinänen, P., Peltonen, L., Kortejärvi, H., Tanninen, V. P., Christiansen, L., Hirvonen, J., Yliruusi, J. and Rantanen, J., "In-situ measurement of solvent-mediated phase transformations during dissolution testing," *J. Pharm. Sci.* **95**(12), 2730–2737 (2006).
13. Debnath, S., Predecki, P. and Suryanarayanan, R., "Use of glancing angle X-ray powder diffractometry to depth-profile phase transformations during dissolution of indomethacin and theophylline tablets," *Pharm. Res.* **21**, 149–159 (2004).
14. Ando, H., Ishii, M., Kayano, M. and Ozawa, H., "Effect of moisture in crystallization of theophylline in tablets," *Drug. Dev. Ind. Pharm.* **18**, 453–467 (1993).
15. Windbergs, M., Jurna, M., Herek, J. L., Offerhaus, H. L., Kleinebudde, P. and Strachan, C. J., "Visualization of the physicochemical structure of oral solid dosage forms and changes upon dissolution using coherent anti-Stokes Raman scattering microscopy," submitted to *Anal. Chem.*

